603 024

ARO D # 2566:

TR AE 6406

RESEARCH ON THE DYNAMICS OF A VEHICLE IN A TUBE

Under Grant No. DA-ORD-31-124-61-G88
U. S. Army Research Office (Durham)

FINAL PROGRESS REPORT

342 p $7.00 hc
$1.75 mf

DEPARTMENT OF AERONAUTICAL ENGINEERING AND ASTRONAUTICS
RENSSELAER POLYTECHNIC INSTITUTE
TROY, NEW YORK

June, 1964

INDEX

INTRODUCTION

J. V. Foa

This report is a summary of work done at Rensselaer since 1961, as part of a program of research on the dynamics of a body moving in a tube, under a three-year grant from the U. S. Army Research Office (Durham). More specifically, this report covers the portion of the program that dealt with problems relating to a transportation system in which a vehicle would propel itself at high velocity (250 to 2000 mph) through a tube.

Other research activities under the same grant have been reported separately (Refs. 1-3).

THE CONCEPT

Land vehicles are of necessity constrained to travel along narrowly defined paths. Therefore, unless the prescribed path is a straight line, a land vehicle traveling at very high speed must be supported from all sides. This kind of support is best provided within a tube, also because there are safety features that are intrinsic in the operation of a high-speed vehicle within a tube.

However, in conventional tube transportation systems, the vehicle, in traveling within the tube, acts in relation to the adjacent air masses either as a driving piston (as in the case of a

train in a tunnel) or as a driven piston (as in pneumatic dispatch systems), and therefore its motion is accompanied by large displacements of the air masses in the tube. In contrast to the incompressible-flow situation (Ref. 4), where these displacements decrease the drag of the vehicle, their effect in a compressible medium is found to be an increase of drag. The increase is so large that the required thrust could not be produced by wheel traction at speeds much above those of present-day land transportation even if there were no structural limitations to the use of this kind of propulsion at high speeds. Propulsion by linear induction could extend the range of attainable speeds somewhat, but only at a prohibitive cost in power consumption. To overcome this difficulty, schemes have been proposed for the operation of vehicl in evacuated tubes, but any systems of this sort would be very cos ly to operate (despite its low power demands) and highly vulnerabl Furthermore, at speeds at which the use of wheels, levapads, or other direct-contact or low-clearance supports must be ruled out, the evacuation of the tube aggravates the problem of supporting th vehicle and leaves a magnetic suspension, with its own peculiar difficulties and hazards, as the only workable solution.

A study of the broad problem of high-speed land transportatio with consideration of the intertwined difficulties that this probl involves, led, in 1947, to the conception of the scheme that is

discussed in the present report. The work that was done on this scheme at Rensselaer, as an internal research project, prior to the initiation of the studies that are summarized here, is described in Refs. 5-7.

The system under discussion overcomes the speed limitations of conventional land-transport systems without requiring an evacuated tube. Its main feature will now be described in some detail.

PROPULSION

The vehicle propels itself by the fore-to-aft transfer, through the space which separates it from the tube wall, of the air which fills the remainder of the tube. The transfer is the process by which the motion of the vehicle is produced and maintained, not the consequence of a motion that is produced by other means. Its volumetric rate is such that the flow perturbations in the tube are kept at the lowest level that is compatible with the maintenance of the required motion of the vehicle. This condition would be ideally and automatically satisfied if the fluid filling the tube were incompressible and if, in addition, its motion were fully prevented at some station by means of a gate or simply by keeping one end of the tube closed. In this case, the volumetric transfer rate would always be equal to the product of the cross-sectional area of the tube and the velocity of the

vehicle, and the fluid would be at rest everywhere in the tube except in the transfer passages, regardless of the mode of propulsion. Because of the compressibility of the air, the flow perturbations produced by the pressure disturbances which originate at the vehicle may extend over great distances. However, in contrast to the incompressible-flow situation, the amplitude and distribution of these perturbations depend not only on the boundary conditions but also on the shape of the vehicle, on its blockage ratio, on its speed, and on its mode of propulsion. In particular, it has been found that modes of propulsion of the type specified above ("internal" modes) are capable of producing much smaller flow perturbations, all other conditions being equal, than the conventional ("external") modes, in which the thrust is produced as the reaction to a force exerted on a stationary structure With internal propulsion, if the tube is relatively short and the motion of the fluid is inhibited at any one station, the transient flow velocities that are generated in the tube even during acceleration and deceleration of the vehicle are quite low (Section A). Th analysis also predicts remarkably low flow velocities with the present system, during accelerations of the vehicle, for the idealized case of a tube of infinite length (Section A). This means tha no gate or other flow-inhibiting device is necessary when the accelerations start at such a distance from the nearest opening in the tube that no reflected disturbance can reach the vehicle befor

the acceleration phase is completed. In the steady state that is finally established by the reverberating pressure waves, the flow velocities are higher, but still very much lower than with external propulsion (Section F).

Since the slipstream of the propulsion system is here substantially at rest, its "propulsive efficiency" is close to unity. Furthermore, the wake associated with the drag of the vehicle is also at rest in a stationary frame of reference. Thus the kinetic energy losses associated with fluid motions in both the slipstream and the wake are almost entirely eliminated. The power required for propulsion of the vehicle at steady speed is, accordingly, greatly reduced. At supersonic speed, this power is reduced to that necessary to make up for flow losses inside the vehicle and in the annular space surrounding it within the tube.

In fact, at supersonic speeds, the vehicle itself may be considered as the equivalent of the centerbody of a jet engine, the outer shroud of which is represented by the wall of the tube. The power required at steady speed can then be calculated by analogy with that of a jet engine in the condition of zero thrust. Fig. 1 illustrates this equivalence for a system in which the transfer flow is sustained by the addition of heat alone, as in a ramjet. It should be noted that the outer boundary of the airstream passage

(the internal surface of the tube wall) is not stationary in the vehicle-fixed frame of reference as it is in conventional jet engines; instead, it moves in this frame of reference in the direction of the relative air flow. Energy losses due to viscous forces are therefore substantially reduced.

Problems relating to drag and propulsion are discussed in Sections A, E, F, G, H and J of this report.

SUPPORT

It has already been noted that a land vehicle traveling at very high speed must be supported on all sides. In the lower range of speeds the required support may be provided by wheels or skids or low-clearance devices, such as the "levapads". Large-clearance suspensions are preferable at high speeds. Over the entire range of speeds, the vehicle may be kept on a centered path through the use of suitably arranged GEM pads. Since the air curtains in these supports would be blowing against the solid walls of the tube, their "rigidity" would not be limited as it is in conventional ground effect machines that are to operate over soft ground or water. Therefore, this kind of support could be made to operate effectively within the tube at speeds far above the maximum permissible with "conventional" ground effect machines. In forward motion, the rearward momentum of the deflected curtains contributes to the thrust (Section B). Floating suspensions of

this type also have the important merit that a vehicle so provided, if its center of gravity is appropriately low, will automatically tilt itself to the correct angle of bank in every turn, independently of the speed at which the turn is negotiated.

Problems of stability and ground-effect support of the vehicle are discussed in Sections B, C, and D of this report.

TRANSONIC ACCELERATION

In dealing with supersonic vehicles, a variety of schedules of acceleration through the transonic regime may be considered. Some aspects of two of these schedules are discussed in Section I. According to the first one, the transfer flow is permitted to choke, with the formation of a forward-facing shock ahead of the vehicle; and the vehicle is then made to overtake this shock. The second schedule calls for surge chambers around the tube walls, or for wall perforations, over those stretches of the tube within which the transonic acceleration is expected to take place. Others yet are based on the utilization of nonsteady processes in the transfer flow.

BRAKING

The presence of large and confined masses of air within the tube provides a safe and simple solution to the problem of bringing the vehicle to rest from speeds at which it would not be practicable

to dissipate all the stored kinetic energy through sliding friction between solid surfaces. As soon as the input of propulsive power to the transfer flow is shut off, the behavior of the vehicle in relation to the adjacent fluid masses changes to the already discussed pistonlike action of conventionally-driven vehicles. The result is a large retarding force, which may be increased further through the insertion of spoilers in the transfer passage or may be decreased through the opening of appropriate vents. It is easy to verify that this mechanism is capable of producing, at high forward speeds, any braking action that may be desired or required even under severe circumstances. As the vehicle slows down this braking force decreases, until the velocity of the vehicle becomes low enough that it can be brought to a full stop by conventional sliding-friction means. In any case, the dissipation of the kinetic energy initially stored in the vehicle does not entail any difficulty with local heating or wear, because the mechanism just described causes this energy to become distributed over long stretches of the tube.

ILLUSTRATIVE EMBODIMENTS

Illustrative embodiments of the concept are shown in Figures 2 through 6. Fig. 2 shows a low-speed, wheel-supported vehicle with a propeller-energized flow. In the arrangement of Fig. 3 a

compressor energizes the flow both for propulsion and for ground-effect support.

Fig. 4 shows a vehicle with a driving mechanism which is essentially an ejector pump. The primary gas is discharged from a compressor or other suitable gas generator into a mixing duct behind the vehicle, where the ejector action takes place. The mixing duct is formed by the tube itself, as shown in the lower portion of the figure. There is a similarity between this embodiment and that of Fig. 1, in that the transfer flow is energized, in both cases, in a region where the addition of energy to the flow would have no useful effect if the tube were absent. The tube constitutes, in both cases, an integral part of the propulsion system. For example, when the primary gas generator is a turbojet (as in the embodiment of Fig. 4), the thrust generator may be said to be a shrouded turbojet in which the shroud is replaced by a stationary tube.

In the embodiment of Fig. 5 the driving mechanism is again an ejector pump, but the transfer flow is energized upstream of the throat.

Fig. 6 shows a supersonic arrangement in which the transfer flow is energized by a cryptosteady energy exchanger (Ref. 8) ahead of the throat and by heat addition downstream of the throat. In a

variation of this embodiment, the addition of heat is effected behind the vehicle by sources which are fixed to the tube and successively activated by the passing vehicle (Section F).

REFERENCES

1. Foa, J. V., "Evaluation of the Increase of Missile Payload That Can Be Obtained from Atmospheric Boost at Take Off," (Project Mountainwell), September 1961.

2. Burr, J.W., Adair, W.R., and Madden, J.J., "Performance Analysis of the Murray-Kumar Missile-Boost System," Rensselaer Polytechnic Institute, Tech. Rept. TR AE 6110, December 1961.

3. Adair, W.R., McGrath, P.A., and Burr, J.W., "Small-Scale Experimental Study of the Murray-Kumar Missile Boost System," Rensselaer Polytechnic Institute, Tech. Rept. TR AE 6207, May 1962.

4. Tollmien, W., "Luftwiderstand und Druckverlauf bei der Fahrt von Zügen in einem Tunnel," Zeitschrift des Vereines deutsche Ingenieure, 71, No. 6, 199-203, 5 February 1927.

5. von Keszycki, H.J., "The Motion of a Self-Propelled Body in a Tube," Rensselaer Polytechnic Institute, Tech. Rept. TR AE 5905, December 1959.

6. Lopez, H., "An Experimental Investigation of the Dynamics of a Self-Propelling Body in a Tube," Rensselaer Polytechnic Institute, Tech. Rept. TR AE 5903, December 1959.

7. Burr, J., "A Contribution to the Dynamics of a Self-Propelled Vehicle in an Infinite Duct," Rensselaer Polytechnic Institute Tech. Rept. TR AE 6101, January 1961.

8. Foa, J.V., "A New Method of Energy Exchange," ARS Journal, 32 1396-1398 (1962).

FIG. 1

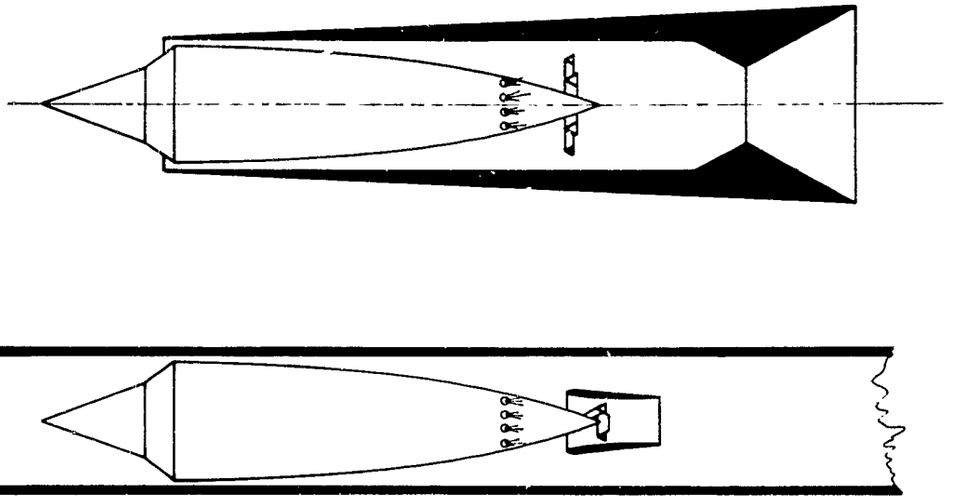

FIG. 2

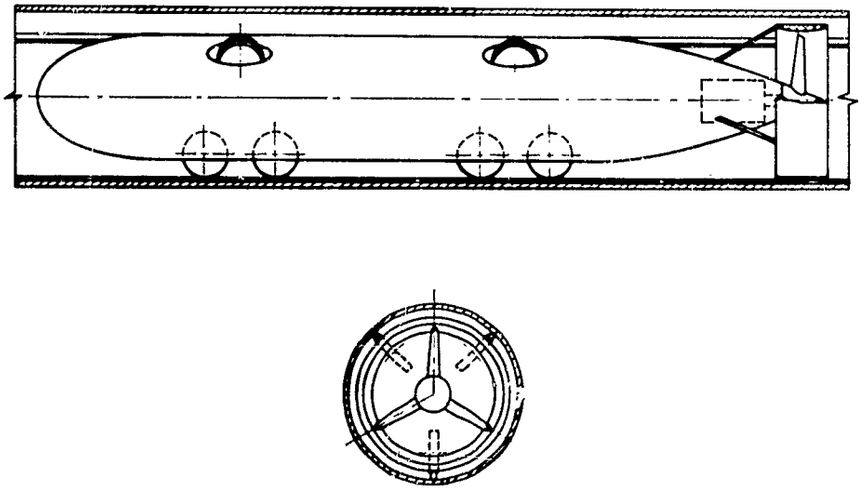

FIG. 3

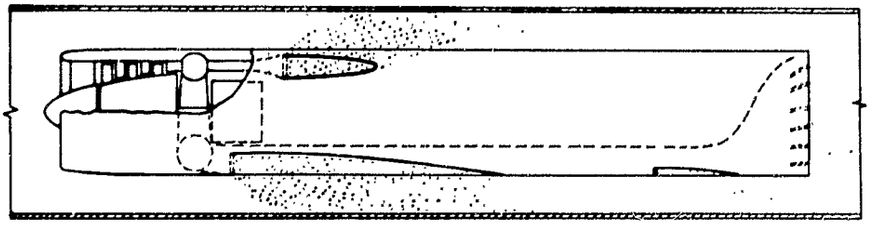

FIG. 4

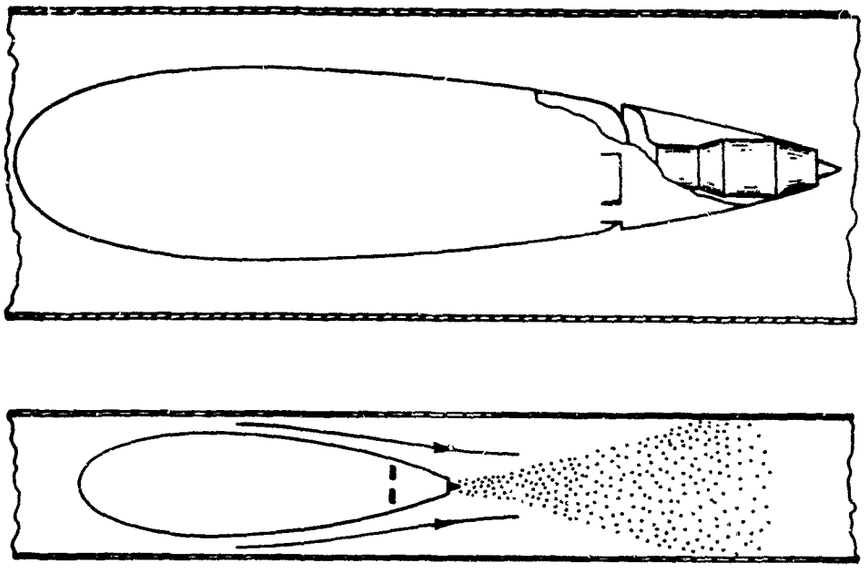

FIG. 5

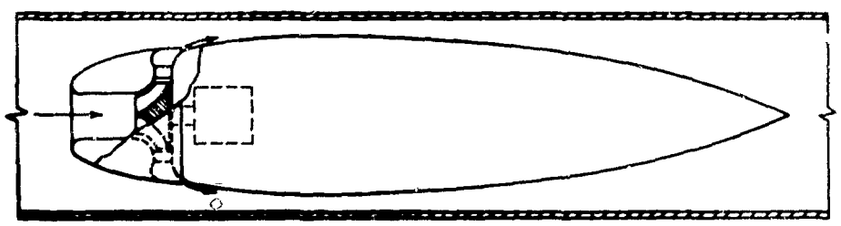

FIG. 6

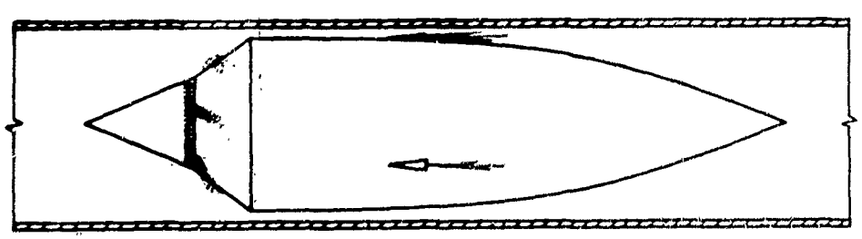

SECTION A

AN APPROXIMATE ANALYSIS OF A SELF-PROPELLED VEHICLE IN A TUBE WITH CONSIDERATION OF VARIOUS TUBE END CONDITIONS

by

Peter McGrath
John W. Burr
William Adair

First issued as TRAE 6204
October 1963
"The Flow Induced by a New Type
of Self-Propelled Vehicle in a Duct"

SUMMARY

An analysis is carried out to determine the magnitude of the flow velocities that are induced inside a tube in the presence of a vehicle which propels itself by the fore-to-aft transfer, at appropriate rates, of the fluid in the adjacent layers within the tube itself. A fixed schedule of accelerations of the vehicle is considered, with various tube end conditions.

The greatest induced air velocities are produced if the tube is open at both ends. If the tube is closed at one or both ends the induced air velocities are more than an order of magnitude lower. In an infinite or half-infinite tube the induced air velocities are greater than those produced in a closed tube, but still an order of magnitude lower than those produced in a tube open at both ends.

TABLE OF CONTENTS

SYMBOLS

A	nondimensional speed of sound, $\frac{a}{a_*}$
a	speed of sound (ft/sec)
b	nondimensional terminal velocity, $\frac{u_t^2}{gL}$
C	force ratio, $\frac{m_v g}{p_* \alpha}$
e	base of natural logarithms
g	gravitational constant
L	tube length (ft)
M	Mach number, $\frac{u}{a}$
m_v	mass of vehicle (slug)
m	mass of air (slug)
$\dot{m}$	mass flow of air (slug/sec)
p	pressure (lb/ft^2)
P	Riemann parameter
Q	Riemann parameter
R	gas constant ($ft\text{-}lb/lb_m\text{-}^oR$)
T	temperature (^oR)
t	time (sec)
U	nondimensional velocity, $\frac{u}{a_*}$
u	velocity (ft/sec)
V	volume (ft^3)
v	specific volume (ft/lb_m)
x	coordinate along tube (ft)
α	cross sectional area of tube

γ ratio of specific heats

ϵ a constant less than 1.0, see Eq. (2)

θ thrust (lbs)

ρ density (slugs^{+}/ft^3)

Subscripts

0 reference state

1 region ahead of vehicle

2 region behind vehicle

x axial distance along tube

t terminal

v vehicle

1x axial location in Region 1

2x axial location in Region 2

1v refers to conditions adjacent to front face of vehicle

2v refers to conditions adjacent to rear face of vehicle

Superscripts

o stagnation conditions

INTRODUCTION

In recent years a number of reports have been written (Refs. 1, 2, 3, and 4) concerning a method of high-speed land transportation involving a self-propelled vehicle operating in a tube. This concept of transportation, first proposed by Foa at Cornell Aeronautical Laboratory in 1947, consists of a vehicle propelling itself through a tube by the fore-to-aft transfer, through or around itself, of the air which fills the remainder of the tube. This is in contrast to conventional systems of transport in tubes, or of pneumatic dispatch, where the column of air filling the entire length of the tube (or twice that length in the case of a closed-loop system) must be moved about the same distance as the vehicle, at about the same velocity.

The proposed system employs the air in the tube to provide both thrust for propulsion and drag for braking, and its operation is accompanied by disturbances in the air columns adjacent to the vehicle. The present report is concerned only with the acceleration phase and more particularly with a determination of the order of magnitude of the induced air velocities which are produced by accelerating vehicles of the type described above, operating in tubes with various end conditions (open, closed, and half-open tubes, finite, infinite, and half-infinite tubes).

ANALYSIS

Statement of the Problem

A rigorous study of the dynamical situation considered here would require a detailed analysis of the fluid flow around or through the vehicle. Great simplifications are possible if viscous stresses are assumed to be negligible, with the understanding that the validity of this assumption is to be checked in the light of the results (and particularly of the flow velocities) so obtained. Then, the flow may be treated as one-dimensional everywhere, except for a limited region comprising the fluid-transfer passages and their immediate neighborhood. Furthermore, if the duct is sufficiently long, this region may be treated as a discontinuous "actuate disk", and the flow may accordingly be treated as one-dimensional everywhere. A schematic representation of this analytical model is shown in Fig. 1 with the vehicle moving to the right and the flow relative to the vehicle moving to the left. All velocities and distances relative to the duct are considered positive to the right.

In the present analysis only subsonic vehicle speeds are considered. To obtain a common basis for comparison, the stipulated schedule of accelerations of the vehicle is the same for all conditions considered.

Vehicle Performance

The thrust acting on the vehicle is equal to the change of

stream force (relative to the vehicle) of the flow as it passes through the vehicle, or

$$\theta = \dot{m}\left\{(u_v - u_{2v}) - (u_v - u_{1v})\right\} + \alpha(p_{2v} - p_{1v}) \qquad (1)$$

where θ is the thrust, $\dot{m}$ is the mass flow through the vehicle, relative to the vehicle, u_{2v} and p_{2v} are the velocity and pressure, respectively, of the flow just behind the vehicle, and u_{1v} and p_{1v} are the velocity and pressure, respectively, of the flow just ahead of the vehicle. Since the velocity change across the vehicle is small, the contribution of the momentum change to the thrust is small and will consequently be neglected in the present analysis.* Let the pressure rise across the vehicle be

$$p_{2v} - p_{1v} = \epsilon p_0 \left(1 - \frac{u_v}{u_t}\right) \qquad (2)$$

where p_0 is a reference pressure, u_v the vehicle velocity, u_t the terminal velocity of the vehicle, and ϵ a constant less than 1.0. Then

$$\theta = \alpha(p_{2v} - p_{1v}) = m_v \frac{du_v}{dt} \qquad (3)$$

* The absolute value of the thrust contributed by the momentum change is small for all cases considered in the Numerical Example, but the percentage of the total thrust which the momentum change contributes increases from less than 10% when the vehicle first starts, to 20% or 30% at higher vehicle velocities when the pressure difference drops to a small value. Therefore the approximation of the present analysis is poor in the latter range of speeds, which is, however, the range of least interest, in that it involves the lowest flow velocities.

or

$$\frac{du_v}{dt} = \epsilon \frac{P_o \alpha}{m_v}\left(1 - \frac{u_v}{u_t}\right) \tag{4}$$

Introducing the nondimensional parameter $c = \frac{m_v g}{P_o \alpha}$

$$\frac{du_v}{dt} = \frac{\epsilon g}{c}\left(1 - \frac{u_v}{u_t}\right) \tag{5}$$

With $u_v = 0$ and $x_v = 0$ at $t = 0$,

$$\frac{u_v}{u_t} = 1 - e^{-\frac{\epsilon g}{c u_t} t} \tag{6}$$

and

$$x_v = \int_0^t u_v dt = u_v t - \frac{u_t^2 c}{\epsilon g}\left(1 - e^{-\frac{\epsilon g}{c u_t} t}\right)$$

or

$$x_v = -\frac{c u_t^2}{\epsilon g}\left\{ \ln\left(1 - \frac{u_v}{u_t}\right) + \frac{u_v}{u_t} \right\} \tag{7}$$

From Eq. (6) it can be seen that the vehicle velocity is an exponential function of time, asymptotically approaching the termi velocity u_t . At any distance x_v from the starting point, t vehicle will have attained only a fraction $\frac{u_v}{u_t}$ of the termina velocity. From Eq. 7,

$$\ln\left(1 - \frac{u_v}{u_t}\right) + \frac{u_v}{u_t} = -\frac{P_o \alpha}{m_v g} \cdot \frac{\epsilon g x_v}{u_t^2} \tag{8}$$

This relation is plotted in Fig. 2.

Air Velocities Induced by the Vehicle

The air velocities which are induced in the tube by the accelerating vehicle depend on the tube end conditions on both sides of the vehicle. The end conditions considered here are: (1) fully open end, (2) fully closed end, and (3) no end (tube extending to infinity). Two of the nine possible combinations of these conditions at the two ends admit no solution for the analytical model used. These two cases are those of a half-infinite tube on either side of the vehicle with the tube end closed on the other side. They require a gradual increase of the pressure increment from zero to the value given by Eq. 2, whereas the analytical model used here requires a finite pressure rise across the vehicle from the start.

Each of the other seven cases must be solved separately, as they require different assumptions and simplifications.

1) Both ends closed

For this tube configuration, the flow processes are treated as quasi-static. The air temperature is stipulated to be constant with respect to time and uniform throughout the tube, so that the density is dependent only on the pressure. The pressure is considered constant throughout each of the two regions ahead of and behind the vehicle ($p_{1x} = p_{1v} = p_1$, $p_{2x} = p_{2v} = p_2$). Since the total mass of air within the tube is constant

$$p_2 x_v + p_1 (L - x_v) = p_0 L$$

where L is the total length of the tube. The pressure ahead of vehicle (on its right side in the figures) is then

$$P_1 = P_0 - (P_2 - P_1)\frac{x_v}{L}$$

or

$$P_1 = P_0\left\{1 - \epsilon\frac{x_v}{L}\left(1 - \frac{u_v}{u_t}\right)\right\} \tag{9}$$

and from Eq. (2)

$$P_2 = P_0\left\{1 + \epsilon\left(1 - \frac{u_v}{u_t}\right)\left(1 - \frac{x_v}{L}\right)\right\} \tag{10}$$

Consider the layer of air which at time t is at a distance x from the left end, in region 1. The volume and mass of air enclosed between this layer and the right end of the tube are $(L-x)$ and $(L-x)\frac{\alpha P_1}{RT_0}$, respectively. The latter is constant, whe the former changes with time. Denoting the velocity of this laye by u_{1x},

$$\frac{dv_1}{dt} = \frac{d}{dt}\left(\frac{V_1}{m_1}\right) = \frac{\frac{d}{dt}\{(L-x)\alpha\}}{(L-x)\frac{\alpha P_1}{RT_0}} = -\frac{u_{1x}RT_0}{(L-x)P_1}$$

For an ideal gas,

$$\frac{dv_1}{dt} = -\frac{RT_0}{P_1^2}\frac{dP_1}{dt}$$

Thus,

$$u_{1x} = (L-x)\frac{1}{P_1}\frac{dP_1}{dt}$$

Substituting for R and $\frac{dR}{dt}$ from Eq. 9 yields:

$$\frac{u_{1x}}{u_t} = \epsilon\left(1 - \frac{x}{L}\right)\left(1 - \frac{u_v}{u_t}\right)\left\{\frac{\ln\left(1 - \frac{u_v}{u_t}\right) + 2\frac{u_v}{u_t}}{\epsilon\frac{x_v}{L}\left(1 - \frac{u_v}{u_t}\right) - 1}\right\} \qquad (11)$$

This equation gives the velocity distribution in region 1 at the time when the instantaneous velocity of the accelerating vehicle is u_v .

Similarly, in region 2, denoting the instantaneous flow velocity at x by u_{2x} .

$$\frac{u_{2x}}{u_t} = \epsilon\frac{x}{L}\left(1 - \frac{u_v}{u_t}\right)\left\{\frac{\frac{\epsilon}{bc} + \ln\left(1 - \frac{u_v}{u_t}\right) + 2\frac{u_v}{u_t}}{1 + \epsilon\left(1 - \frac{u_v}{u_t}\right)\left(1 - \frac{x_v}{L}\right)}\right\} \qquad (12)$$

where b is the terminal velocity parameter $\frac{u_t^2}{gL}$. Both u_{1x} and u_{2x} are linear functions of x , zero at the closed ends and maximum at the vehicle. Thus, at any instant the maximum induced air velocities are obtained from Eqs. (11) and (12) evaluated at $x = x_v$.

2) <u>One end open and the other closed.</u>

When the tube is open at one end the mass of air in the tube does not remain constant during the acceleration of the vehicle. However, as will be verified, the induced flow velocities are small in this situation also. Therefore the pressure in the region of the tube between the open end and the vehicle remains close to atmospheric

pressure, and the flow in this region can be treated as incompr ible. If the pressure is also considered constant throughout t region between the closed end and the vehicle, then at each ins the pressure is uniform throughout both regions, or $p_{1x} = p_{1v}$ and $p_{2x} = p_{2v} = p_2$. If the temperature is stipulated to be stant with time and uniform throughout the tube, then the flow velocity may be considered uniform throughout the region betwe open end and the vehicle. The continuity equation across the gives

$$\rho_{2v}(u_v - u_{2v}) = \rho_{1v}(u_v - u_{1v}) \qquad (1.$$

For the case in which the closed end is behind the vehicl (region 2) the flow velocity in region 1 is

$$u_{1v} = u_1 = \frac{p_2}{p_1}(u_{2v} - u_v) + u_v \qquad (1$$

where the pressure ratio, as given by Eq. (2), is

$$\frac{p_2}{p_1} = \frac{p_2}{p_0} = 1 + \epsilon\left(1 - \frac{u_v}{u_e}\right) \qquad (1$$

The air velocity in the closed region behind the vehicle (u can be found using the same approach as in case 1.

$$u_{2x} = -\frac{1}{\rho_2}\frac{dp_2}{dt}$$

or

$$\frac{u_{2x}}{u_t} = \frac{x}{L}\left\{\frac{\frac{\epsilon^2}{bc}\left(1 - \frac{u_v}{u_t}\right)}{1 + \epsilon\left(1 - \frac{u_v}{u_t}\right)}\right\} \tag{16}$$

The velocity u_{2x} is at each instant a linear function of x, zero at the closed back end and maximum at the vehicle. Thus,

$$\left(\frac{u_{2x}}{u_t}\right)_{max} = \frac{u_{2v}}{u_t} = -\epsilon\left(1 - \frac{u_v}{u_t}\right)\left\{\frac{\ln\left(1 - \frac{u_v}{u_t}\right) + \frac{u_v}{u_t}}{1 + \epsilon\left(1 - \frac{u_v}{u_t}\right)}\right\} \tag{17}$$

which shows that the maximum induced air velocity in region 2 is dependent only upon ϵ and $\frac{u_v}{u_t}$.

Combining Eqs. 14, 15 and 17 yields

$$\frac{u_1}{u_t} = -\epsilon\left(1 - \frac{u_v}{u_t}\right)\left\{\ln\left(1 - \frac{u_v}{u_t}\right) + 2\,\frac{u_v}{u_t}\right\} \tag{18}$$

Thus, the air velocity in region 1 is dependent also upon ϵ and $\frac{u_v}{u_t}$.

For the case in which the closed end is ahead of the vehicle (Region 1) the flow velocity in the Region 2 is

$$u_{2v} = u_2 = \frac{p_1}{p_2}\left(u_w - u_v\right) + u_v \tag{19}$$

where again the pressure ratio is found from Eq. (2),

$$\frac{p_1}{p_2} = \frac{p_1}{p_0} = 1 - \epsilon\left(1 - \frac{u_v}{u_t}\right)$$

The air velocity in Region 1 can again be found by using the same approach as in case 1.

$$u_{1x} = (L - x) \frac{1}{P_1} \frac{dP}{dt}$$

or

$$\frac{u_{1x}}{u_t} = \left(1 - \frac{x}{L}\right) \frac{\epsilon^2}{bc} \left\{ \frac{\left(1 - \frac{u_v}{u_t}\right)}{1 - \epsilon\left(1 - \frac{u_v}{u_t}\right)} \right\} \qquad (20)$$

Thus, u_{1x} is at each instant a linear function of x, maximum at the vehicle and zero at the front end. By substituting the value of $\frac{u_{1x}}{u_t}$ into Eq. (19), the velocity in the open-end region (Region 2) is obtained as:

$$\frac{u_2}{u_t} = \epsilon\left(1 - \frac{u_v}{u_t}\right)\left\{ \frac{\epsilon}{bc}\left(1 - \frac{x_v}{L}\right) + \frac{u_v}{u_t} \right\} \qquad (21)$$

It can be verified that the air velocity in Region 2 is maximum when $u_v = 0$, which occurs at $x_v = 0$:

$$\left(\frac{u_2}{u_t}\right)_{max} = \frac{\epsilon^2}{bc} = \frac{\epsilon^2 \alpha P_0 L}{\eta_v u_t^2} \qquad (22)$$

From this expression it can be seen that the initial flow-velocity a function of tube length (L) and that, for very long tubes, ver high air velocities will result. This result is a consequence of t quasi-static approach used. The pressure in the open-end region is

atmospheric and because of the pressure ratio across the vehicle (which is maximum when $u_v = o$) the closed-end region ahead of the vehicle is under low pressure. As the vehicle begins to move, the pressure (which is assumed constant throughout the length of the tube) begins to rise. In order to satisfy the conditions of the quasi-static approach, the inflow velocity must be very high to supply the large amount of air necessary to raise the pressure in the entire tube. The implausibility of the result indicates that the present analysis for this condition (tube closed ahead of the vehicle) is applicable only to very short tubes.

3) Infinitely long tube

The effect of the compression and expansion waves which the vehicle generates as it accelerates is determined in the following nonsteady-flow analysis. To avoid the complicated interactions of outgoing waves with reflected waves, an infinite tube will be considered. In this case, if no entropy producing disturbances exist in the tube, the value of the Riemann parameters (see Ref. 5) on the characteristics which reach the vehicle from both sides remains constant:

$$P_2 = \frac{2}{\gamma-1} A_{2x} + U_{2x} = \frac{2}{\gamma-1} A_{2v} + U_{2v} = \frac{2}{\gamma-1} \qquad (23)$$

$$Q_1 = \frac{2}{\gamma-1} A_{1x} - U_{1x} = \frac{2}{\gamma-1} A_{1v} - U_{1v} = \frac{2}{\gamma-1} \qquad (24)$$

Since the flow is assumed to be homentropic, Eq. 2 yields

$$U_v = \frac{u_v}{a_o} = \frac{u_t}{a_o}\left\{1 + \frac{1}{\epsilon}\left(A_{2v}^{\frac{2\gamma}{\gamma-1}} - A_{1v}^{\frac{2\gamma}{\gamma-1}}\right)\right\} \qquad (25)$$

Substituting the above expressions for U_v, U_{1v} and U_{2v} int the equation for the conservation of mass across the vehicle,

$$\left(U_v - U_{1v}\right) = \frac{\rho_2}{\rho_1}\left(U_v - U_{2v}\right) \qquad (26)$$

and using the isentropic relationship between ρ and T, yields

$$U_t\left\{1 + \frac{1}{\epsilon}\left(A_{2v}^{\frac{2\gamma}{\gamma-1}} - A_{1v}^{\frac{2\gamma}{\gamma-1}}\right)\right\}\left\{\left(\frac{A_{2v}}{A_{1v}}\right)^{\frac{2}{\gamma-1}} - 1\right\} = \frac{2}{\gamma-1}\left\{\left(\frac{A_{2v}}{A_{1v}}\right)^{\frac{2}{\gamma-1}}\left(1-A_{2v}\right) - \left(A_{1v}-1\right)\right\} \qquad (27)$$

This equation, which can be solved numerically, gives a relation between A_{1v} and A_{2v}. Once this relationship is established, the corresponding values of u_{1v}, u_{2v} and u_v can be determined from Eqs. (23), (24) and (25).

This solution gives the waves which are generated as the vehicle accelerates along the tube. The only transient this solution omits is the one generated when the power is first applied to the vehicle which is at rest in the tube. It does, however, give, under the conditions stipulated, the velocity of the flow after the power has been applied.

4) Semi-infinite tube

As mentioned previously, when the tube is closed on one side of the vehicle and infinitely long in the other direction there is no solution similar to those outlined above, if the pressure difference given by Eq. (2) is considered to be established when the vehicle is still at rest. Such a solution does exist, however, if the tube is open on one side of the vehicle and infinitely long in the other direction.

If the region between the open end and the vehicle is considered to remain at atmospheric pressure, then for the case where the open end is behind the vehicle, Eq. (2) and the isentropic relations give

$$\frac{u_v}{u_t} = 1 - \frac{1}{\epsilon}\left\{1 - A_{IV}^{\frac{2\gamma}{\gamma-1}}\right\} \qquad (28)$$

The invariance of the Riemann parameter on the characteristics which reach the vehicle from the front gives

$$\frac{2}{\gamma-1} = \frac{2}{\gamma-1} A_{Ix} - U_{Ix} = \frac{2}{\gamma-1} A_{IV} - U_{IV} \qquad (29)$$

Substituting these two equations into the continuity equation across the vehicle gives

$$U_v\left\{A_{IV}^{-\frac{2}{\gamma-1}} - 1\right\} = A_{IV}^{-\frac{2}{\gamma-1}} U_{2V} + \frac{2}{\gamma-1}\left(1 - A_{IV}\right) \qquad (30)$$

The corresponding equations for the case when the open end is ahead of the vehicle and the tube is infinitely long behind it are:

$$\frac{u_v}{u_t} = 1 - \frac{1}{\epsilon}\left(A_{2v}^{\frac{2\gamma}{\gamma-1}} - 1\right) \tag{28'}$$

$$\frac{2}{\gamma-1} = \frac{2}{\gamma-1} A_{2x} + U_{2x} = \frac{2}{\gamma-1} A_{2v} + U_{2v} \tag{29'}$$

$$U_v\left\{A_{2v}^{-\frac{2}{\gamma-1}} - 1\right\} = A_{2v}^{-\frac{2}{\gamma-1}} U_{1v} - \frac{2}{\gamma-1}\left(1 - A_{2v}\right) \tag{30'}$$

The speed of sound A in the region adjacent to the vehicle on the infinite tube side can be obtained from either Eq. (28) or (28') for any value of $\frac{u_v}{u_t}$. Once this is determined, the corresponding value of the flow velocity on both sides, u_{1x} u_{2x} , can be obtained from either Eqs. (29) and (30) or Eqs. (and (30').

5) Both ends open

When both ends of the tube are open the static pressure at th outflow end and the stagnation pressure at the inflow end are equa to atmospheric pressure. If the inlet and exit flows are consider incompressible at constant temperature, then

$$P_1\left(1 - \frac{u_1^2}{2gRT_0}\right) = P_0^* = P_0 \tag{31}$$

Equations 2 and 31 give

$$u_1 = \sqrt{2gRT_0}\left\{\frac{1}{1 - \epsilon\left(1 - \frac{u_v}{u_t}\right)} - 1\right\}^{\frac{1}{2}} \tag{32}$$

and, from the continuity equation across the vehicle,

$$u_2 = u_v - \frac{u_v - u_1}{\left(1 + \frac{u_1^2}{2gRT_0}\right)} \qquad (33)$$

Numerical Example

Because of the differences of approach in the above analyses of the various configurations considered, the results could not be compared on the basis of a common set of equations or nondimensional charts. For this reason a numerical example will be given here to provide an indication of the order of magnitude of the induced air velocities produced in the various configurations. Consider the following vehicle and tube:

m_v = 100,000 lbs

u_t = 500 ft/sec = 340 mph

L = 100 miles

α = 177 ft^2

ϵ = 0.1

and the following atmospheric conditions:

P_0 = 2100 psf

T_0 = 540°R

thus $b = \frac{u_t^2}{2g} = 0.0147$

$C = \frac{m_v g}{P_0 \alpha} = 0.269$

For these conditions the vehicle velocity and the time to travel to a given location are plotted on Fig. 3 as functions of the vehicle location. The corresponding induced air-velocities the various end conditions are presented on Figs. 4, 5, and 6. the maximum induced air velocities, which always occur immediat in front of and immediately at the rear of the vehicle, are pre sented on these figures.

The calculated air velocities for the case of a tube which open behind the vehicle and closed ahead of it are not presente on the curve because the analytical model used becomes unrealis in this case, for the reasons discussed previously. Also, onl of the half-infinite-tube cases is shown on the figures; for th other case, only the total pressure level throughout the tube w be changed. The pressure ratio and velocity change across the vehicle, and the absolute value of the air velocity would remai same.

The maximum induced air velocity, which occurs for a tube at both ends, is 452.5 ft/sec, which is a speed at which compre bility effects (as reflected in the ratio between total and sta pressure) are still negligible. Therefore the assumption of in pressible flow is valid for all cases in which this assumption made.

It is also noteworthy that for the case of the tube closed at both ends changes of the parameter bc up to 0.2, which would most likely be the maximum value desirable (see Fig. 2), the change in the induced air velocities is so small that it cannot be plotted on the same graph. Also the parameter c does not appear in any of the other cases.

DISCUSSION

The results of the analysis, as applied to a specific numerical example, indicate that, as could be expected, the lowest induced flow velocities are produced when the tube is closed at one or both ends, and that these velocities are in either case one order of magnitude lower than those that would be produced by a vehicle with the same thrust schedule in a tube open at both ends.

In a tube that is infinitely long in both directions, or in a half-infinite tube with an open end, the same vehicle will induce air velocities much more nearly equal to those of the closed tube case than to those of the open tube. This indicates that, although placing a gate behind the vehicle to produce a closed-end condition would give the best results, very little would be lost by not using such a gate if the tube is so long that waves reflected from either end do not return to the vehicle before the latter has reached cruising speed.

In the case of the short, open tube, the velocities induced by the vehicle considered here in the acceleration phase are of the same order of magnitude (but of the opposite sign) as those that would be induced by a wheel-traction vehicle - or as those that would be required to propel a pneumatic-dispatch vehicle - at the same terminal velocity.

Viscous effects, which are neglected in this analysis, are unimportant in all cases except that of the acceleration in proximity to an open end, because the maximum calculated flow velocities in all such cases are actually very low, and also because these maximum velocities appear only as brief and localized transients.

REFERENCES

1. Lopez, H., An Experimental Investigation of the Dynamics of a Self-Propelling Body in a Tube, Rensselaer Polytechnic Institute, TR AE 5903, 1959.

2. von Keszycki, H., The Motion of a Self-Propelled Body in a Tube, Rensselaer Polytechnic Institute, TR AE 5905, 1959.

3. Burr, J., A Contribution to the Dynamics of a Self-Propelled Vehicle in an Infinite Duct, Rensselaer Polytechnic Institute, TR AE 6101, 1961.

4. Foa, J.V., "Land Transport at Air Transport Speeds with Speed and Economy," National Defense Transportations Journal, July-August 1962.

5. Foa, J.V., Elements of Flight Propulsion, John Wiley and Sons, 1960.

FIGURE A-1

SCHEMATIC REPRESENTATION OF MODEL

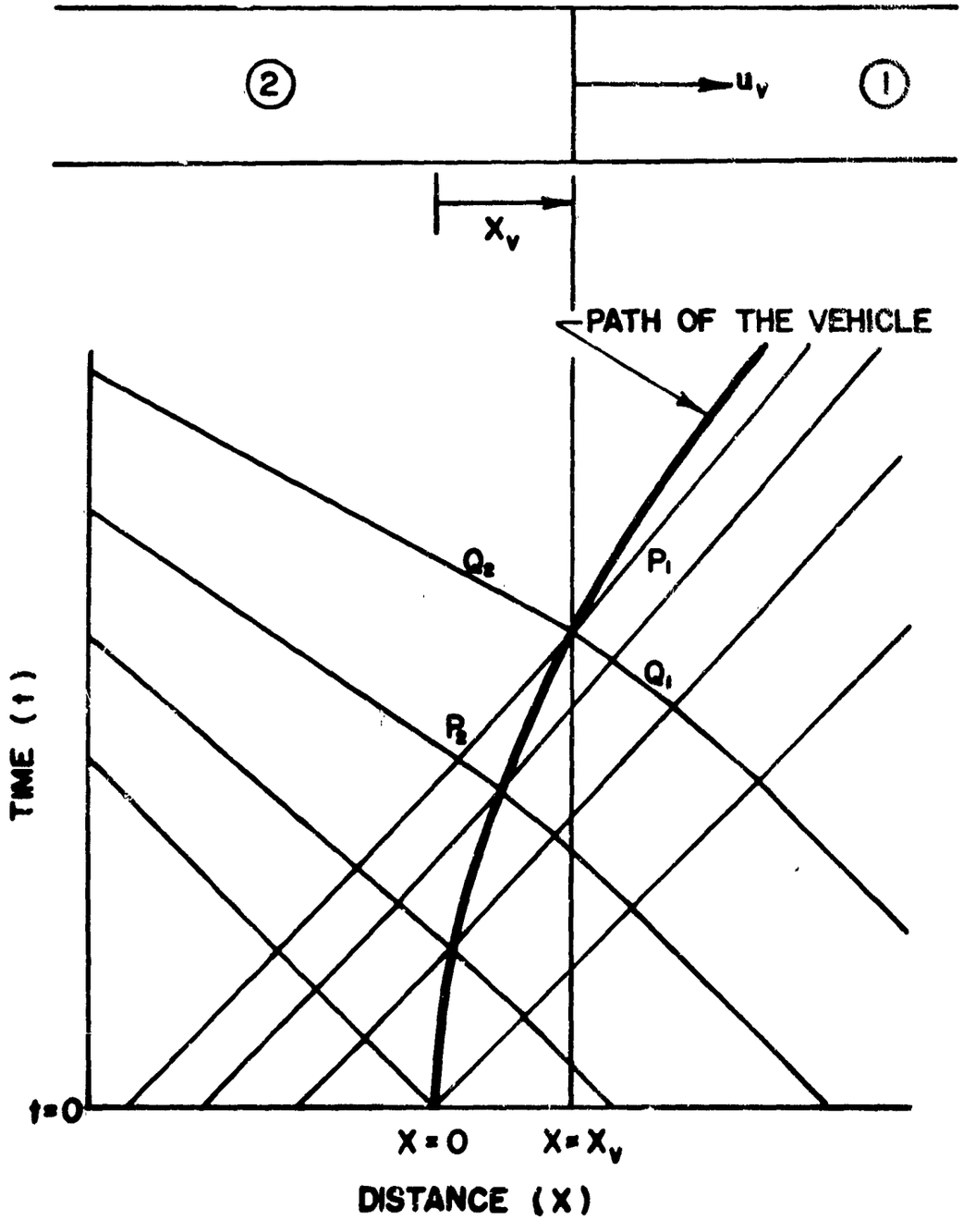

FIGURE A-2

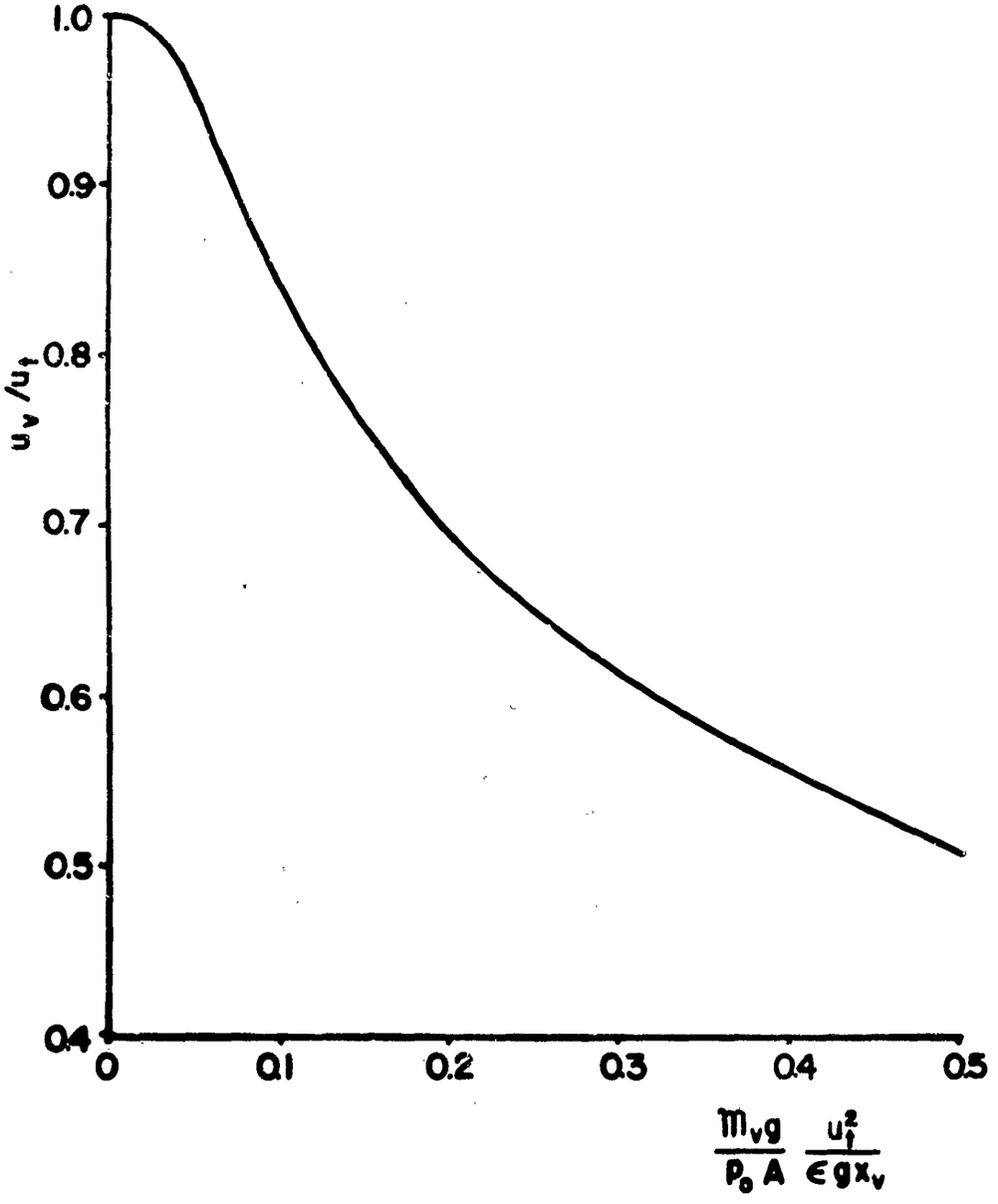
1.0
0.9
0.8
0.7
0.6
0.5
0.4
u_v / u_t
0
0.1
0.2
0.3
0.4
0.5
$\frac{\dot{m}_v g}{P_0 A} \frac{u_t^2}{\epsilon g x_v}$

VEHICLE
AS A FUNCTI

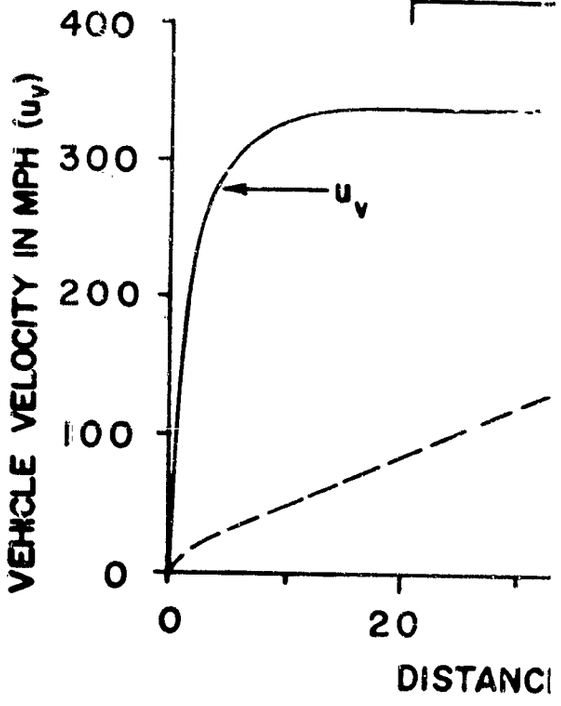

JRE A-3

OCITY AND TIME
: THE DISTANCE TRAVELED

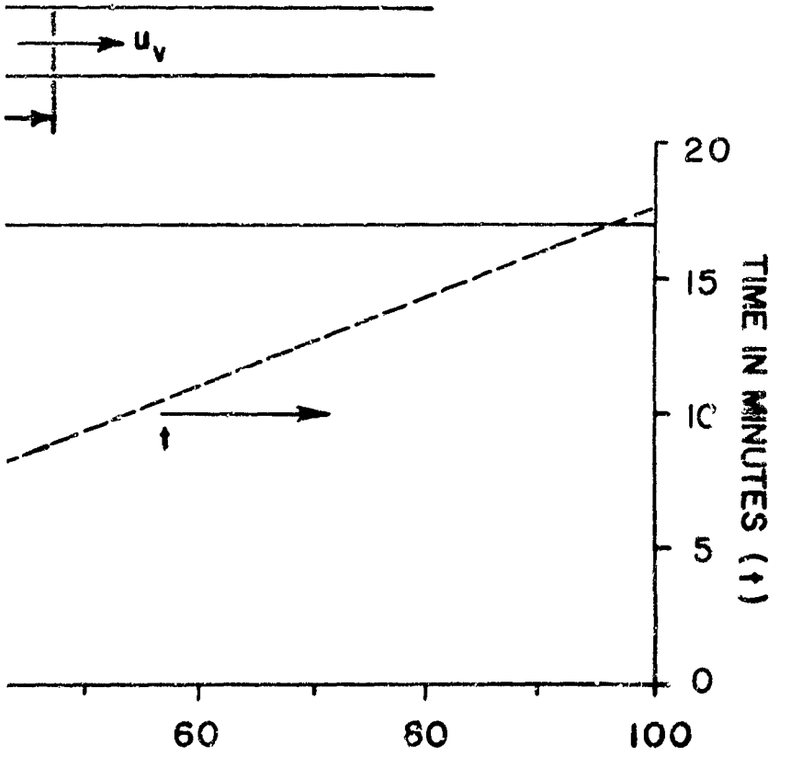

VELED IN MILES (X_v)

u_t = 500 FT/SEC = 340.9 MPH
α = 0.1
p_0 = 2100 PSF
a = 177 FT^2 (D = 15 FT)
L = 100 MILES
gm_v = 100,000 LBS

MAXIMUM AIR VE

②

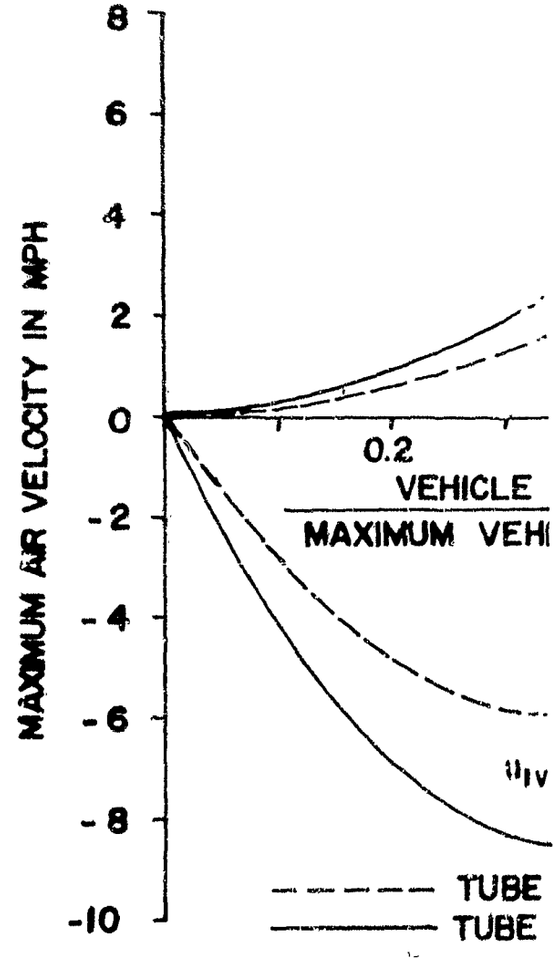

RE A-4

INDUCED BY THE VEHICLE

$\rightarrow u_v$ ①

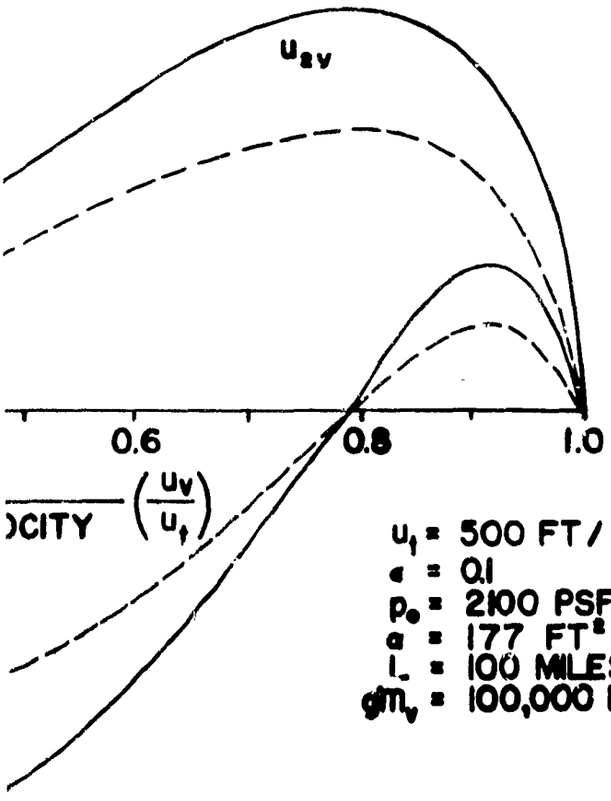

OCITY $\left(\frac{u_v}{u_1}\right)$

u_1 = 500 FT / SEC = 340.9 MPH
α = 0.1
p_o = 2100 PSF
a = 177 FT^2 (D = 15 FT)
l_- = 100 MILES
gm_v = 100,000 LBS.

AT BOTH ENDS (STARTS AT ONE END)
BEHIND & OPEN AHEAD OF THE VEHICLE
(STARTS AT CLOSED END)

MAXIMUM AIR VE

(2

MA

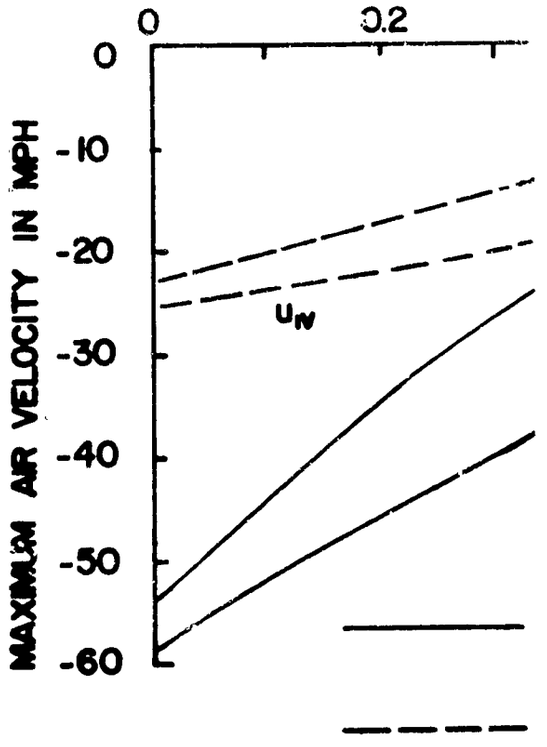

GURE A-5

INDUCED BY THE VEHICLE

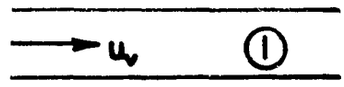

VELOCITY / HICLE VELOCITY $\left(\frac{u_v}{u_1}\right)$

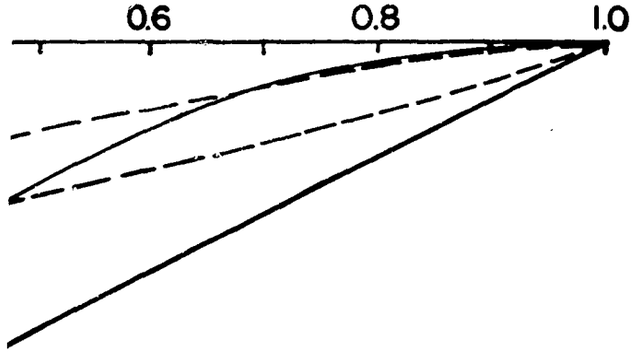

$\epsilon = 0.1$
$T_0 = 540°R$
$u_1 = 500$ FT/SEC = 340.9 MPH

TUBE AHEAD & OPEN FINITE TUBE BEHIND
ICLE (STARTS AT OPEN END)

WITHIN AN INFINITE TUBE

AIR VEL

(T

②

M

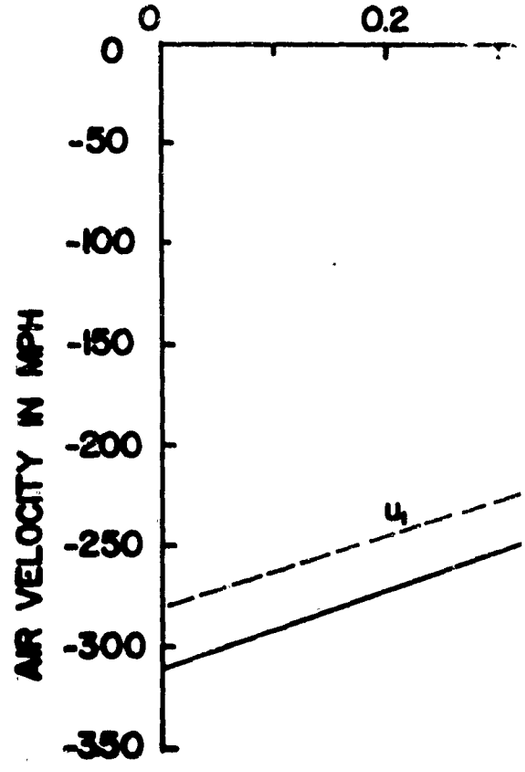

FIGURE A-6

INDUCED BY THE VEHICLE

N AT BOTH ENDS)

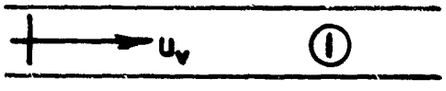

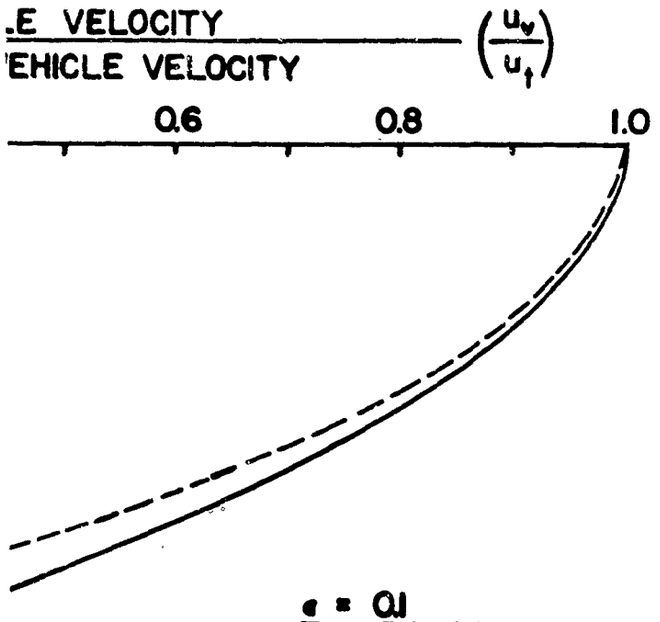

ϵ = 0.1
T_0 = 540°R
u_1 = 500 FT/SEC = 340.9 MPH

SECTION B

THE EFFECT OF SIMULATED HIGH FORWARD SPEED ON A TWO-DIMENSIONAL GROUND EFFECT SUPPORT

by

Anthony A. West

SUMMARY

Preliminary tests have been conducted to investigate the feasibility of using ground effect supports to provide suspension and propulsion of a vehicle at high forward speeds. The effects of simulated high forward speeds on the lift and drag of a two-dimensional ground effect support are correlated through a forward-speed parameter which is derived in this report.

TABLE OF CONTENTS

SYMBOLS

A augmentation ratio for GES configuration = $\frac{L_H}{M_T \ell}$

c chord length of model = 7.5 in.

C_D drag coefficient = $\frac{D}{S q_\infty}$ $C_{D_o} = 0.07$

C_L lift coefficient = $\frac{L}{q_\infty S}$

C_L' aerodynamic lift coefficient = $\frac{L'}{q_\infty S}$

C_R recovery factor = $\frac{D_o - D}{M_T \ell}$

C_μ jet momentum coefficient $\left[\frac{M_T \ell}{q_\infty S} \text{ for GES}\right]\left[\frac{M_o \ell}{q_\infty S} \text{ for JFW}\right]$

D drag

h height of model from groundboard

ℓ nozzle length - length of exposed model span = 9.75 in.

L total lift

L_H lift at zero forward speed for GES

L' aerodynamic lift = L - L_H for GES

M momentum flux/unit length of nozzle = $\frac{\dot{m} V_j}{\ell}$

M_T total momentum flux/unit length of nozzle = $M_F + M_R$ for GES

$\dot{m}$ total nozzle mass flow rate measured from venturi meter

p pressure

q dynamic head = $\frac{1}{2}\rho V^2$

S exposed model plan area = ℓc = 0.508 ft^2

V velocity

V_j jet velocity calculated assuming the air in the chambers is expanded isoenergetically and isentropically down to the free-stream static pressure

V_∞ wind tunnel free stream velocity = simulated forward speed of model

θ jet angle (see Fig. 4)

ρ air mass density

ϕ forward speed parameter - defined in Appendix

Subscripts

c critical condition at which jets are swept under model (see Figs. 1(c) and 1(f).)

F front jet

0 no air supplied to nozzles

R rear jet

∞ wind tunnel free-stream condition

Superscript

o stagnation condition

I. INTRODUCTION

In a report on a proposed high-speed self-propelled air-breathing vehicle in a tube, Foa (Ref. 3) has suggested that ground effect supports could be used for suspension of the vehicle. The tube wall would provide the kind of transverse guidance and control that is absent in ground-effect supports operating over open terrain or water surfaces. Furthermore, the rigidity of the tube wall should permit much higher velocities in the air curtains than are permissible over soft ground or water, and should therefore make possible the utilization of ground-effect support at very high forward speeds. At the present time, however, there is little information available on the effects of high forward speeds on the air cushion of a ground effect support and the present work was undertaken to provide a fundamental understanding of the problem. For this purpose it was believed that a two-dimensional rather than a three-dimensional study would be more fruitful. The specific aims of this preliminary investigation were to determine:

(a) the feasibility of ground effect support at high subsonic forward speeds.

(b) the possibility of utilizing the momentum of the ground effect curtain in the generation of thrust.

The work on this project has been carried out under the auspices of the Army Research Office (Durham) Grant No. DA-ORD-31-124-61-G88.

II. DESCRIPTION OF APPARATUS

Wind Tunnel and Balance

The dynamic experiments on the model were carried out in the RPI 4x6 ft. subsonic wind tunnel, which is of the closed-throat return type. The wind tunnel control panel and test section are shown in Figs. B-2 and B-3 respectively. The maximum airspeed in the test section was 200 fps. The aerodynamic forces on the model were measured on a six-component mechanical balance.

Model

The model is two-dimensional, and its section consists of a flat undersurface and a circular arc top surface of 11.5 in. radius, as shown in Fig. B-4. The air is supplied to the front and rear chambers independently, and is distributed within each chamber by means of the distribution tubes which contain a 0.03 in. longitudinal slit. Two pressure taps in each chamber are located in the base plate to measure the stagnation pressure in the chamber. A small block is welded to the base plate just "downstream" of these taps to ensure that the flow is brought to rest at the tap. The leading-edge and trailing-edge nozzle gaps are adjustable but were maintained at 0.05 ins. for the present series of tests. The dimensions of the model are given in Figs. B-4 and B-5.

The model was mounted in the test section on two main struts as shown in Fig. B-6. The angle of attack was 0^{o} for all tests. The model tips were recessed into the sideboards which were carefully cut to prevent the model fouling the boards. The sideboards were attached to the tunnel floor by slotted angle-iron and the groundboard was mounted between the sideboards by four brackets as shown in Fig. B-7. The clearance between the model and the groundboard could be adjusted from 0-18 in. The dimensions of the sideboards and groundboards used during the tests are shown in Fig.B-8.

Jet Air Supply

High pressure air was supplied from a reservoir to a manual regulator which in turn supplied the air to the front and rear distribution tubes by means of the air supply pipes as shown in Fig. B-9. A gate-valve was fitted in each of these air supply pipes so that by suitable adjustment of these gate valves and the manual regulator any desired mass flow to the front and rear chambers could be obtained independently. A venturi meter was fitted to each supply pipe to measure mass flow supplied to the chambers.

III. EXPERIMENTAL PROCEDURE

Measurement of Momentum Flux and Jet Angle Along the Nozzles

In consideration of the possibility of flow changes due to structural deformation under pressure, the jet angle and the

distribution of the momentum flux along the leading-edge and trailing-edge nozzles were measured for various chamber pressures using the apparatus shown in Fig. B-10. The jet angle was 82^{o} for both nozzles and was found to be invariant with chamber pressure. The maximum variation of jet angle along the nozzle was $\pm 2^{o}$. It was found, for both nozzles, that the momentum flux at the midspan position was a maximum of 5% greater than the momentum flux at the outer ends. It was assumed that this variation was sufficiently small to be neglected for the purposes of this series of tests.

Determination of Chamber Pressure

The rig shown in Fig. B-10 was used with the pitot tube at the jet exits to determine the variation of the stagnation pressure along the span for a series of different chamber pressures. These readings were compared with those obtained from the interr pressure taps in the baseplate. The readings agreed within 4% and a calibration curve was constructed to convert the chamber pressure readings into the average value of the stagnation pressure along the nozzle.

Wind Tunnel Tests

After the preliminary experiments described above, the mode was mounted in the wind tunnel as shown in Fig. B-7. The lift a drag on the model were measured at 0^{o} incidence for different ai

speeds in the test section, chamber pressures, heights above ground, and groundboards. During each run the air speed in the test section was changed from 0 to 200 fps and the mass flow to the chambers was kept constant by adjustment of the regulator. An equal mass flow of air was supplied to the front and rear nozzles in those tests in which the model was tested as a ground effect support. The test conditions are summarized in Table B-I.

IV. RESULTS AND DISCUSSION

Fig. B-11 shows that there is close agreement, both in trend and magnitude, between the experimental results and those predicted by the simple momentum theory of Reference 1. The graph also shows that an error of a few degrees in the measurement of the jet angle can result in appreciable changes in the value of the augmentation ratio and it is believed that this is the major cause of the discrepancy between the theoretical and experimental results.

Fig. B-12 shows how the total lift acting on the model increases with forward speed in the ground effect support and jet flap wing configurations.

Fig. B-13 reveals that the aerodynamic lift coefficient increases rapidly with increasing forward speed in the subcritical regime, reaches a maximum around the critical forward speed, and thereafter decreases slowly in the supercritical regime. This

graph confirms the fundamental correctness of the chosen forward speed parameter. It will be noticed that for Run 1 the maximum value of C_L' is attained at a value of the forward speed parameter greater than 1.0. The reason for this is that the forward speed parameter is based on the free-stream velocity but the model is in the boundary layer of the groundboard. This is borne out by a comparison of Runs 1 and 2. The jet velocity is the same for both runs but in Run 2 the model is further from the groundboard.

From Fig. B-14 it can again be seen that, with the exception of Run 6, the maximum value of the aerodynamic lift coefficient is attained close to a value of 1.0 of the forward speed parameter. The effect of the broundboard boundary layer is very pronouced in Run 6, which was performed using a very low jet velocity. With this low jet velocity, the wind tunnel airspeed at the critical condition is relatively small and thus the boundary layer on the groundboard is fairly thick. This can be seen by a comparison of Runs 2 and 8 in which a higher jet velocity was used; both runs were performed with the model at the same distance above the ground board.

Fig. B-15 shows the effect on the aerodynamic lift coefficient of changing the groundboard size. The jet velocity and the distance of the model from the groundboard was the same for both runs. The use of the larger groundboard with its attendant thicker

boundary layer, has two consequences -- firstly, the maximum value of C_L' is attained at a higher value of the forward speed parameter for the reasons given above. Secondly, the magnitude of the maximum value of C_L' is less because the total lift is less due to the model being in a lower velocity boundary layer. For the above reasons the results obtained using the large and small groundboards are presented separately.

Fig. B-16 confirms that for the jet flap wing configuration out of ground effect there is a linear relationship between the lift coefficient and the radical of the jet momentum coefficient -- a result already reported in Reference 2.

For the ground effect support configuration in the supercritical regime, Fig. B-17 reveals a similarly unique relationship between the aerodynamic lift coefficient and the radical of the jet momentum coefficient, irrespective of the actual magnitude of the jet velocity. This would suggest that the aerodynamic lift experienced by the model in the supercritical regime is derived in the same way as the lift on a jet flap wing out of ground effect i.e. mainly from the low pressure region on the top surface of the model. The airflow in these two cases is shown in Figs. B-1(d) and B-1(g) for the ground effect support and for the jet flap wing, respectively. The above is only a tentative suggestion and would need to be checked by a survey of the pressure distribution around the model at various forward speeds.

Fig. B-18 presents typical results for the model in the ground effect support configuration. It will be noticed that, although the total drag is less than the profile drag, the net force is still a drag. In none of the tests carried out was a net thrust experienced by the model. The reason for this is t high value of the profile drag resulting from the relatively thick section and blunt trailing edge of the model.

Fig. B-19 reveals a rapid increase of the thrust recovery coefficient with forward speed in the subcritical regime. Thi is probably mainly due to the fact that as the forward speed i increased more of the jet curtain is swept under the model rat than escaping over the top surface of the model. As can be se from a comparison of Figs. B-1(b) and B-1(d) the possibility o thrust recovery is inherently greater for the smoother, less d sipative airflow. It can be seen from this graph that C_R is also a function of the ratio of forward speed to jet velocity. It will be noted that values of C_R greater than 1.0 are obtai in the supercritical regime. It is suggested that this is due the airflow over the top of the model being entrained by the r jet as shown in Fig. B-1(d). The increase in C_R with forward speed in the supercritical regime is due to the fact that the losses associated with the mixing of two airstreams decrease a the difference between their velocities is decreased.

Fig. B-20 exhibits more clearly the strong dependence of the thrust recovery factor on the ratio of the forward speed to the jet velocity. The scatter in the experimental data is due to the smallness of the forces being measured.

V. CONCLUDING COMMENTS

Depsite the complications arising from the interaction between the jet curtain and the groundboard boundary layer, it is believed that the following valid conclusions for a two-dimensional model may be drawn from the experimental data:

1. For a ground effect support employing a thin jet curtain, the lift at zero forward speed is satisfactorily predicted by the theory of Ref. 1.

2. For constant height and constant jet momentum flux, the lift increases with forward speed both in the ground effect support and jet flap wing configurations.

3. The forward speed parameter which is developed in the Appendix is shown to be significant.

4. In none of the test runs was there a net thrust experienced by the model. However, the feasibility of utilizing the momentum flux from an "aerodynamically clean" ground effect support as a significant contribution to thrust has been demonstrated.

5. For maximum thrust recovery the ideal operating condition is apparently obtained by operating near the critical point and arranging for the jet velocity to be equal to the forward speed of the support. This conclusion requires verification from data obtained for values of $V_\infty/V_j > 1.0$ (see Fig. B-20).

6. In the ground effect support configuration tests, the flows were essentially incompressible as the maximum value of the free-stream and jet flow Mach numbers was 0.25. However it should be realized that high forward speeds were simulated by values of V_∞/V_j up to 1.5. It is believed that the derived forward speed parameter would be significant for high subsonic speeds as compressibility effects would not change the fundamental nature of the flow.

The above remarks are only strictly applicable to two-dimensional models and to the plane of symmetry of three-dimensional models. However, there is no reason to believe that a similar approach to the problem of a three-dimensional model at high subsonic speeds would not yield qualitatively similar results.

REFERENCES

1. Crewe, P.R. and Eggington, W.J. "The Hovercraft - A New Concept in Maritime Transport" presented at the meeting of the Royal Institution of Naval Architects. Nov. 19, 1959.

2. Poisson-Quinton P. "Two-dimensional Studies of a Ground Effect Platform" presented at the "Symposium on Ground Effect Phenomena" held at Princeton University, Oct. 1959.

3. Foa, J.V. "A Fast Carrier", Department of Aeronautical Engineering and Astronautics, Rensselaer Polytechnic Institute, TR AE 6206, May 1962.

4. Foa, J.V. "Elements of Flight Propulsion", John Wiley and Sons, New York, 1960.

TABLE B-I

SUMMARY OF TEST CONDITIONS

Run No.	Groundboard	h (ins)	Chamber Pressure Gauge (lb/ft^2) Front	Rear	Remarks
1	Small	0.38	56	56	ground effect sup
2	"	0.69	56	56	"
3	"	1.00	47	47	"
4	"	2.00	120	120	"
5	Large	0.69	56	56	"
6	"	1.63	17	17	"
7	"	1.63	52	52	"
8	"	1.63	78	78	"
9	"	2.50	120	120	"
10	"	4.60	0	197	jet flap Wing
11	"	8.50	0	78	"
12	"	12.50	0	310	"
13	"	12.50	0	78	"
14	"	12.50	0	318	"
15	"	16.60	0	78	"
16	"	16.60	0	470	"
17	"	4.60	0	0	determination of C_D
18	"	16.60	0	0	"

APPENDIX

The nature of the airflow around the model is characterized by a "forward-speed parameter" Φ defined as the ratio

$$\Phi = \frac{\text{height of model above ground}}{\text{critical height of model above ground}} = \frac{h}{h_c}$$

It is assumed that at the critical forward speed the pressure acting on the upstream side of the front jet curtain is the freestream stagnation pressure p^o_∞ . It is further assumed that the free stream static pressure p_∞ acts on the downstream side of the rear jet curtain.

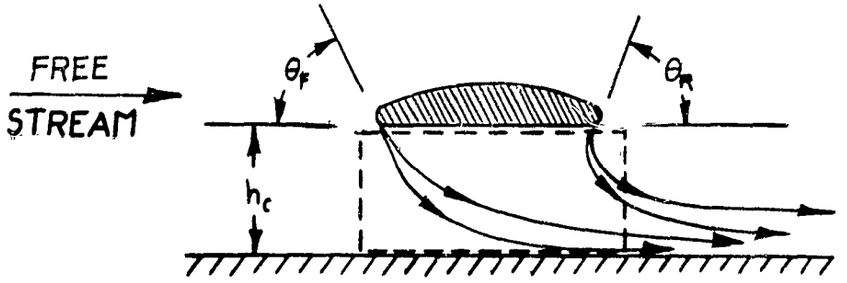

Applying the momentum theorem to the control volume shown and assuming inviscid flow:

$$p^o_\infty h_c = M_F(1-\cos\theta_F) + M_R(1+\cos\theta_R) + p_\infty h_c$$

$$\therefore \quad h_c = \frac{M_F(1-\cos\theta_F) + M_R(1+\cos\theta_R)}{p^o_\infty - p_\infty}$$

The forward speed parameter is then

$$\Phi = \frac{h\,(P_\infty^\circ - P_\infty)}{M_F(1-\cos\theta_F) + M_R(1+\cos\theta_R)}$$

There are two special cases to be considered:

(1) <u>The Ground Effect Support Configuration</u>

In this case the momentum flux issuing from the front and rear jets is the same i.e. $M_F = M_R$. The front and rear jet angles are also the same $\theta_F = \theta_R$

$$\therefore \quad \Phi = \frac{h(P_\infty^\circ - P_\infty)}{M_F + M_R} = (P_\infty^\circ - P_\infty)\frac{h}{M_T}$$

(2) <u>The Jet Flap Wing Configuration</u>

In this case there is no front jet i.e. $M_F = 0$.

$$\therefore \quad \Phi = \frac{h(P_\infty^\circ - P_\infty)}{M_R(1+\cos\theta_R)}$$

LIST OF ILLUSTRATIONS

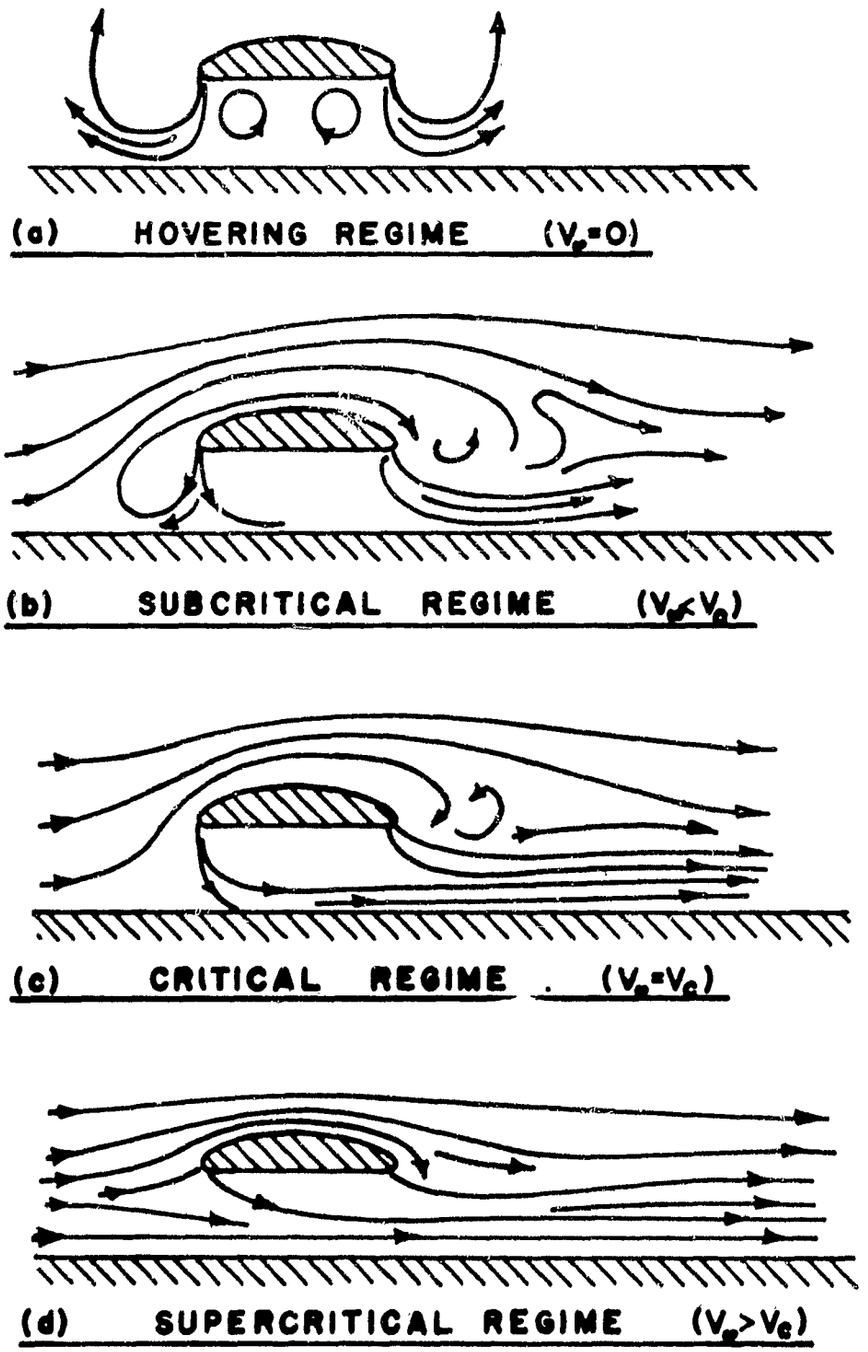

FIG. B-1 THE EFFECT OF FORWARD SPEED ON THE AIRFLOW AROUND A TWO-DIMENSIONAL SUPPORT; (a) - (d) GROUND EFFECT SUPPORT

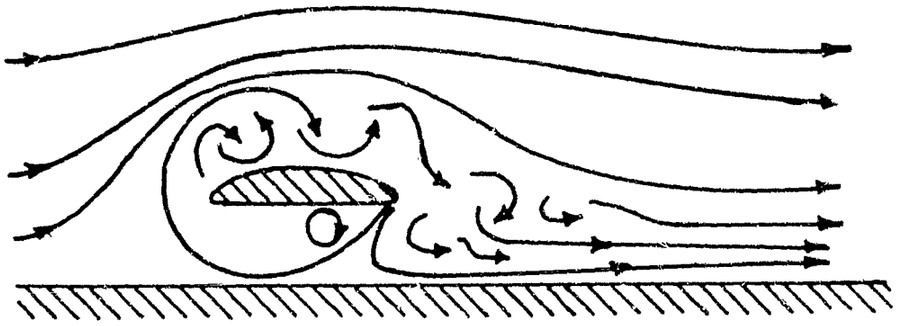

(e) IN GROUND EFFECT ($V_\infty < V_c$)

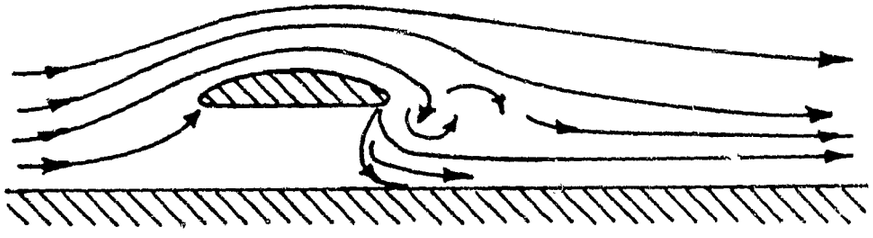

(f) AT CRITICAL SPEED ($V_\infty = V_c$)

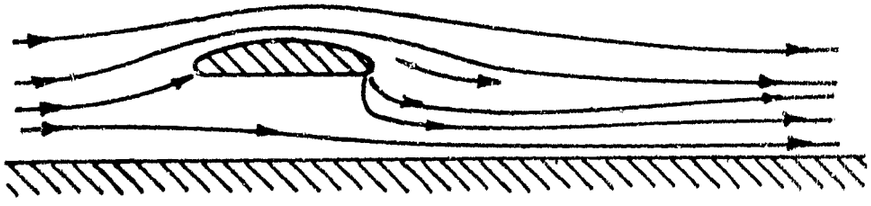

(g) OUT OF GROUND EFFECT ($V_\infty > V_c$)

FIG. B-1 Cont'd. THE EFFECT OF FORWARD SPEED ON THE AIRFLOW AROUND A TWO-DIMENSIONAL SUPPORT; (e) - (g) JET FLAP WING

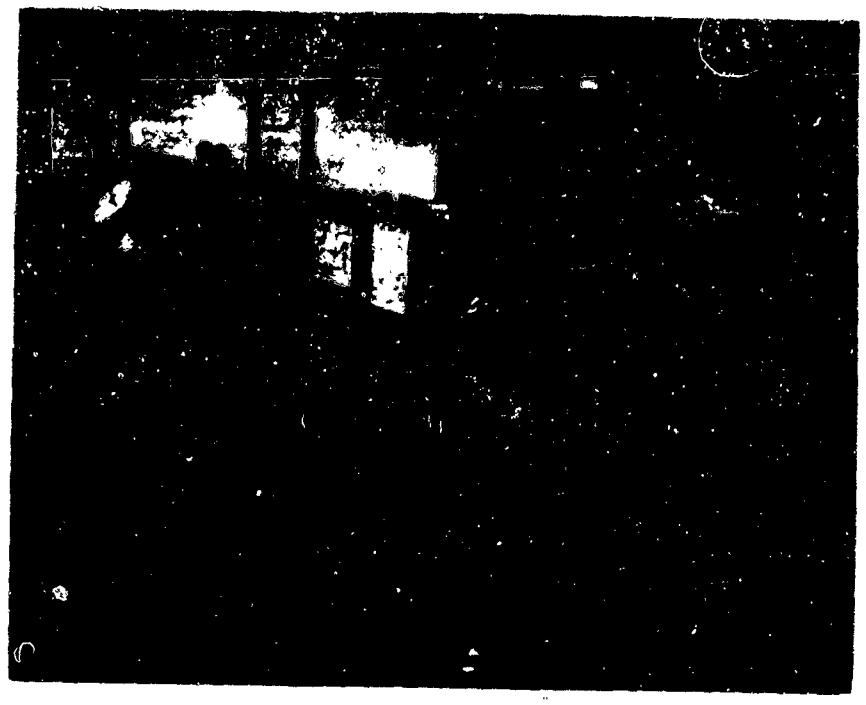

FIG. B-2 WIND TUNNEL CONTROL PANEL

FIG. B-3 WIND TUNNEL TEST SECTION

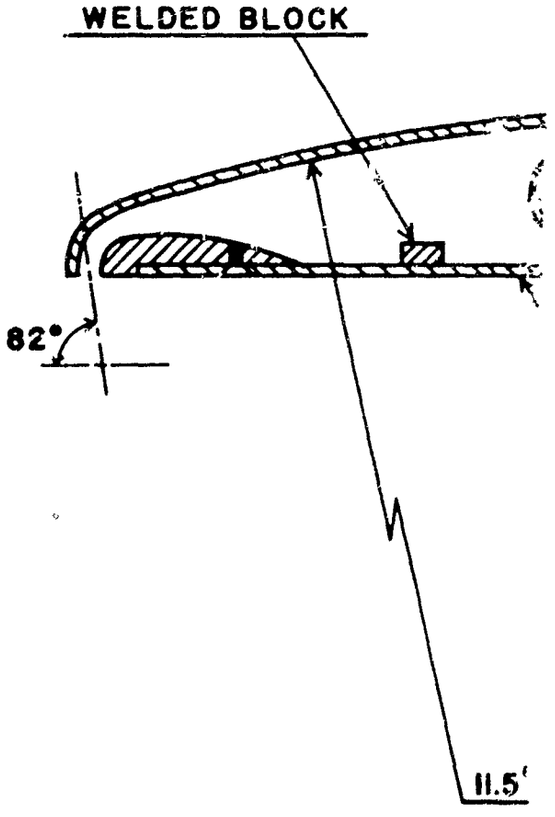

SCALE: 1:1

FIG. B

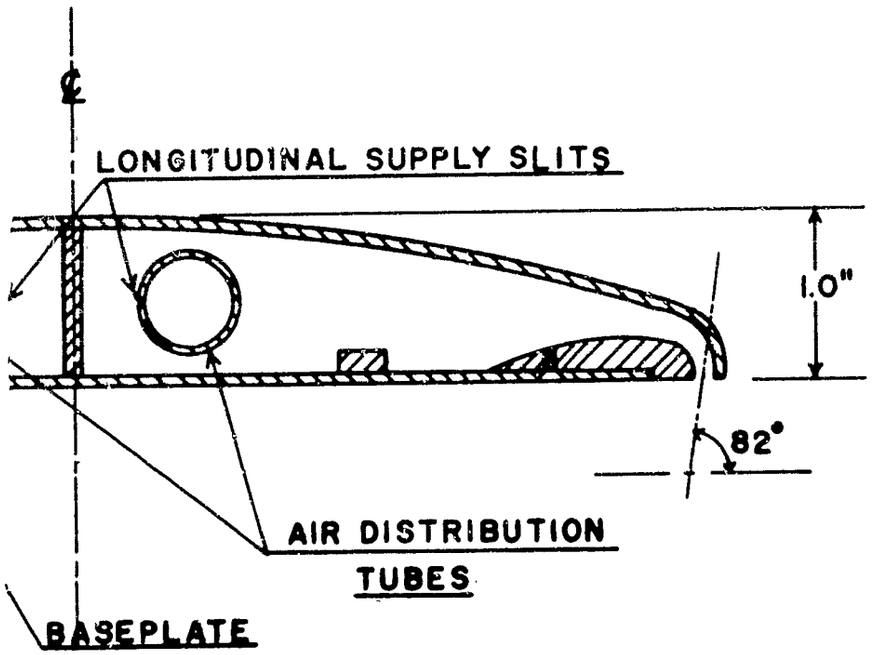

MODEL IS SYMMETRICAL ABOUT ℄

SECTION THROUGH MODEL

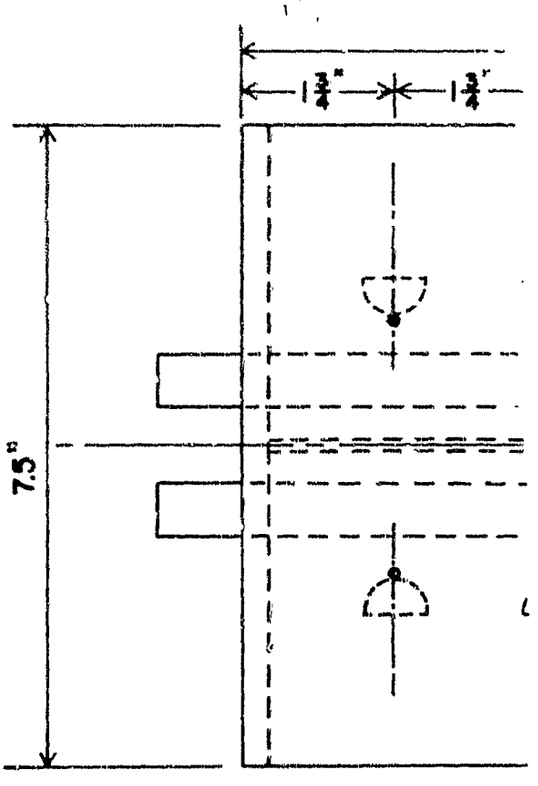

SCALE: ½ FULL SIZE

FIG. B-5

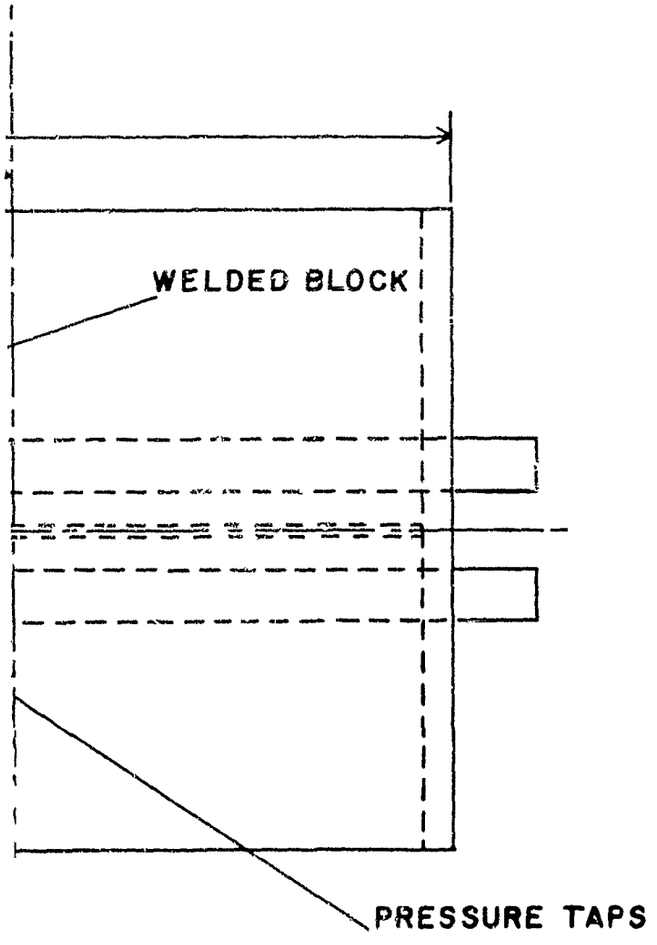

EW OF MODEL

FIG. B-6 INSTALLATION OF MODEL WITH SIDEBOARDS REMOVED

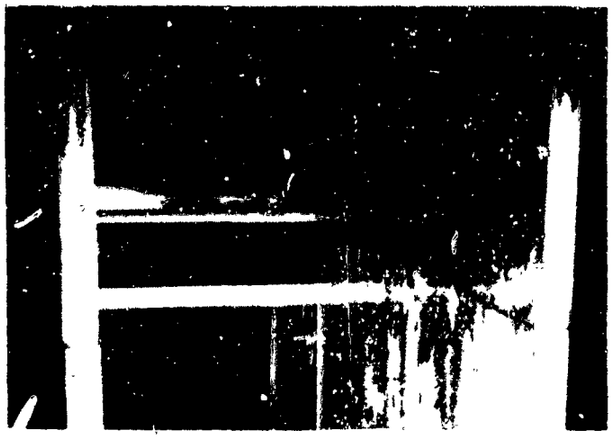

FIG. B-7 REAR VIEW OF INSTALLED MODEL WITH SMALL GROUNDBOARD

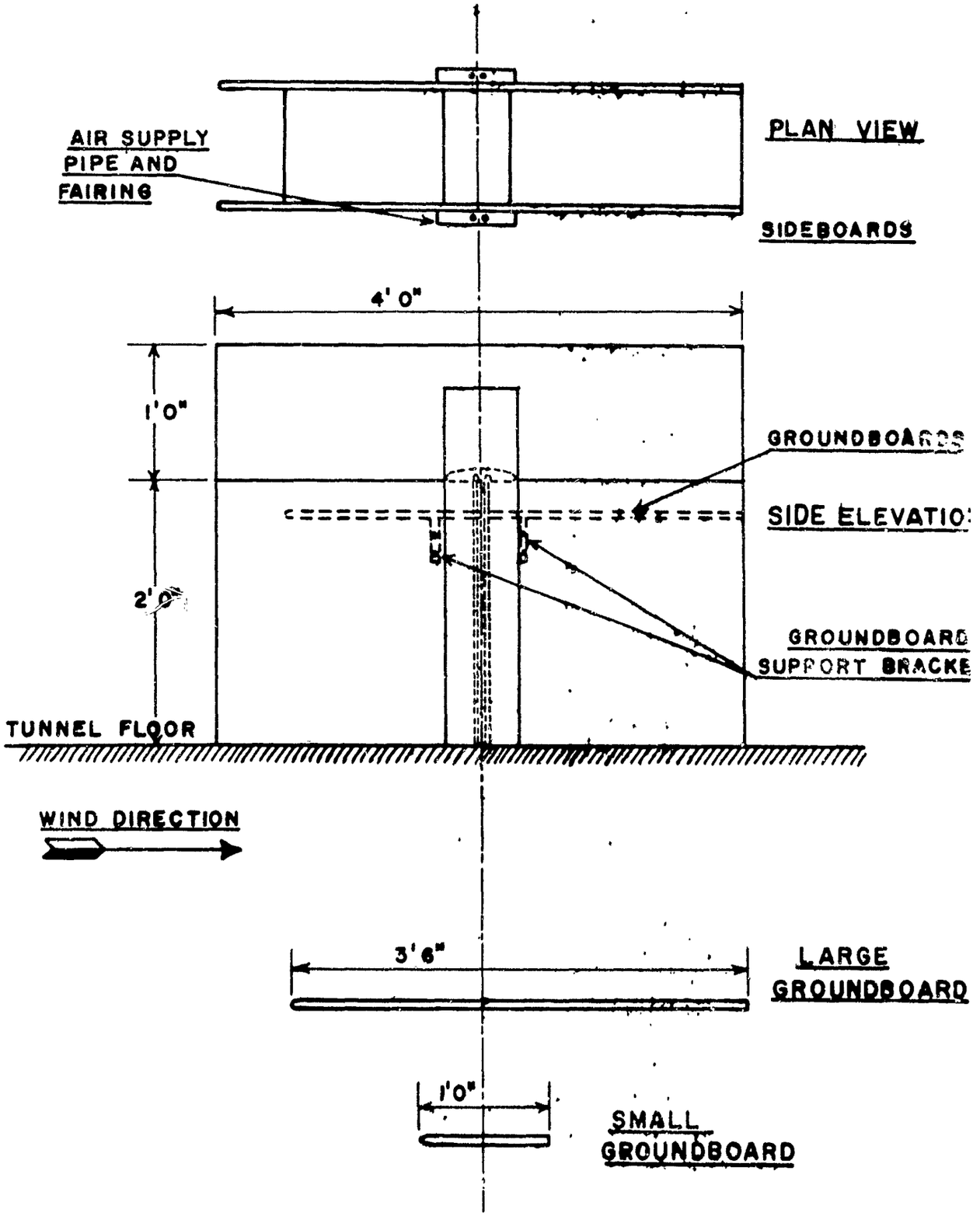

FIG. B-8 SCHEMATIC DRAWING OF MODEL INSTALLATION

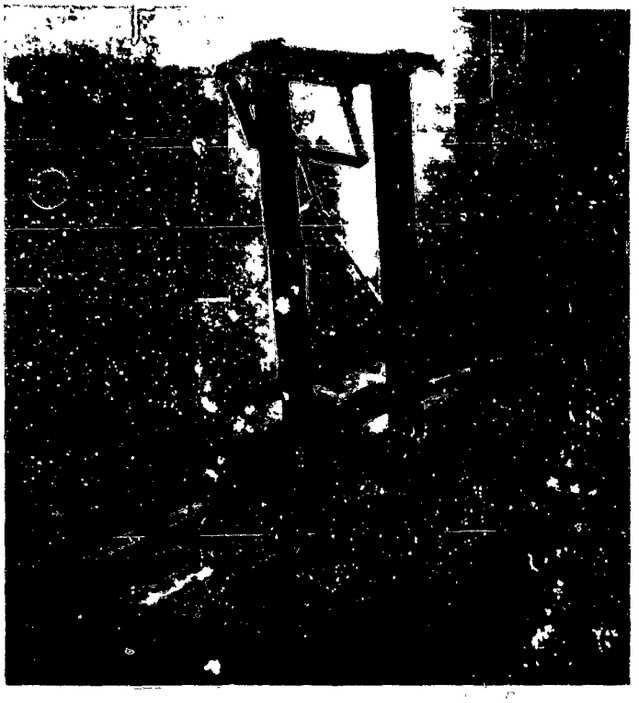

FIG. B-9 MODEL SHOWING AIR SUPPLY LINES

FIG. B-10 RIG TO MEASURE JET ANGLE AND MOMENTUM FLUX DISTRIBUTION ALONG THE NOZZLE

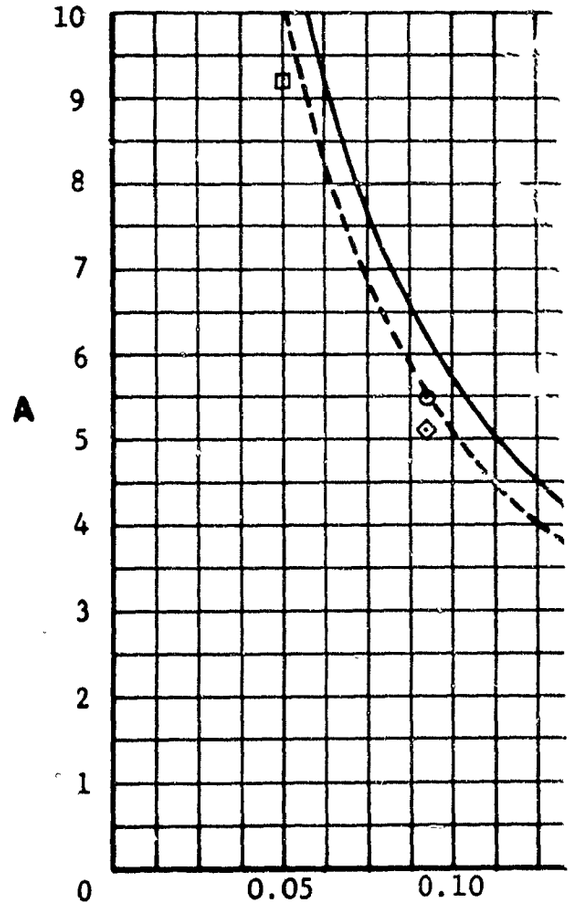

FIG. B-11 AUGMENTATION

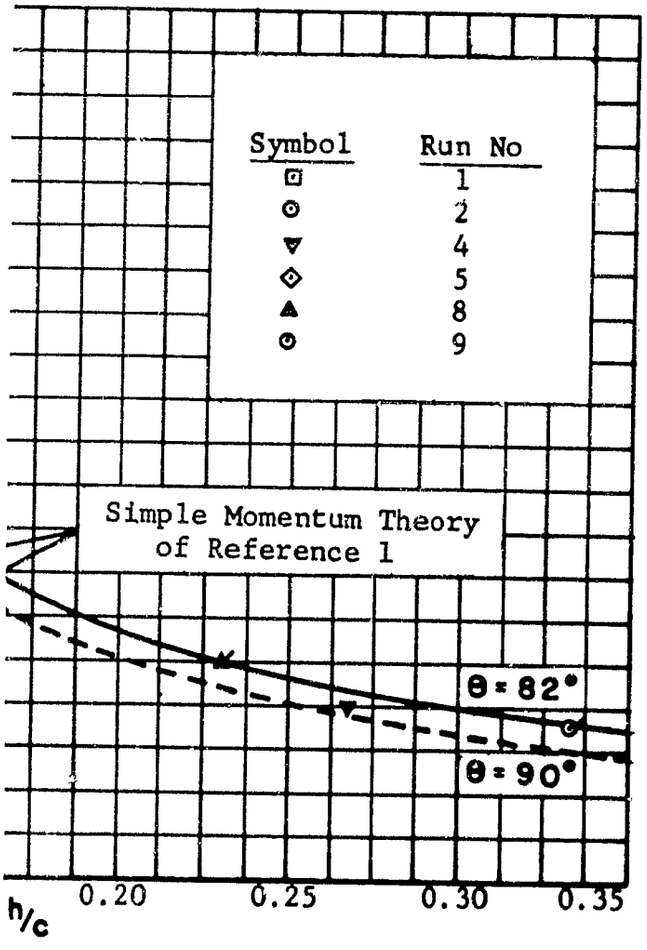

vs. HEIGHT-CHORD RATIO FOR $V_{\infty} = 0$

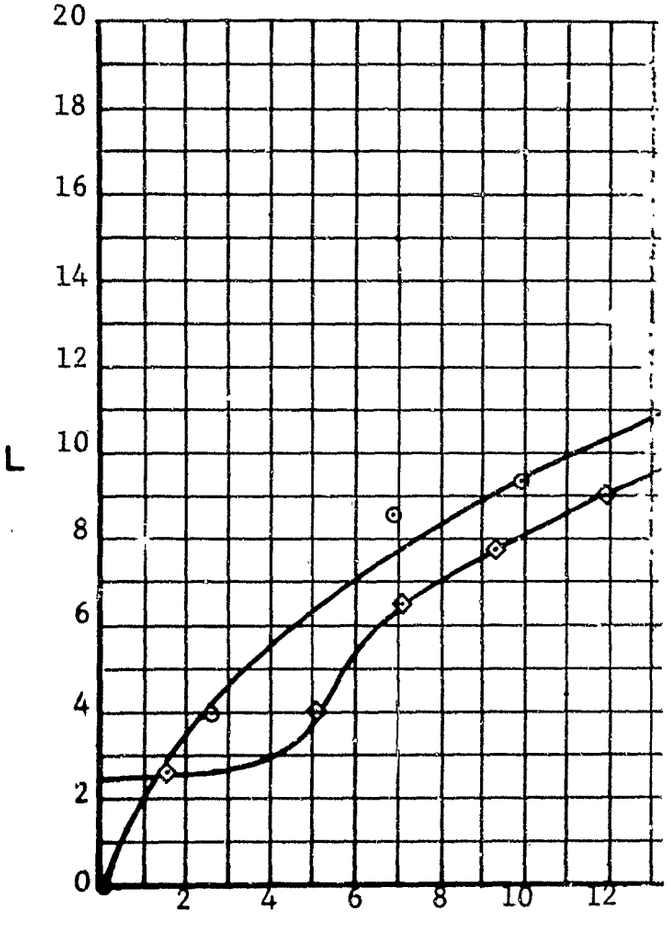

FIG. B-12 TOTAL LIFT vs. WIND TU

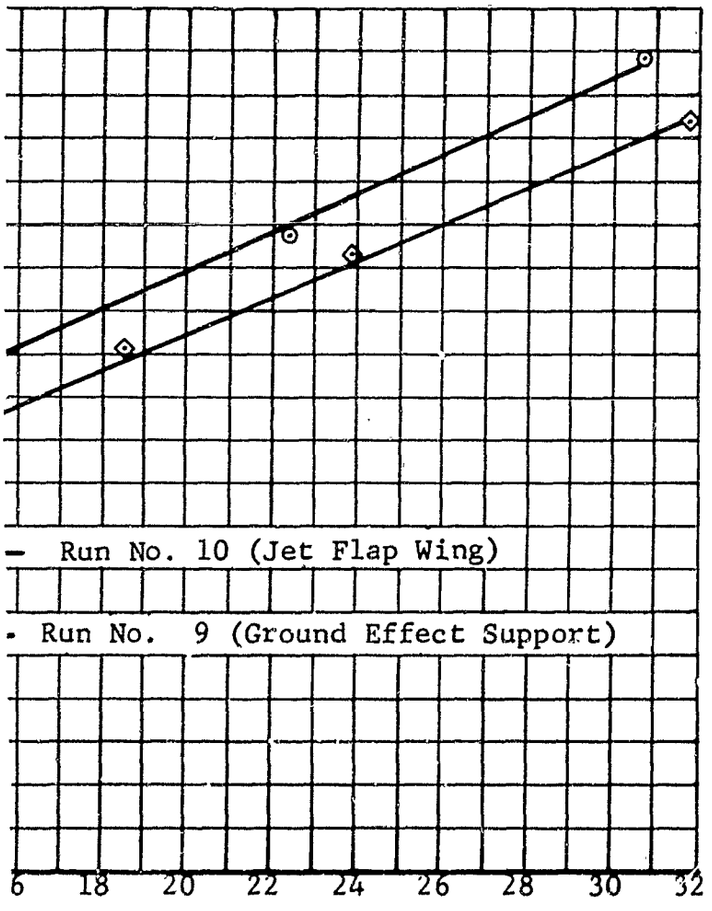

YNAMIC HEAD

q_∞ (Slugs/ft-sec^2)

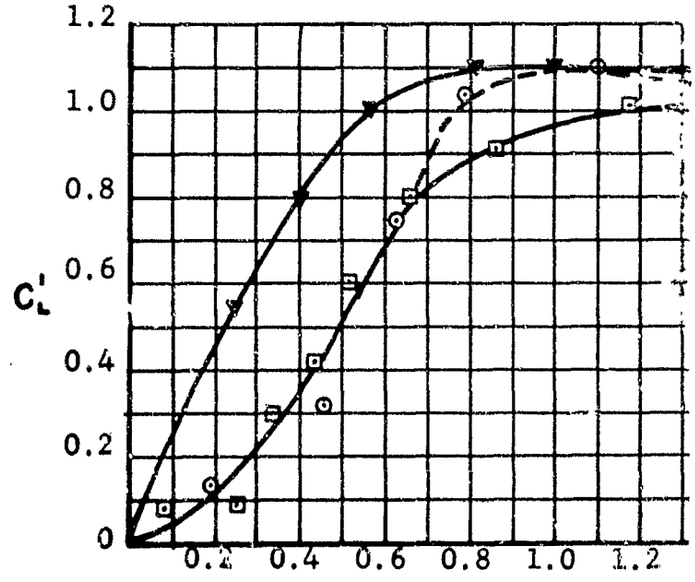

FIG. B-13 AERODYNAMIC LIFT COEFFICIEN
EFFECT SI

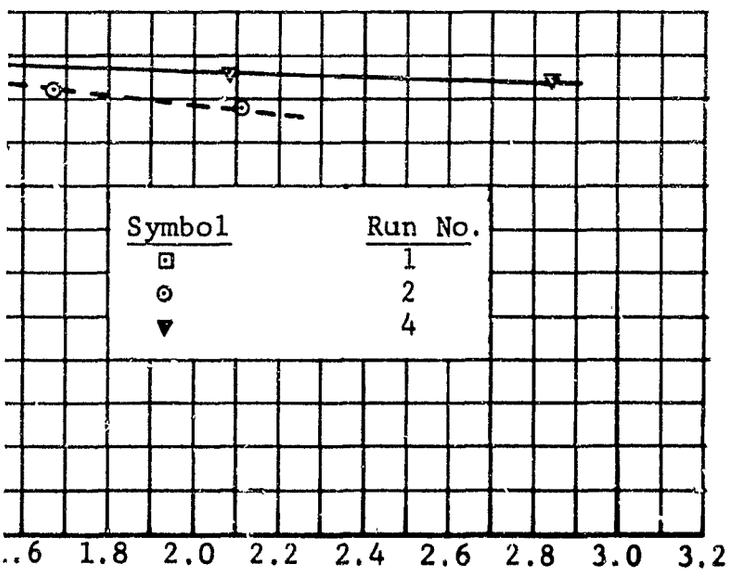

FORWARD SPEED PARAMETER FOR GROUND
SMALL GROUNDBOARD.

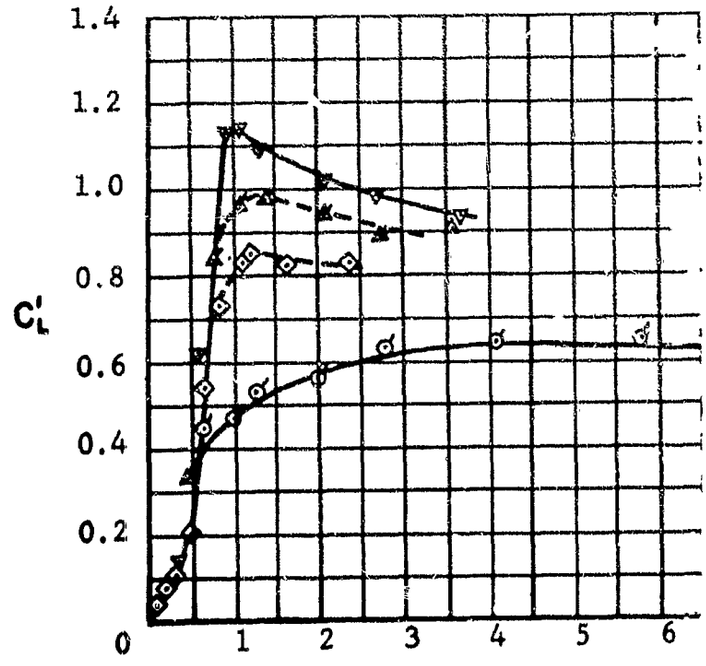

FIG. B-14 AERODYNAMIC LIFT COEFFI
FOR GROUND EFFEC

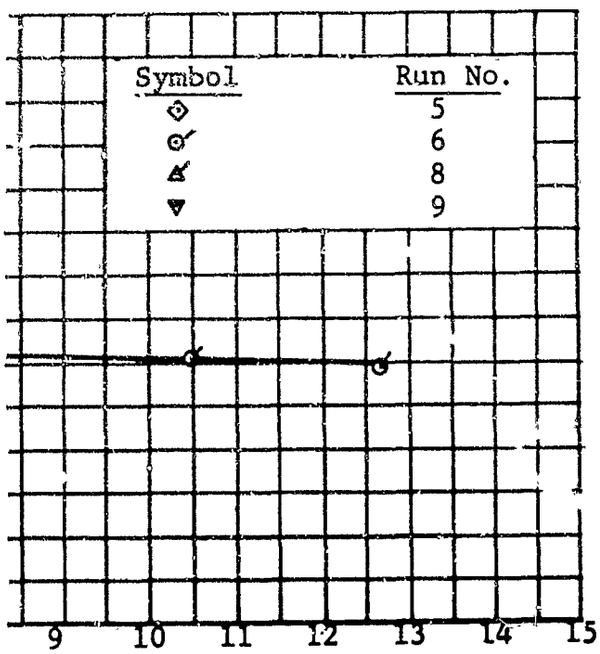

FORWARD SPEED PARAMETER
-LARGE GROUNDBOARD

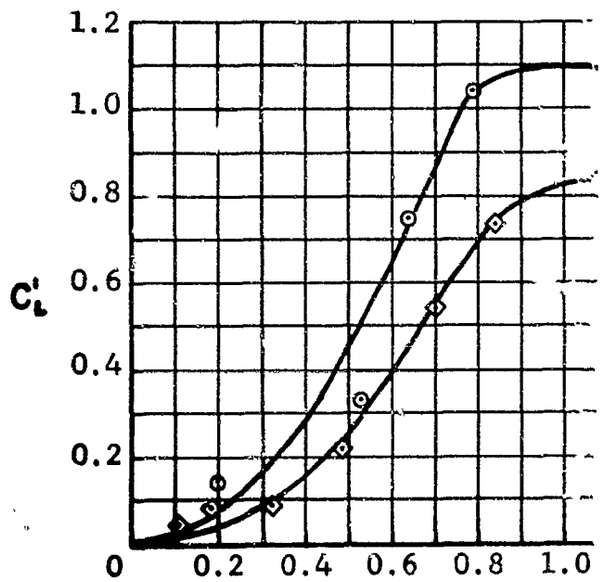

FIG. B-15 AERODYNAMIC LIFT COE
FOR (

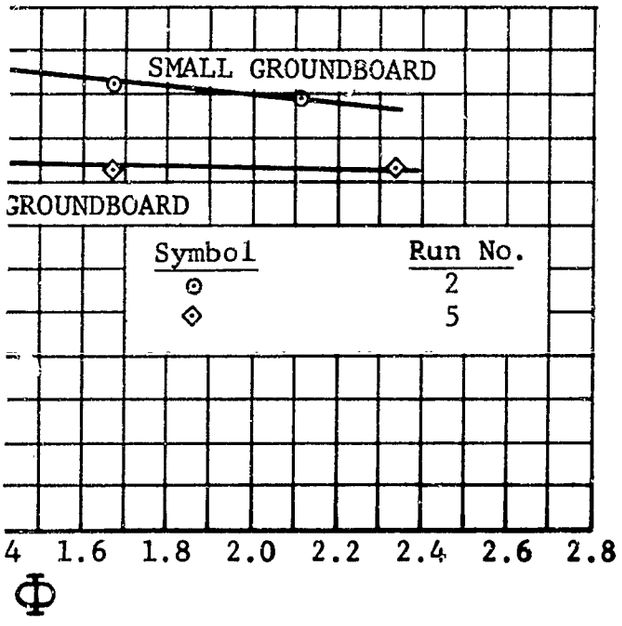

vs. FORWARD SPEED PARAMETER
FECT SUPPORT

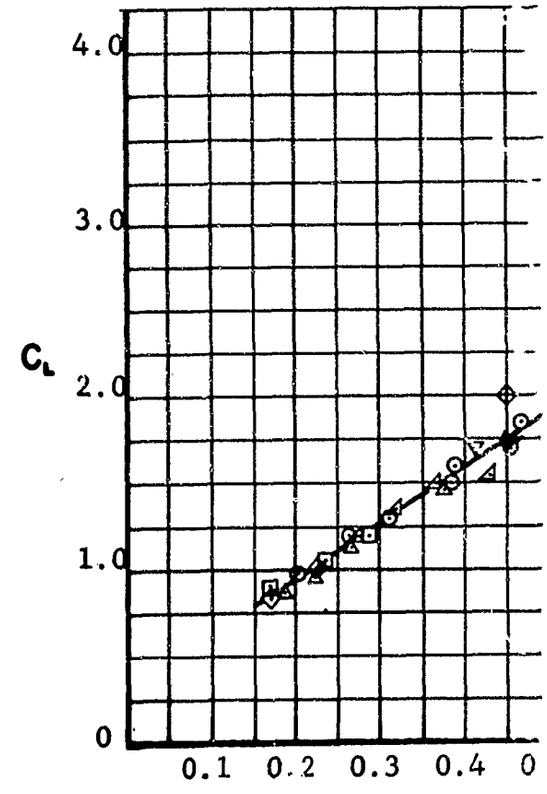

FIG. B-16 LIFT COEFFICIENT
FLAP WIN

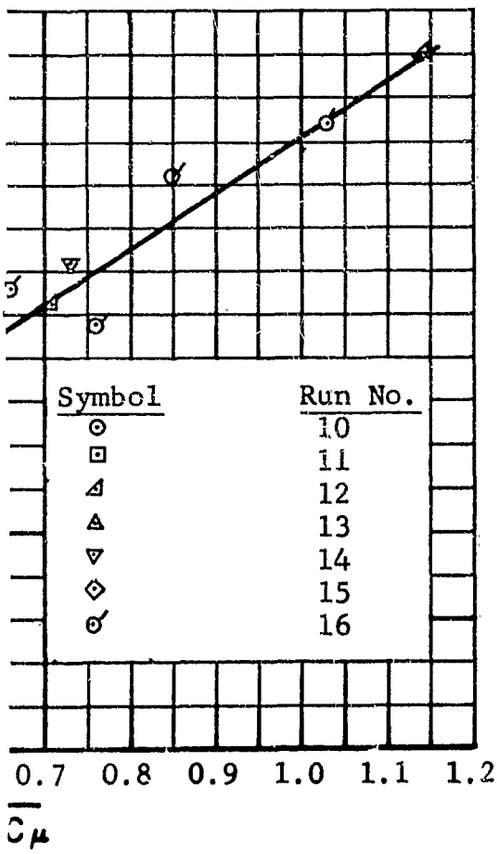

MOMENTUM COEFFICIENT FOR JET
GROUND EFFECT

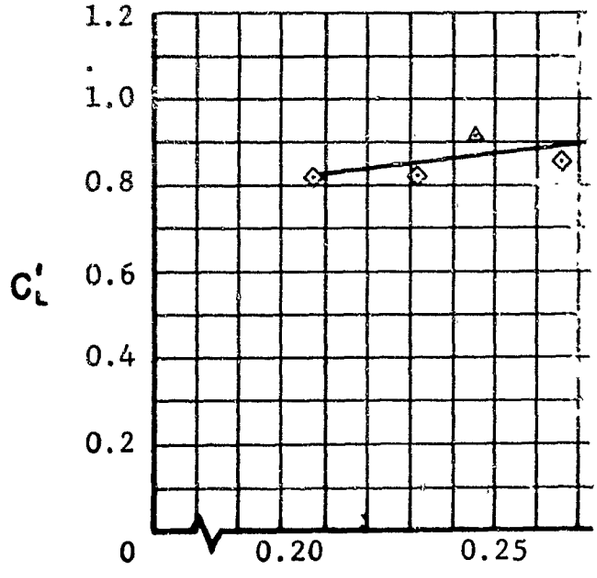

FIG. B-17 AERODYNAMIC LI
GROUND E

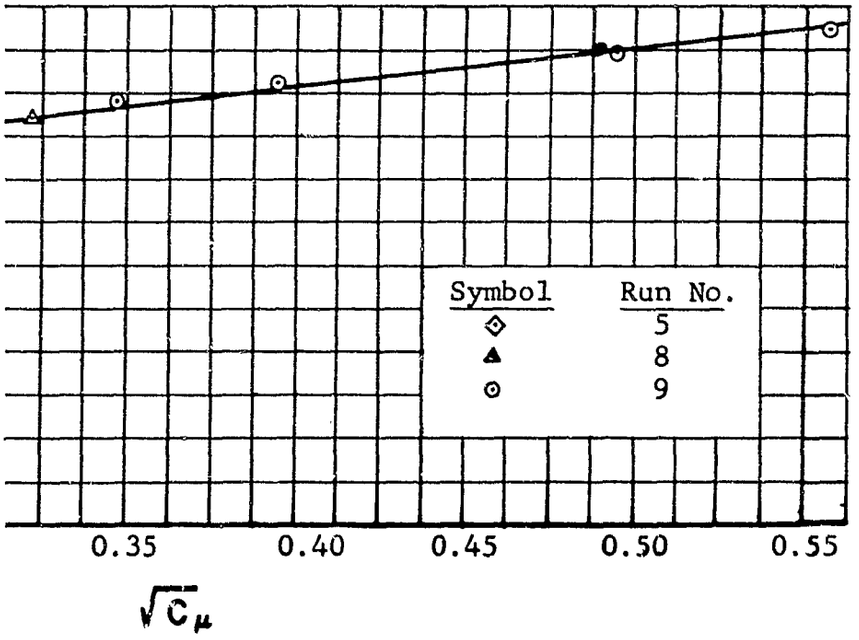

FICIENT vs. MOMENTUM COEFFICIENT FOR
UPPORT IN SUPERCRITICAL REGIME

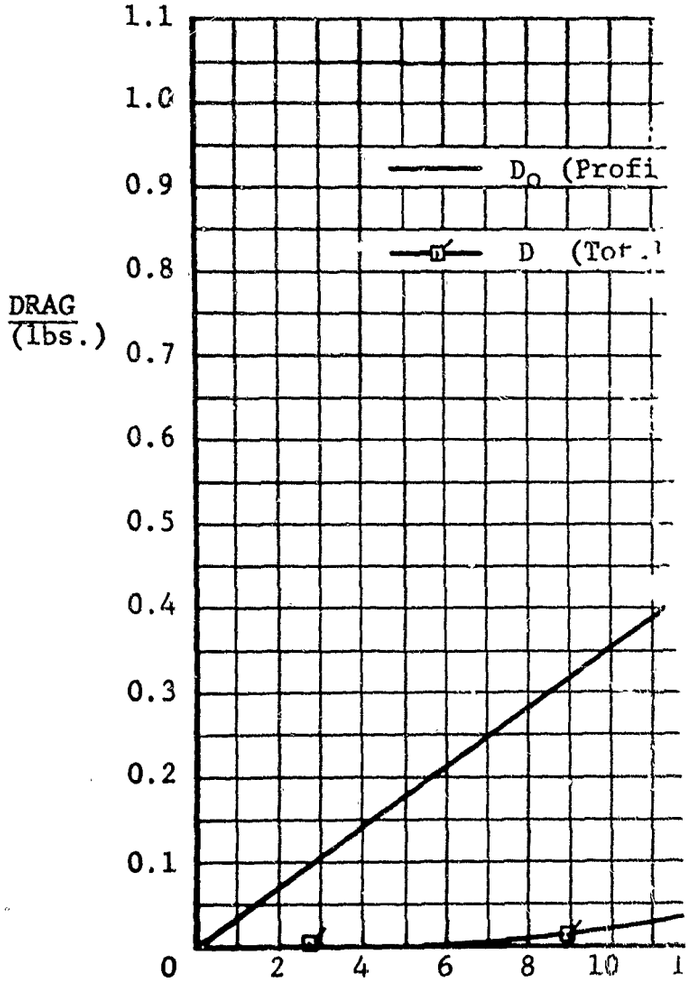

FIG. B-18 DRAG OF GROUND EFFE

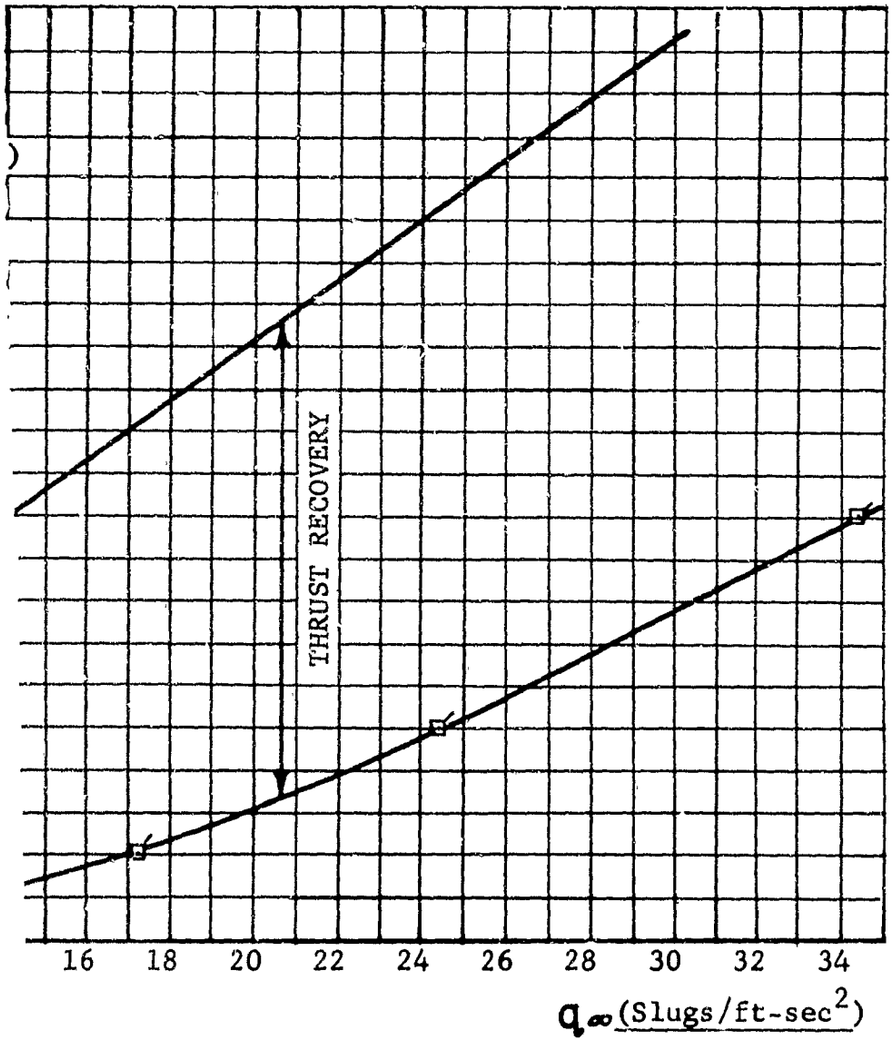

ORT vs. WIND TUNNEL DYNAMIC HEAD

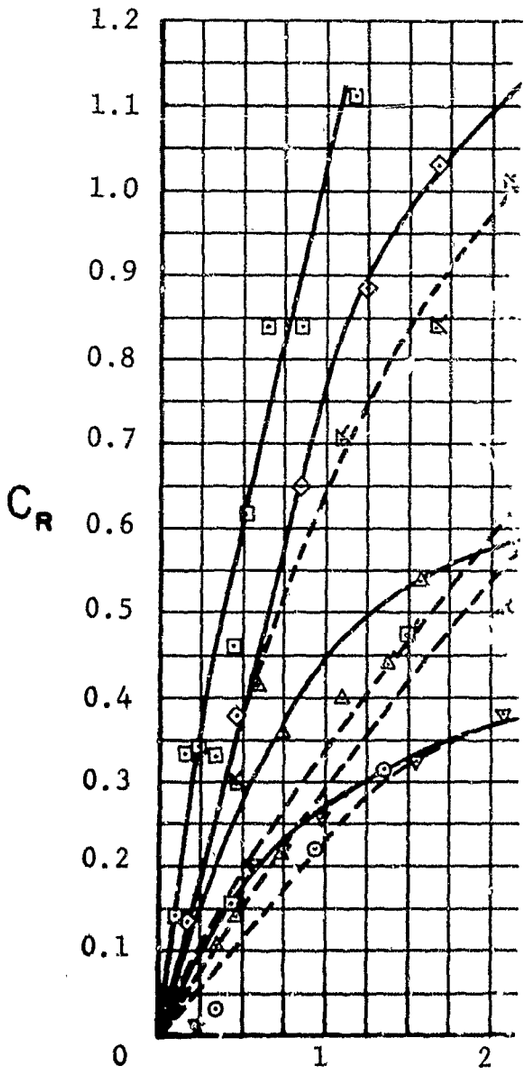

FIG. B-19 GROUND EF

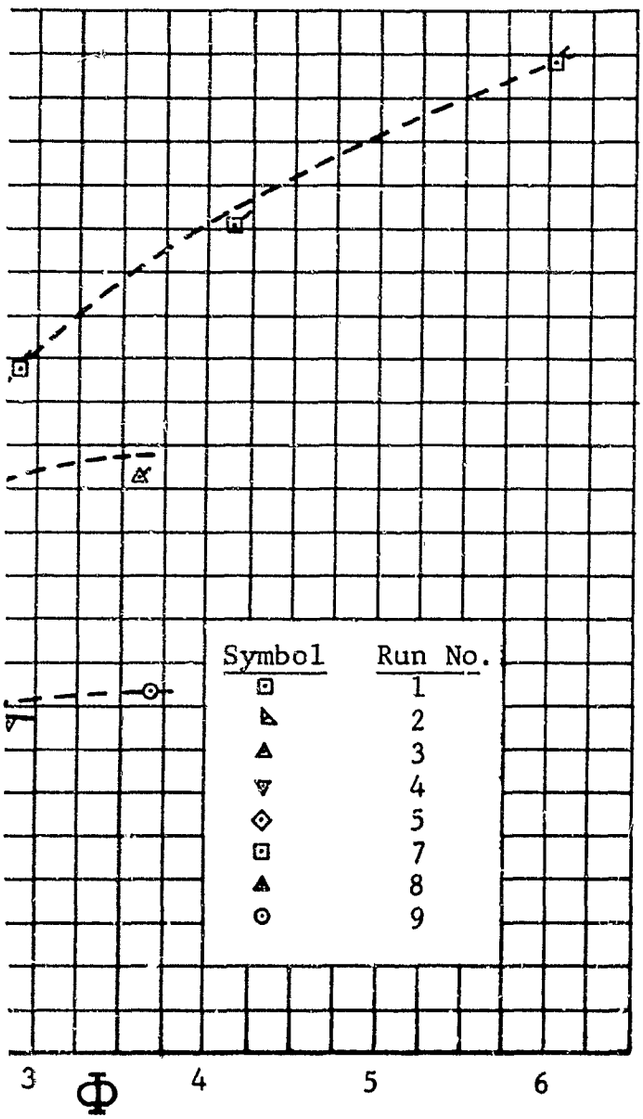

PPORT: THRUST RECOVERY COEFFICIENT
'ORWARD SPEED PARAMETER

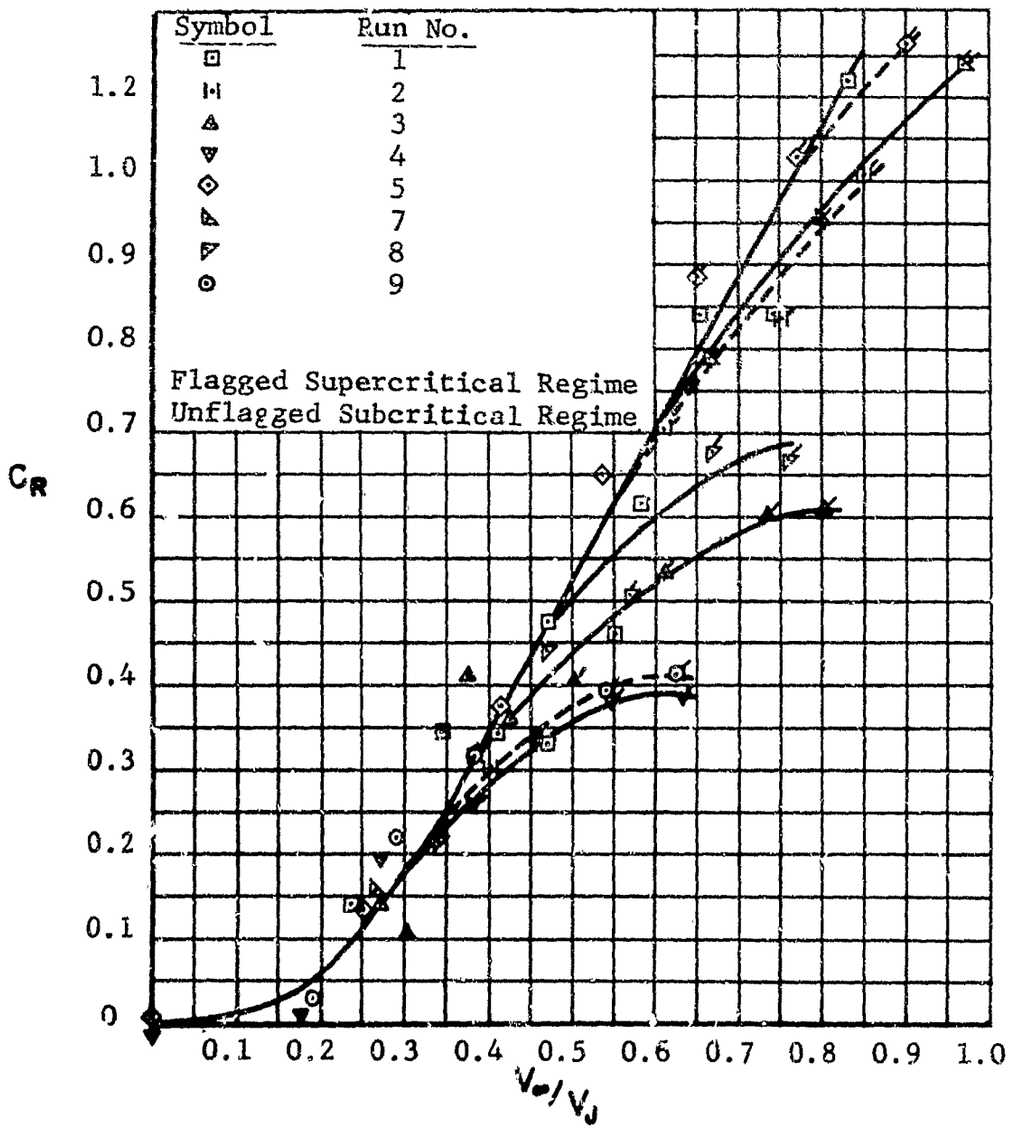

FIG. B-20 GROUND EFFECT CHART: THRUST RECOVERY COEFFICIENT vs. RATIO OF FORWARD SPEED TO JET VELOCITY
$V_F = V_R = V_J$

Section C

FLOW FIELD AROUND A HOLLOW CYLINDER MOUNTED IN A TUBE

by

Gerald M. Davey
Mark H. Siegel
John W. Burr
Duane E. Cromack

First issued as TR AE 6402, January 1964

SUMMARY

Preliminary tests have been carried out to investigate the pressure distribution on the outside surface of a vehicle moving at high speed within a tube. The vehicle was simulated by a hollow cylinder mounted in a tube of circular cross section. The contribution of these surfaces to the lift and pitching moment on the vehicle are determined. The contribution to pitching moment is found to be destabilizing.

These tests are supplemented by flow visualization tests at low flow velocities.

TABLE OF CONTENTS

LIST OF ILLUSTRATIONS

SYMBOLS

c	length of models. For all models = 7"
d	outside diameter of models. For all models = 3"
S	model planform area cd, (see Appendix)
C_l	local lift coefficient

$$C_l = \oint C_{p_x} d(x/c) \cos\phi$$

C_L	overall lift coefficient; average found from C_l vs ϕ curves
$C_{m_{L.E.}}$	local pitching moment coefficient

$$C_{m_{L.E.}} = \oint C_{p_x} \left(\frac{x}{c}\right) d\left(\frac{x}{c}\right) \cos\phi$$

$C_{M_{L.E.}}$	overall pitching moment coefficient about leading edge. Average found from $C_{m_{L.E.}}$ vs ϕ curves
C_{p_x}	pressure coefficient at position x

$$C_{p_x} = 1 - \frac{p_x}{p_{TANK}}$$

L	total lift due to external pressure distribution. Here lift is defined to act in that plane which contains the axis of the cylinder both before and after any change of disturbance in angle of attack.
$M_{L.E.}$	total moment about the leading edge due to external pressure distribution.
M	flow Mach number
p_{tank}	manometer reading when connected to atmosphere at one end and to settling tank at the other.

p_x	manometer reading when connected to atmosphere at one end and a model pressure tap at the other
V	flow velocity
q	dynamic pressure, $\frac{1}{2}\rho V^2$.
X, Z	See Figure C-7
α	angle of attack in pitch, see Figure C-7
α_e	compound angle of atta , i.e., effective angle of attack involving bo pitch and yaw, see Appendix
Θ	angle of attack in yaw, see Figure C-7
Φ	circumferential position being simulated by placing model at a compound angle, see Figure C-7

I. INTRODUCTION

In a report on a proposed high speed, self-propelled, air-breathing vehicle in a tube, Foa (Ref. 1) has suggested that ground effect supports could be used for suspension of the vehicle. West (Ref. 2) has investigated further the feasibility of this system to provide both suspension and propulsion of the vehicle at high forward speeds. One criterion in determining the required strength of the ground effect support is the stability of the vehicle when disturbed from its axi-symmetric position within the containing tube.

This report gives the results of a preliminary program to investigate the stability of the vehicle. At the time of writing, the shape of the vehicle was not clearly defined. Hence a very simple shape, i.e., a hollow cylinder, was used. It is with the pressure distribution on the outside surface of the vehicle that this report is concerned.

II. DESCRIPTION OF APPARATUS

Two separa e series of experiments were made.

1. Pressure tap models.

Two models were tested; one with a blunt leading edge (Model I) and the other with a round leading edge (Model II). The models and apparatus are shown in Figs. C-1 thru C-7. Fig. C-1 shows Model I and the location of its six pressure taps. Fig. C-2 shows

Model II and the accompanying mechanism for incidence adjustmen and measurement in pitch and yaw. Figs. C-3 thru C-5 show the detailed configuration and dimensions of the two models. Fig.C- shows the model mounted centrally within its containing tube. This tube had a bellmouth inlet open to the atmosphere and an airflow induced by operating a compressor downstream of a settl tank. The manometers were external to the rest of the test ce Since there must necessarily be some clearance between the stin and the tube, an inflow of air and resultant distortion of the main airflow over the model was of some concern. Originally, tests were run in a cell in which a compressor was mounted up- stream of the model. As a result the static pressure at the ne (which was fairly close to the duct exit) was equal to the ambi static pressure and hence leakage losses about the model sting were negligible. Mechanical failure of this facility necessita- ted installation of the model in the present cell. Consequentl the static pressure in the region near the model was no longer at the ambient static value and leakage became appreciable, giv rise to the need for a sealing shield, as indicated in Fig. C-6.

2. Flow visualization model.

This model was made from a transparent plastic tube as sho in Fig. C-8; it was the sam size as the pressure tap model and also mounted in a 6" diameter containing tube. Provision was ma

to alter the angle of attack in pitch only. The whole apparatus was mounted in the Rensselaer Polytechnic Institute low speed, low turbulence smoke tunnel. A flow velocity of 20 ft/sec was used in all flow visualization tests.

III. EXPERIMENTAL PROCEDURE

1. Pressure tap model.

A traverse was made, across the working section of the tube where the model would be, to measure static and stagnation pressure. Once out of a reasonably thin boundary layer these parameters were constant thus ensuring a uniform Mach number.

We wish to measure the pressure on the outside surface of the model at as many places as possible. On the other hand model complication and strut interference increase as the number of taps is increased. It was possible, however, to obtain a complete survey of pressures around the model at any given effective angle of attack by adopting the following procedure:

a) the model was set at α_e in pure pitch; then 6 more readings were obtained by using $-\alpha_e$ in pure pitch.

b) the model was set at α_e in pure yaw. Due to symmetry this gives the same result as $-\alpha_e$ in yaw.

Thus the pressure at six lengthwise stations can be determined at 4 circumferential positions.

Now, due to the fact that a plane of symmetry for the model and the containing tube can always be made to exist through the

axis of the model, it is possible by the use of compound rotations to measure the pressure at any circumferential position. All rotations should be about the geometric center of the model. For pitch rotations this was the case but for yaw rotations a small error was incurred due to the fact that the axis of rotation could not be made to pass through the geometric center. Simple geometric formulae were derived which gave the required pitch and yaw angles for any given effective angle of attack α_e and circumferential position, ϕ . (See Appendix).

Tests were made at two different Mach numbers, and for two different effective angles of attack, for both the blunt and the rounded leading edged models.

Some distortion of the flow field results from the presence of the sting in the airflow. This distortion was kept to a minimum by suitable shaping, see Figs. C-1 thru C-5.

2. Flow visualization model.

The crux of the problem being investigated is that the flow field around and through the model is influenced by the containing tube in a manner which is not qualitatively predictable on the basis of existing theories or previous observations.

To get some idea of the disturbed airflow pattern, the transparent flow visualization model was constructed to enable

photographs to be obtained. Liquid titanium tetrachloride was introduced in small quantities into the recess of a small, smooth rake some distance upstream of the model. The air passing over the rake caused a steady, white stream of gaseous titanium tetrachloride to be drawn downstream. The vertical position of the rake relative to the model was adjustable and the airflow over several parts of the model could be visualized.

IV. RESULTS AND DISCUSSION

1. Pressure survey tests.

In order to calculate the lift and pitching moment on the model due to the pressure distribution on its outside surface a plot of C_p vs X/C is made. As we are dealing with an essentially three dimensional flow a scheme must be adopted to produce overall values of C_L and C_M from the many C_p values.

There must be a stagnation point at or extremely near to the leading edge of the model around the whole circumference. Thus assuming an isentropic flow for the stagnation streamtube we can fix $C_p = 1$ at the leading edge throughout. Secondly, assume that the pressure inside the model is uniform at any lengthwise station over the whole cross section; no restriction need be put on the lengthwise variation of pressure. This is believed to be a valid assumption over most of the length of the tube, and is further supported by Fig. C-9a, where an internal streamline is

seen to become parallel to the walls almost instantaneously on entering the model and to keep in this position throughout. In particular, the pressure at the trailing edge of the model is uniform. Now, with the above conditions, pairs of C_p vs X/C curves can be plotted together to form closed curves. This has been done in Figs. C-11 and C-12 using C_p values on those longitudinal strips having a common projection on a plane bisecting the cylinder into its upper and lower surfaces; i.e., results for $\phi = \phi_1$, and $\phi = \pi - \phi_1$ (or for one value of Z/C) are plotted together (see Appendix). The area enclosed by these curves gives the sum of the forces normal to the surface at the two points chosen. The resultant local lift coefficient is easily found from this curve.

Figs. C-13 and C-14 show these C_l values versus radial distance measured from the center of the tube along the bisecting plane (see Fig. C-7). The overall value C_L is found as the average C_l . The included table summarizes the values so obtained.

Fig. C-15 shows C_L vs α_e for both models. As would be expected the rounded leading edge model generated more lift than the blunt leading edge model throughout. Both curves appear to be slightly nonlinear, which is not surprising in view of the essentially three dimensional nature of the flow. This is further emphasized by Figs. C-13 and C-14 that reveal that a fundamental

change in the external flow pattern must take place around the models between $\alpha_e = 5^o$ and $\alpha_e = 10^o$ in order to produce such a change in the shape of the loading or C_l values.

The value of C_m is determined as the moment of the area under the C_p vs X/C curve with respect to a suitable position along the length of the model; the result being factored by $\cos\phi$. It is convenient to use the leading edge as a datum for the measurement of moment arms.

Figs. C-16 and C-17 demonstrate the variation of $C_{m_{L.E.}}$ with radial position from the center of the tube. Again the fundamental changes between $\alpha_e = 5^o$ and $\alpha_e = 10^o$ are seen.

Fig. C-18 shows $C_{M_{L.E.}}$ vs α_e for both models. In accordance with expectation, Model II everywhere develops larger moments than Model I.

Finally, Figs. C-19 and C-20 show that the pressure distribution on the external surface of the model has a destabilizing effect. The internal flow may modify this situation. It should be noted that the model with the rounded leading edge, although more acceptable aerodynamically, could also be more unstable, at least as far as the external pressure field is concerned, for certain locations of the center of gravity.

Peripheral pressure distributions represented in the form of polar plots of C_p vs ϕ are shown in Figs. C-22 thru C-29.

Results are included for tests run at M = 0.17 and M = 0.26 with $\alpha_e = 5^\circ$ and $\alpha_e = 10^\circ$, for both Models I and II.

2. Flow Visualization Tests

The results are shown as Figs. C-9 and C-10. Fig. C-9 shows three smokelines with the model set at $\alpha = 7^\circ$. The auxiliary sketches show the position of the smokeline before it is influenced by the model, as seen from upstream.

In Fig. C-9a the smokeline was divided by allowing it to impinge on the leading edge. The early and continuing alignment of the internal streamline parallel to the model is noteworthy; separation occurs at the blunt leading edge as would be expected.

Fig. C-10 shows extreme angles of $\alpha = 17^\circ$ and 18° respectively, and consequently large displacements of the smokeline. Note, however, that the smokeline reverts to being parallel with the containing tube very much sooner at this large α than for $\alpha = 7^\circ$.

As noted in the introduction, these experiments were related to a proposed vehicle moving along a tube. Our simulation here is not quite complete as we have the whole airflow having a high velocity relative to the tube whereas in the proposed system only the air in the region near the vehicle has a significant velocity relative to the tube.

V. CONCLUSION

The results of these tests clearly show the vehicle to be unstable when displaced from its equilibrium position. This conclusion is a result of tests concerning the external flow of the vehicle only. It is not obvious at the time of writing whether the resultant of all moments acting on the vehicle, considering both its internal and external flows, is stabilizing or not.

The quantitative evaluation of the instability of the vehicle will provide useful criteria for the design of the support system (proposed to be of the ground effect type), which is itself stabilizing.

Nevertheless, in view of the inherent assumptions and approximations used in obtaining the results reported here, these results should be accepted as quantitative information only in relation to the idealized model by which the vehicle was simulated and to the specific conditions under which the tests were performed.

At the time of writing, tests are being conducted on a vehicle of the type discussed in this report, in which forces and moments are being measured directly. Early results are in good agreement with those obtained in this report.

Further tests will have to be performed on vehicles of different geometries, with the inclusion of internal fairings and gates to study the effects of blockage and the like, before a full evaluation can be made of the stability of an air-breathing vehicle traveling within a tube.

REFERENCES

1. Foa, J.V., "Land Transport at Air Transport Speeds", National Defense Transportation Journal, July-August 1962.

2. West, A.A., "The Effect of Similated High Forward Speed on a Two-Dimensional Ground Effect Support", Rensselaer Polytechnic Institute Tech.Report, TR AE 6304, October 1963.

APPENDIX

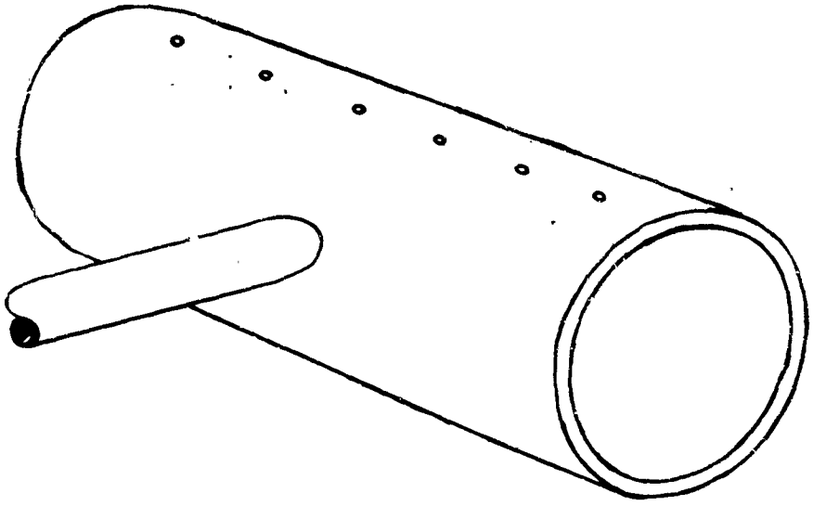

Imagine the cylinder split into a number of longitudinal strips, i.e.,

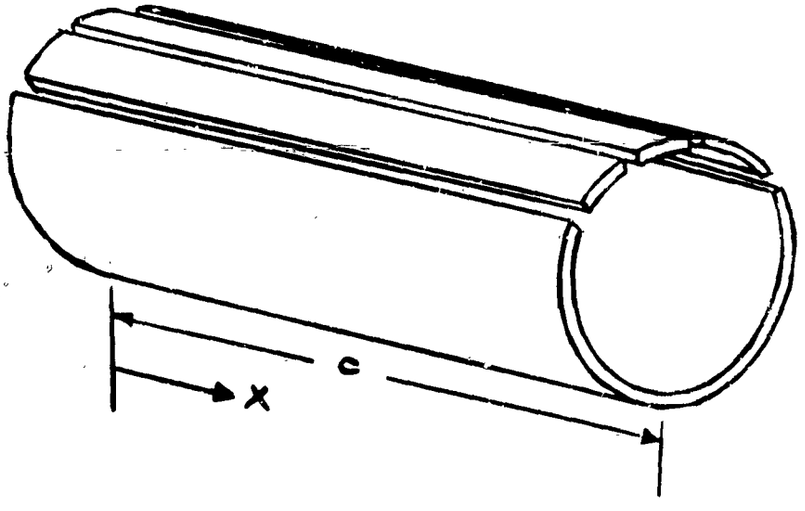

Each of the longitudinal strips is treated as a 2-d flat plate airfoil, along which the pressure distribution is recorded. Consider now two typical strips, chosen at the angles ϕ, and π -

respectively, such that both strips corresponding to the same value of Z have a common projection on an imaginary plane bisecting the cylinder into its upper and lower surfaces:

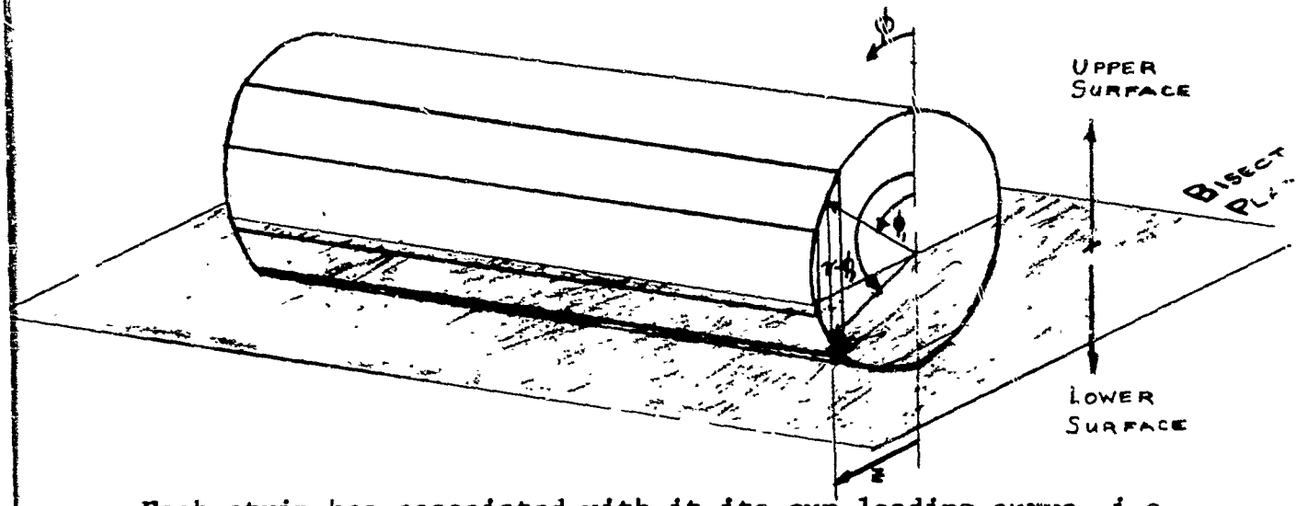

Each strip has associated with it its own loading curve, i.e.,

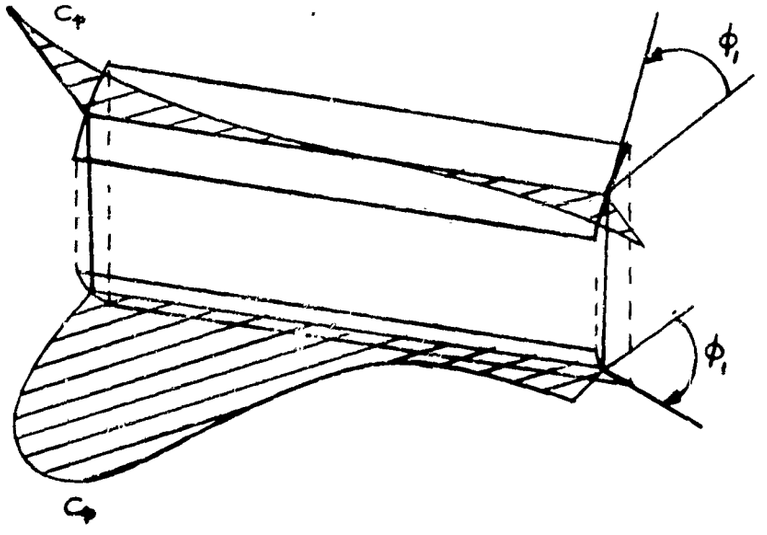

Because the strips were chosen such that they are both disposed from the imaginary bisecting plane by equal amounts, the loading curves may be factored by cos ϕ_1 and plotted together to form a

closed curve from which lift and moment coefficients may be obtained.

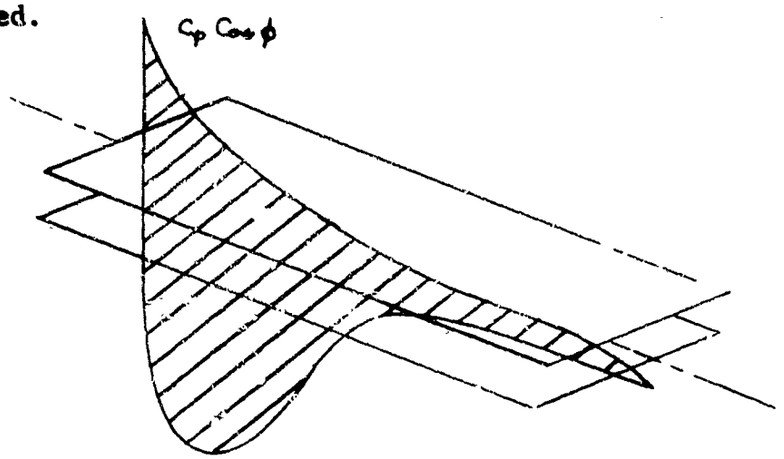

Thus,

$$C_2 = \oint C_p \cos\phi \, d(x/c)$$

$$C_{m_{L.E.}} = \oint C_p \cos\phi \, \frac{x}{c} \, d(x/c)$$

$$C_L = C_{2_{AVE.}}$$

$$C_{M_{LE}} = C_{m_{LE\,AVE}}$$

$$L = C_L q S$$

$$M_{LE} = C_{M_{LE}} q S c$$

where S ≡ projected area of model on bisecting plane = cd.

Establishing the Equivalent Angle of Attack

$\alpha_e \equiv$ equivalent angle of attack

$\Theta \equiv$ angle of yaw

$\phi \equiv$ angle of roll

$\alpha \equiv$ angle of pitch

At the outset we have four unknowns; the procedure followed is to stipulate α_e and ϕ. We require two equations in the two unknowns, Θ and α. Having stipulated α_e and ϕ these equations are solved for Θ and α and the model adjusted accordingly.

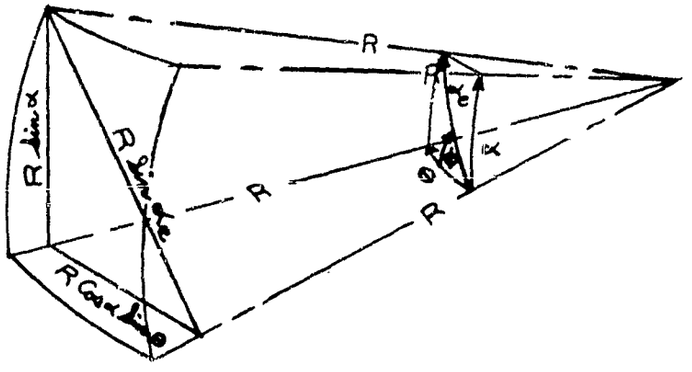

From the geometry of the figure,

$$R \sin \alpha_e \cos \phi = R \cos \alpha \sin \Theta$$

Making a small angle approximation ($\cos \alpha \approx 1.0$) to facilitate computation at no appreciable loss in accuracy there

results:

$$\sin\theta = \sin\alpha_e \cos\phi$$

Similarly,

$$R \sin\alpha_e \sin\phi = R \sin\alpha$$

$$\sin\alpha = \sin\alpha_e \sin\phi$$

It is worthy of note that the small angle approximation is equivalent to saying that the order of finite rotations may be interchanged for small angles.

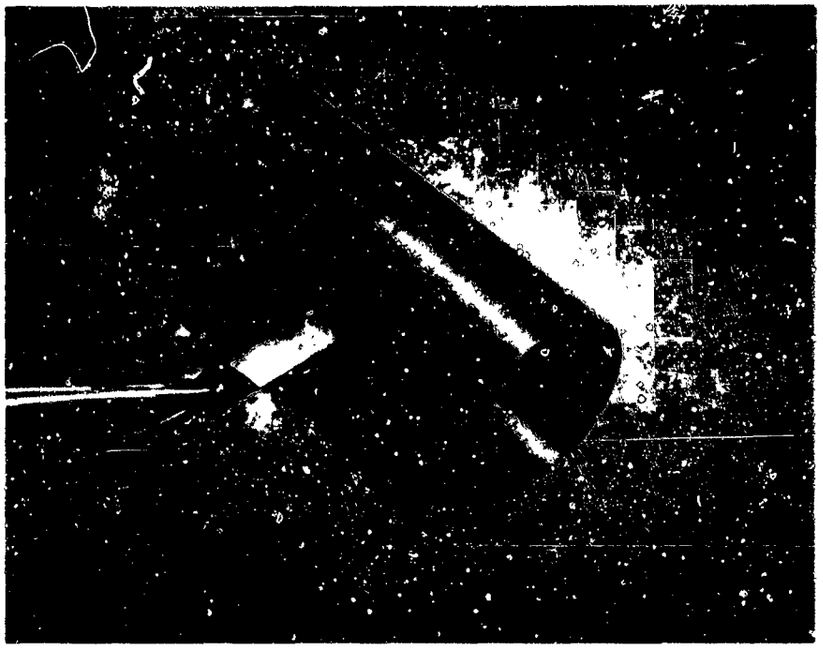

FIG. C-1

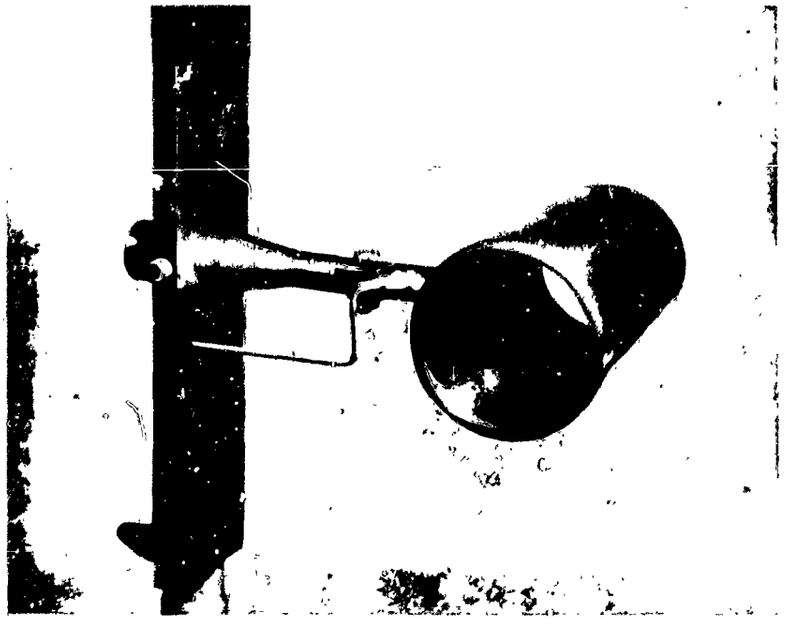

FIG. C-2

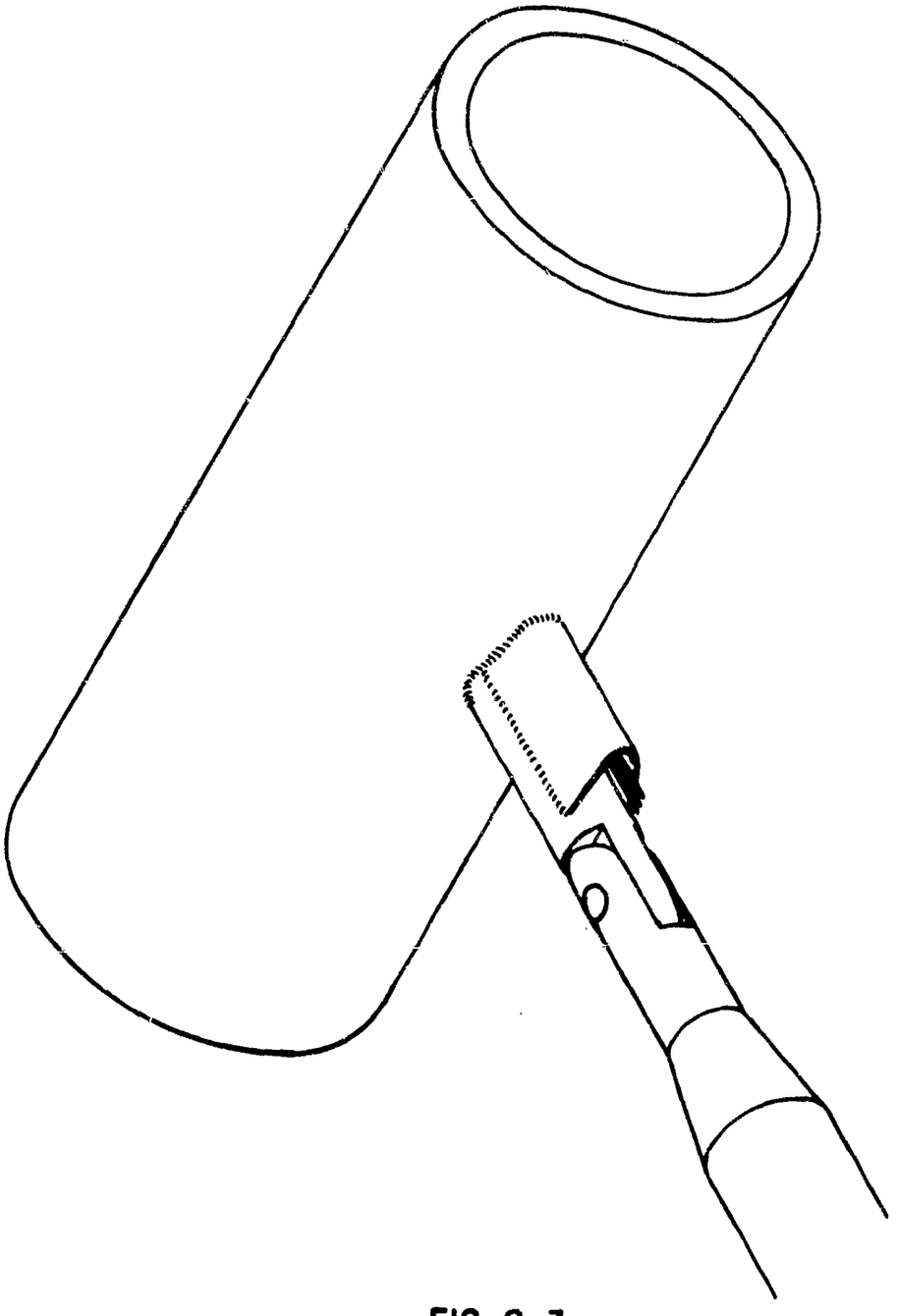

FIG. C-3

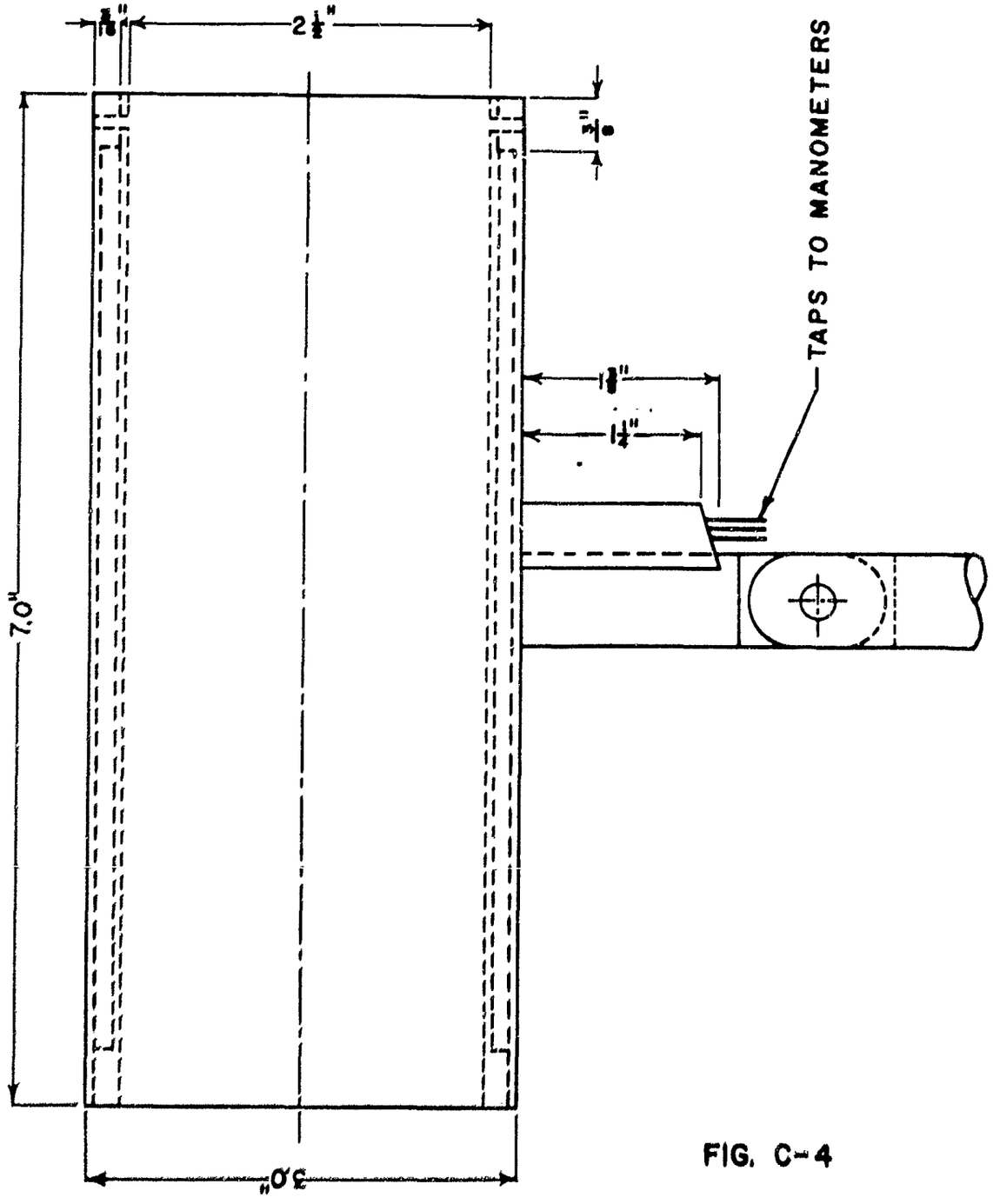

FIG. C-4

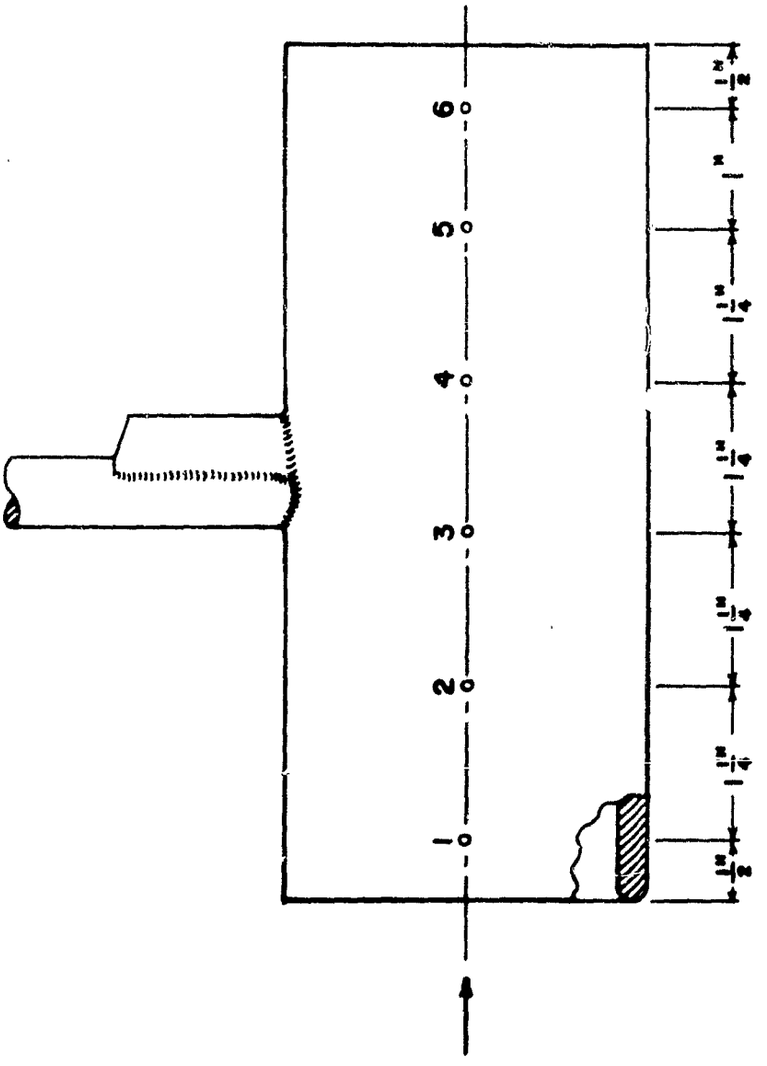

FIG. C-5

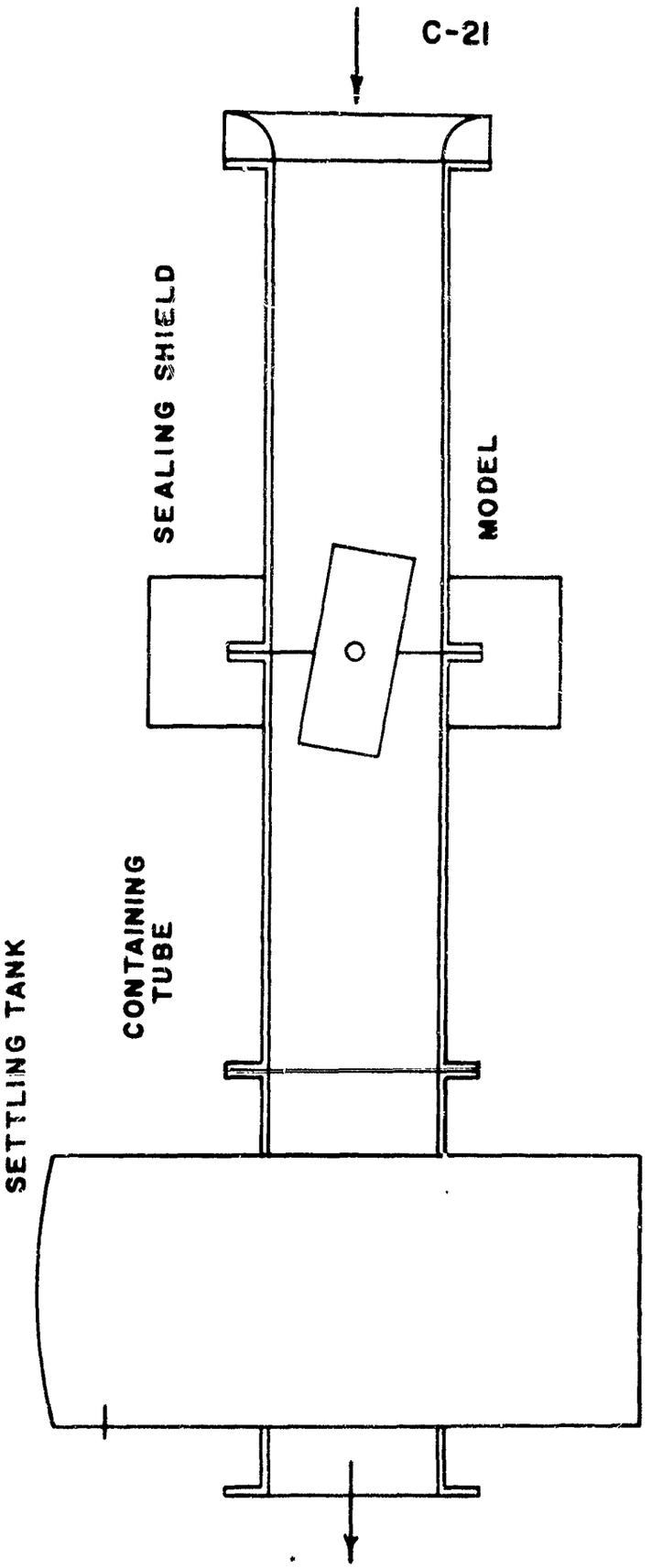

FIG. C-6

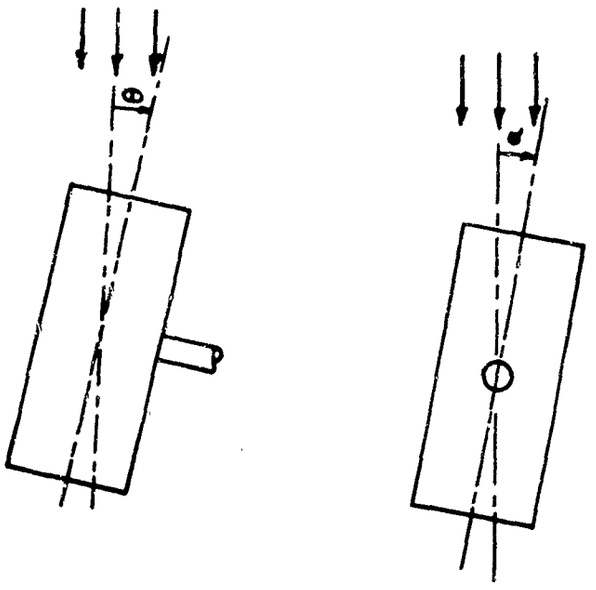

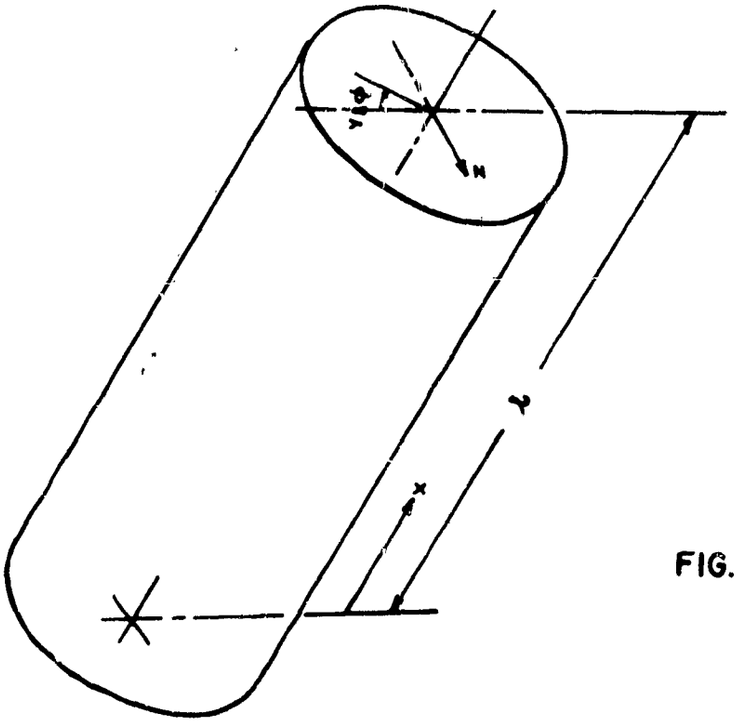

FIG. C-7

FIG. C—8

FILAMENT POSITION VIEWED FROM UPSTREAM

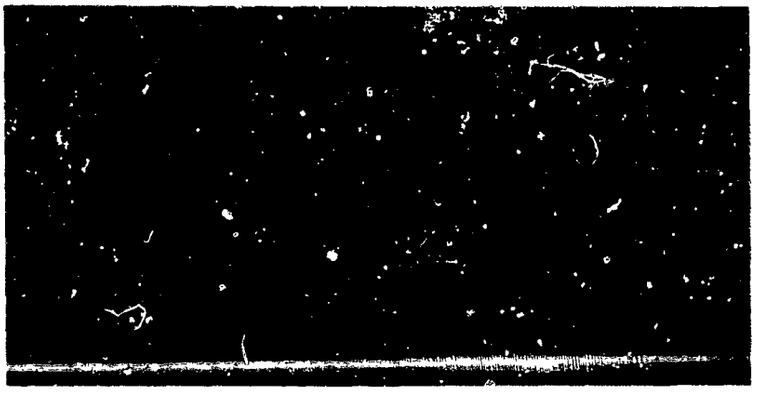

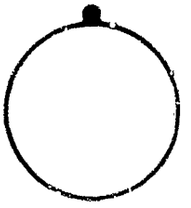

$\alpha = 7°$

FIG. C-9a

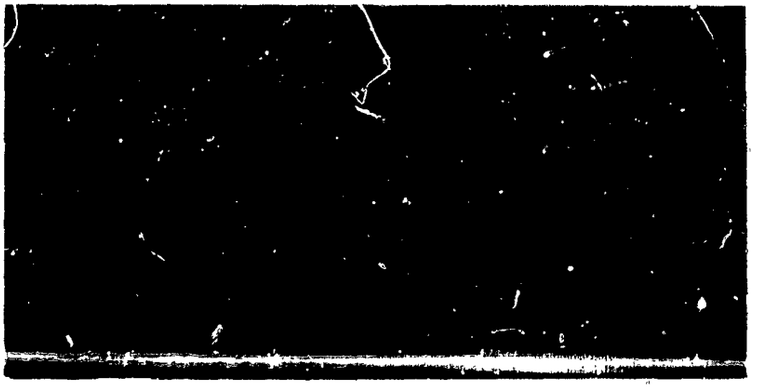

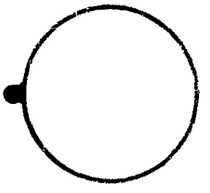

$\alpha = 7°$

FIG. C-9b

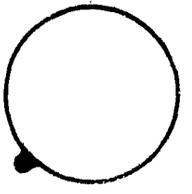

$\alpha = 7°$

FIG. C-9c

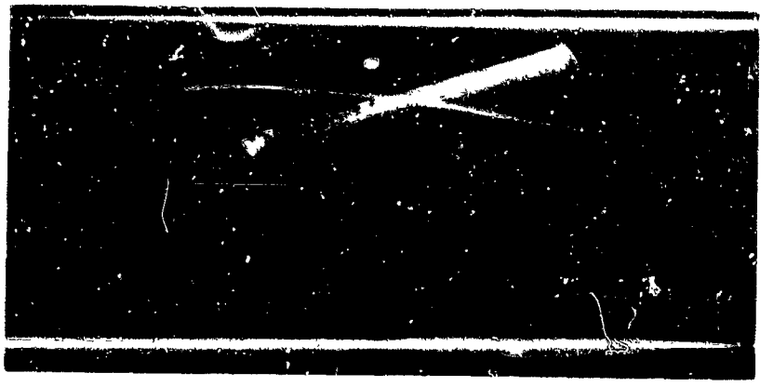

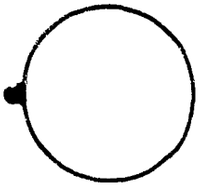

$\alpha = 17°$

FIG. 10a

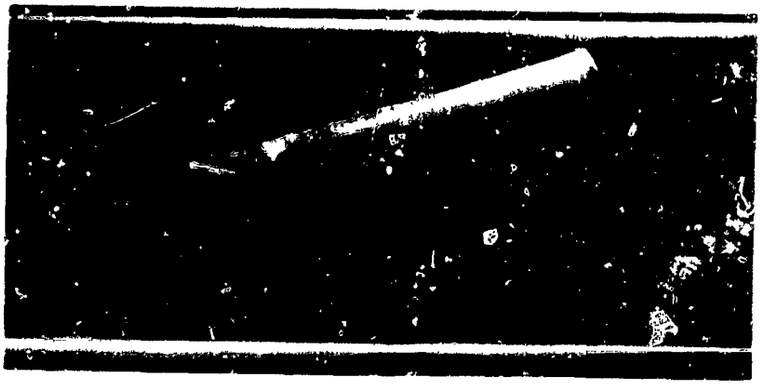

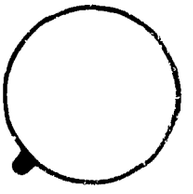

$\alpha = 18°$

FIG. 10b

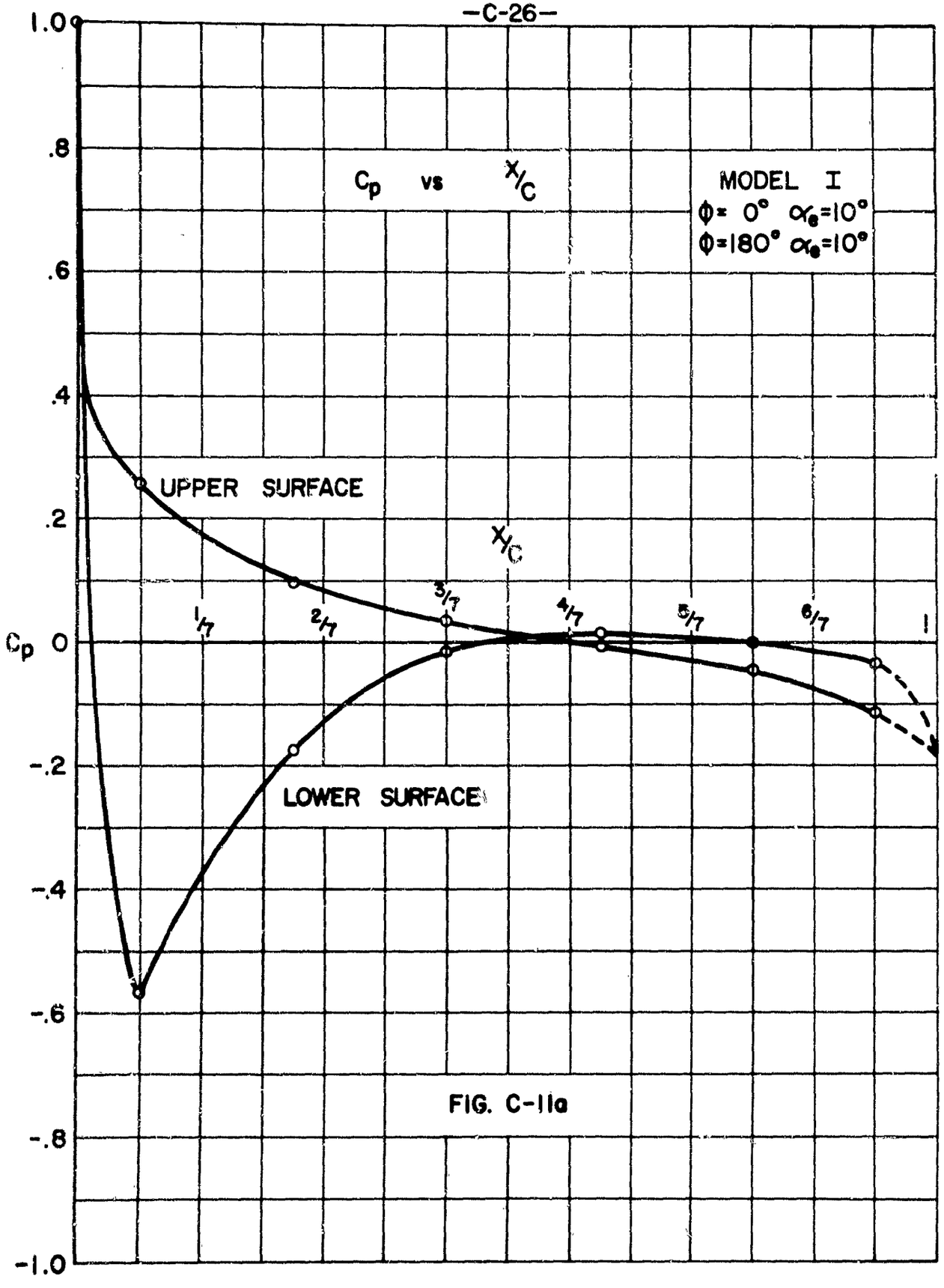
1.0
.8
.6
.4
.2
0
-.2
-.4
-.6
-.8
-1.0
Cp
Cp vs X/C
MODEL I
Φ= 0° α₀=10°
Φ=180° α₀=10°
UPPER SURFACE
LOWER SURFACE
X/C
1/7
2/7
3/7
4/7
5/7
6/7
1

FIG. C-11a

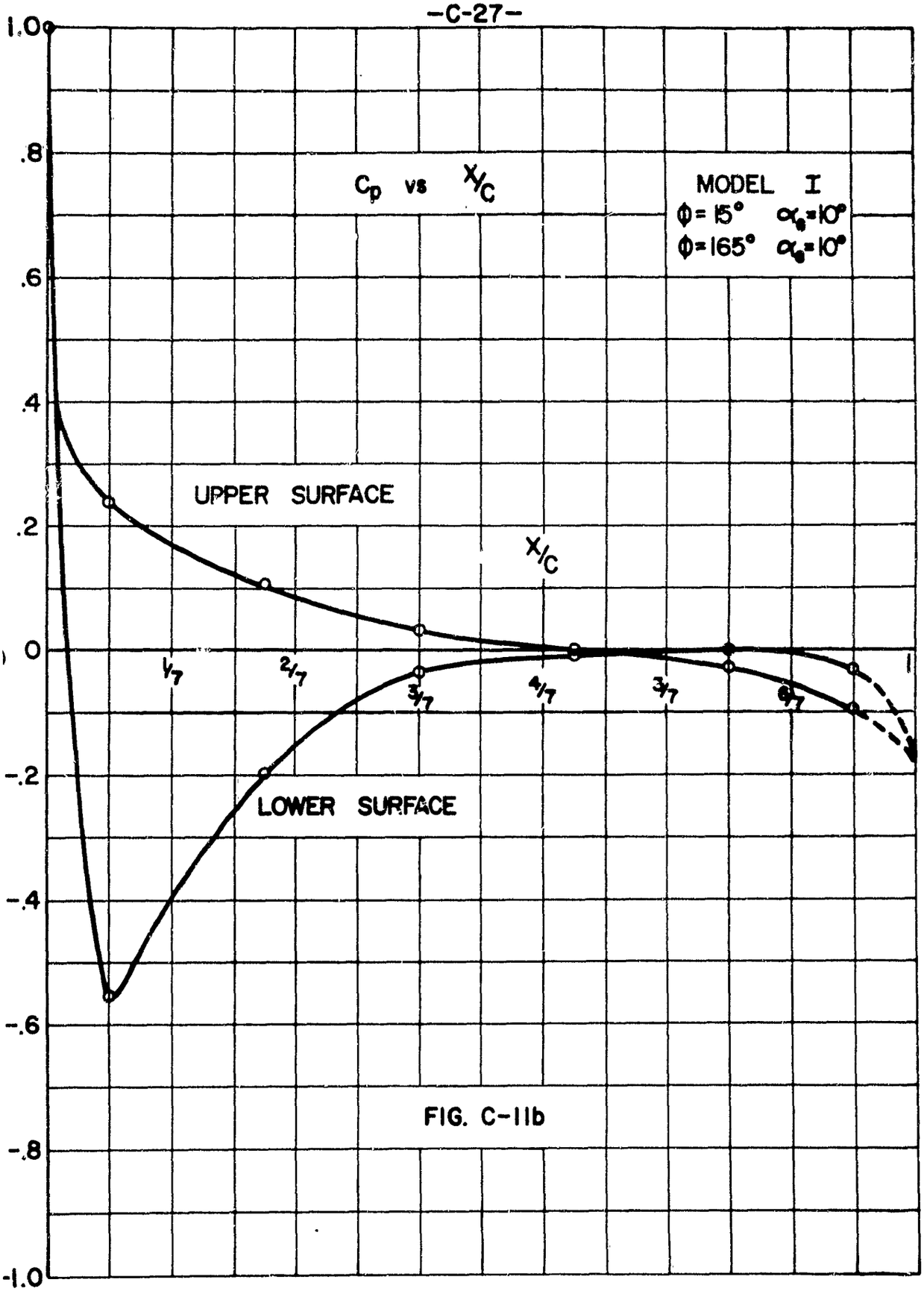
1.0
.8
.6
.4
.2
0
-.2
-.4
-.6
-.8
-1.0
C_p vs X/C
MODEL I
$\phi = 15°$ $\alpha_s = 10°$
$\phi = 165°$ $\alpha_s = 10°$
UPPER SURFACE
LOWER SURFACE
X/C
1/7
2/7
3/7
4/7
5/7
6/7
1

FIG. C-11b

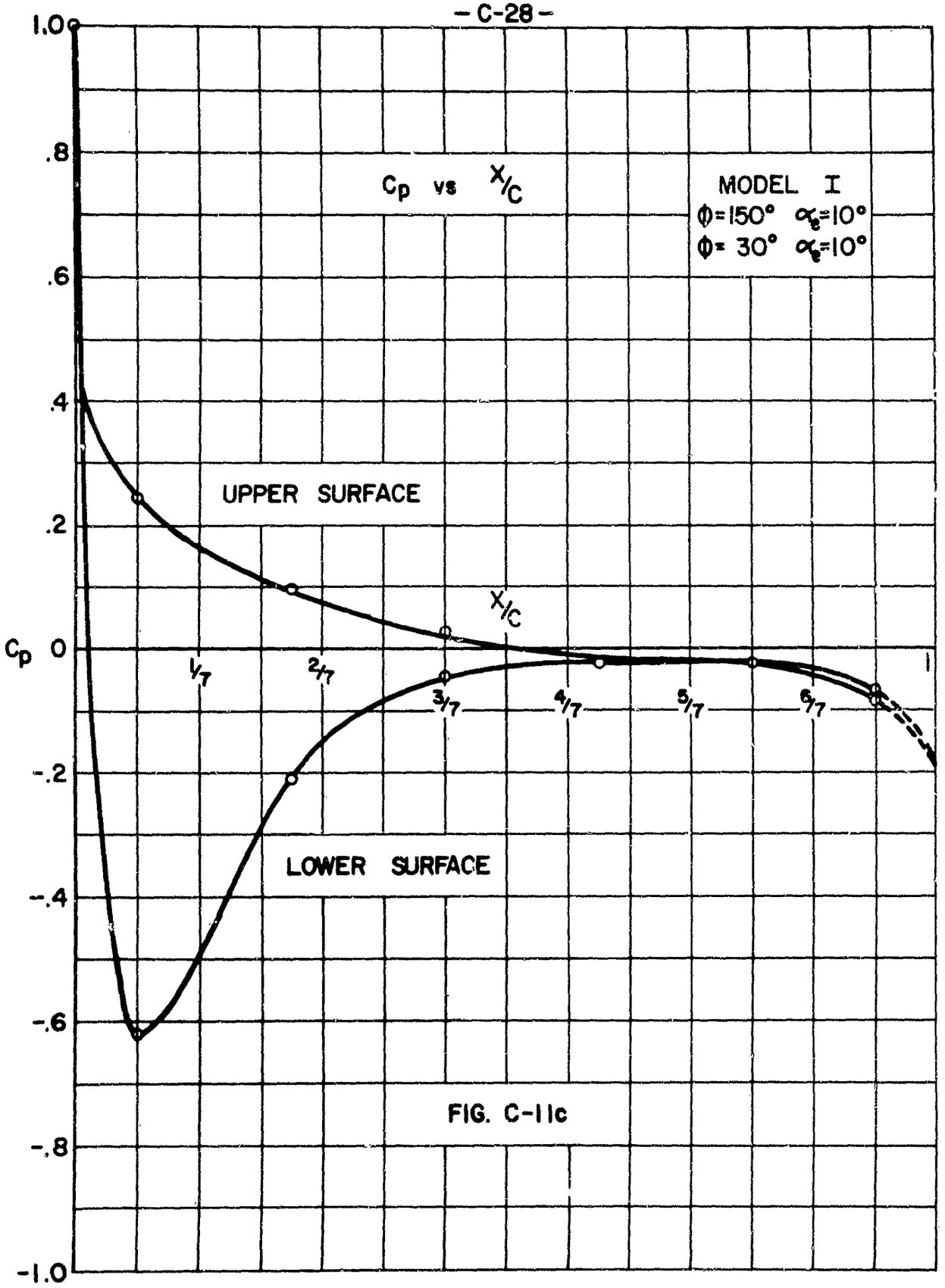
1.0
.8
.6
.4
.2
0
-.2
-.4
-.6
-.8
-1.0
C_p
C_p vs X/C
MODEL I
Φ=150° α_t=10°
Φ= 30° α_t=10°
UPPER SURFACE
LOWER SURFACE
X/C
1/7
2/7
3/7
4/7
5/7
6/7

FIG. C-11c

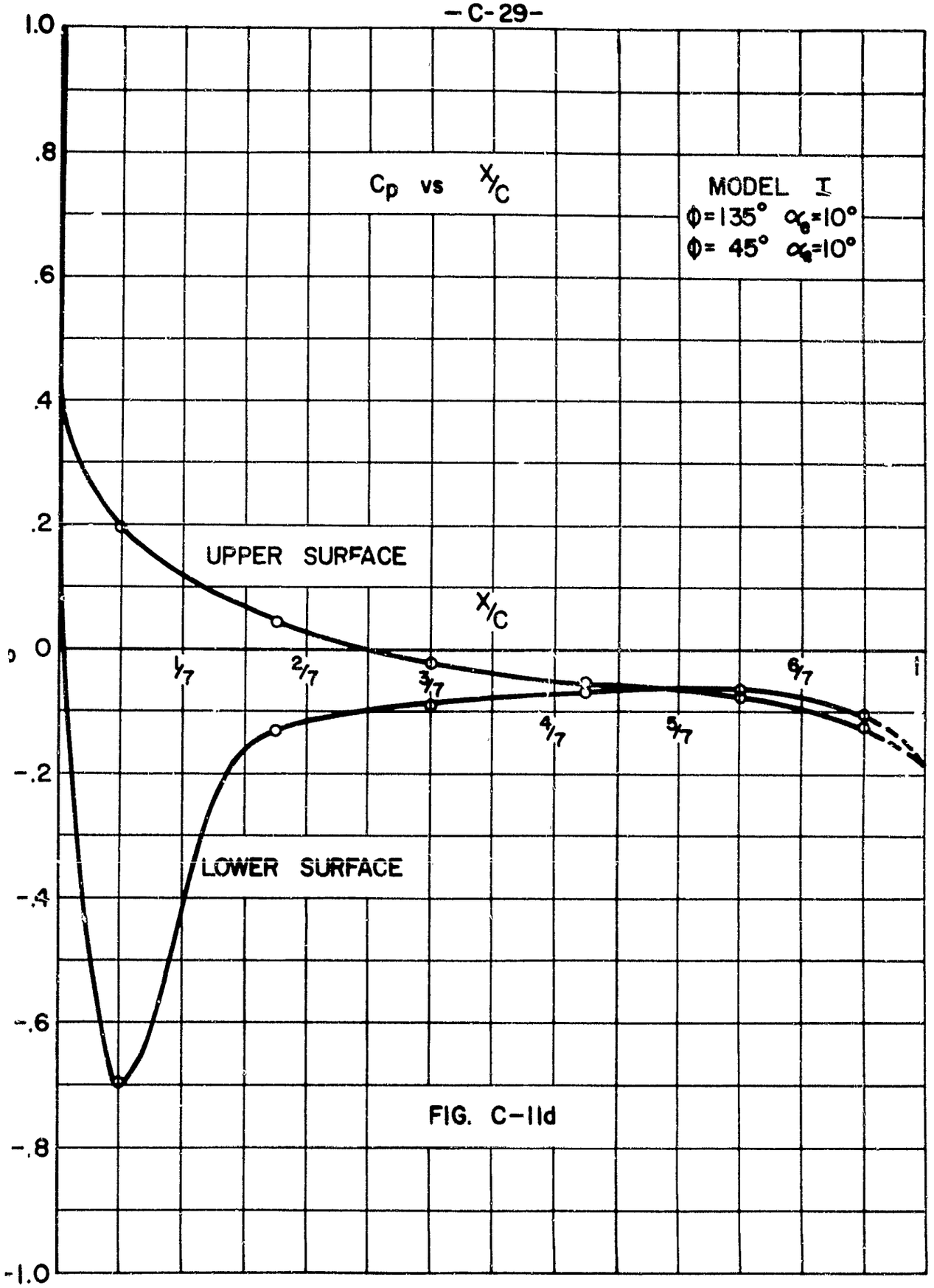
1.0
.8
.6
.4
.2
0
-.2
-.4
-.6
-.8
-1.0
Cp vs X/C
MODEL I
Φ=135° α=10°
Φ= 45° α=10°
UPPER SURFACE
X/C
1/7
2/7
3/7
4/7
5/7
6/7
1
LOWER SURFACE

FIG. C-11d

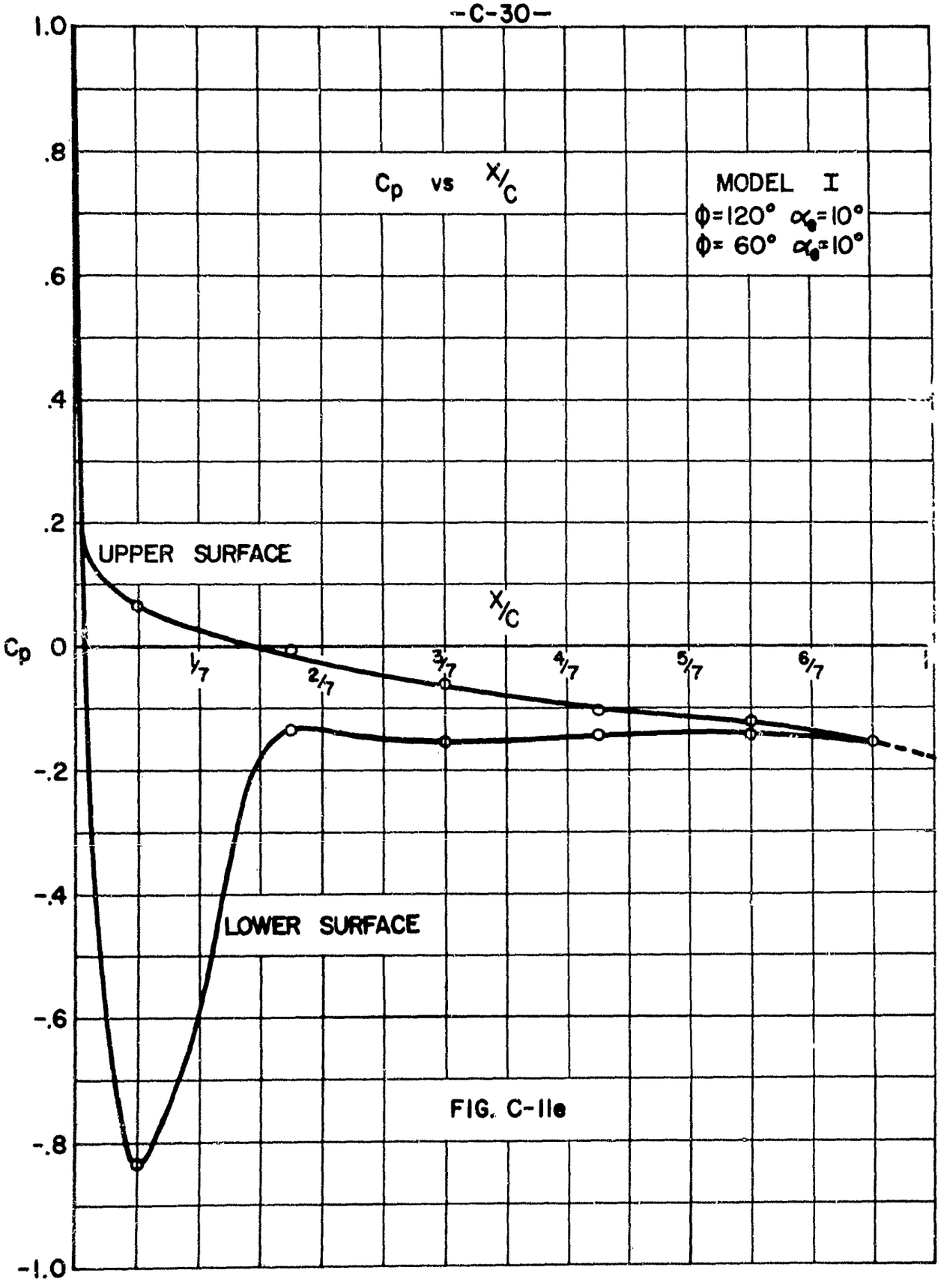
1.0
.8
.6
.4
.2
0
-.2
-.4
-.6
-.8
-1.0
Cp
Cp vs X/C
MODEL I
Φ=120° α=10°
Φ= 60° α=10°
UPPER SURFACE
X/C
1/7
2/7
3/7
4/7
5/7
6/7
LOWER SURFACE

FIG. C-11e

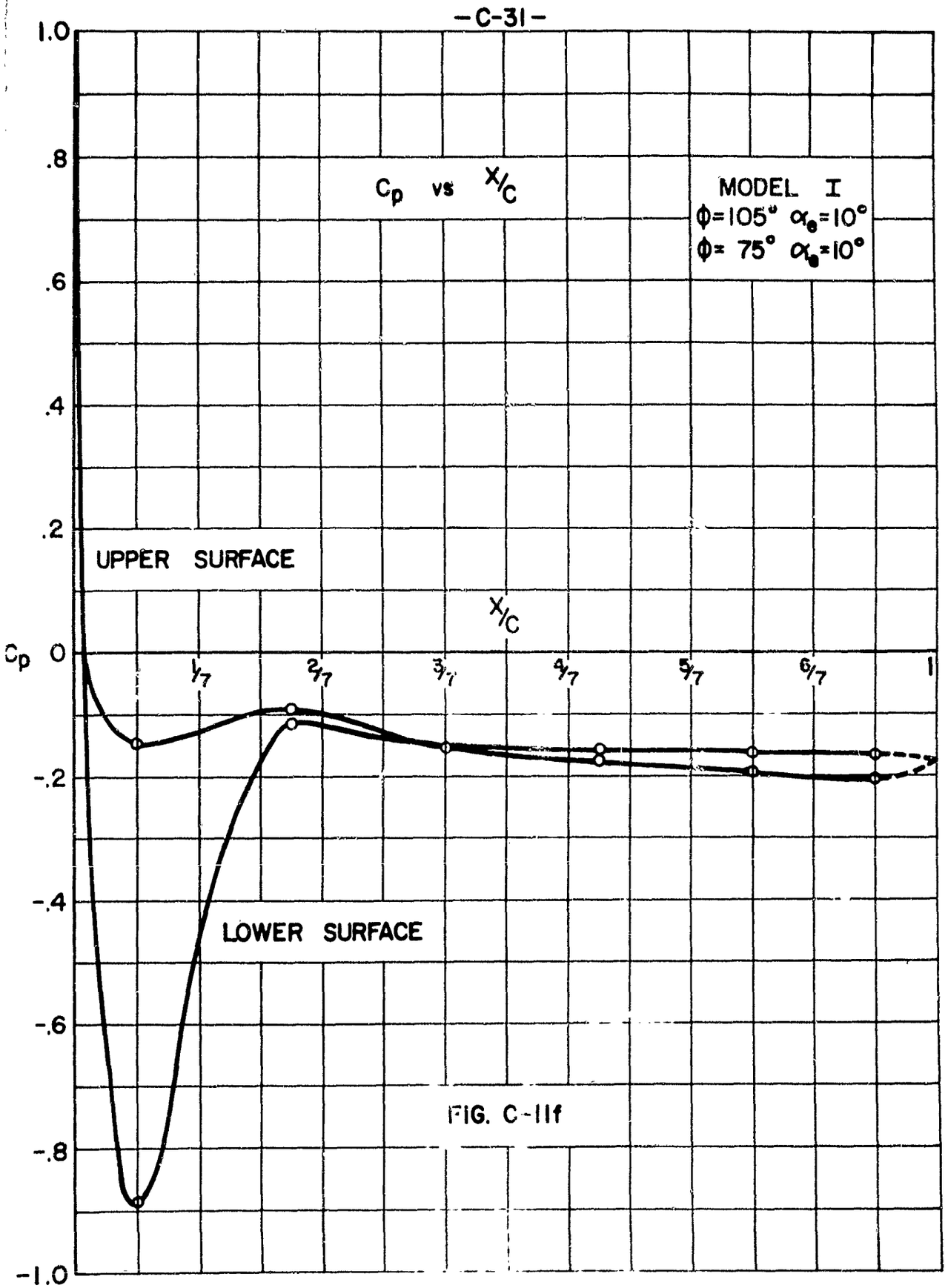
1.0
.8
.6
.4
.2
0
-.2
-.4
-.6
-.8
-1.0
C_p
C_p vs X/C
MODEL I
ϕ=105° α_a=10°
ϕ= 75° α_a=10°
UPPER SURFACE
LOWER SURFACE
X/C
1/7
2/7
3/7
4/7
5/7
6/7
1

FIG. C-11f

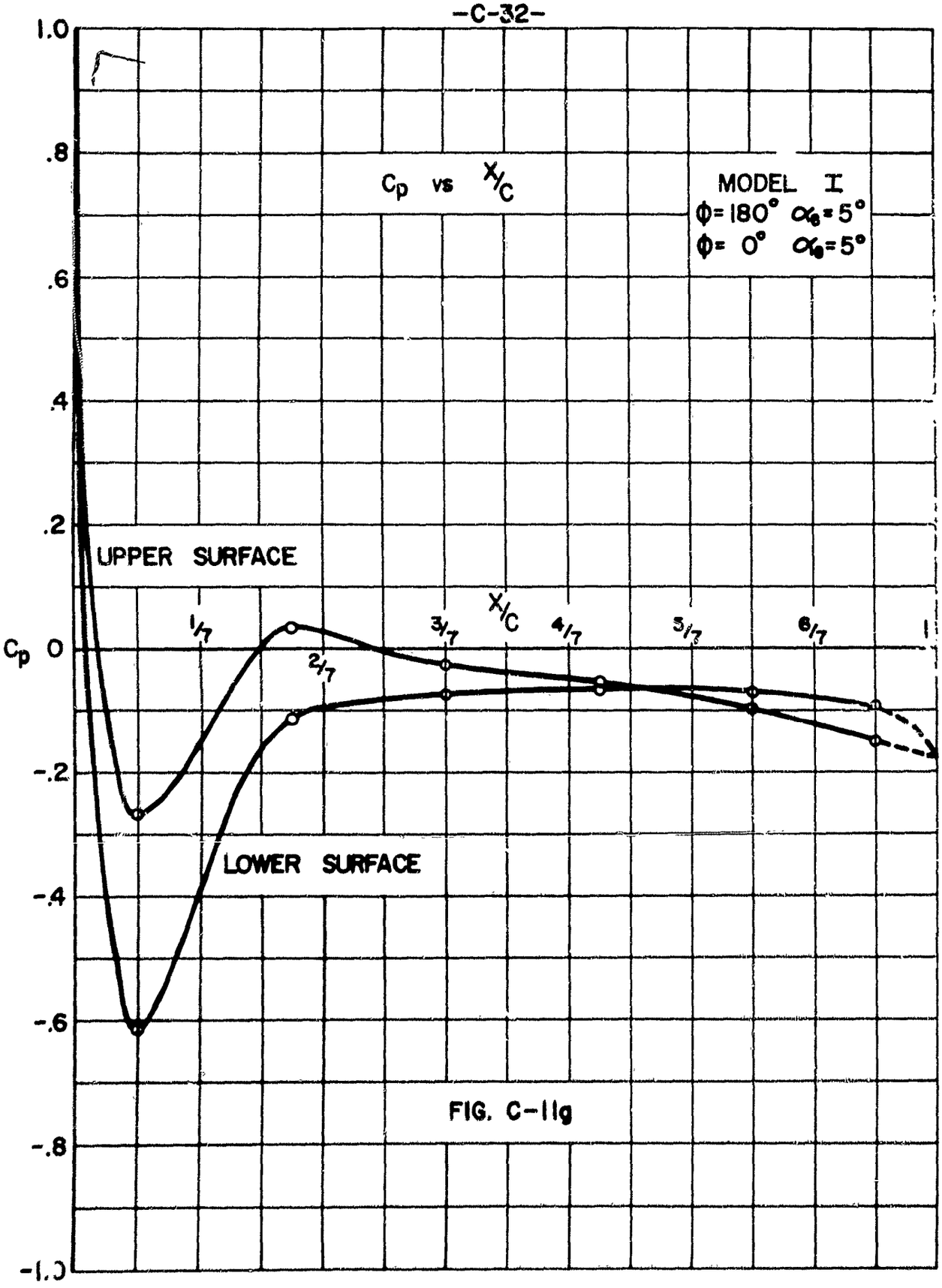
1.0
.8
.6
.4
.2
0
-.2
-.4
-.6
-.8
-1.0
Cp
Cp vs X/C
MODEL I
Φ= 180° α₀= 5°
Φ= 0° α₀= 5°
UPPER SURFACE
LOWER SURFACE
X/C
1/7
2/7
3/7
4/7
5/7
6/7
1

FIG. C-11g

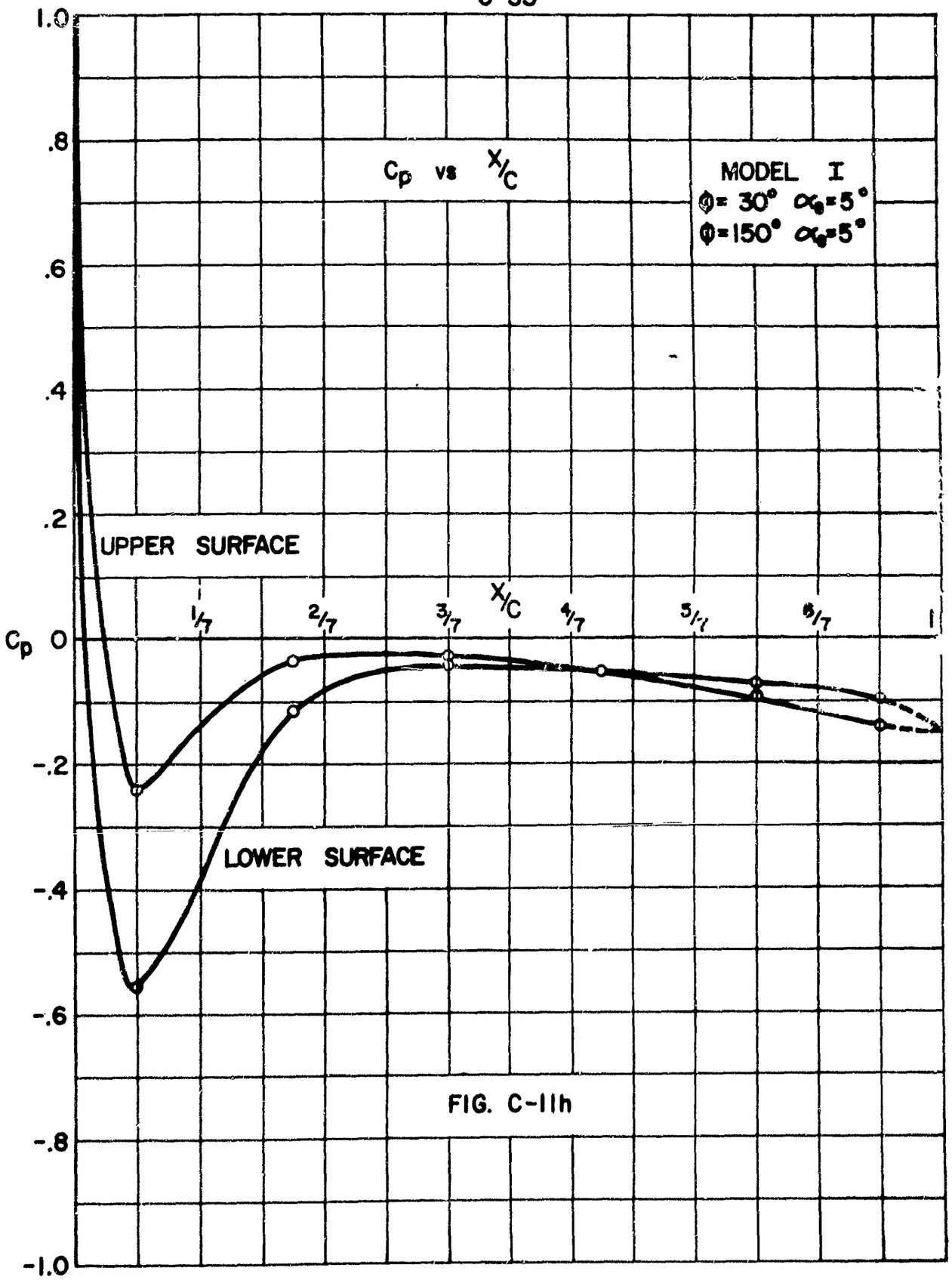
1.0
.8
.6
.4
.2
0
-.2
-.4
-.6
-.8
-1.0
Cp
Cp vs X/C
MODEL I
Φ= 30° α=5°
Φ=150° α=5°
UPPER SURFACE
LOWER SURFACE
X/C
1/7
2/7
3/7
4/7
5/7
6/7
1

FIG. C-11h

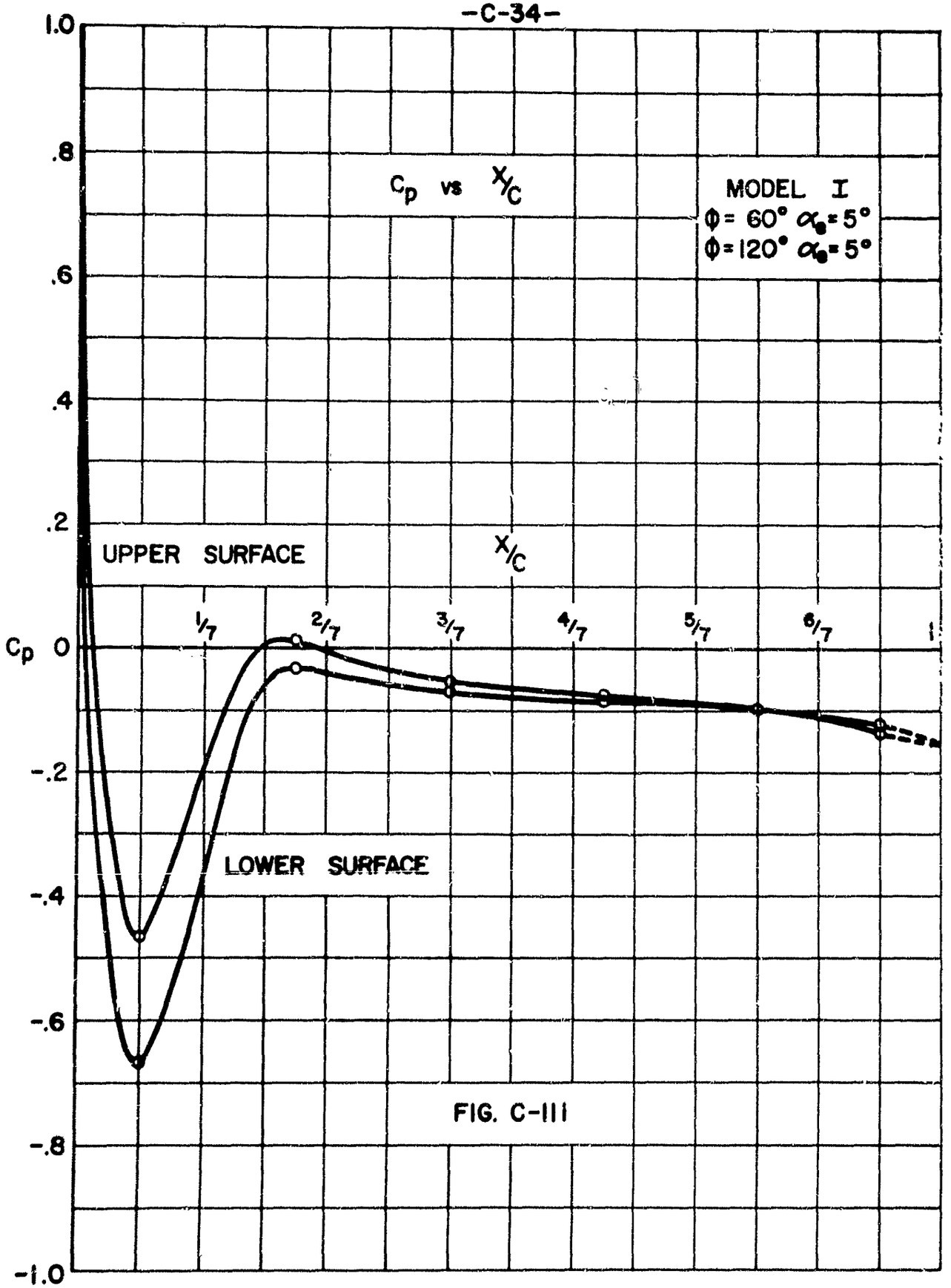
1.0
.8
.6
.4
.2
0
-.2
-.4
-.6
-.8
-1.0
Cp
Cp vs X/C
MODEL I
Φ = 60° α = 5°
Φ = 120° α = 5°
UPPER SURFACE
LOWER SURFACE
X/C
1/7
2/7
3/7
4/7
5/7
6/7
1

FIG. C-111

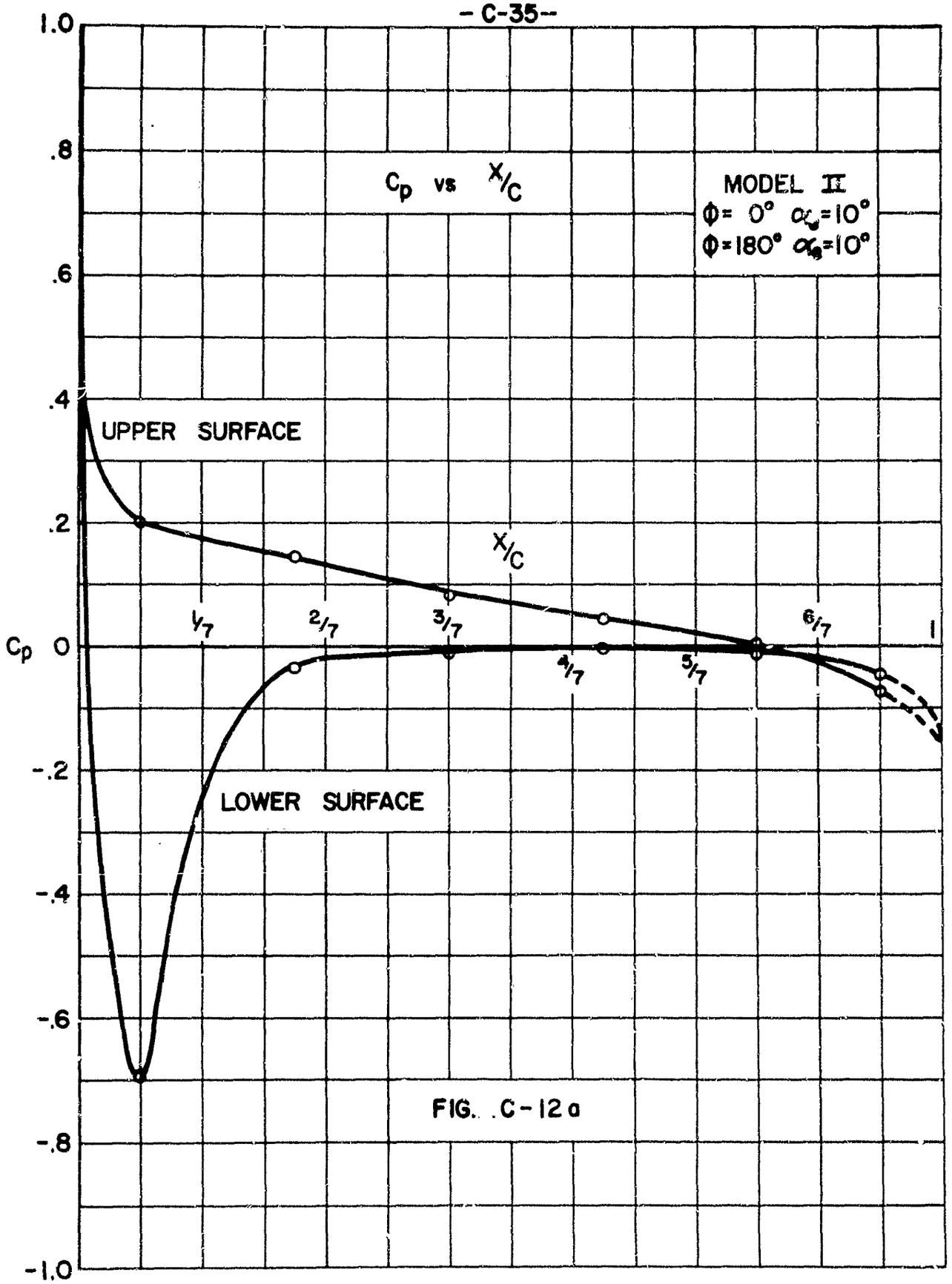
1.0
.8
.6
.4
.2
0
-.2
-.4
-.6
-.8
-1.0
Cp
Cp vs X/C
MODEL II
Φ= 0° α=10°
Φ=180° α=10°
UPPER SURFACE
LOWER SURFACE
X/C
1/7
2/7
3/7
4/7
5/7
6/7
1

FIG. C-12a

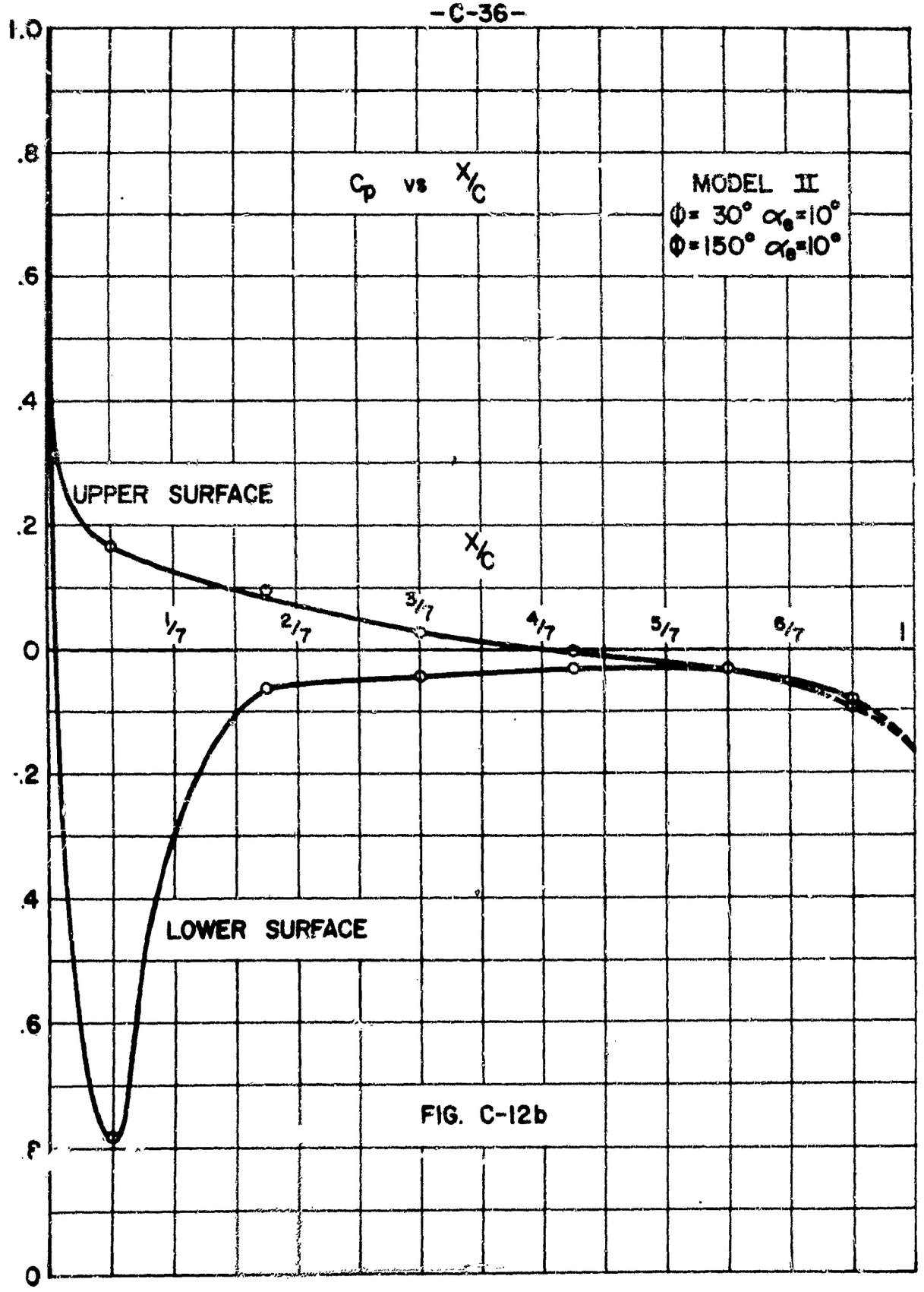
1.0
.8
.6
.4
.2
0
.2
.4
.6
.8
1.0
C_p vs X/C
MODEL II
$\Phi = 30°$ $\alpha_0 = 10°$
$\Phi = 150°$ $\alpha_0 = 10°$
UPPER SURFACE
LOWER SURFACE
X/C
1/7
2/7
3/7
4/7
5/7
6/7
1

FIG. C-12b

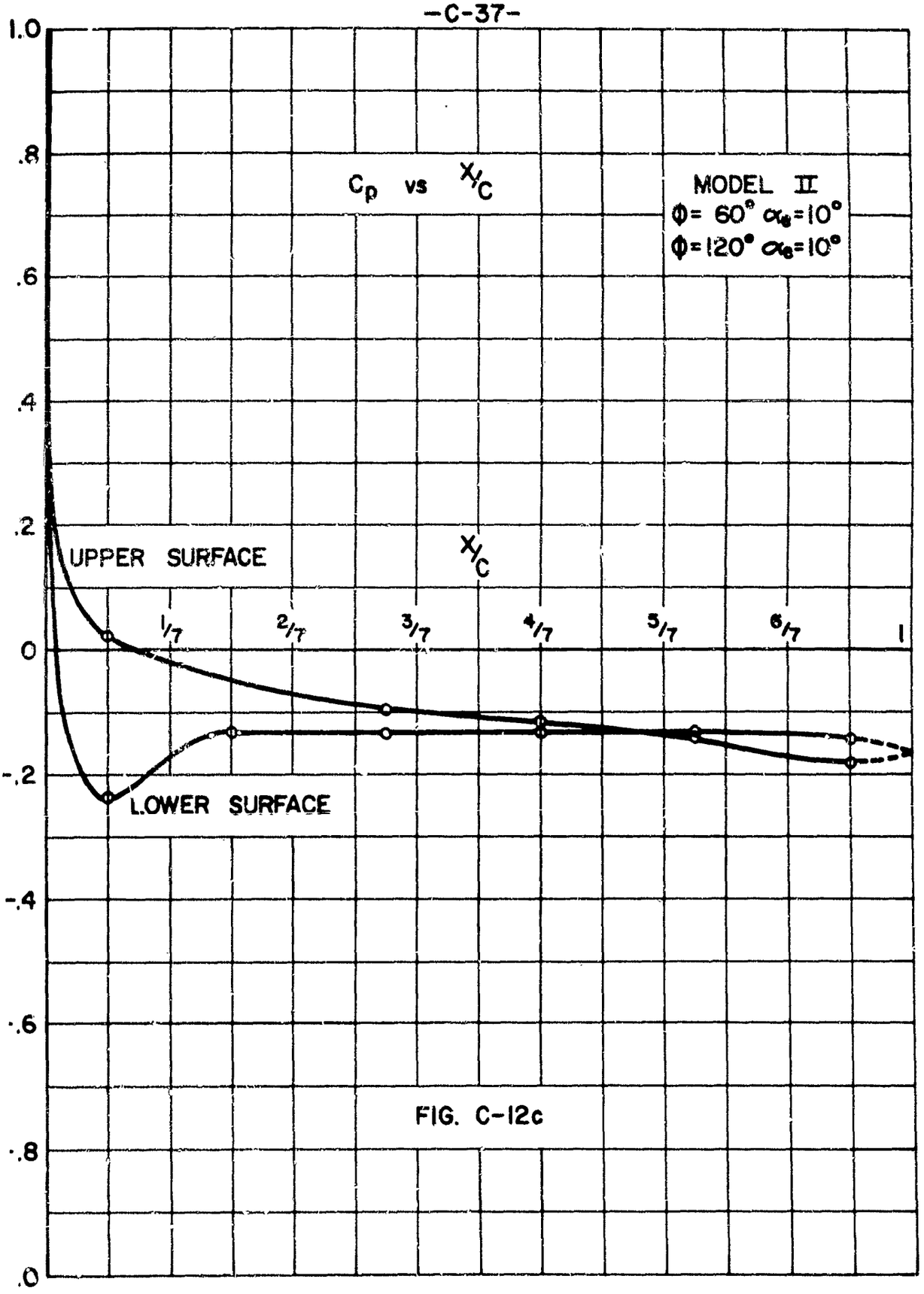
1.0
.8
.6
.4
.2
0
-.2
-.4
·.6
·.8
.0
C_p vs X/C
MODEL II
$\Phi = 60^\circ$ $\alpha_s = 10^\circ$
$\Phi = 120^\circ$ $\alpha_s = 10^\circ$
UPPER SURFACE
LOWER SURFACE
X/C
1/7
2/7
3/7
4/7
5/7
6/7
1

FIG. C-12c

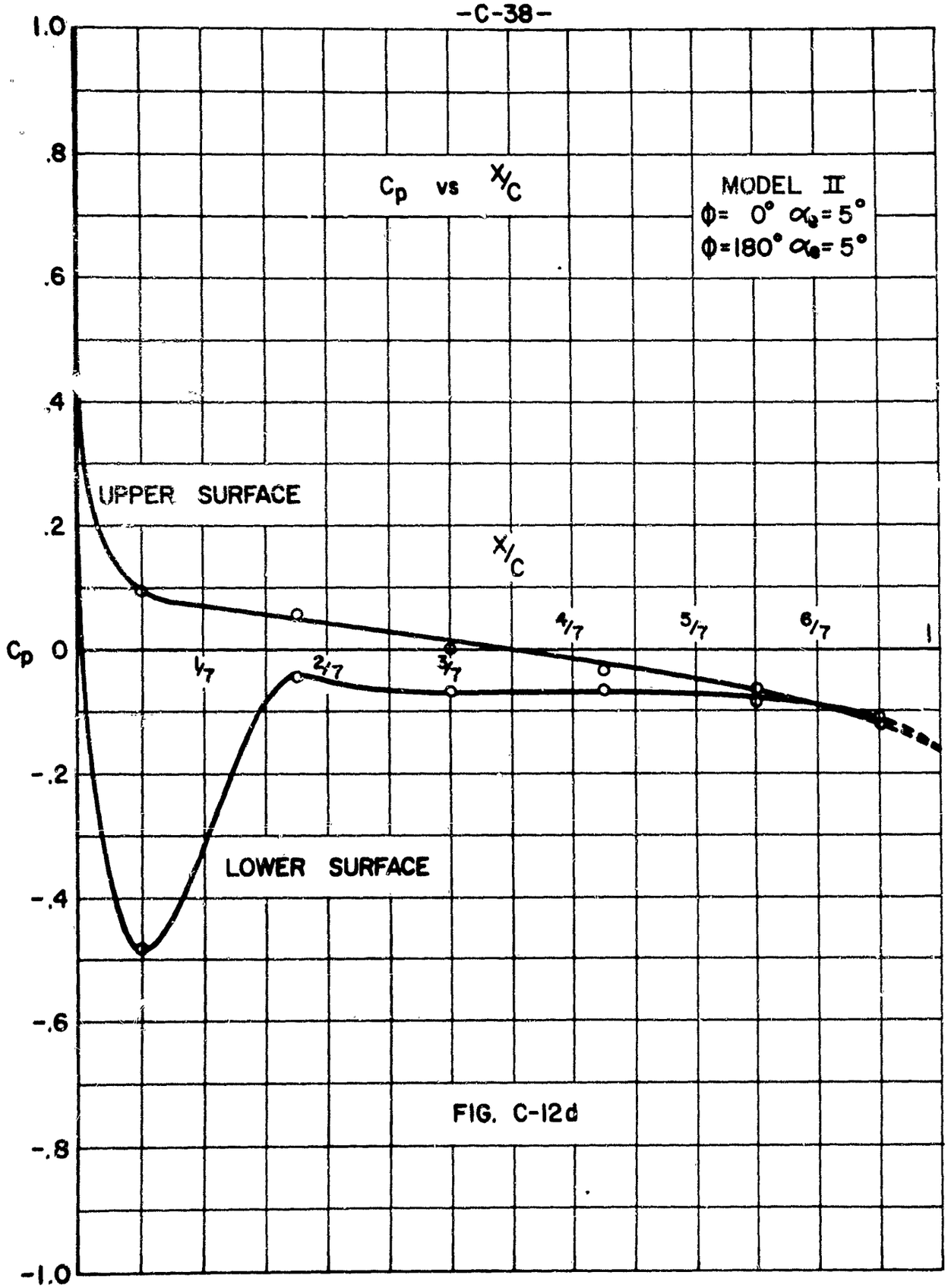
1.0
.8
.6
.4
.2
0
-.2
-.4
-.6
-.8
-1.0
C_p
C_p vs X/C
MODEL II
$\phi = 0°$ $\alpha_0 = 5°$
$\phi = 180°$ $\alpha_0 = 5°$
UPPER SURFACE
LOWER SURFACE
X/C
1/7
2/7
3/7
4/7
5/7
6/7
1

FIG. C-12d

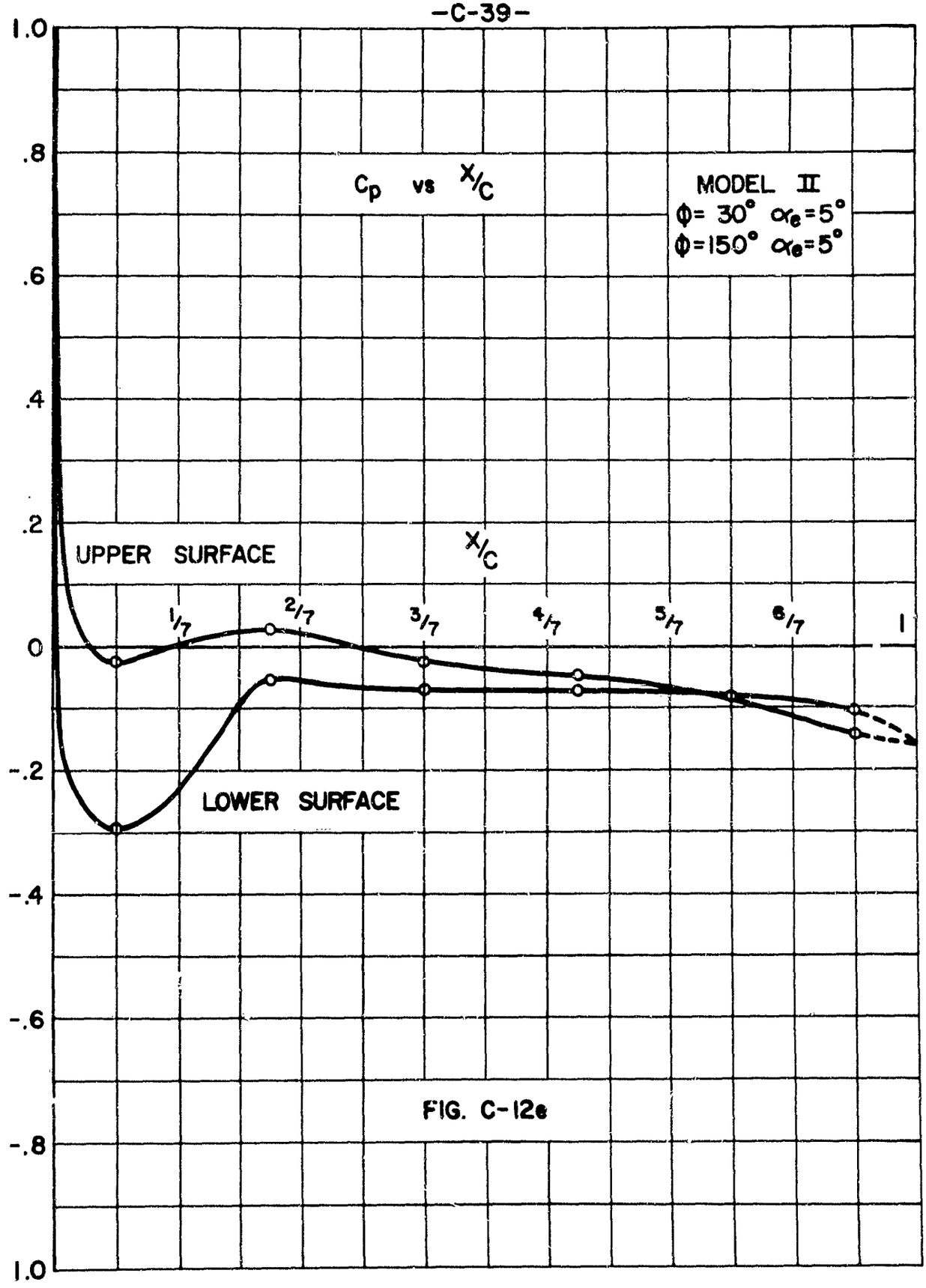
1.0
.8
.6
.4
.2
0
-.2
-.4
-.6
-.8
1.0
C_p vs X/C
MODEL II
ϕ= 30° α_e=5°
ϕ=150° α_e=5°
UPPER SURFACE
X/C
1/7
2/7
3/7
4/7
5/7
6/7
1
LOWER SURFACE

FIG. C-12e

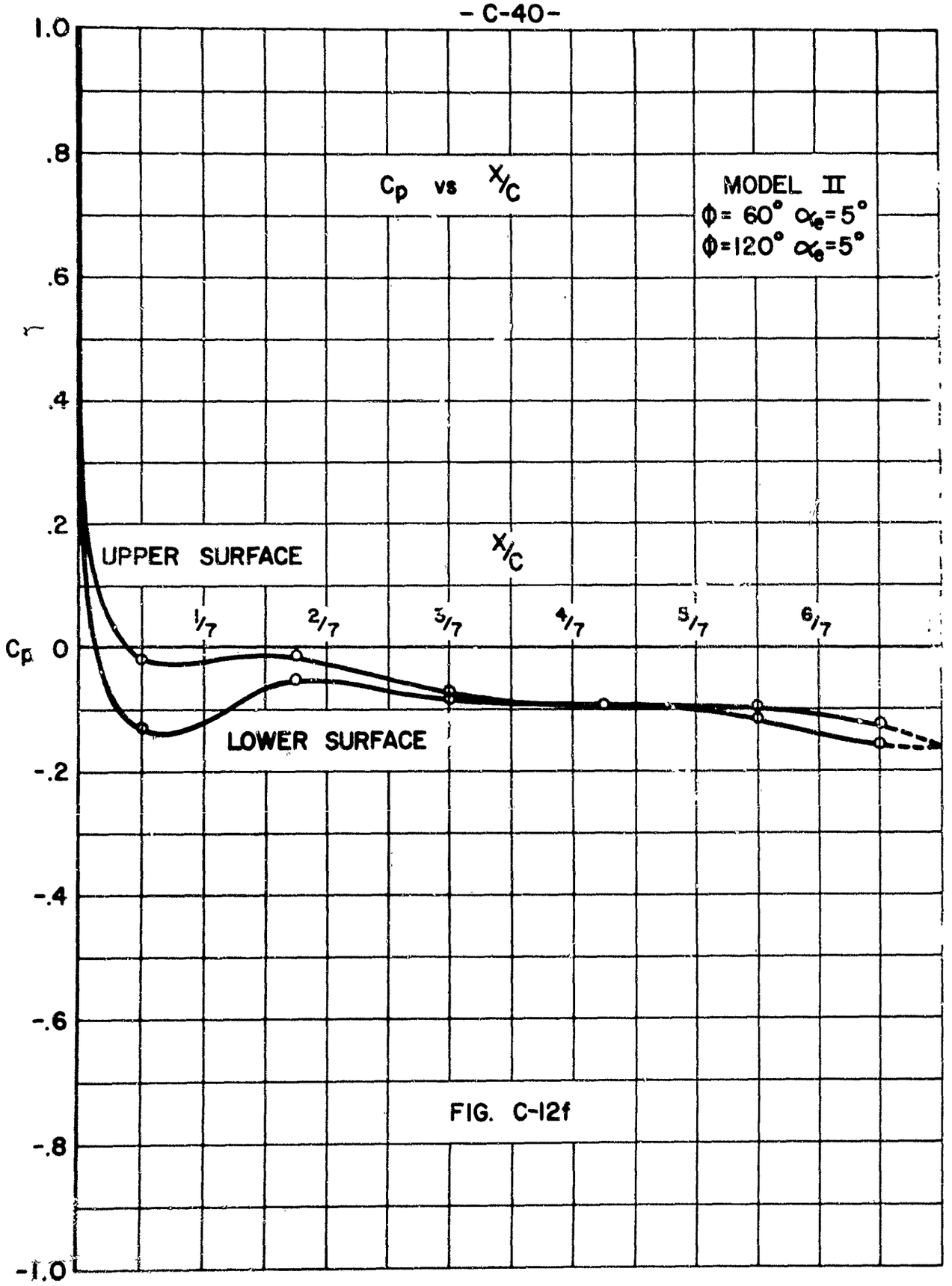
1.0
.8
.6
.4
.2
0
-.2
-.4
-.6
-.8
-1.0
C_p
C_p vs X/C
MODEL II
$\Phi = 60^\circ$ $\alpha_e = 5^\circ$
$\Phi = 120^\circ$ $\alpha_e = 5^\circ$
UPPER SURFACE
LOWER SURFACE
X/C
1/7
2/7
3/7
4/7
5/7
6/7

FIG. C-12f

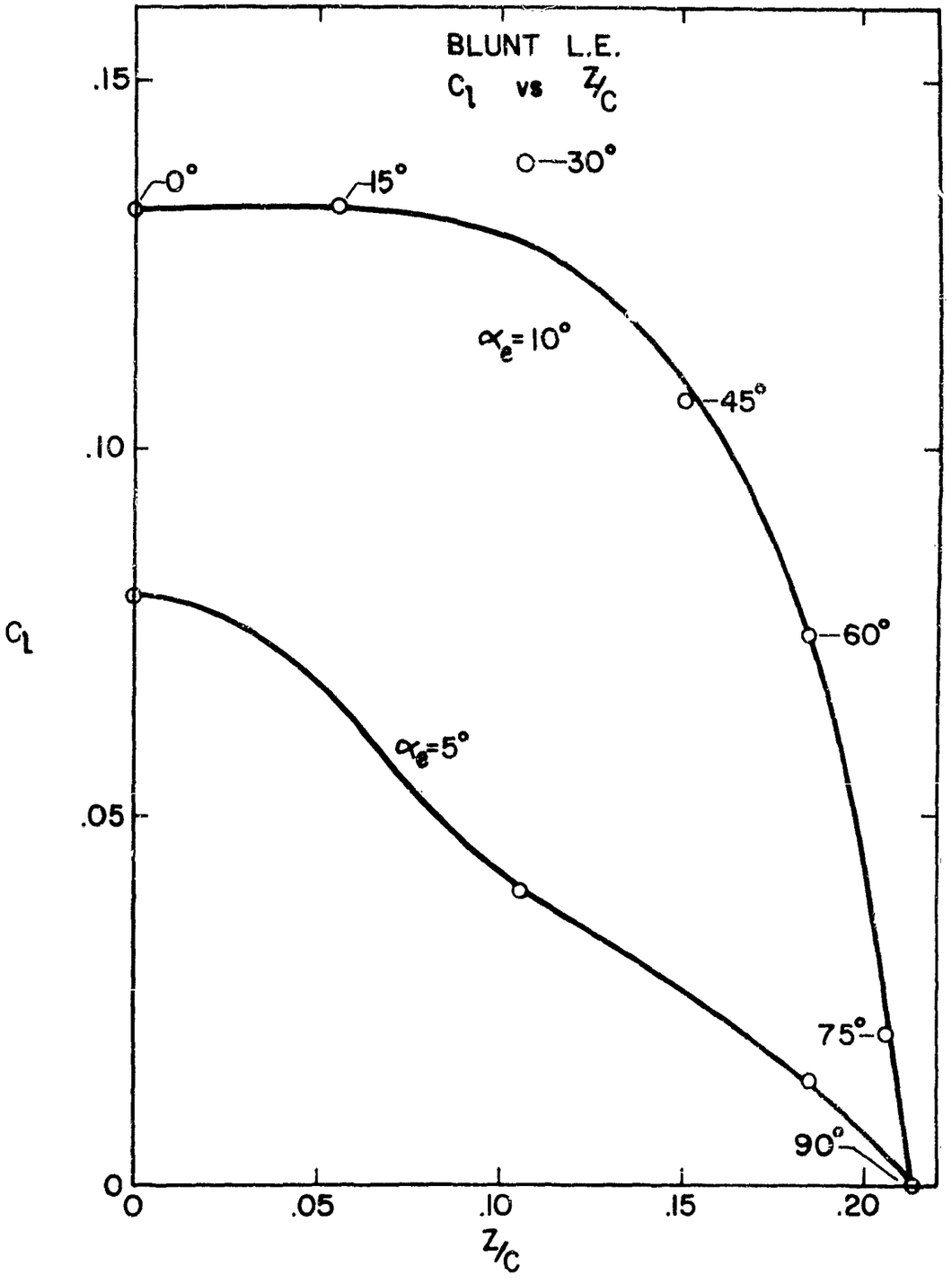
BLUNT L.E.
C_l vs Z/C
○—30°
0°
15°
α_e=10°
45°
60°
α_e=5°
75°
90°
.15
.10
.05
0
0
.05
.10
.15
.20
C_l
Z/C

FIG. C-13

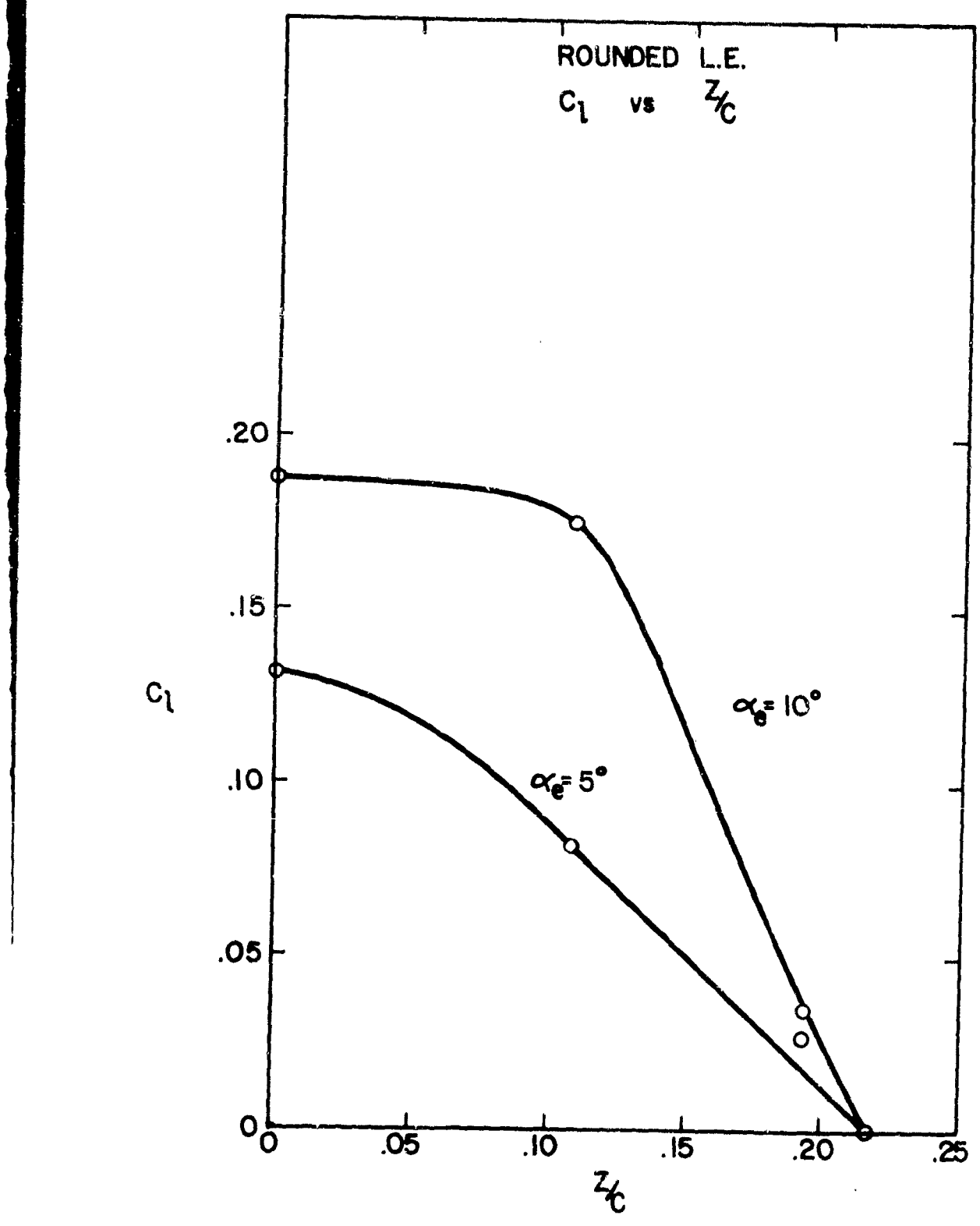
ROUNDED L.E.
C_l vs Z/C
.20
.15
.10
.05
0
C_l
α_e= 10°
α_e= 5°
0
.05
.10
.15
.20
.25
Z/C

FIG. C-14

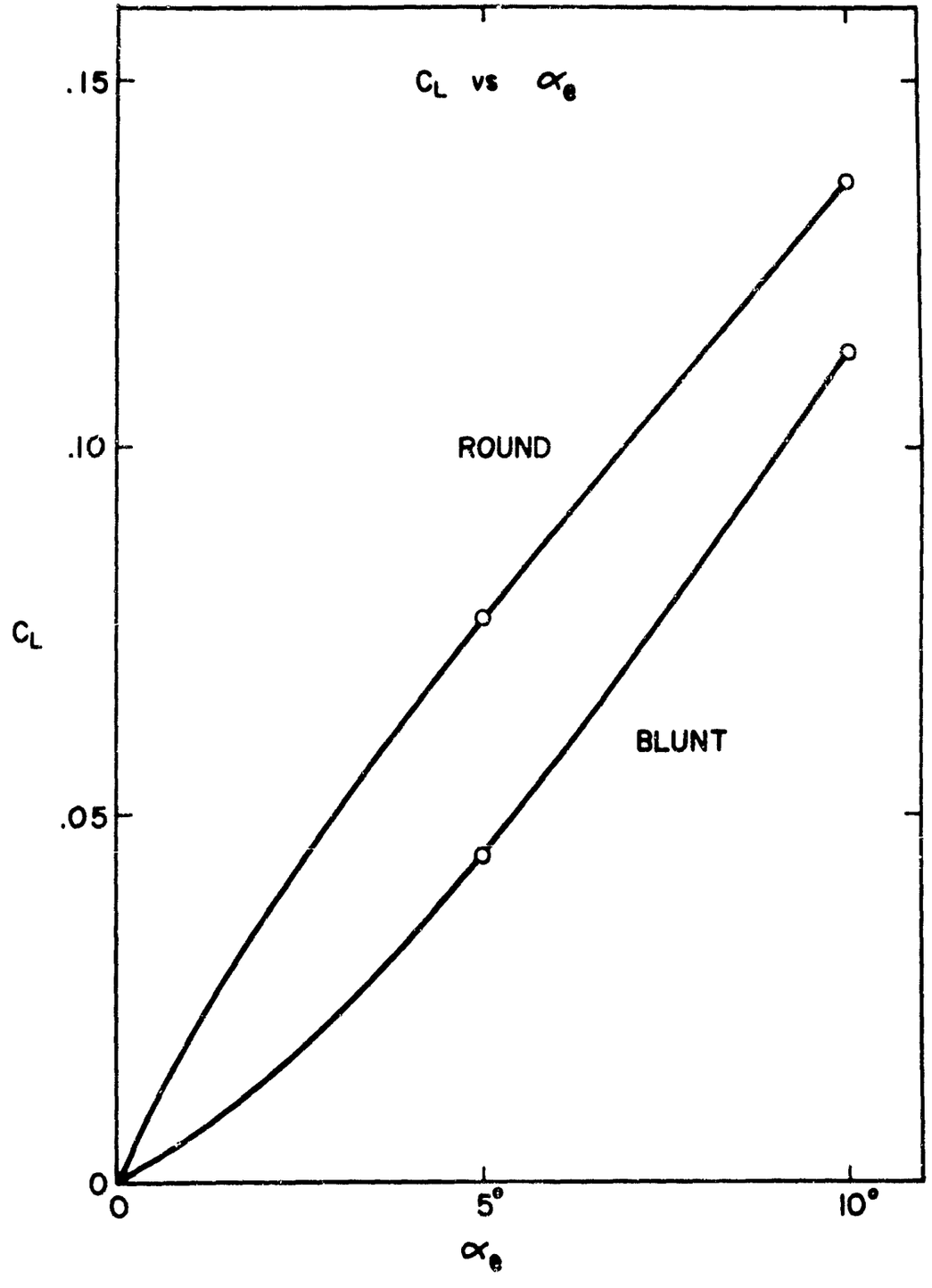

FIG. C-15

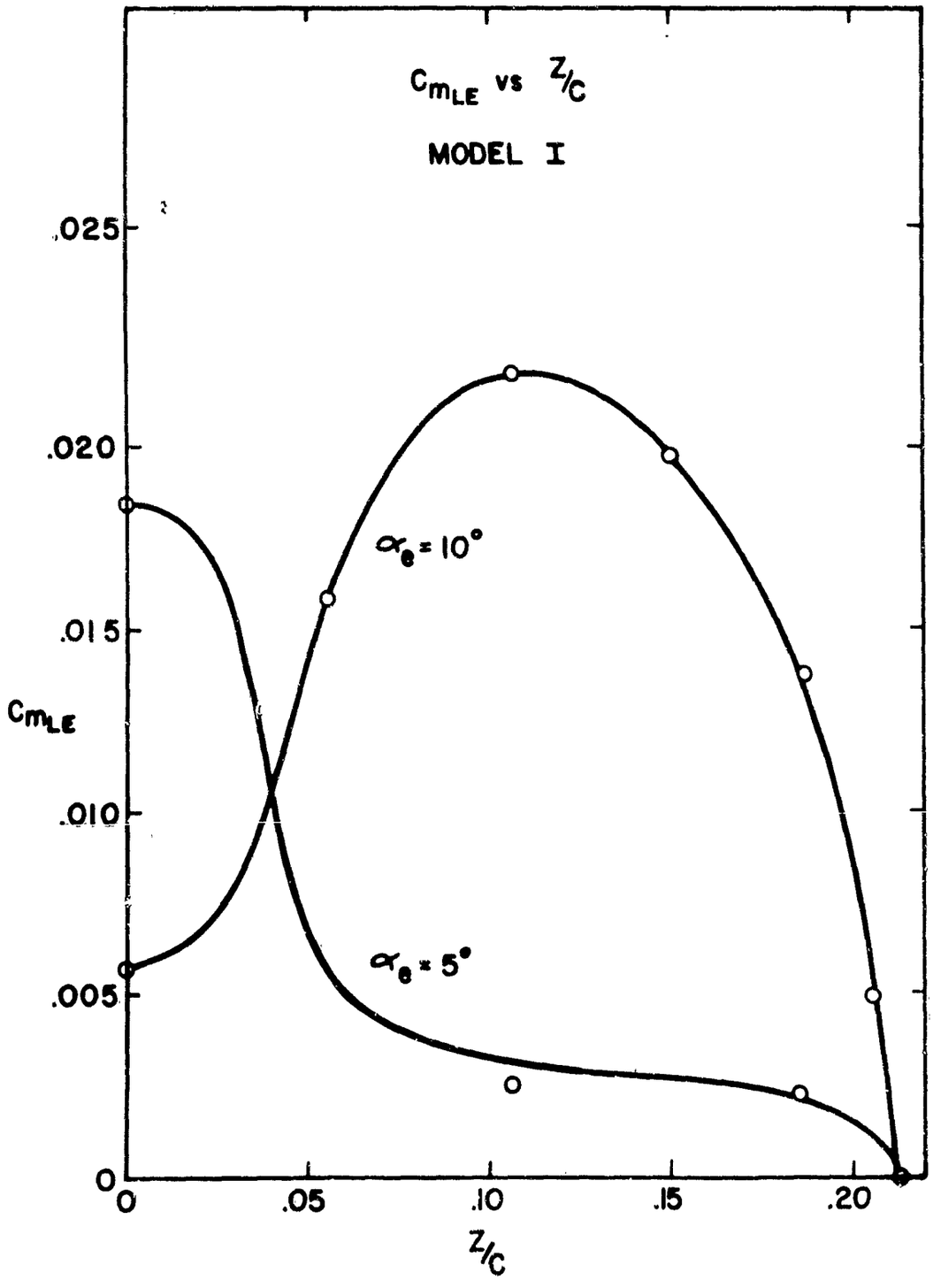
$C_{m_{LE}}$ vs Z/C
MODEL I
.025
.020
.015
.010
.005
0
$C_{m_{LE}}$
$\alpha_e = 10°$
$\alpha_e = 5°$
0
.05
.10
.15
.20
Z/C

FIG. C-16

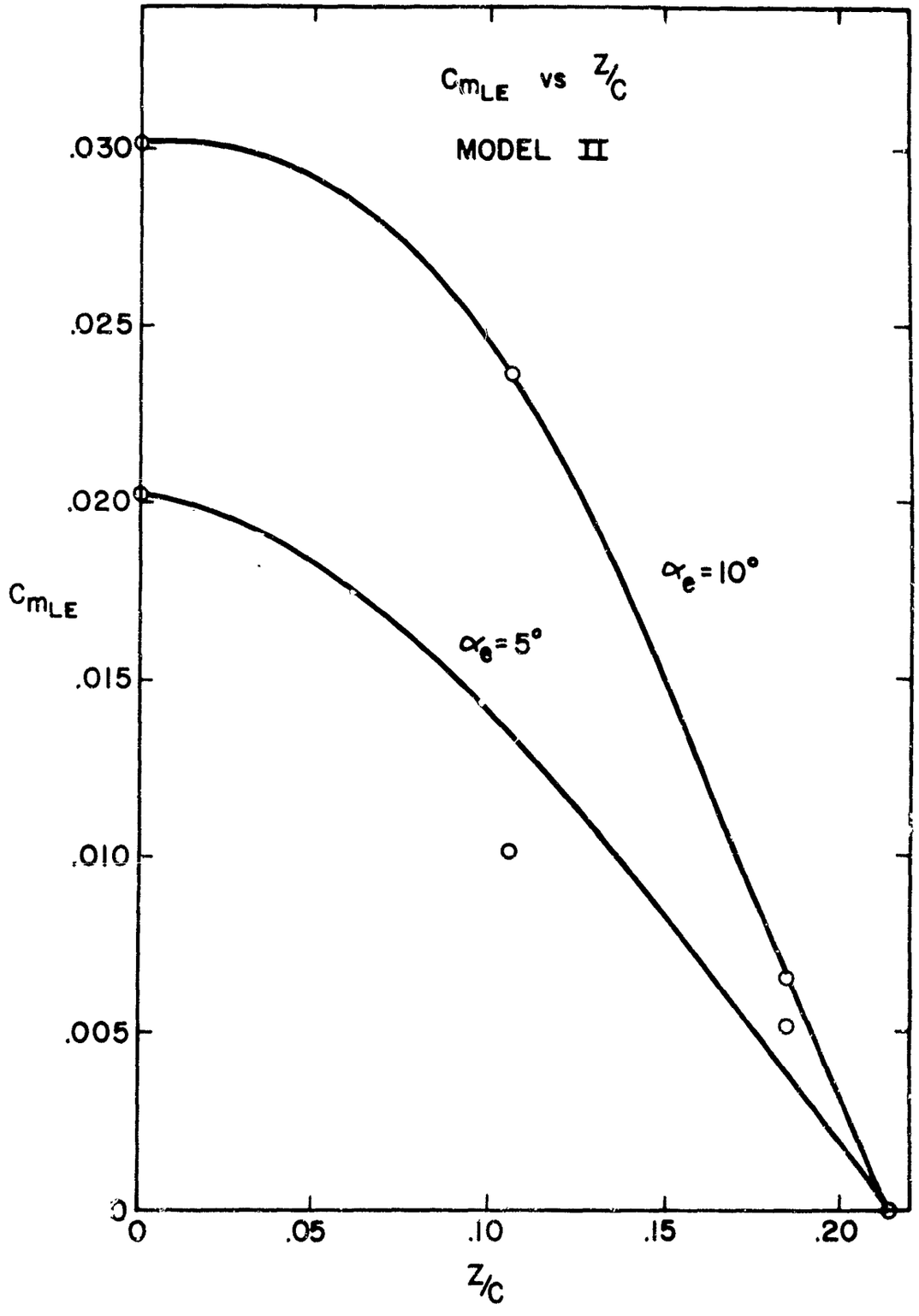
$C_{m_{LE}}$ vs Z/C
MODEL II
.030
.025
.020
.015
.010
.005
0
$C_{m_{LE}}$
$\alpha_e = 10°$
$\alpha_e = 5°$
0
.05
.10
.15
.20
Z/C

FIG. C-17

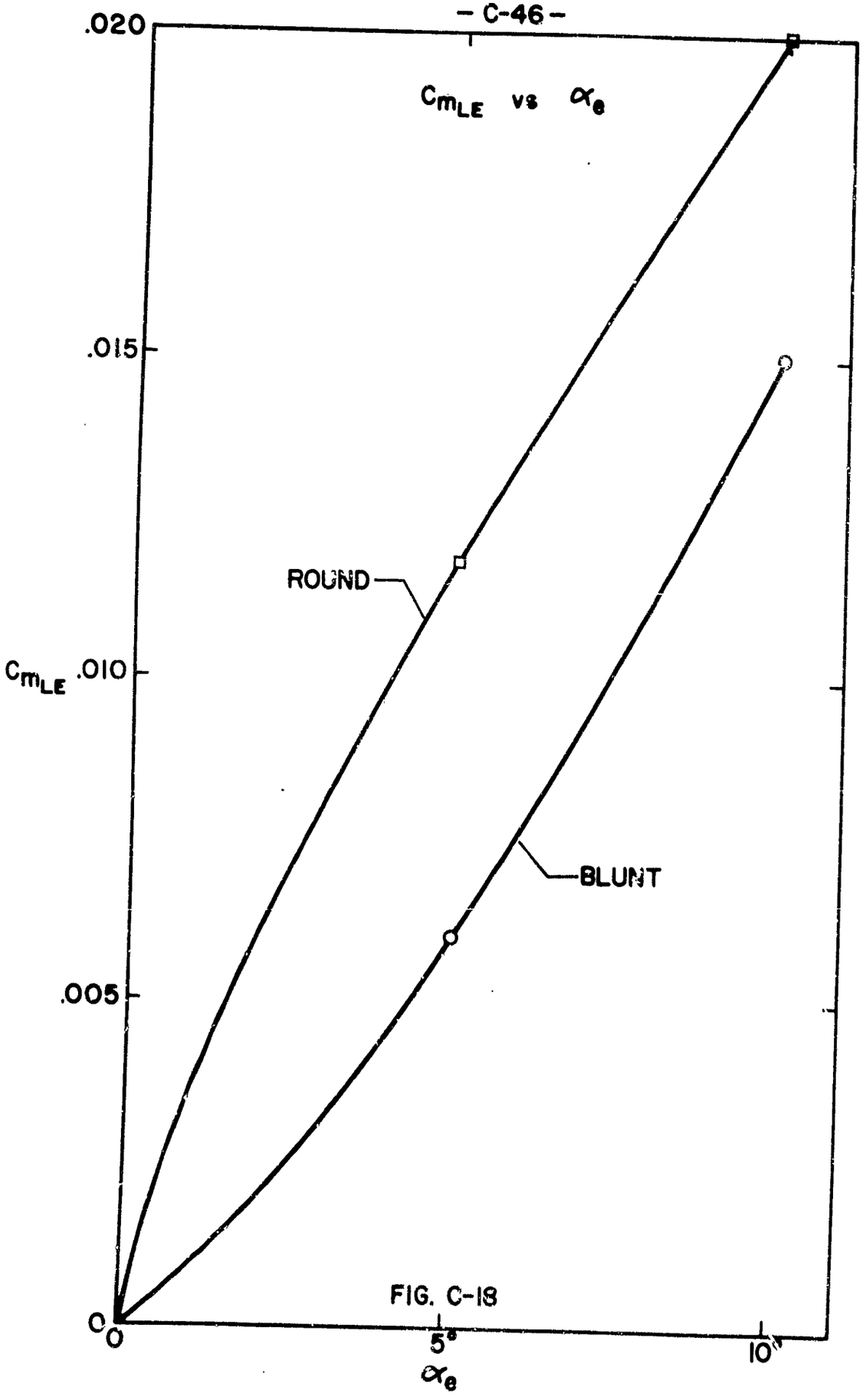

FIG. C-18

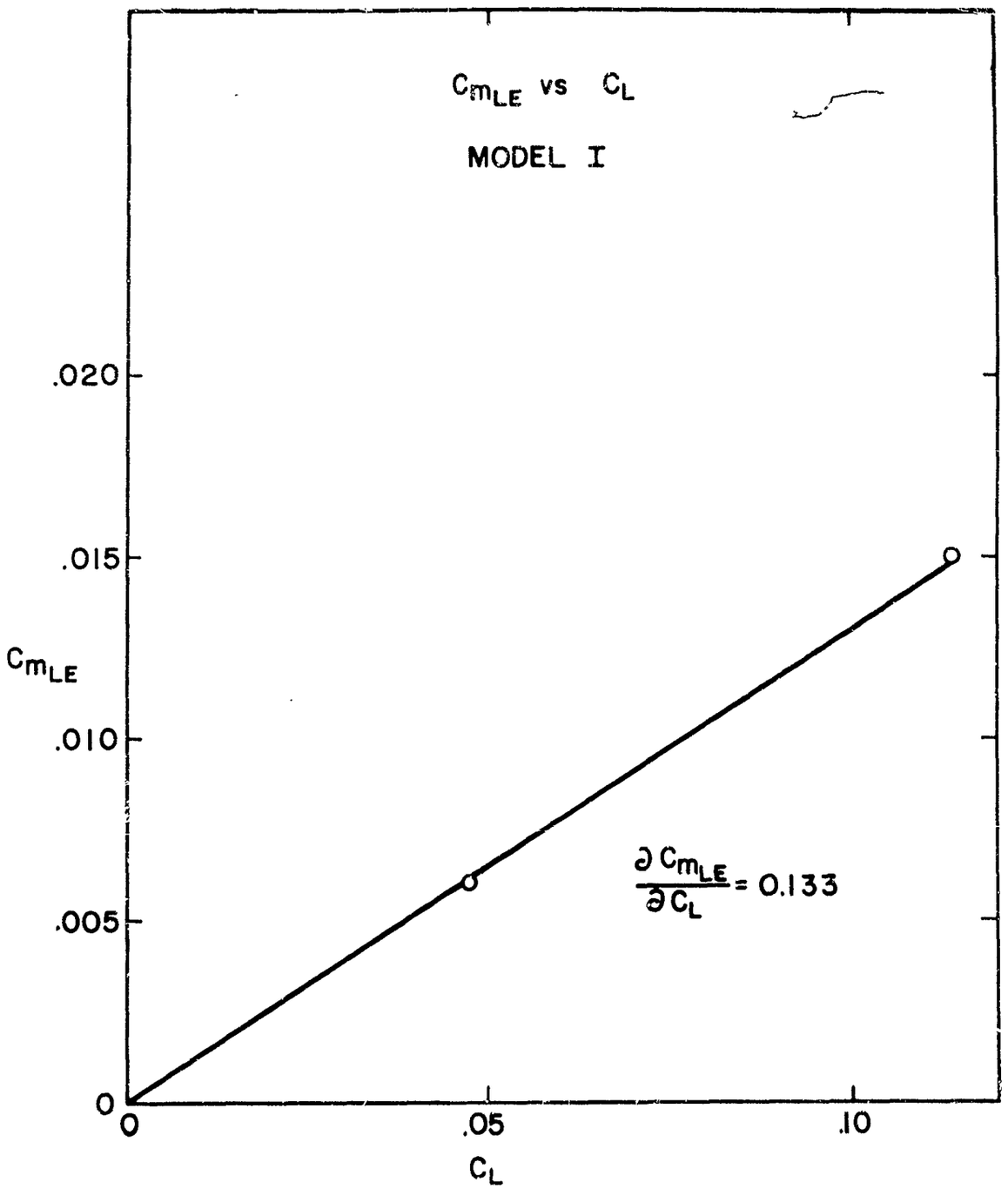
$C_{m_{LE}}$ vs C_L
MODEL I
.020
.015
.010
.005
0
$C_{m_{LE}}$
0
.05
.10
C_L
$\frac{\partial C_{m_{LE}}}{\partial C_L} = 0.133$

FIG. C-19

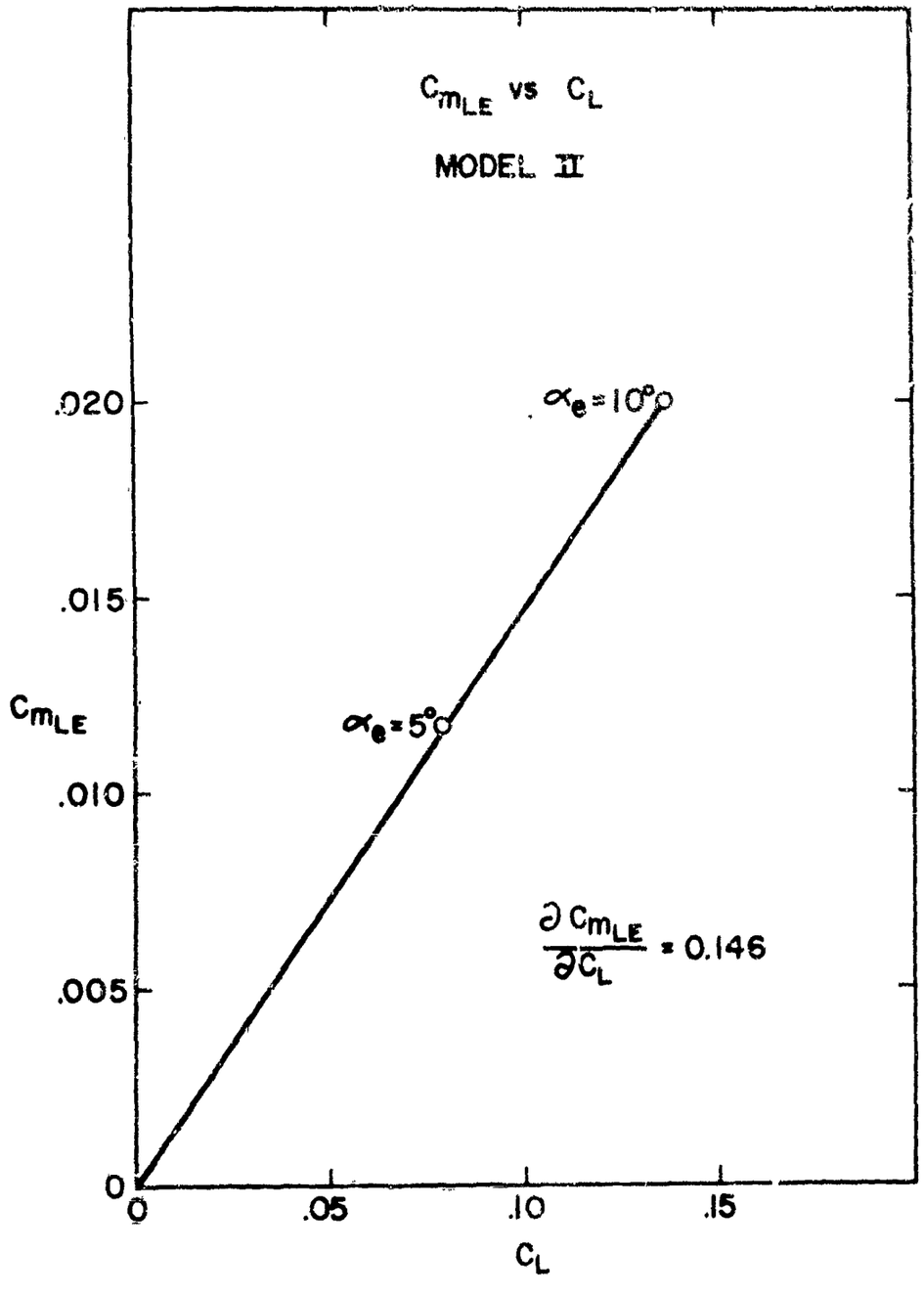
$C_{m_{LE}}$ vs C_L
MODEL II
.020
.015
.010
.005
0
$C_{m_{LE}}$
$\alpha_e = 10°$
$\alpha_e = 5°$
$\frac{\partial C_{m_{LE}}}{\partial C_L} = 0.146$
0
.05
.10
.15
C_L

FIG. C-20

RESULTS

r = 0.26

MODEL	α_e	C_L	$C_{M_{LE}}$	$\frac{\partial C_{M_{LE}}}{\partial C_L}$
I	5	.044	.0060	0.133
I	10	.113	.0150	0.133
II	5	079	.0118	0.146
II	10	.137	.0200	0.146

FIG. C-21

C_p vs ϕ, POSITIONS ① - ⑥

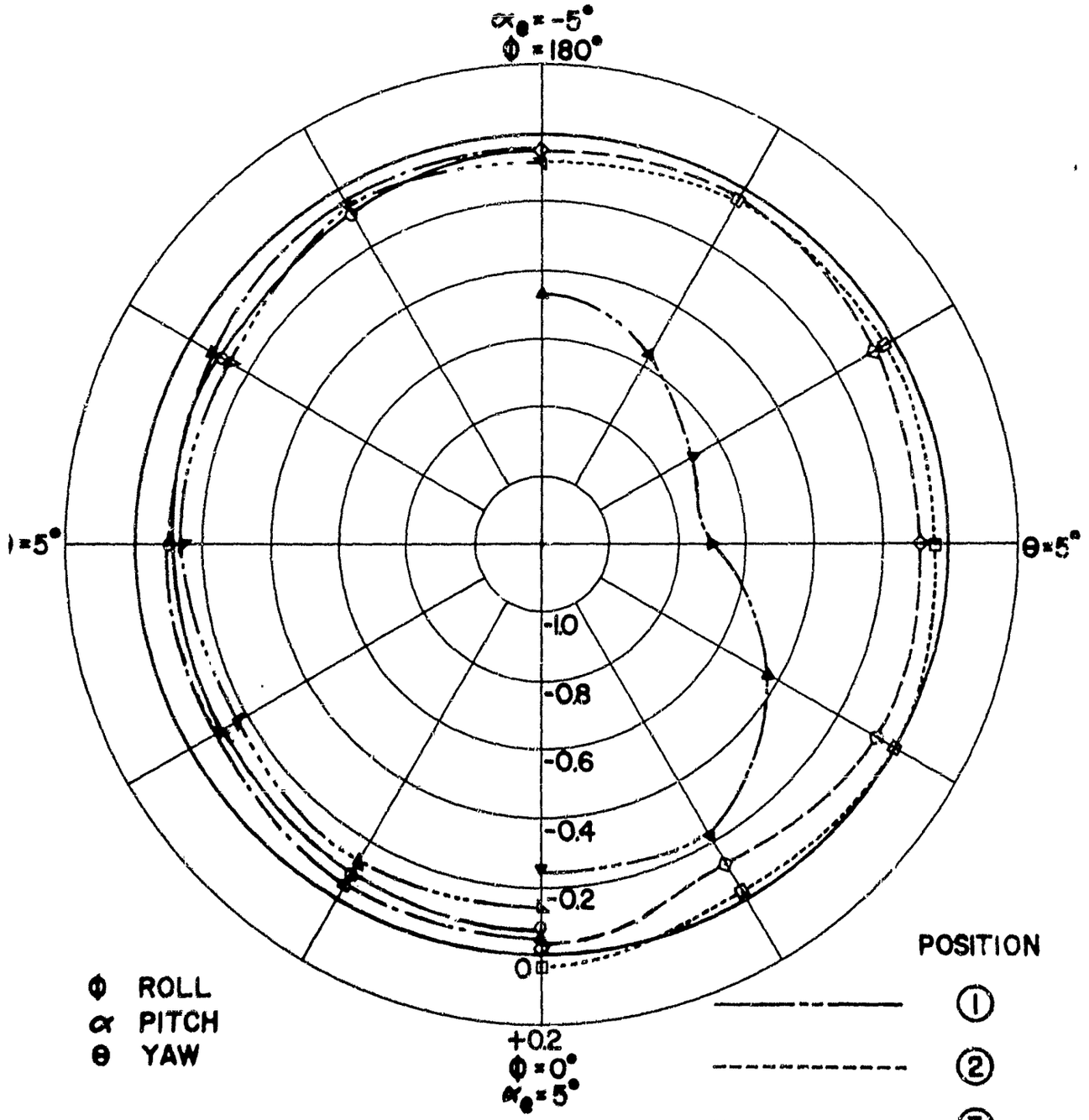

ϕ ROLL
α PITCH
θ YAW

MODEL I
r = 0.17
α_θ = ±°

FIG. C-22

C_p vs ϕ, POSITIONS ① - ⑥

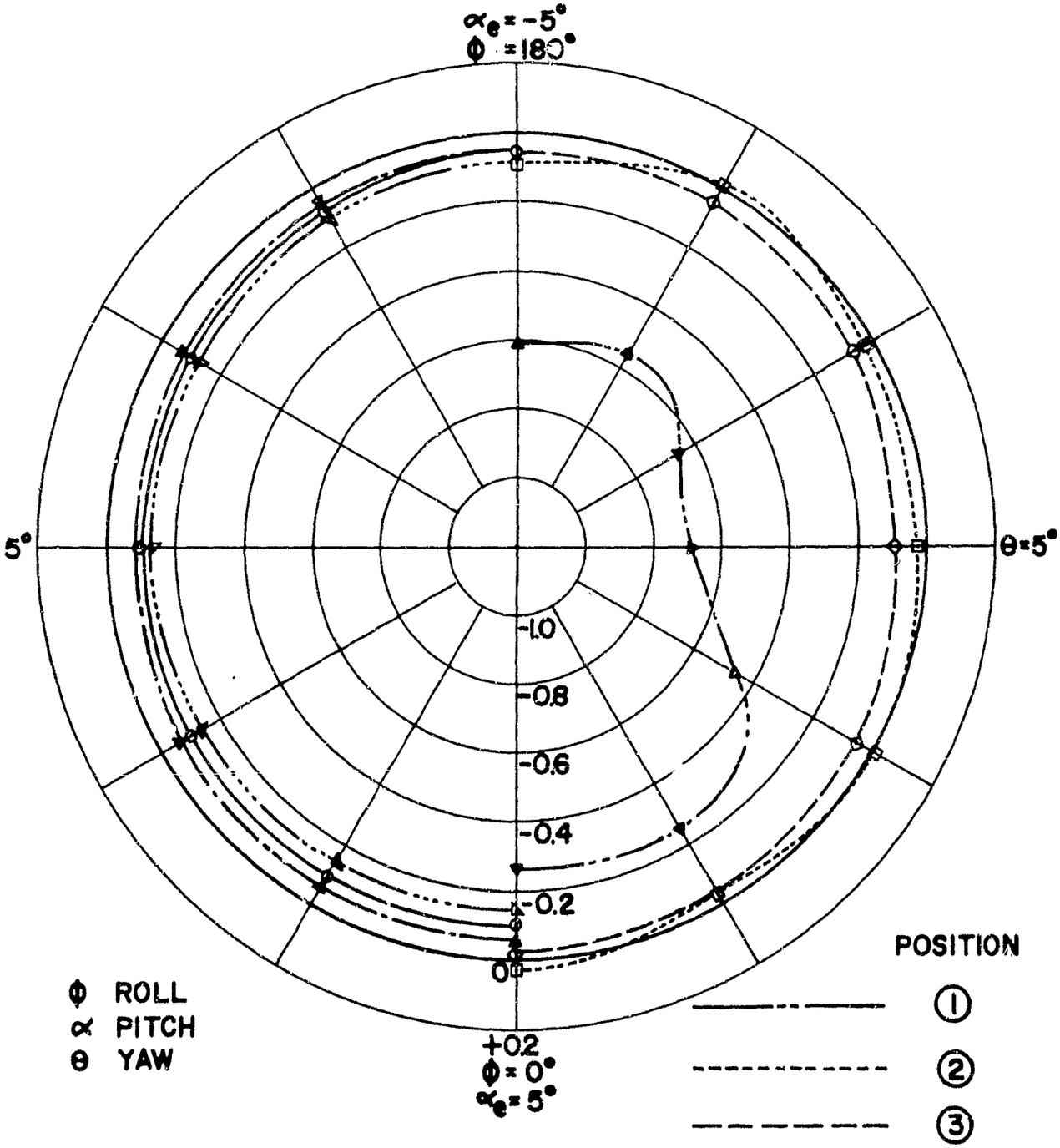

ϕ ROLL
α PITCH
θ YAW

POSITION
① ——·——
② - - - - -
③ — — — —
④ ———
⑤ ———
⑥ ——·——

MODEL I
r = 0.26
$\alpha_e = 5°$

FIG. C-23

C_p vs ϕ POSITIONS ① - ⑥

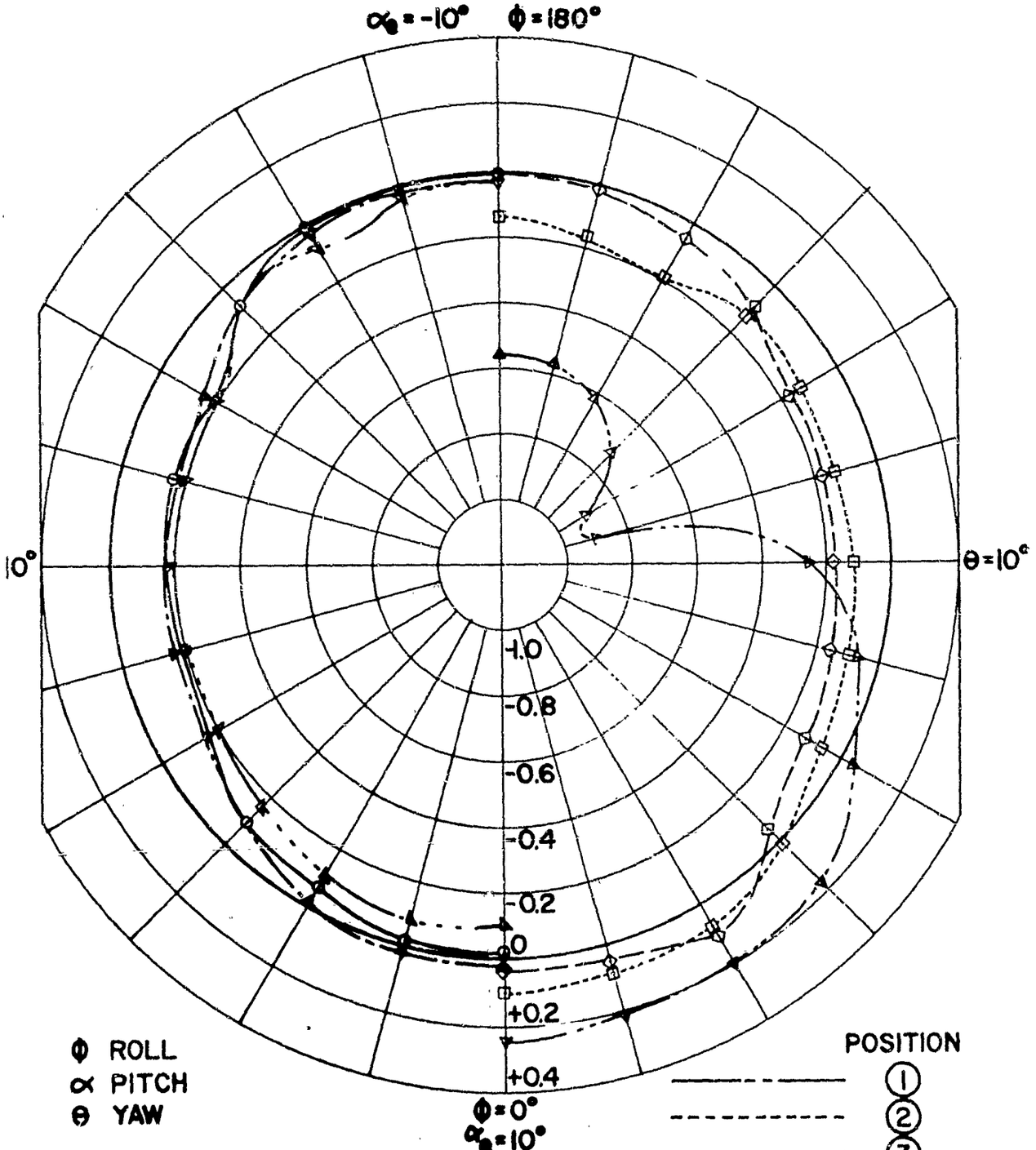

MODEL I
r = 0.17
α_s = 10°

FIG. C-24

C_p vs Φ

$\alpha_e = -10°$

POSITIONS ① – ⑥

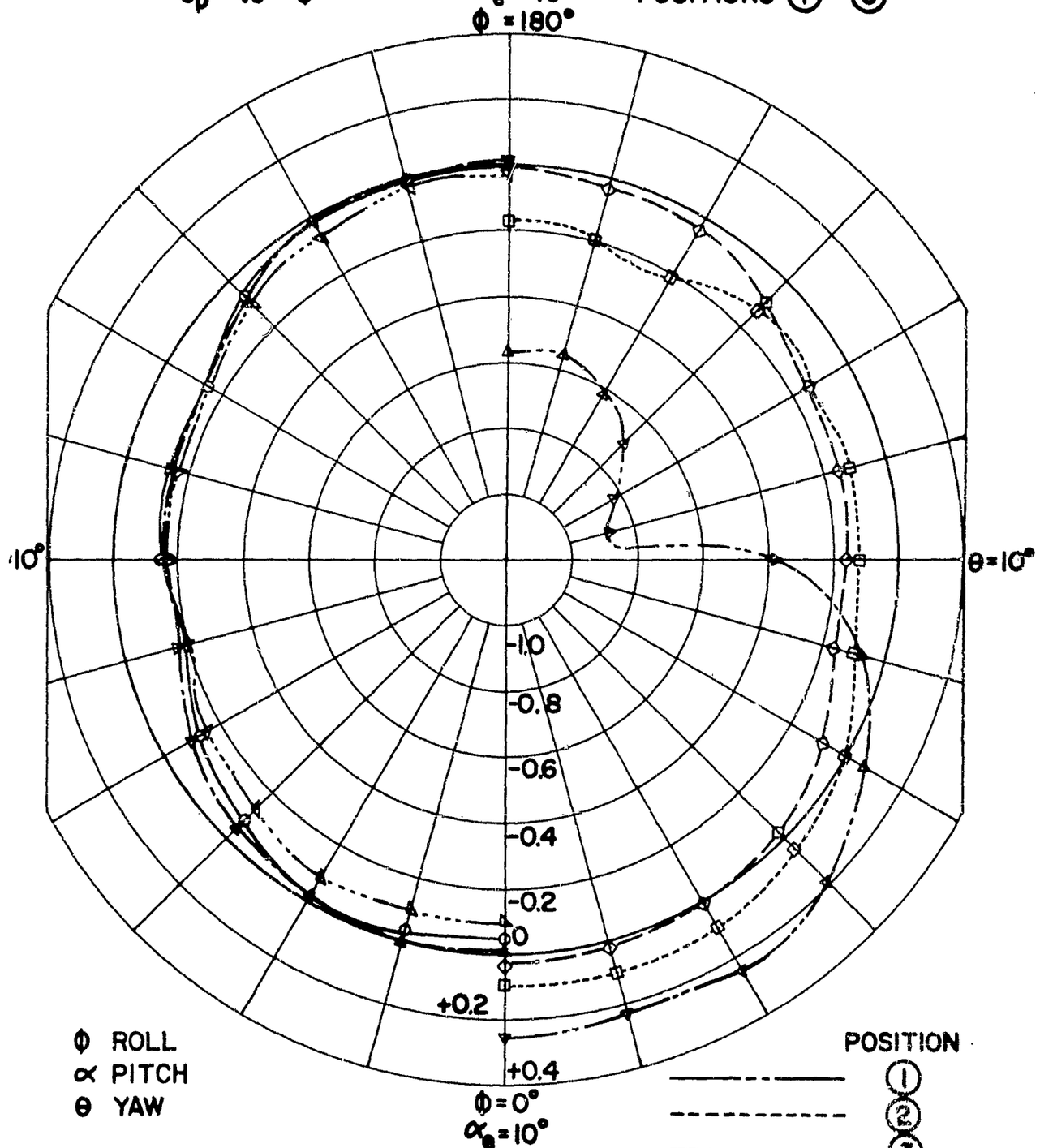

Φ ROLL
α PITCH
θ YAW

MODEL I
r = 0.26
$\alpha_e = 10°$

POSITION
① ——— ———
② ----------
③ — — — —
④ ——— ———
⑤ ———————
⑥ ——— ———

FIG. C-25

Cp vs ϕ

$\alpha_\theta = -5°$
$\phi = 180°$

POSITIONS ① - ⑥

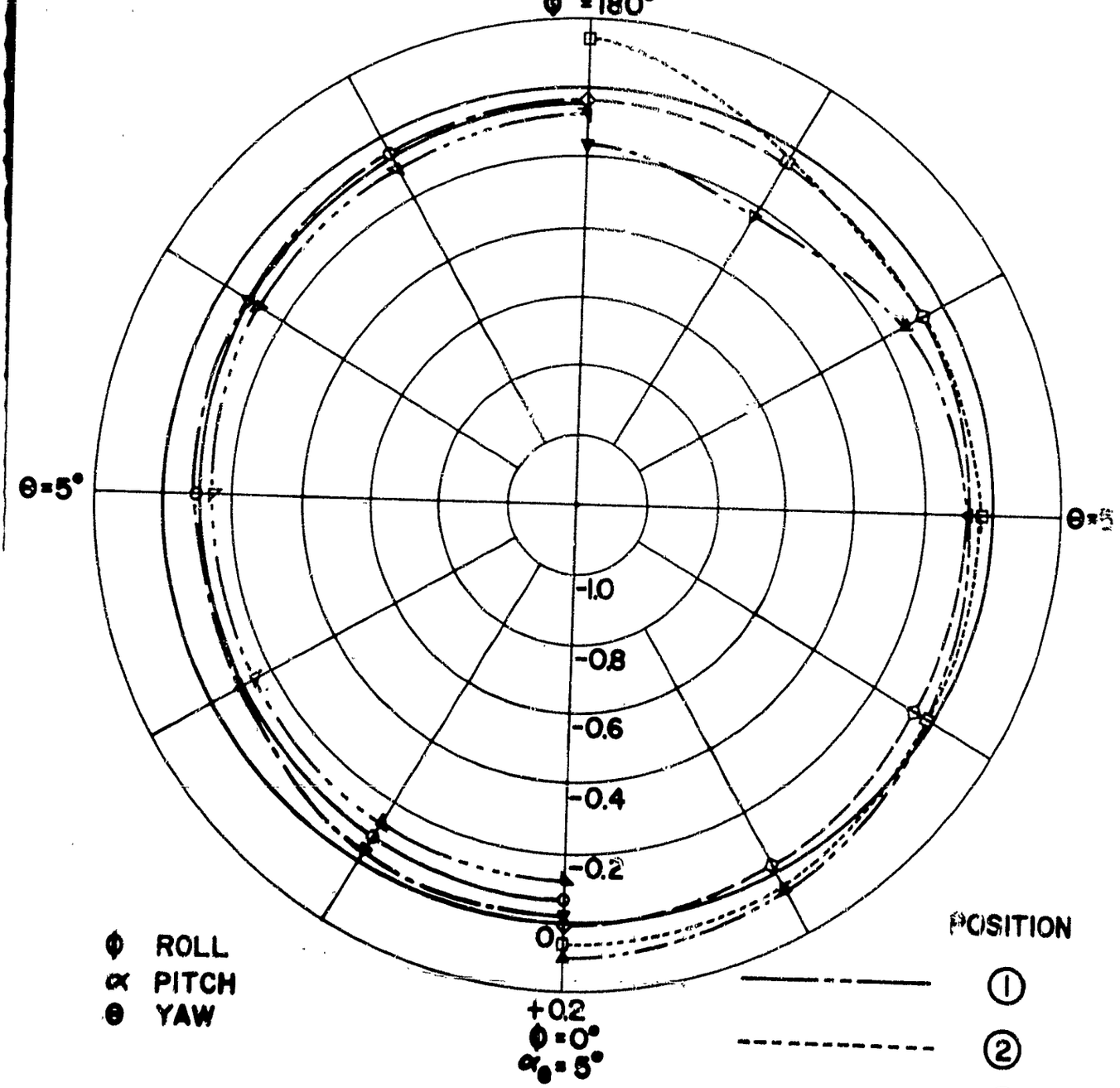

ϕ ROLL
α PITCH
θ YAW

POSITION

① ——— ———
② ----------
③ — — — —
④ ——— ———
⑤ ———————
⑥ ——— ---

MODEL II
r = 0.17
$\alpha_\theta = 5°$

FIG. C-26

C_p vs Φ, POSITIONS ① - ⑥

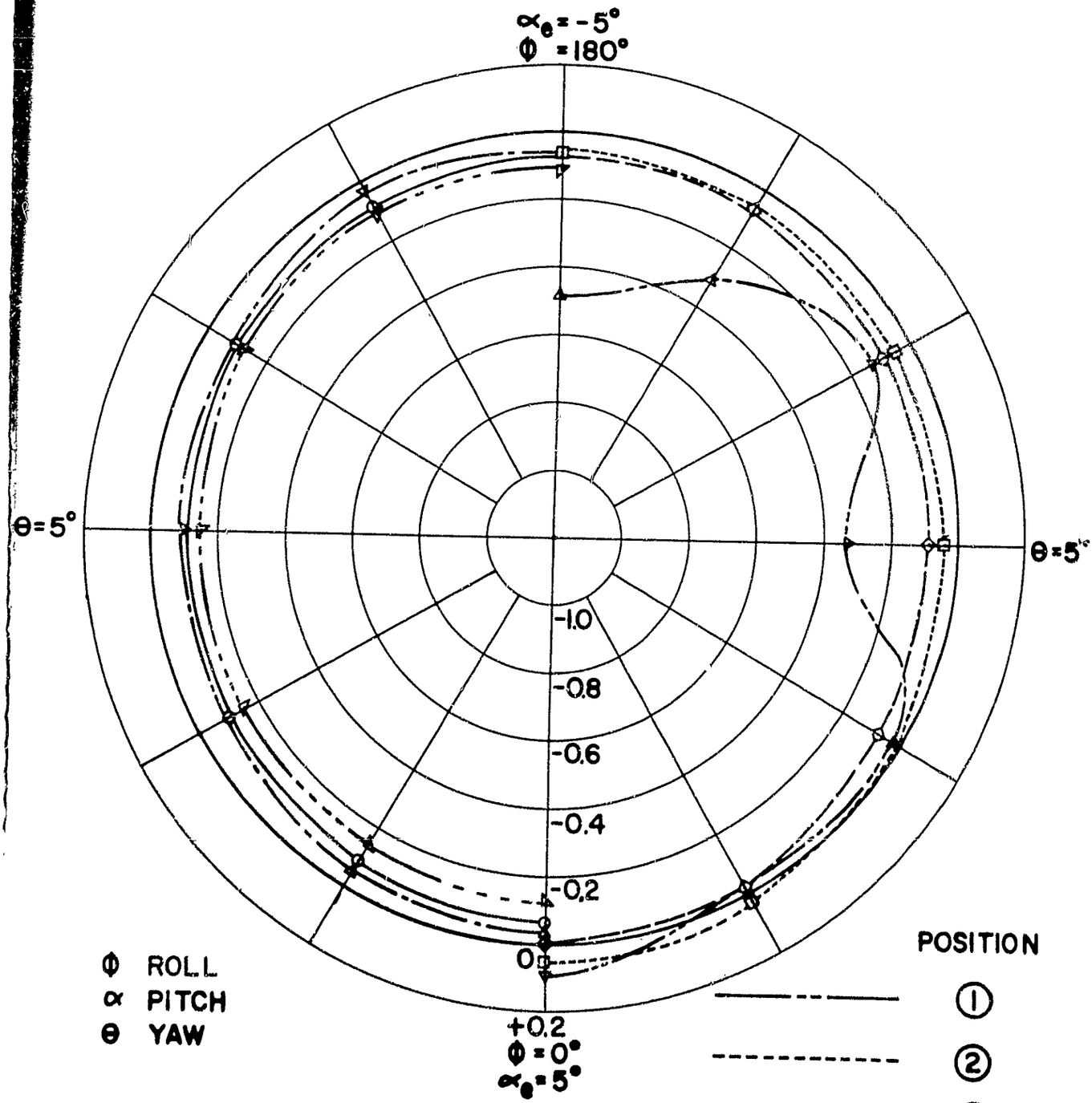

Φ ROLL
α PITCH
Θ YAW

POSITION

① ——— ———
② ----------
③ — — — —
④ ——— —
⑤ ———
⑥ ——— ———

MODEL II
r = 0.26
$\alpha_e = 5°$

FIG. C-27

C_p vs ϕ

α_e=-10°
ϕ =180°

POSITIONS ① – ⑥

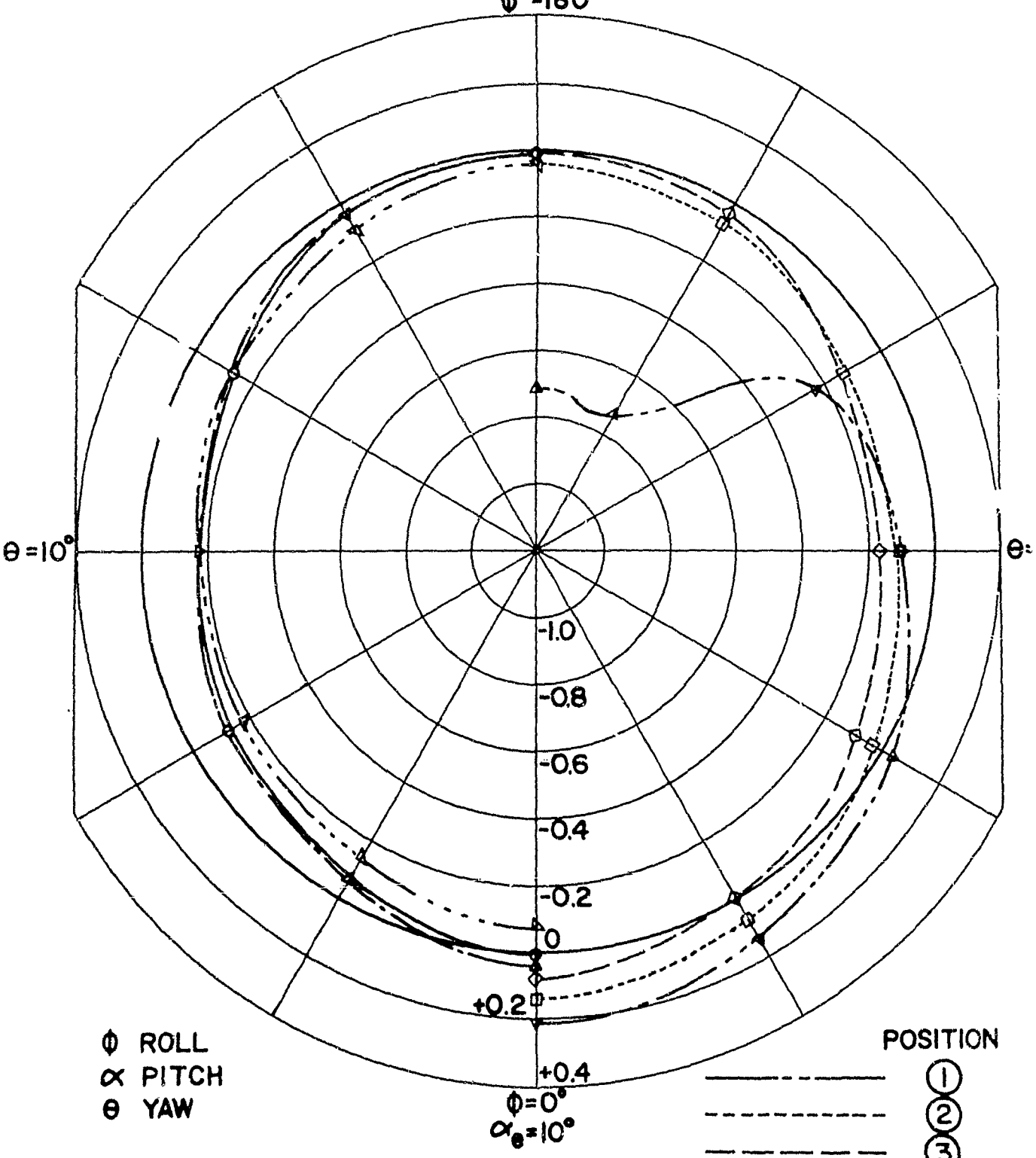

φ ROLL
α PITCH
θ YAW

MODEL II
r = 0.17
α_e= 10°

POSITION
① ——— ———
② – – – – –
③ — — — —
④ ——— ———
⑤ ———
⑥ ——— ———

FIG. C-28

C_p vs ϕ, POSITIONS ① – ⑥

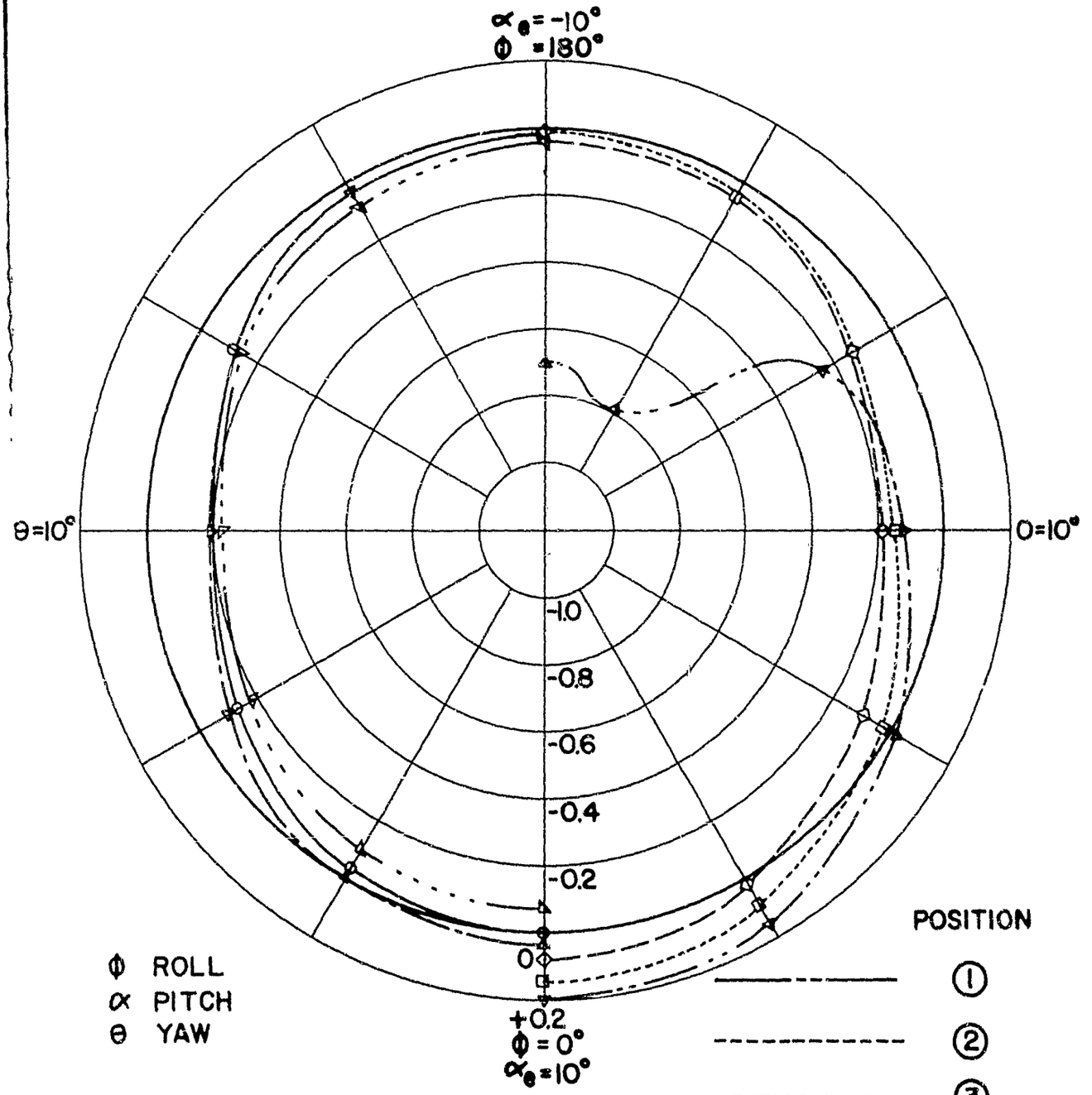

ϕ ROLL
α PITCH
θ YAW

POSITION
① ——— ———
② ----------
③ — — — — —
④ ——— ———
⑤ ———————
⑥ ———————

MODEL II
r = 0.26
α_e = 10°

FIG. C-29

SECTION D

MEASUREMENT OF FORCES AND MOMENTS ACTING ON A VEHICLE IN A TUBE

by

John W. Burr

INTRODUCTION

The question as to whether a vehicle traveling in a tube would be aerodynamically stable or unstable has been examined in the light of experimental pressure surveys in Section C of this report. The present section deals with tests for the re-examination of the same question in the light of direct measurements of forces and moments.

Because of a series of failures in the facilities used for the tests reported here, the planned experimental program could not be completed. The present experimental rig, however, is satisfactory and will be used in further tests. Only initial results are presented here.

EXPERIMENTAL APPARATUS

Facility

The tests reported here were conducted in one of the test cells of the Department of Aeronautical Engineering and Astronautics of Rensselaer Polytechnic Institute Contained within this cell is a Rolls Royce Merlin supercharger driven by a variable speed dynamometer. The supercharger is connected to a large reservoir (see Fig. D-1) and can evacuate this reservoir to pressures ranging from atmospheric to twenty inches of vacuum, depending upon the mass flow delivered. While running, the

supercharger can hold the pressure in the reservoir steady to within 0.2 of an inch of water.

Model

The tube of the tube-transport system is simulated by a stationary 6" diam. tube connected to the reservoir at its discharged end, and with a bellmouth opening to the atmosphere at its inlet end (see Fig. D-2). The model of the vehicle is held within the tube with its center about fifteen inches downstream of the inlet.

The model of the vehicle, shown in Fig. D-3, consists of a tube seven inches long, 2 and 7/8 inches in diameter with a 3/16 inch thick wall. The model has interchangeable leading edges.

The model is supported at mid station with a 1/2 inch thick sting which is in turn connected to a framework totaly supported by strain beam members. Since the sting must go through the wall of the tube without touching it, a space must be left around the sting. This would permit leakage of atmospheric air into the tube if a seal were not provided. To provide this seal the entire supporting structure including the strain beams is enclosed in a chamber which was in turn sealed (see Fig. D-4).

Instrumentation

The strain beam members consist of two drag beams and two lift beams connected directly above and below the model. A third drag beam is connected in the horizontal plane to provide yaw stability. This beam is connected to the framework by two ball joints to prevent the beam from providing any lift or side motion support. The force on all three drag beams must be added to give the total drag, the upper and lower drag beams must be subtracted and the result multiplied by the distance between the pin joints to give the pitching moment, and the force on the two lift beams must be added to give the total lift. Each of the three drag beams is instrumentedwith four Baldwin strain gages which are connected into a Wheatstone bridge. Each of the two lift beams is instrumented with two Baldwin strain gages and these four strain gages are connected to form a single Wheatstone bridge. The output from these four Wheatstone bridges is read on a Brown Verticle-Drum Millivoltmeter. The instrument rack containing the millivoltmeter and the balancing and control resistor is shown in Fig. D-5.

Procedure

The system was calibrated by attaching a long rod to the model and hanging weights from the rod in such a manner as to

simulate lift, drag and pitching moment and the deflection of the millivoltmeter was recorded. These readings were then converted to calibration curves. The calibration curve for lift is shown on Fig. D-6.

During the running the Mach number in the tube was determined from the atmospheric total pressure and the pressure in the reservoir tank. Since the reservoir was only about four tube diameters downstream of the model, the tank pressure was assumed to be equal to the static pressure in the tube.

Discussion

A plot of the model lift coefficient, defined as

$$C_L = \frac{Lift}{\frac{1}{2}\rho V^2 A}$$

where A is the total external wetted area of the model, is presented on Fig. D-7. The effect at Mach number is seen to be small over the range of the Mach numbers tested. Also, changing the shape of the leading edge from a rounded edge to a square, blunt edge does not seem to affect the lift coefficient appreciably.

Comparison of these results with the results of the pressure tests presented in Section C indicates good agreement (Fig. 7).

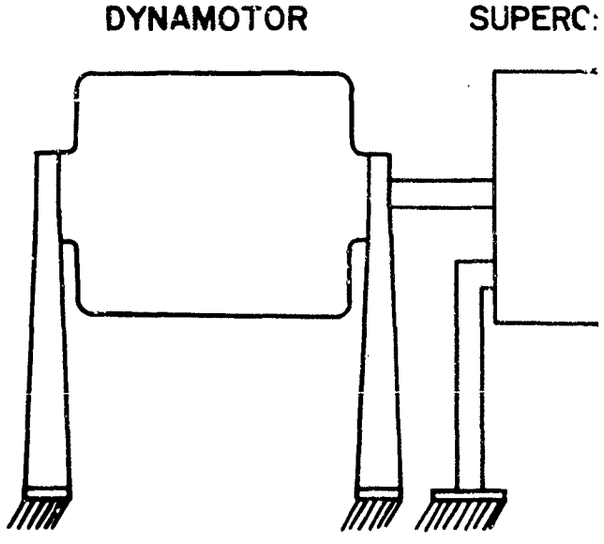

FIG. D-1: Schematic Di

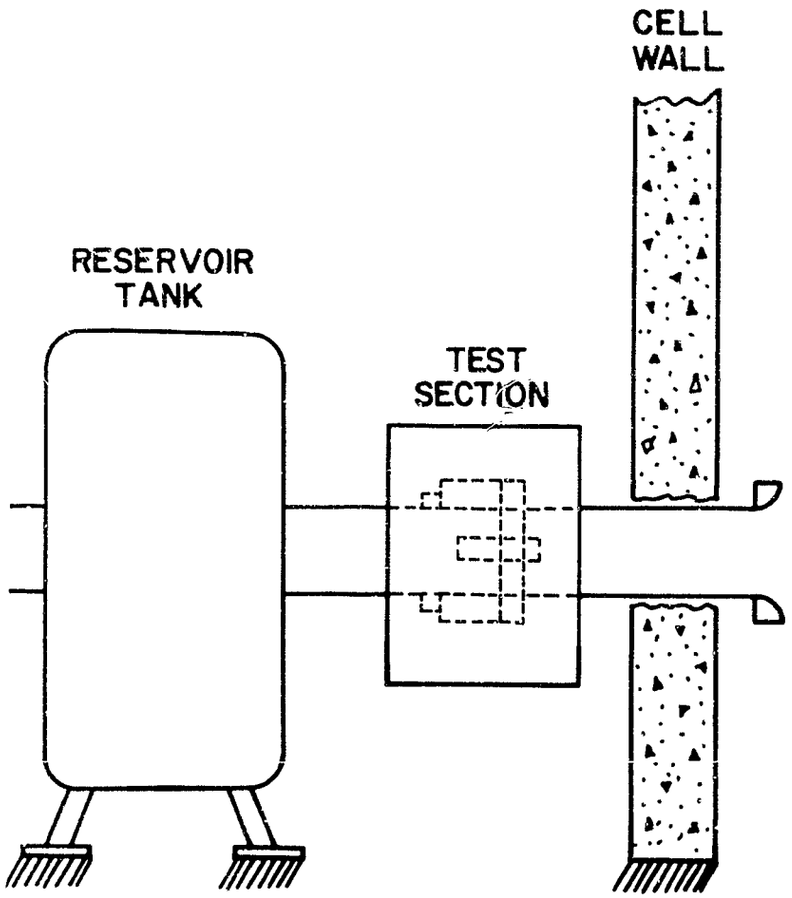

the Experimental Apparatus

Fig. D-2. Installation of the Test Rig
(sealing shroud removed)

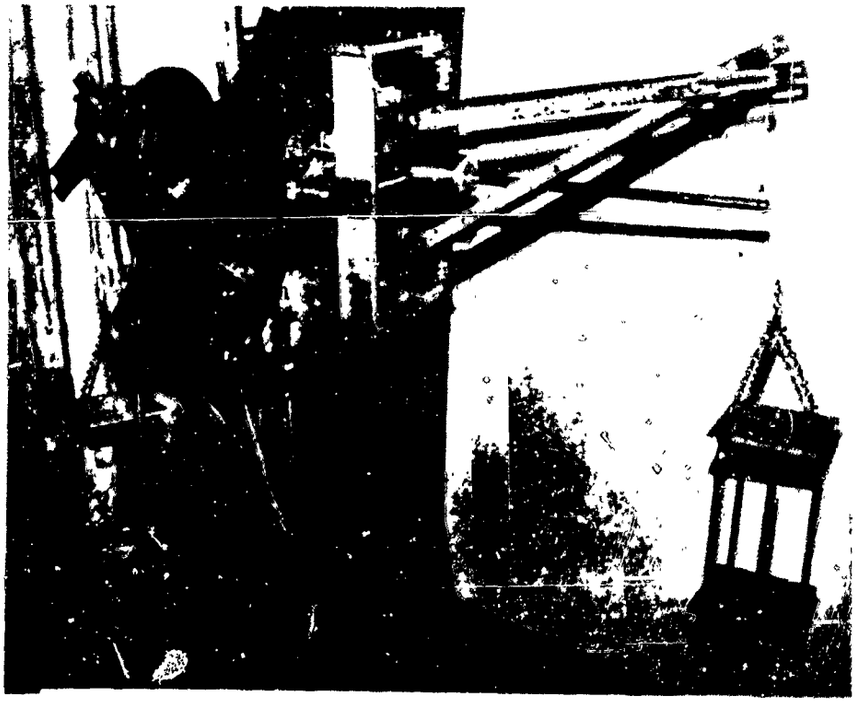

Fig. D-3. Test Model showing Calibration Rig
and Sealing Chamber
(model moved outside sealing chamber for calibration)

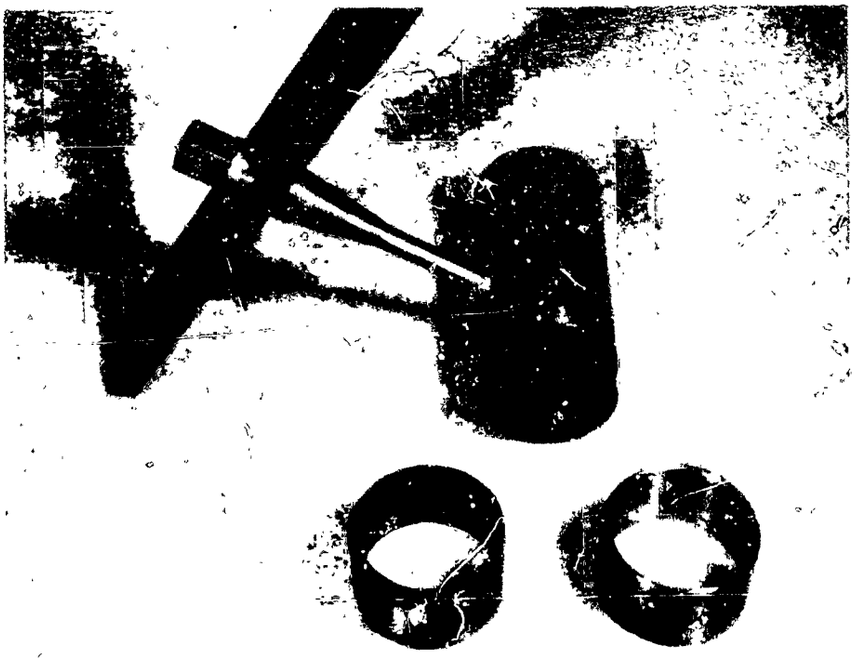

Fig. D-4. Test Model with Interchangeable Leading Edges.

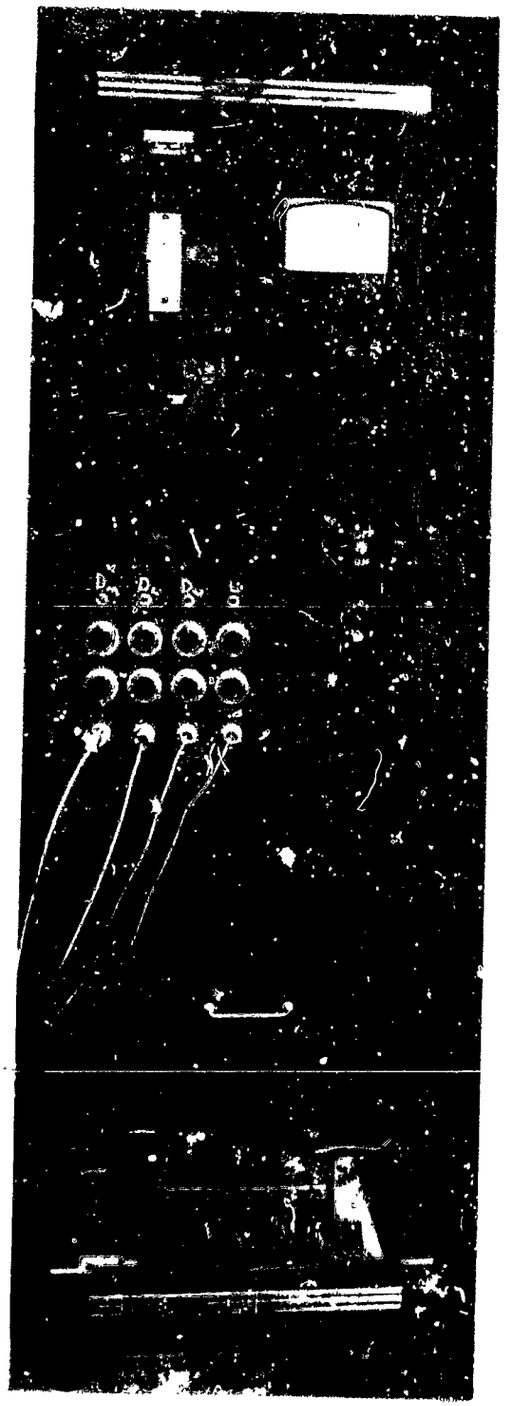

Fig. D-5. Recording Millivoltmeter

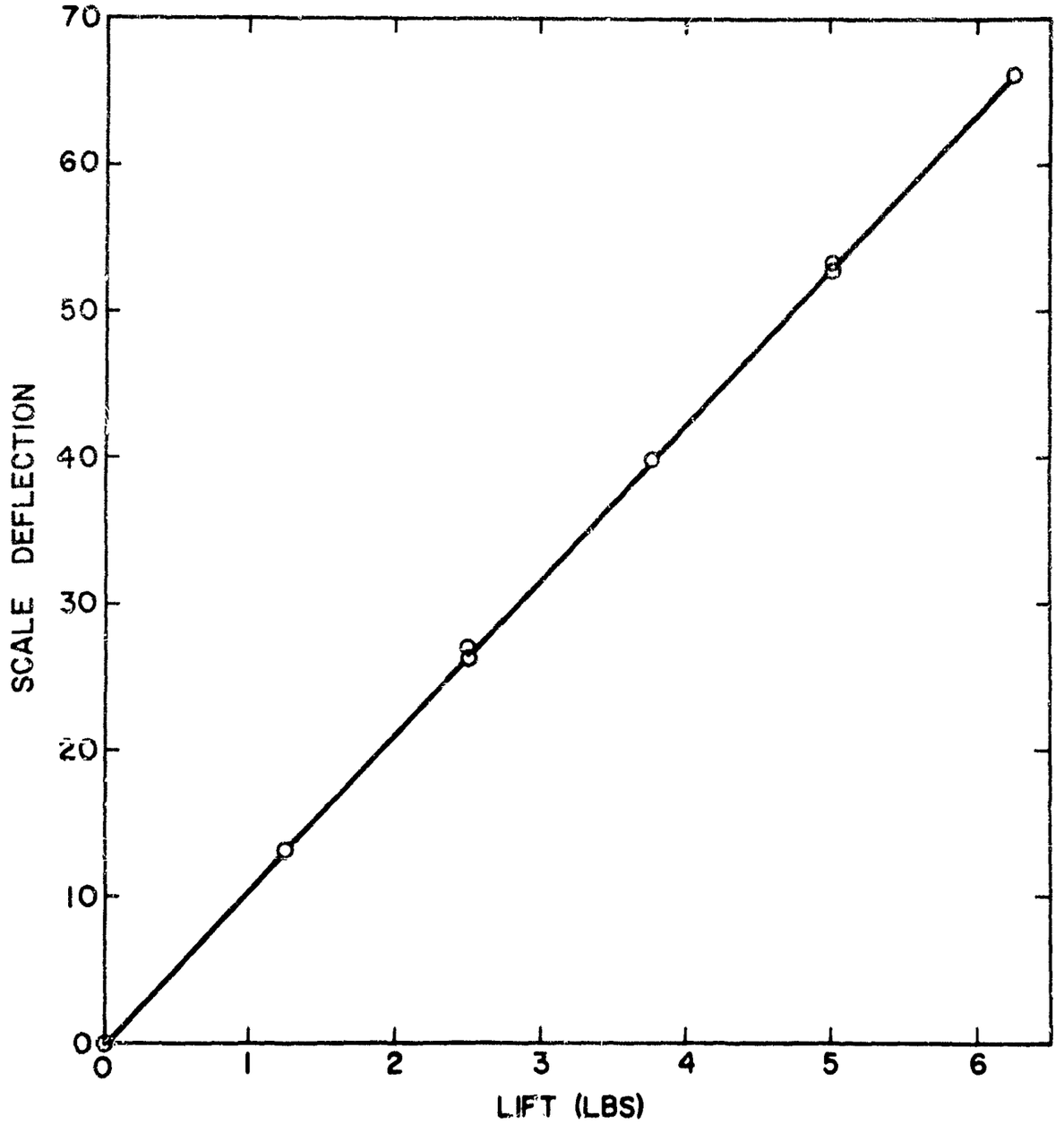

FIG: D-6: Calibration Curve

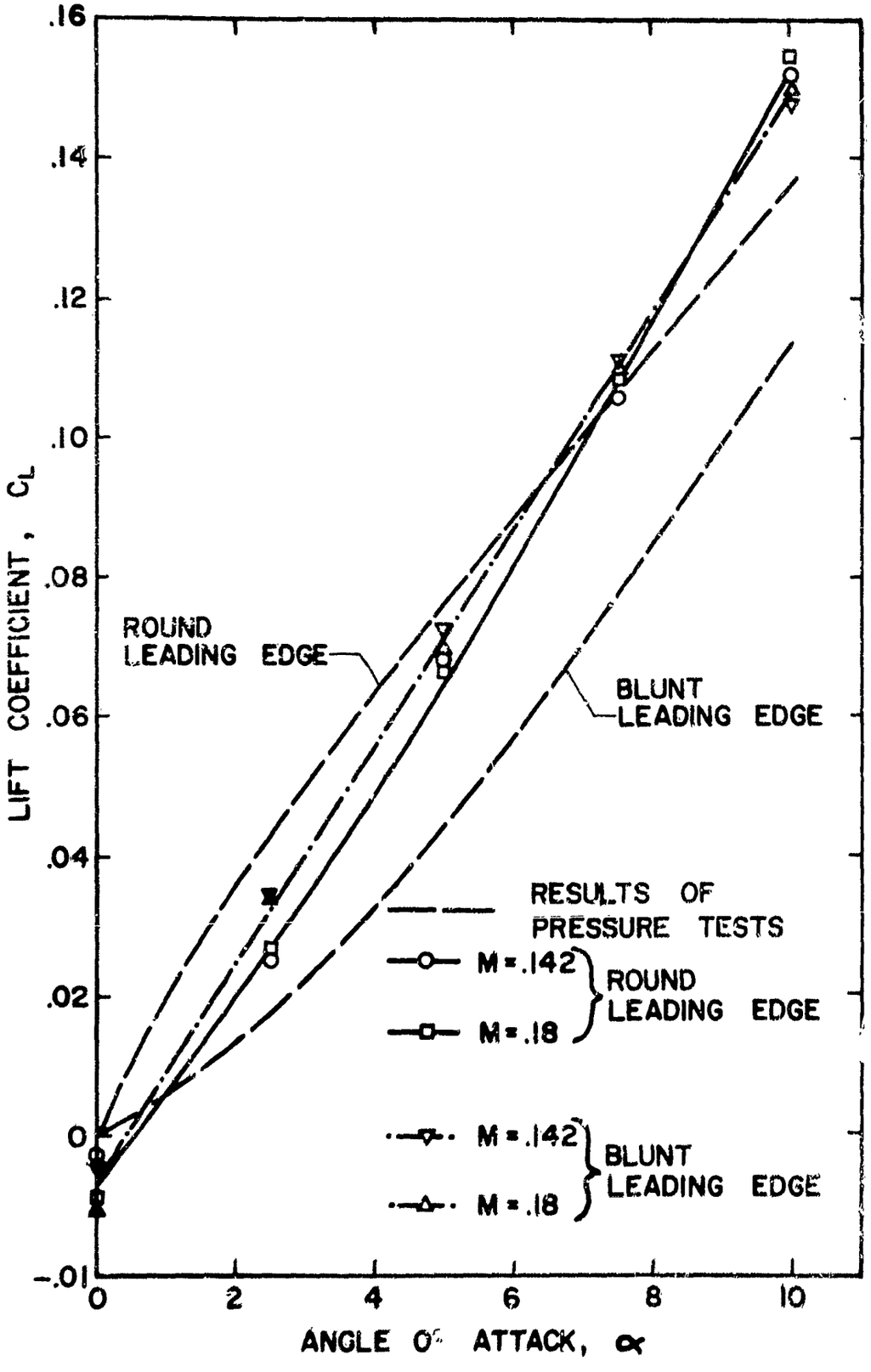

FIG. D-7: Lift Coefficient vs. Angle of Attack

Section E

WALL EFFECTS ON THE DRAG OF A BODY MOVING IN A TUBE

by

Peter N. Szucs

WALL EFFECTS ON THE DRAG OF A BODY MOVING IN A TUBE

Summary

Drop tests have been conducted to determine how the drag of a body moving inside a tube is affected by the tube walls. Measurements have been made for various end conditions, Reynolds numbers, body-to-duct diameter ratios, and body shapes. Only steady-state conditions have been considered.

Introduction

The effect of walls on the motion of a sphere falling in a viscous medium within a vertical tube was studied for low Reynolds numbers by Ladenburg (Ref. 1). The present investigation covers higher Reynolds numbers and a wider variety of shapes.

As in Ref. 1, drag measurements were made on bodies falling within vertical tubes. The tubes were filled with water. In some of the tests the lower end of the tube was open (Fig. E-1a), whereas in others it was closed (Fig. E-1b).

Apparatus and procedure

The experimental apparatus used in these tests is shown in Fig. E-2. The test tube was held in a vertical position within a lucite tank of square (1' x 1') cross section and was topped by an electromagnetic mechanism for the support and release of the body. The motion of the falling body was followed and recorded through an

array of vertically arranged light sources and photo-electric cells and a Hathaway recording oscillograph.

Four test tube diameters were used: 1-1/4", 1-3/4", 2" and 2-1/2".

Fig. E-3 shows the bodies used in the tests. The weights of the streamlined bodies could be adjusted by means of mercury ballast.

The "drag coefficients" C_D, defined as

$$C_D = \frac{F}{\frac{1}{2}\rho A_B V_B^2}$$

(where F is the drag force on the body, A_B its maximum cross sectional area, ρ the density of the medium, and V_B the velocity of the body relative to the walls), were calculated from the measured terminal velocities, at which F was equal to the weight of the body in water.

In some tests, an aluminum powder suspension was used for the purpose of visualizing the particle path lines in the tube-fixed frame of reference (see, e.g., Fig. E-4).

Results and Discussion

The measured drag coefficients are plotted in Fig. E-5 for the spherical bodies and in Fig. E-6 for the streamlined bodies.

The range of Reynolds numbers for the conditions of these tests is from 1×10^4 to 4×10^4.

It will be noted that, although the drag coefficient is always higher in the closed-end than in the open-end condition, the difference decreases as D/d increases and becomes negligible for D/d greater than about 2.5. Furthermore, the drag coefficient becomes substantially independent of D/d (indicating that the wall effect has substantially vanished) when D/d is greater than about 4. This result is in sharp contrast with the low-Reynolds number situation described in Ref. 1, where it is pointed out that, when viscous effects are predominant, significant wall effects are observed even with D/d in excess of 100.

From Fig. E-7 it can be seen that the asymptotic (free flight) value of C_D is approached more rapidly - hence that the wall effect decreases more rapidly -with increasing D/d when the moving body is a sphere than when it is a streamlined body. This result is understandable, in view of the fact that viscous effects are more important in the latter than in the former case.

It should be noted that the drag coefficient C_d is referred here to the velocity of the body relative to the tube (V_B) rather than to the velocity of the body relative to the fluid. The latter velocity may be taken to be $V_B - V$, where V is the volumetric flow

rate divided by the cross-sectional area A_t of the tube. It is unlikely that even a drag coefficient based on the relative velocity $V_B - V$ will be totally independent of the end conditions, but this may be assumed to be the case, in first approximation. Then, letting subscripts o and c denote open-end and closed-end conditions, respectively, one has, for any given body in any given tube,

$$\tfrac{1}{2} C_{D_o} \rho A_B V_B^2 = \tfrac{1}{2} C_{D_c} \rho A_B (V - V_B)^2$$

whence

$$\frac{V}{V_B} = 1 - \left(\frac{C_{D_o}}{C_{D_c}}\right)^{\frac{1}{2}}$$

The drag in the open-end condition is

$$F = A_t \Delta p_f + \tfrac{1}{2} \rho A_t V^2$$

where $A_t \Delta p_f$ is the resultant of the frictional forces exerted by the flow on the walls over the entire length of the tube, A_t being the cross-sectional area of the tube and Δp_f the loss of static pressure produced by these forces. It follows that

$$\frac{A_t \Delta p_f}{F} = 1 - \frac{A_t}{C_{D_o} A_B}\left(\frac{V}{V_B}\right)^2$$

$$= 1 - \frac{1}{C_{D_o}}\left[\frac{D}{d}\left(1 - \sqrt{\frac{C_{D_o}}{C_{D_c}}}\right)\right]^2$$

For example, for the conditions of the tests reported in Fig. E-5 with $A_t/A_B = 2$ (i.e., $D/d = 1.414$), the drag coefficients C_{D_c} and C_{D_o} are 2.7 and 1.55, respectively, and Eqs. (1) and (2) yield

$$V = .242\ V_B$$

$$A_t \Delta p_f = .9245\ F$$

Thus, the resultant of the frictional forces on the tube walls is, under these conditions, equal to about 92.5% of the drag of the body. As the length of the tube is increased, V decreases, C_{D_o} approaches C_{D_c}, and the frictional force on the tube wall increases asymptotically to 100% of F. Similarly, the fact that C_{D_o}/C_{D_c} approaches 1.0 as D/d is increased finds its obvious explanation in the decrease of V/V_B that is associated with increasing area ratios A_t/A_B.

Reference

1. Ladenburg, B., "On the Effect of Walls on the Motion of a Sphere in a Viscous Fluid", translated by J. Frohlich, Dept. of Aero. Eng. and Astr. Renss. Poly. Inst., TR AE 6305, Nov. 1963. Original in Annalen der Physik, 23 (1907) 447

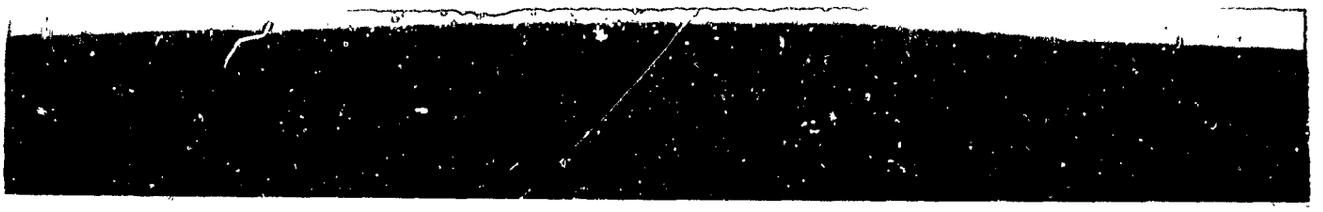

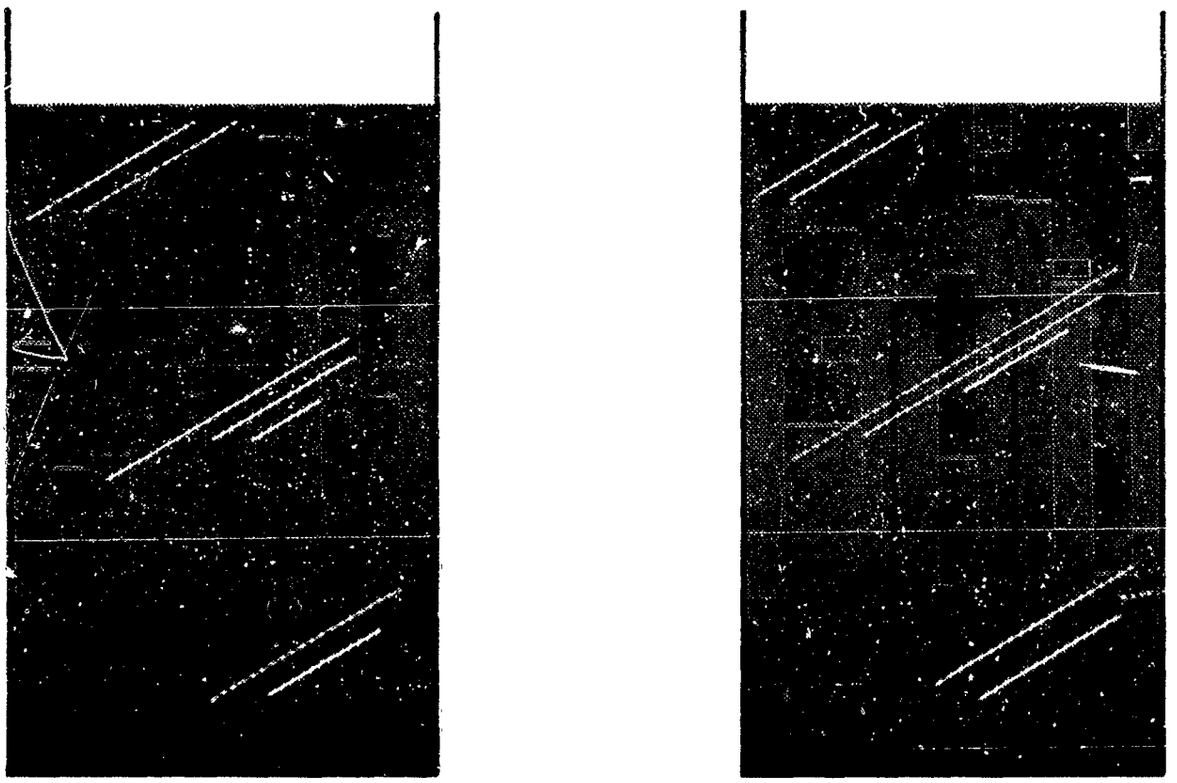

(a) (b)

FIG. E-1

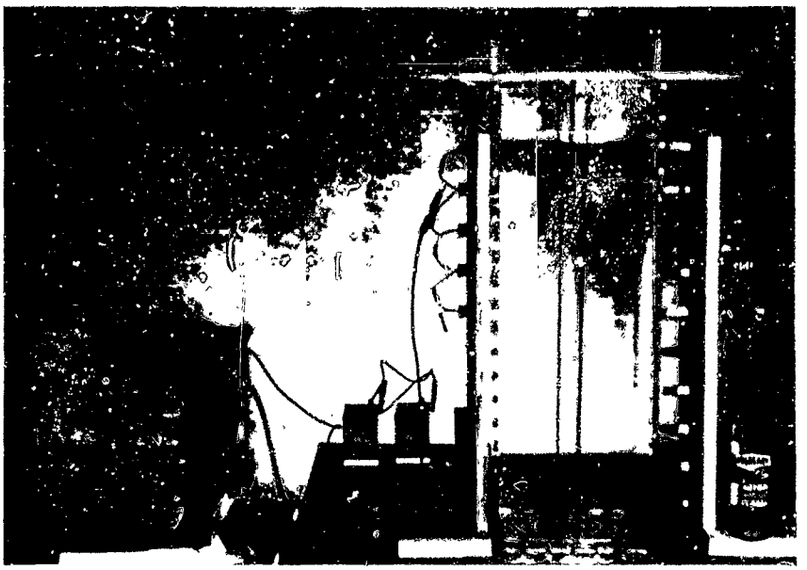

FIG. E-2

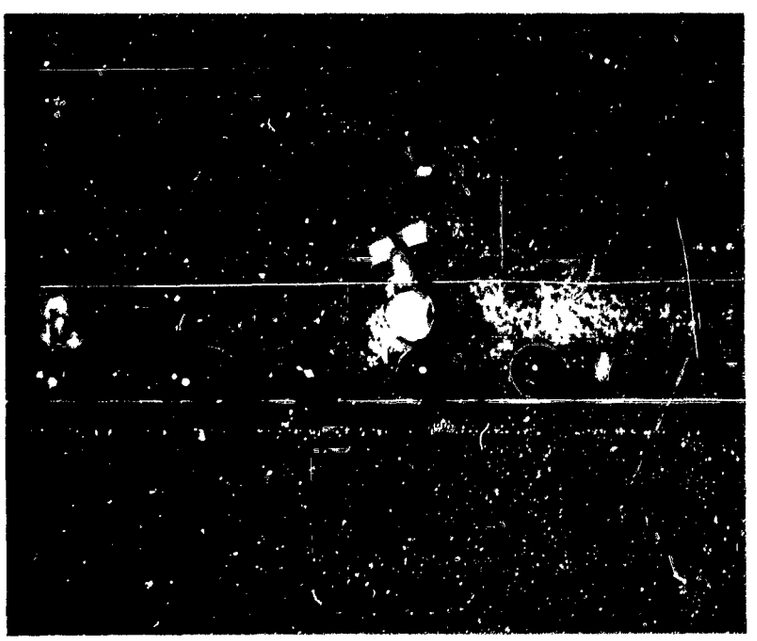

FIG. E-3 BODIES USED IN TESTS. SPHERE DIAMETERS (1 to r): 1", 7/8", 3/16", 3/4", 11/16", 1/2", 13/32". MAXIMUM TEARDROP DIAMETERS ARE 1" FOR LARGER BODY AND 3/4" FOR THE SMALLER ONE.

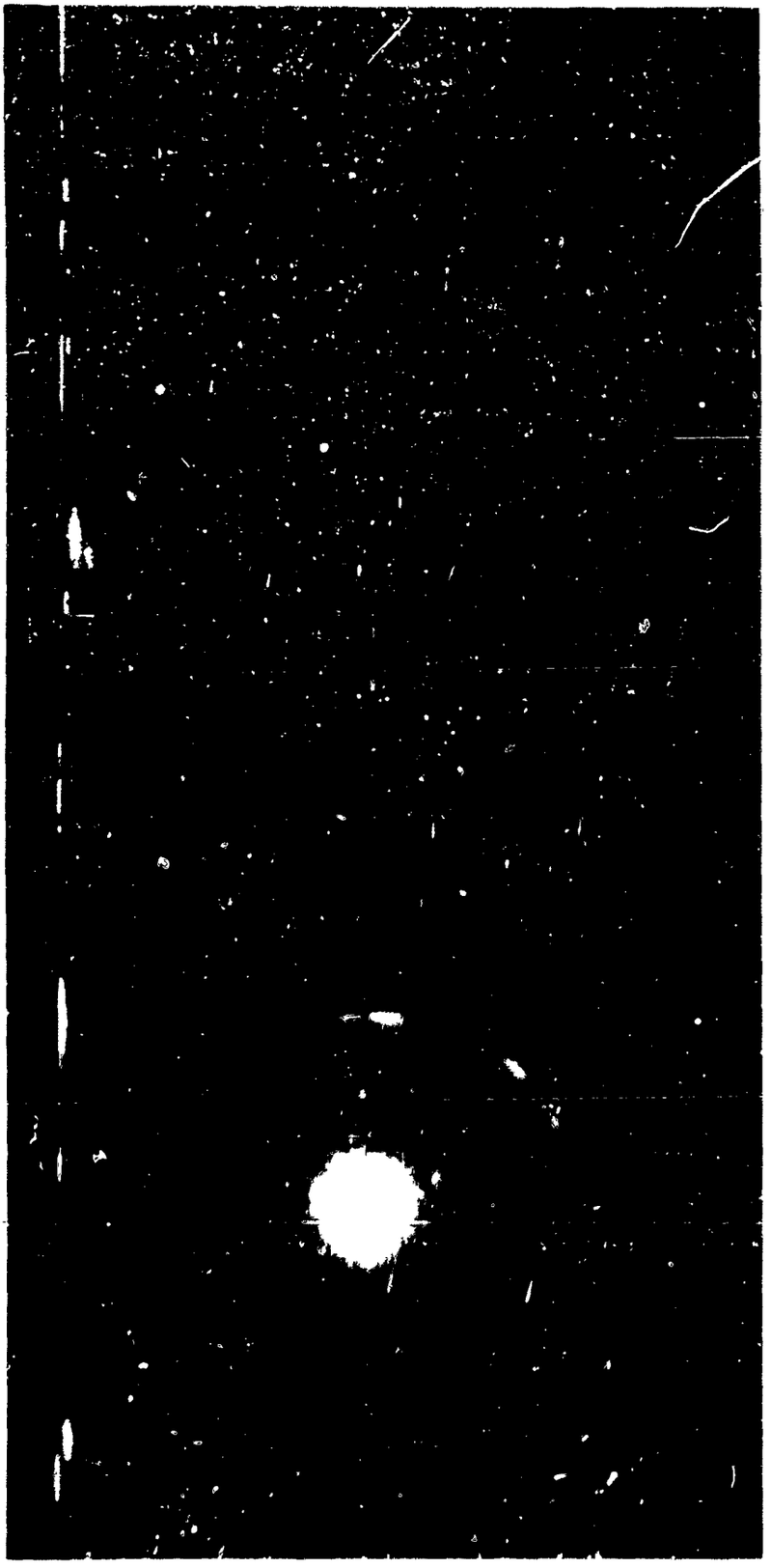

FIG. E-4 PARTICLE PATH LINES AROUND 1" DIAMETER SPHERE FALLING WITHIN 1¼" DIAMETER TUBE WITH CLOSED LOWER END.

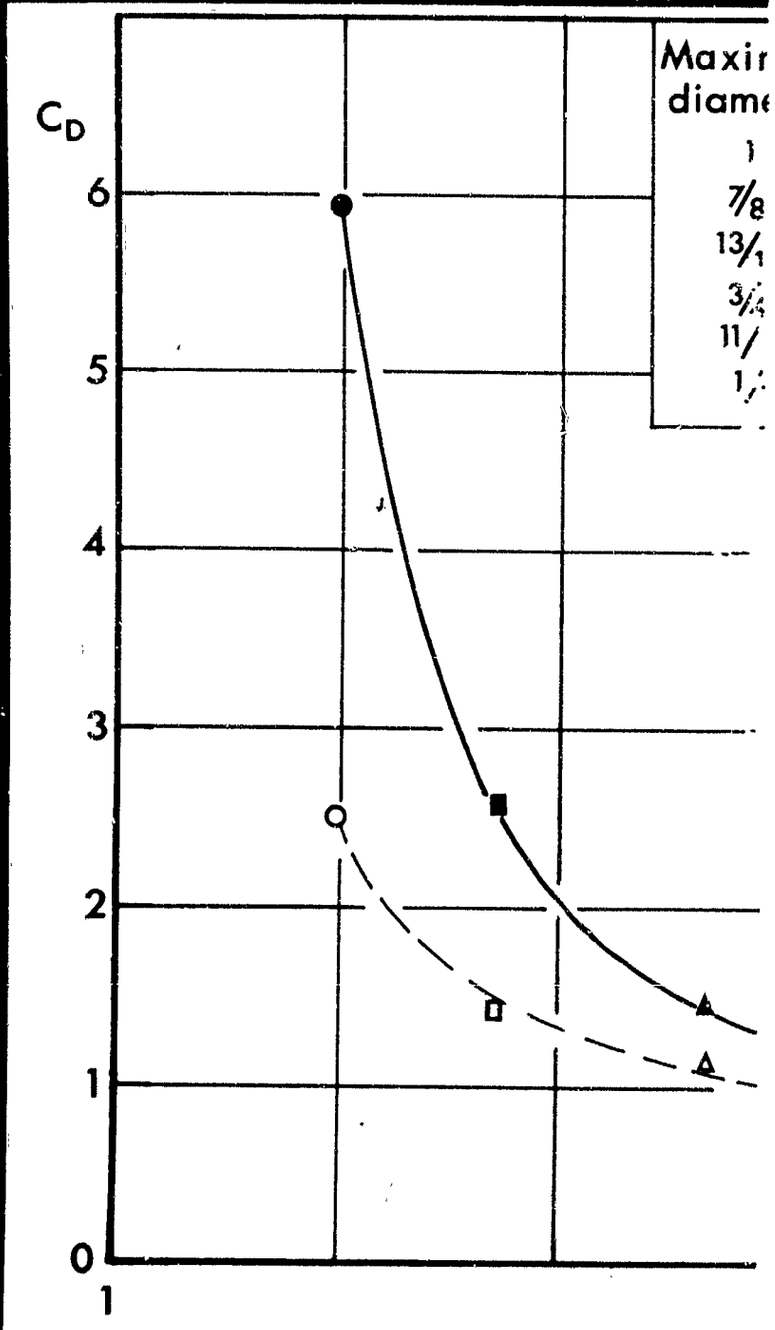

FIG. E-5 EFFECTIVE DRAG COEFFICIEN
TO SI

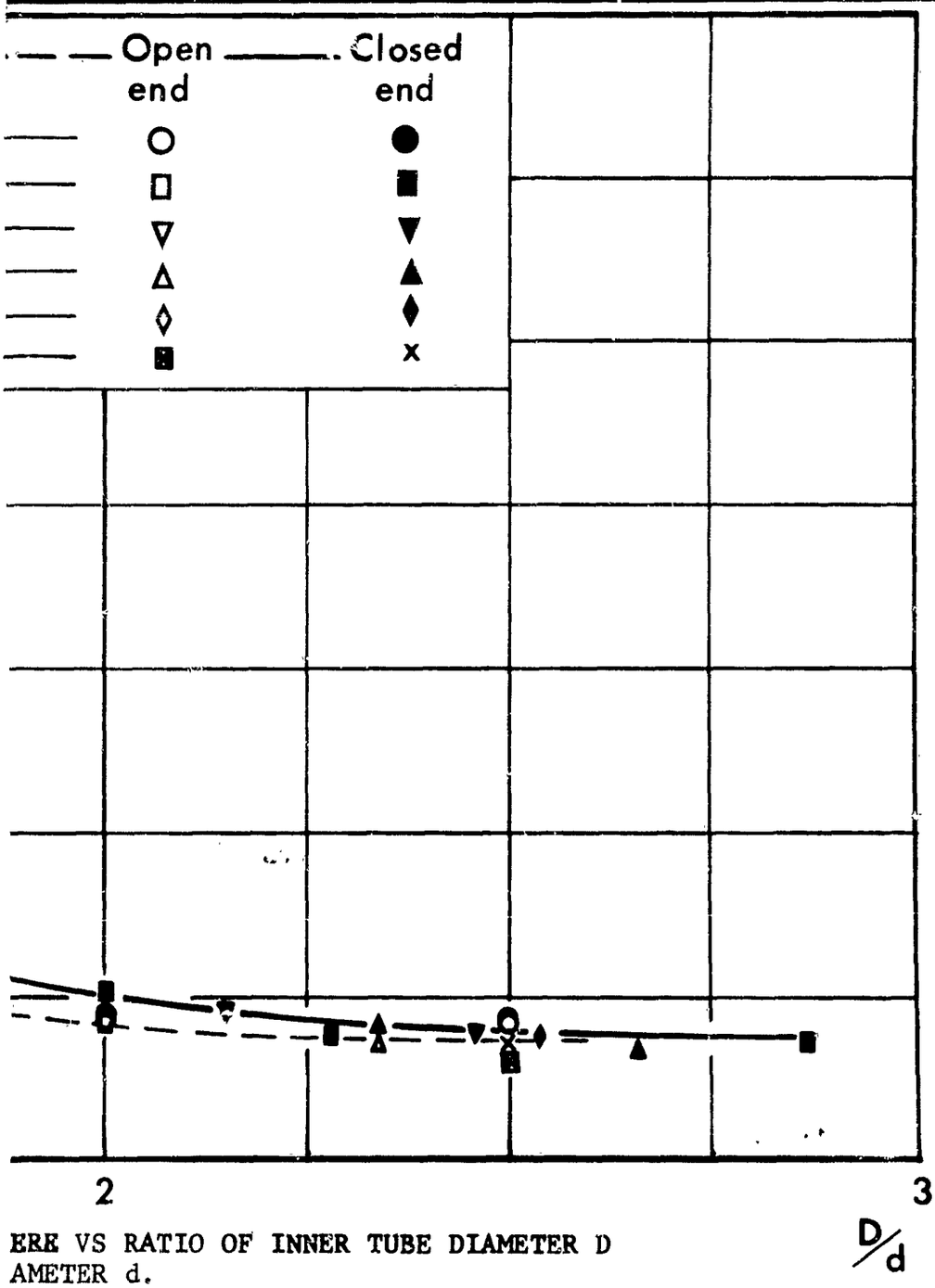

ERE VS RATIO OF INNER TUBE DIAMETER D
AMETER d.

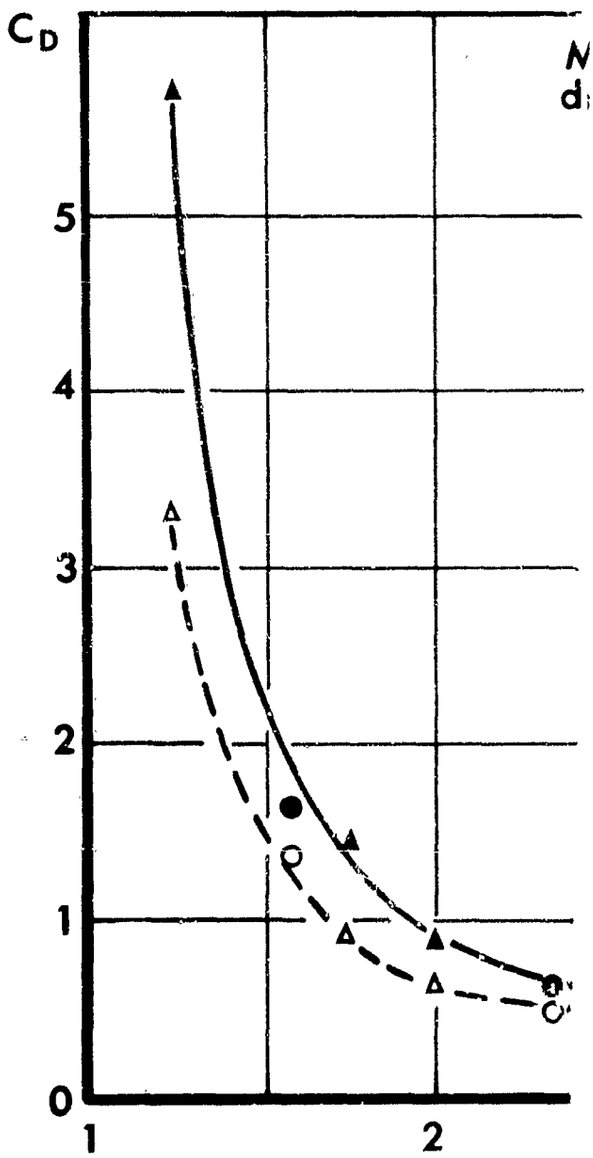

FIG. E-6 DRAG COEFFICIENT
DIAMETE

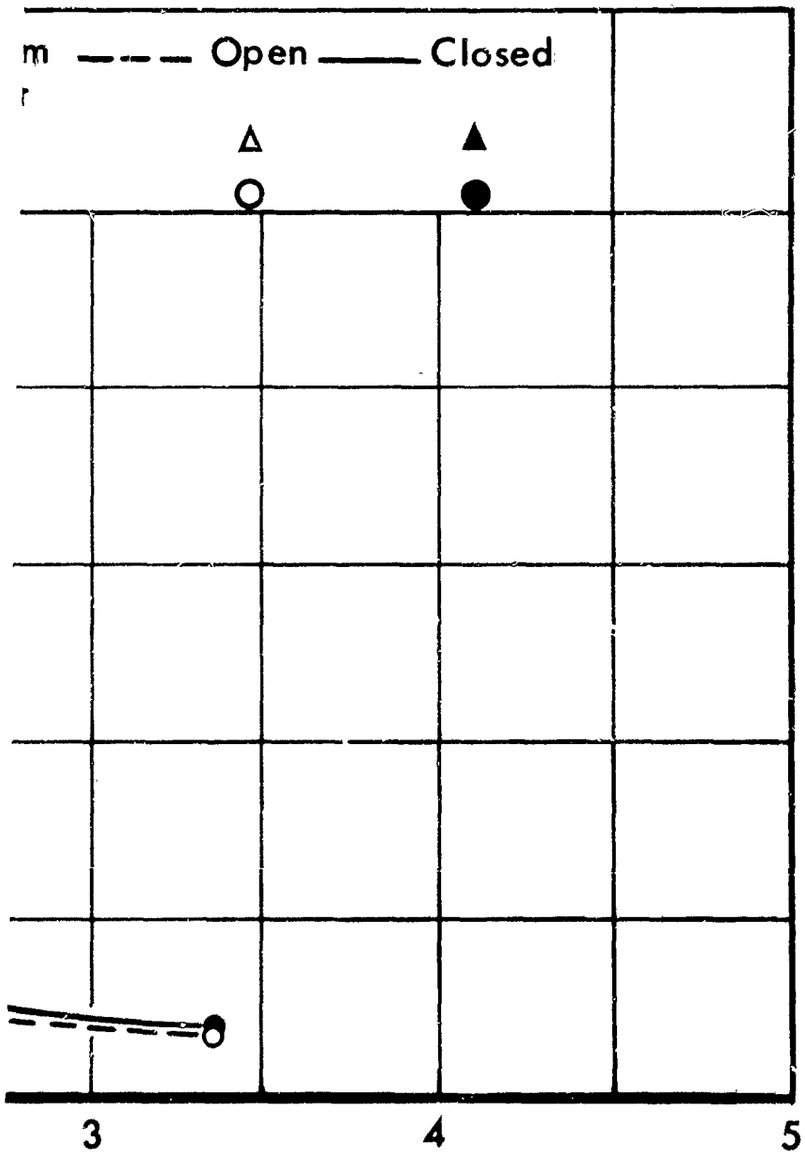

AMLINED BODY VS RATIO OF INNER TUBE
MAXIMUM BODY DIAMETER d_{max}

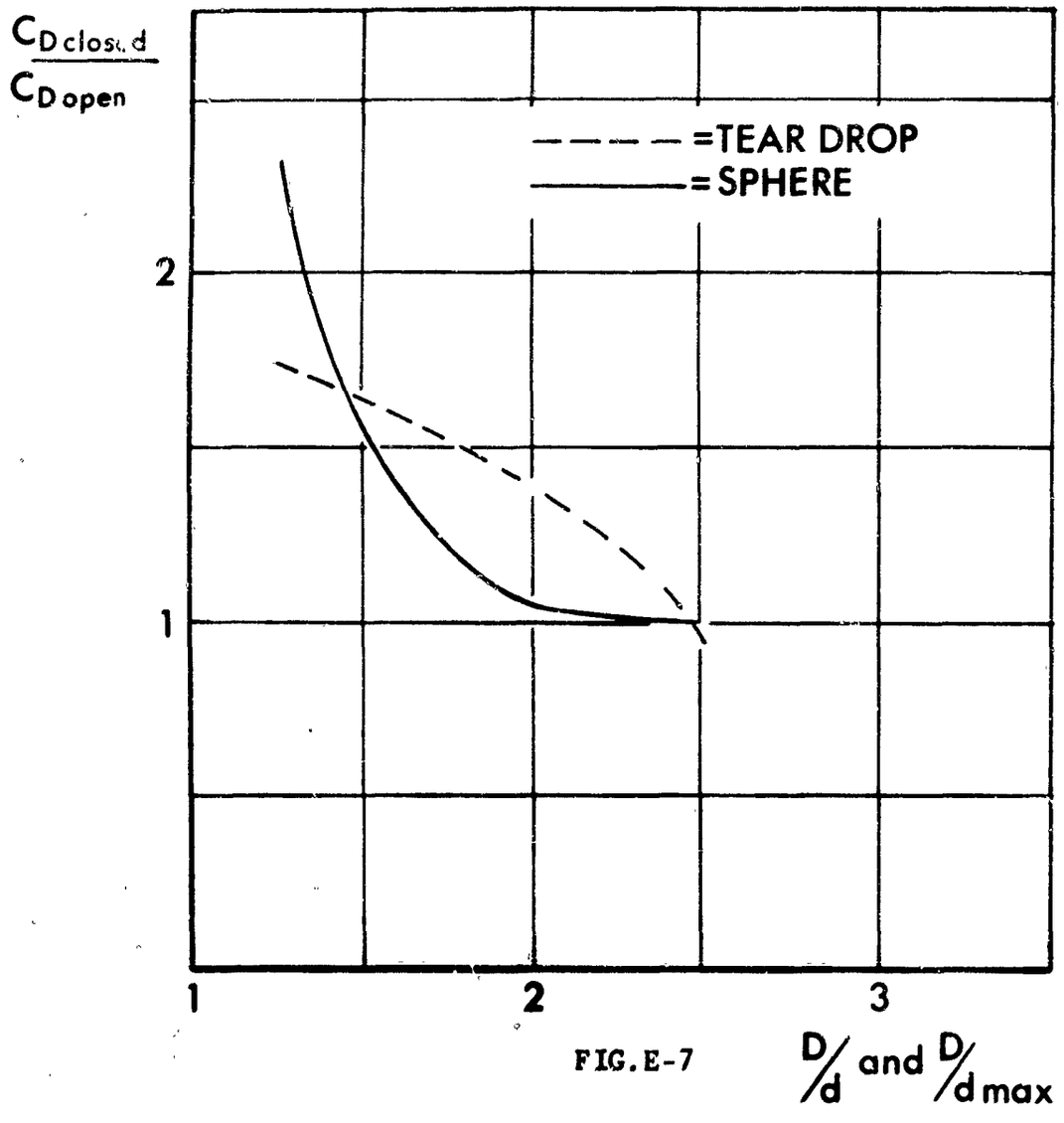

FIG. E-7

SECTION F

ERRATA SHEET

PAGE	LINE	CHANGE	TO
111	11	pAu	ρAu
8	5	quantitative	qualitativ
11	eq. (10)	$\frac{dT^\circ}{T^\circ}$	$\frac{dT^\circ}{T^\circ}$
16	eq. (16)	$\frac{1}{M_\infty^2}\ \frac{\gamma+1}{2}(1-y)^2$	$\frac{1}{M_\infty^2} - \frac{\gamma+1}{2}(1-y)^2$
17	15	$\left[\frac{\gamma+1}{2}(1-y)^2 + \frac{\gamma-1}{2}\right]^{-1}$	$\left[\frac{\gamma+1}{2}(1-y)^2 + \frac{\gamma-1}{2}\right]^{-1}$
18	6	vehicles	vehicle
19	eq. (9')	$\left[1 - \frac{\gamma-1}{2} M_\infty^2(2y_4 - 1)\right]$	$\left[1 - \frac{\gamma-1}{2} M_\infty^2(2y_4 - 1)\right]$
21	eq. (25)	$\frac{F_1 - F_2}{\rho_\infty A u_w}$	$\frac{F_1 - F_2}{\rho_\infty A}$
27	13	72.7%	72.5%
38	7	synchromism	synchronism

Section F

PROPULSION OF A VEHICLE IN A TUBE

by

Joseph V. Foa

Also issued as TR AE 6404

SUMMARY

This study concerns the flow disturbances and energy transformations that a vehicle traveling in a tube produces in the adjacent columns of air. The analysis accounts for compressibility, friction, and heat exchanges. The results are applied to the calculation of the power required in relation to blockage ratio, vehicle speed, and mode of propulsion. At the higher speeds, the power required is found to depend very critically on the mode of propulsion.

SYMBOLS

a speed of sound, fps

A cross-sectional area of the tube, sq. ft.

A_V maximum cross-sectional area of the vehicle, sq.ft.

$B = A_V/A$ (blockage ratio)

c_p specific heat at constant pressure, ft-lb/slug ^oR

c_f nondimensional friction factor

$D = M\left(1 + \frac{\gamma-1}{2}M^2\right)^{\frac{\gamma+1}{2(\gamma-1)}}$

$F = pA + \dot{m}u = pA(1+\gamma M^2)$ (stream force)

$G = (1+\gamma M^2)\left(1 + \frac{\gamma-1}{2}M^2\right)^{-\frac{\gamma}{\gamma-1}}$

h^o specific stagnation enthalpy, ft-lb/slug

$\dot{m} = \rho A u$ (mass flow rate in vehicle-fixed frame of reference), slugs/sec

M Mach number in vehicle-fixed frame of reference

$M_o = u_w/a_o$

$N = M\left(1 + \frac{\gamma-1}{2}M^2\right)^{\frac{1}{2}}(1+\gamma M^2)^{-1}$

p static pressure, psf

p^o stagnation pressure in vehicle-fixed frame of reference, psf

P power factor = (power required)/$p_o A\, u_w$

q heat input per unit mass, ft-lb/slug

r radius of tube, ft.

R gas constant, ft-lb/slug ^oR

T static temperature, ^oR

T^o stagnation temperature in vehicle-fixed frame of reference, ^oR

T^{o*} stagnation temperature in tube-fixed frame of reference, ^oR

u flow velocity relative to the vehicle, fps

u_v velocity of the vehicle relative to the tube, fps

$u_w = -u_v$ (velocity of the tube in vehicle-fixed frame of reference), fps

x distance from vehicle along tube, ft.

$y = (u_w - u)/u_w$ (ratio between velocity of the flow and velocity of the vehicle, as measured in tube-fixed frame of reference)

$Z = N^6 D$ (See tabulation in the Appendix, for $\gamma = 1.4$)

γ ratio of specific heats

θ thrust required, lb.

ρ density of gas in the tube, slugs/cu. ft.

Subscripts (see Fig. 1):

0 conditions outside the tube, assumed to be uniform

1 nearest station ahead of the vehicle where the flow can be treated as one-dimensional

2 station at tail end of vehicle

3 terminal station of energy addition in internal propulsion; upstream end of wake

4 wake station downstream of which T^{o*} is constant

e external propulsion

i internal propulsion

t throat of fluid transfer passage

INTRODUCTION

A vehicle may be propelled through a tube in an infinite variety of ways, but these may be grouped, for convenience of analysis, in three main categories. The first category, which includes conventional wheel traction and linear induction motor drives, is that in which thrust is generated as the reaction to a force exerted by the vehicle on a stationary external structure. Here the fluid in the tube merely acts as a resisting medium. In the second category (typified by pneumatic dispatch systems), the fluid is driven through the tube by a pump or by a high-pressure supply, and the vehicle is carried along by the fluid in this motion. In the third category, the vehicle still derives its propulsion from displacements of the fluid columns within the tube but these displacements are produced by the forces which are exerted on the fluid by the vehicle itself. The vehicle propels itself in this case by the fore-to-aft transfer, through itself and/or through the space which separates it from the tube wall, of the air or other fluid that fills the remainder of the tube.

The present study deals with propulsion modes of two of these three categories: the first and the third. For lack of better designations, the former will be referred to as "external propulsion" and the latter as "internal propulsion". Combinations of internal and external modes of propulsion will also be considered.

The situation studied here is that of a straight, horizontal and infinitely long tube, within which a vehicle is traveling at constant speed. The external air in the vicinity of the tube is at rest and in uniform state throughout, and the tube is open to the surrounding atmosphere at $\pm\infty$. The present investigation concerns the flow disturbances that the moving vehicle produces inside the tube, the associated losses, and the effect that these losses have on the power required to maintain the motion of the vehicle.

Similar situations have been treated, for incompressible fluids, by Tollmien (Ref. 1). One of the consequences of neglecting compressibility is that, the power available being finite, the calculated flow velocities must become everywhere vanishingly small as the tube length considered is increased indefinitely. In contrast, when compressibility is taken into account, the vehicle is found to be capable of generating large flow disturbances over long stretches of the tube even when the length of the tube is infinite. As a result of these disturbances and of the attendant thermodynamic transformations, each particle of the air in the tube undergoes a thermal cycle as it travels from $-\infty$ to $+\infty$ in the vehicle-fixed frame of reference. With external propulsion, the work output in this thermal cycle is negative, whereas with internal propulsion the cycle is utilized for the propulsion of the vehicle itself.

It is precisely with such motions and cycles that this study is concerned, and special attention is given to their dependence on blockage ratio, mode of propulsion and vehicle speed, and to their effects on the required power. The dependence of the power required on the mode of propulsion is found to be very critical, particularly at the higher speeds.

General governing equations for the flow outside of region 1-3.

In the vehicle-fixed frame of reference the flow is steady. Therefore, tne governing equations for the flow outside of region 1-3 can be derived, in this frame of reference, in the same manner as the familiar equations of steady one-dimensional flow with friction, heat exchanges and chemical reactions. The distinguishing feature of the present situation is that the walls of the tube are moving at the uniform velocity u_w in the direction of the relative flow, which is taken to be the positive x direction. The velocity u_w is, of course, equal and opposite to the velocity of the vehicle relative to the ground.

From the definitions of c_f and F,

$$dF = \rho A \frac{c_f}{r} (u_w - u)|u_w - u| dx$$

$$F = \rho A (1 + \gamma M^2)$$

Therefore,

$$\frac{dF}{F} = \frac{\gamma M^2}{1 + \gamma M^2} \frac{c_f}{r} \frac{y|y|}{(1-y)^2} dx \qquad (1)$$

From the energy equation

$$\dot{m} dh^\circ = u_w dF + \dot{m} dq$$

and neglecting changes of specific heats, there follows, after some manipulation,

$$\frac{dT^\circ}{T^\circ} = \frac{\gamma-1}{\gamma} \frac{1+\gamma M^2}{1+\frac{\gamma-1}{2}M^2} \frac{1}{1-y} \frac{dF}{F} + \frac{dq}{c_p T^\circ}$$

or

$$\frac{dT^\circ}{T^\circ} = \frac{(\gamma-1)M^2}{1+\frac{\gamma-1}{2}M^2} \frac{c_\tau}{r} \frac{y|y|}{(1-y)^3} dx + \frac{dq}{c_p T^\circ}$$

The continuity equation may be written in the form (Ref.

$$\frac{dF}{F} + \frac{dN}{N} - \frac{1}{2}\frac{dT^\circ}{T^\circ} = 0$$

whence

$$\frac{dN}{N} = \left(\frac{\gamma-1}{2\gamma} \frac{1+\gamma M^2}{1+\frac{\gamma-1}{2}M^2} \frac{1}{1-y} - 1\right)\frac{dF}{F} + \frac{1}{2}\frac{dq}{c_p T^\circ}$$

or

$$\frac{dN}{N} = M^2 \frac{c_\tau}{r}\left[\frac{1}{(1-y)\left(\frac{2}{\gamma-1}+M^2\right)} - \frac{\gamma}{1+\gamma M^2}\right]\frac{y|y|}{(1-y)^2} dx + \frac{1}{2}\frac{dq}{c_p T^\circ}$$

Since A is constant

$$\frac{dF}{F} = \frac{dp^\circ}{p^\circ} + \frac{dG}{G}$$

or

$$\frac{dF}{F} = \frac{dp}{p} + \frac{d(1+\gamma M^2)}{1+\gamma M^2}$$

From the definitions of G and N

$$\frac{dG}{G} = \gamma M^2 \frac{dN}{N}$$

$$\frac{dM}{M} = \frac{1+\frac{\gamma-1}{2}M^2}{1-M^2}(1+\gamma M^2)\frac{dN}{N}$$

Therefore,

$$\frac{dp^\circ}{p^\circ} = \left[\frac{1}{1+\frac{\gamma-1}{2}M^2} - y\right]\gamma M^2 \frac{c_f}{r}\frac{y|y|}{(1-y)^3}dx - \frac{1}{2}\gamma M^2 \frac{dq}{c_p T^\circ} \quad (4)$$

$$\frac{dp}{p} = \frac{\gamma M^2}{1-M^2}\left\{\left[1 \quad y-(\gamma-1)M^2 y\right]\frac{c_f}{r}\frac{y|y|}{(1-y)^3}dx - \left(1+\frac{\gamma-1}{2}M^2\right)\frac{dq}{c_p T^\circ}\right\} \quad (5)$$

Finally,

$$\frac{du}{u} = \frac{1}{2}\frac{dT}{T} + \frac{dM}{M}$$

$$= \frac{1}{2}\frac{dT^\circ}{T^\circ} + \frac{1}{1+\frac{\gamma-1}{2}M^2}\frac{dM}{M}$$

$$= \frac{1}{2}\frac{dT^\circ}{T^\circ} + \frac{1+\gamma M^2}{1-M^2}\frac{dN}{N} \quad (6)$$

Eqs. 1, 2, 3, 3', and 6 yield

$$\frac{dy}{y} = \frac{M^2}{1-M^2}\frac{1-\gamma y}{(1-y)^2}|y|\frac{c_f}{r}dx - \frac{1-y}{y}\frac{1+\frac{\gamma-1}{2}M^2}{1-M^2}\frac{dq}{c_p T^\circ} \quad (6')$$

<u>A special case: adiabatic flow.</u>

The governing equations for the adiabatic case are eqs. 1 through 6' with dq = 0 throughout. When $u_w = 0$, they reduce to

the Fanno flow equations.

Adiabatic flows are of limited interest in relation to the problem at hand. The following discussion concerns only the main trends of the transformations in such flows.

Eq. 3' shows that $\frac{dN}{dx} < 0$ if y is in the range

$$0 < y < \frac{\gamma+1}{2\gamma\left(1+\frac{\gamma-1}{2}M^2\right)}$$

or, for air (γ = 1.4),

$$0 < y < \frac{.857}{1+.2M^2}$$

When y is within this range, the local flow Mach number (relative to the vehicle) increases or decreases in the direction of the flow depending on whether the local flow velocity (relative to the vehicle) is supersonic or subsonic. The converse is true if y falls outside of the range indicated above.

$\frac{dF}{dx}$ and $\frac{dT^*}{dx}$ are, as expected, positive or negative depending on whether y is positive or negative.

Eq. 4 reveals that the stagnation pressure (relative to the vehicle) increases or decreases in the direction of the flow, regardless of whether the local flow is subsonic or supersonic,

depending on whether y falls within the range

$$0 < y < \left(1 + \frac{\gamma-1}{2} M^2\right)^{-1}$$

or outside of it.

Finally, Eq. 6' shows that, if y falls within the range $0 < y < \frac{1}{\gamma}$, then the flow velocity increases or decreases in the direction of the flow, depending on whether the flow is supersonic or subsonic. The converse is true when y is outside this range.

Qualitative information of this kind is useful in the quick detection of solutions that are incompatible with the boundary conditions, as will be shown in the discussion of somewhat different situations in the following sections.

Selection of an analytical model for the present investigation.

In the application of the general equations developed above to the study of the flow in tube-transport systems, special attention must be paid to the evaluation of the heat-exchange derivatives. These derivatives depend not only on the thickness and thermal conductivity of the tube walls but also, at each station of the tube and at each instant, on the local time derivatives of the enthalpy and velocity of the internal flow, hence on the local gradients of these quantities in the vehicle-fixed frame of reference and on the velocity of the vehicle.

It is obvious, however, that the actual program of heat exchange between the internal flow and the surrounding atmosphe must lie between two extremes. At one extreme is the case of ze conductivity - the adiabatic flow. This case is of no more th quantitative interest in relation to the problem at hand. At t other extreme is the case of infinite conductivity whereby th internal boundary layer is kept everywhere at the temperature o the external air. For moderate velocities of the vehicle, the latter extreme is believed to be very close to the actual situa tion.

Under the conditions that are to be considered in this pr lem, the flow is fully turbulent in those regions where it und goes its most significant transformations. Furthermore, as wil be shown presently, all these transformations, throughout mos the subsonic range of vehicular speeds, take place very gradu and over great distances, both ahead of the vehicle and behind i except in its immediate proximity. These observations suggest simple analytical model, whereby the tube wall is viewed as act like a very large heat exchanger, through which the heat flows such a manner that the stagnation temperature T^{o*} of the flow relative to the tube wall is made to remain everywhere (except around and immediately behind the vehicle) substantially equal t the external temperature T_o.

A more exact, but necessarily only numerical, analysis of the same problem is carried out in Ref. 3, where Eqs. 1 through 6 of the present paper are applied with the stipulation that

$$\frac{dq}{dx} = -K(T^{o*} - T_o)$$

where K is a constant. The analytical model proposed here, although less exact, is believed to describe the actual physical situation in fair approximation over a wide range of speeds. It also has the advantage that it leads to closed-form solutions which lend themselves to clear and informative interpretation. Nevertheless, its plausibility is limited, as has been noted above, to those situations in which the tube can be viewed as performing the function of a "very large" heat exchanger - very large, that is, in relation to the heat transfer rates that it is called upon to provide. As the speed of the vehicle is increased, the rate at which energy is dissipated in the internal flow increases and the gradients of all flow properties ahead of the vehicle become steeper and steeper. At very high speeds, the constant-T^{o*} condition cannot be maintained, and the path of the transformation must approach that which is finally established when all the flow changes ahead of the vehicle take place through one or more shocks in the neighborhood of station 1. The condition that is approached is that of an isoenergetic process in the vehicle-fixed frame of reference.

The flow transformation ahead of the vehicle will, accordingly, be analyzed as a constant-T^{o*} process for moderate subsonic speeds, and as a constant-T^{o} process for supersonic speed In the transonic range, the flow process may be expected to follow an intermediate path.

Behind the vehicle, the condition T^{o*} = constant is tenabl under all conditions downstream of a station 4 which is itself some distance - as yet unspecified - downstream of station 3 (Fig. 1). The region between stations 1 and 3 is one in which rapid transformations take place and energy is added to the flo in some modes of internal propulsion. The distance from 3 to 4 is the distance required for enough heat to be extracted from t flow to bring T^{o*} to a substantially stationary value.

The flow ahead of the vehicle.

The constant-T^{o*} condition will be analyzed first.

From the definitions of T^{o*} and T^{o} there follows

$$T^{o*} = T^{o} + \frac{(u_\infty - u)^2 - u^2}{2 c_p}$$

$$= T^{o} + \frac{u_\infty^2}{2 c_p}\left(1 - 2\frac{u}{u_\infty}\right) \qquad (7$$

whence, if $T^{o*} = T_o$,

$$dT^{o} = \frac{u_\infty^2}{c_p}\, d\left(\frac{u}{u_\infty}\right) \qquad (8$$

and

$$T^\circ = T_o \left[1 - \frac{\gamma-1}{2} M_o^2 \left(1 - 2 \frac{u}{u_w} \right) \right] \tag{9}$$

Eq. 9 reveals the important (and potentially useful) fact that the stagnation temperature of the internal flow, relative to the vehicle, is lower or higher than the stagnation temperature that would be measured in the free stream at the same Mach number M_o, depending on whether u/u_w is smaller or greater than 1.0 (i.e., depending on whether y is positive or negative). When y = .5, the internal stagnation temperature relative to the vehicle is equal to the external static temperature. This seeming paradox is explained by the above-noted heat exchanger action of the tube.

From Eqs. 8 and 9,

$$\frac{dT^\circ}{T^\circ} = \frac{(\gamma-1) M_o^2}{1 - \frac{\gamma-1}{2} M_o^2 \left(1 - 2 \frac{u}{u_w} \right)} d\left(\frac{u}{u_w} \right) \tag{10}$$

Also,

$$T = T^{\circ *} - \frac{(u_w - u)^2}{2 c_p}$$

$$= T_o \left(1 - \frac{\gamma-1}{2} M_o^2 y^2 \right)$$

and

$$\frac{u}{2 c_p T} = \frac{\gamma-1}{2} M^2$$

whence

$$M^2 = \frac{(1-y)^2 M_0^2}{1 - \frac{\gamma-1}{2} M_0^2 y^2} \tag{11}$$

Finally, Eqs. 1, 6, 11, and the continuity equation

$$\frac{dN}{N} = \frac{1}{2}\frac{dT^\circ}{T^\circ} - \frac{dF}{F}$$

yield

$$\frac{\frac{1}{M_0^2} - \frac{\gamma-1}{2} - \frac{\gamma+1}{2}(1-y)^2}{(1-y)|y|}\frac{dy}{y} = \gamma c_f \, d\left(\frac{x}{r}\right)$$

Therefore, when consideration is given to a flow region in which changes of c_f can be neglected,

$$(\gamma M_0^2 - 1)\left(\frac{1}{y_b} - \frac{1}{y_a}\right) + (1+M_0^2)\ln\frac{y_b}{y_a} + \left(\frac{\gamma-1}{2}M_0^2 - 1\right)\ln\frac{1-y_b}{1-y_a} = \pm\gamma c_f M_0^2 \frac{x_b - x_a}{r} \tag{12}$$

Eq. 12 permits the calculation of the change of velocity from a station a to a station b in any region upstream of station 1 or downstream of station 4. On the right-hand side of the equation, the "+" sign applies when $y > 0$ and the "-" sign when $y < 0$.

If the Reynolds number is found to undergo large changes within the region considered, the calculation should be repeated on subregions small enough that the changes of c_f in each may be neglected or adequately accounted for by the use of suitable averages.

The stream force can be calculated as a function of y from the continuity equation in the form

$$F/\sqrt{T^{o*}} = \text{constant}$$

which, together with Eqs. 9 and 11, yields

$$\frac{F(1-y)}{\frac{1}{M_o^2} - \frac{\gamma-1}{2}y^2 + \gamma(1-y)^2} = \text{constant}$$

At $\pm\infty$, y = 0 and $F = p_o A(1 + \gamma M_o^2)$. Therefore,

$$\frac{F}{p_o A} = \frac{1 - \frac{\gamma-1}{2}M_o^2 y^2}{1-y} + \gamma M_o^2(1-y) \tag{13}$$

$$\frac{p}{p_o} = \frac{F}{p_o A(1+\gamma M^2)}$$

$$= \frac{1}{1-y}\left(1 - \frac{\gamma-1}{2}M_o^2 y^2\right) \tag{14}$$

As has been noted earlier, the assumption of a constant T^{o*} becomes untenable at speeds approaching the speed of sound in the atmosphere surrounding the tube, and at supersonic speeds it becomes more plausible to treat the flow ahead of the vehicle as isoenergetic in the vehicle-fixed frame of reference. When all flow changes take place through shocks around the nose of the vehicle, conditions at station 1 are obviously the same as at infinity, and the flow from station 1 to the throat can be treated like the inflow through a supersonic intake. If, on the other hand, changes occur ahead of station 1, then the flow at 1 is

subsonic, M_1 is determined by conditions further downstream, and the continuity equation gives

$$\frac{F_1}{p_0 A} = \frac{F_0 N_0}{p_0 A N_1} = \frac{M_0 \left(1 + \frac{\gamma-1}{2} M_0^2\right)^{\frac{1}{2}}}{N_1} \qquad (15)$$

An example.

To illustrate the application of Eqs. 9 through 14, consider the flow ahead of a vehicle traveling at 550 fps within a tube surrounded by air at p_0 = 2000 psf and at T_0 = 500 ^{o}R. At this temperature the speed of sound is a_0 = 1100 fps. Therefore, M_0 = .5. Let A = 100 sq. ft., and let the blockage ratio and the mode of propulsion be such that y = .5 just ahead of the vehicle. With the origin (x = 0) at station 1, the equations above provide the following description of the flow:

TABLE I

y	u fps	$\frac{F}{p_0 A}$	M	$\frac{p}{p_0}$	$\frac{p^o}{p_0}$	$\frac{T^o}{T_0}$	average c_f x10^3	distance ahead of vehicle, miles
0	550	1.350	.500	1.00	1.186	1.05		∞
.1	495	1.425	.450	1.11	1.275	1.04	2.25	24
.2	440	1.528	.401	1.249	1.395	1.03	2.0	11
.3	385	1.667	.351	1.442	1.55	1.02	1.8	6
.4	330	1.860	.301	1.651	1.76	1.01	1.75	2
.5	275	2.145	.252	1.971	2.065	1.0		0

The calculated Mach number just ahead of the vehicle, $M_1 = .252$, is the Mach number that would be maintained by a well streamlined body of blockage ratio $B \simeq .58$, i.e., by a vehicle of maximum diameter equal to about 76% of the diameter of the tube.

The stagnation pressure ahead of the vehicle is seen to be considerably higher than the free-stream stagnation pressure at the same Mach number. On the other hand, the stagnation temperature relative to the vehicle is everywhere lower than the stagnation temperature that would be measured in the free stream at the same Mach number, in accordance with the general observations made in the discussion of Eq. 9.

Inspection of Eq. 12 and of Table I reveals a strange difficulty: if one were to carry out a similar calculation for positive values of x, starting, e.g., with $y = .5$ at station 4, y would be found to increase monotonically, approaching 1.0 asymptotically, as x increases indefinitely. This result would indicate that the region behind the vehicle is an infinite wake in which the flow velocity relative to the vehicle continues to decrease with increasing distance from the vehicle. Such a wake would clearly be incompatible with the boundary condition $y_{+\infty} = 0$. It becomes necessary, therefore, to re-examine the solutions in order to determine which flows are possible in the region behind the vehicle

and which are not.

The flow behind the vehicle.

Because of the boundary condition $y_{+\infty} = 0$, the only possible flows behind the vehicle are those in which $\frac{dy}{dx} \gtrless 0$ for $y \lessgtr 0$, respectively.

Eq. 12 yields

$$\frac{dy}{d\left(\frac{x}{r}\right)} = \pm \frac{y^2(1-y)}{\frac{1}{M_0^2} \frac{\gamma+1}{2}(1-y)^2 - \frac{\gamma-1}{2}} \gamma C_\gamma \qquad (1$$

where the " + " sign applies when $y > 0$ and the "-" sign when $y < 0$.

The numerator of the right-hand member of Eq. 16 is alway positive.

Now, if $y > 0$, the " + " sign applies in Eq. 16. On the other hand, where $y > 0$, the stability of the wake demands that dy/dx be negative. Therefore, a wake with $y > 0$ is compatible with the boundary conditions only if the denominator of the right hand member of Eq. 16 is negative, i.e., if

$$M_0^2 > \left[\frac{\gamma-1}{2} + \frac{\gamma+1}{2}(1-y)^2\right]^{-1} \qquad (1$$

This condition must be satisfied everywhere, including station 4, where y will have a higher value than at any statio further downstream.

Where $y < 0$, the "-" sign applies in Eq. 16 but the flow is stable only if $\frac{dy}{dx} > 0$. Therefore, the compatibility condition requires again that the denominator of the right-hand member of Eq. 16 be negative. In this case, however, the highest value of y anywhere downstream of station 4 is zero. It follows then from Eq. 17 that, where $y < 0$, the flow is compatible with the boundary conditions wherever $M_o > \frac{1}{\sqrt{\gamma}}$. The line of demarcation between stable and unstable wake conditions at station 4 is plotted as curve a in Fig. 2. It should be noted that the condition $y_4 = 0$ represents a singularity, because it is a condition that is compatible with the boundary conditions for all values of M_o: when $y_4 = 0$, the flow is at rest relative to the tube everywhere downstream of station 4.

Curve b in Fig. 2 is a plot of the equation

$$M_o^2 = \left[\frac{\gamma+1}{2}(1-y)^2 + \frac{\gamma-1}{2}\right]^{-1}$$

which represents the vanishing of the denomination of the right-hand member of Eq. 16. If y_4 and M_o are such that the initial point lies in the negative quadrant below this curve (like point P in the figure), y will change downstream of station 4 in the manner indicated by the arrow until curve b is reached. At that point y becomes discontinuous, and no solution is found for the flow downstream of the station at which this discontinuity occurs.

The only physical meaning that can be attributed to the "unstable wakes" is that they cannot exist except as nonsteady transients through which the downstream boundary conditions eventually impose on the flow the condition $y_4 = 0$. Therefore, the only steady-flow condition that is possible behind the vehicles, when M_0 is lower than the critical value for wake stability, is one in which the flow is at rest (relative to the tube) everywhere downstream of station 4.

This result is of great importance in the determination of the drag of the vehicle and of the power required to maintain its motion with various means of propulsion.

According to Eq. 16, downstream of station 4 the derivati·· dy/dx can only vanish asymptotically or be identically zero everywhere. Therefore, y in this region can only vary monotoni·cally with x or remain constant.

The flow transformation from station 3 to station 4 can be analyzed as follows:

The energy equation between these two stations, in the vehicle-fixed frame of reference, may be written in the form

$$\dot{m} c_p (T_4^\circ - T_3^\circ) = u_w (F_4 - F_3) + \dot{m} q_{3-4} \qquad (1$$

where q_{3-4} is the heat received by the unit mass of the fluid between the two stations:

$$q_{3-4} = c_p (T_4^{o*} - T_3^{o*})$$

$$= c_p (T_o - T_3^{o*})$$

Equs. 7 and 9 may be re-written as

$$T_3^{o*} = T_3^o + \frac{\gamma-1}{2} M_o^2 (2y_3 - 1) T_o \qquad (7')$$

and

$$T_4^o = T_o \left[1 - \frac{\gamma-1}{2} M_o^2 (2y_4 - 1)\right] \qquad (9')$$

Furthermore,

$$F_3 = p_3 A + \dot{m} u_3$$

$$= p_3 A + \dot{m} u_\infty (1 - y_3) \qquad (19)$$

and, from Eq. 13,

$$F_4 = \frac{p_o A M_o^2}{1 - y_4} \left[\frac{1}{M_o^2} - \frac{\gamma-1}{2} y_4^2 + \gamma (1 - y_4)^2\right] \qquad (13')$$

These equations yield

$$\frac{p_3}{p_o} = \frac{1}{1 - y_4} \left(1 - \frac{\gamma-1}{2} M_o^2 y_4^2\right) \qquad (20)$$

i.e., (by virtue of Eq. 14), $p_3 = p_4$.

Finally, from Eq. 20 and the continuity equation in the form

$$\frac{p_3 u_3}{T_3} = \frac{p_0 u_w}{T_0}$$

one obtains

$$\frac{1}{1-y_3}\,\frac{T_3}{T_0} = \frac{1}{1-y_4}\left(1 - \frac{\gamma-1}{2} M_0^2 y_4^2\right)$$

or

$$\frac{1}{1-y_3}\left[\frac{T_3}{T_0} - \frac{\gamma-1}{2} M_0^2 (1-y_3)^2\right] = \frac{1}{1-y_4}\left(1 - \frac{\gamma-1}{2} M_0^2 y_4^2\right) \qquad (21)$$

When $y_4 = 0$ (i.e., when M_0 is below the critical value for stability of the wake), $p_3 = p_4 = p_0$ and

$$\frac{u_3}{u_w} = 1 - y_3 = \frac{1}{(\gamma-1)M_0^2}\left\{\left[1 + 2(\gamma-1)M_0^2 \frac{T_3}{T_0}\right]^{\frac{1}{2}} - 1\right\} \qquad (22)$$

$$F_3 = p_0 A + \dot{m} u_w (1-y_3) \qquad (23)$$

$$M_3^2 = M_0^2 (1-y_3)$$

$$= \frac{1}{\gamma-1}\left\{\left[1 + 2(\gamma-1)M_0^2 \frac{T_3}{T_0}\right]^{\frac{1}{2}} - 1\right\} \qquad (24)$$

All other flow properties at station 3 are then readily calculated for this case. If, on the other hand, M_0 is above the critical value, the wake is stable and y_4 is no longer uniquely determined by the boundary conditions. The flow at station 3 can then be specified independently of these conditions.

These results will now be applied to calculation of the power required to maintain the steady level motion of simple vehicles by

various means and under various conditions.

Power required.

The following calculations concern only the power required for propulsion and do not account for the drag of supporting and stabilizing devices; nor do they account for the possible utilization of boundary layer air in internal modes of propulsion, or for the efficiencies of the components of machinery through which the required power is delivered from its prime source to the vehicle or to the flow. The vehicle is assumed to be in each case a body of revolution, with its axis in line with the axis of the tube.

The various modes of propulsion are evaluated in terms of a nondimensional power factor P, which is defined as the ratio between the power required and the quantity $p_o A u_w$.

In the case of external propulsion, the power required is the product of the drag and the velocity of the vehicle. Thus,

$$P_e = \frac{\theta u_w}{p_o A u_w} = \frac{F_i - F_e}{A u_w} \tag{25}$$

When internal propulsion is considered, the power required is calculated as the increment of stagnation enthalpy (relative to the vehicle) that must be imparted to the flow in the unit of time in order to maintain the steady motion of the vehicle. The

transfer of energy to the flow is assumed to take place in ev case between stations 1 and 3. Thus,

$$P_i = \frac{\dot{m} c_p (T_3^\circ - T_1^\circ)}{p_0 A u_w}$$
$$= \frac{\gamma}{\gamma - 1} \frac{T_3^\circ - T_1^\circ}{T_0}$$

The following conditions and modes of propulsion will be considered:

(1) $M_0 = 0.8$, with

(1,a) external propulsion, and

(1,b) internal propulsion, by means of a fan ahead of station t.

(2) $M_0 = 2.5$, with

(2,a) external propulsion,

(2,b) internal propulsion by means of a crypto-steady energy exchanger ahead of station t, and

(2,c) internal, ramjet-type propulsion

Condition 1. $M_0 = 0.8$. The diameter of the vehicle consider is equal to 68.5% of the diameter of the tube. Thus, $B = .46$ and $A_t/A = .531$. The relative flow is sonic at station t. Th being a borderline situation, the power factor will be calcul first for a constant-T^{o*} flow and then also for a constant-T^o flow ahead of the vehicle.

With external propulsion, the relative flow is isoenergetic from station 1 to station 3. Assuming the flow to be isentropic from station 1 to station 6, the continuity equation gives $D_1 = .531D(1) = .3077$, hence $M_1 = .328$. Then, Eqs. 11, 13, and 9 yield

$$y_1 = .6$$

$$\frac{F_1}{p_0 A} = 2.739$$

$$\frac{T_1^\circ}{T_0} = .9744$$

Since the flow between 1 and 3 is isoenergetic, $T_3^\circ = T_1^\circ$. Furthermore, M_0 is subcritical. Therefore, $p_3 = p_0$, and Eqs. 22 and 24 give $y_3 = .125$ and $M_3^2 = .56$. Finally,

$$\frac{F_2}{p_0 A} = \frac{F_3}{p_0 A} = 1 + \gamma M_3^2 = 1.784$$

and

$$P_c = \frac{F_1 - F_2}{p_0 A} = .955$$

It should be noted that in this condition the flow receives no energy and is not otherwise disturbed between stations 2 and 3. Therefore, station 3 effectively coincides with station 2. Since the cross-sectional area at 2 is the same as at 1, the stagnation pressure ratio is obtained from the continuity equation for the isoenergetic flow between these two stations as

$$\frac{p_2^\circ}{p_1^\circ} = \frac{D_1}{D_3} = .566$$

The large loss of stagnation pressure is due primarily to a shock between stations t and 2.

For the condition of internal propulsion, the thrust generator considered in this case is a fan located ahead of station t. With $\gamma = 1.4$, and neglecting the entropy increment through the fan, the continuity equation between stations 1 and t may be written as

$$D_1 = \frac{A_t}{A}\left(\frac{T_t^\circ}{T_1^\circ}\right)^3 D(1)$$

Furthermore, $p_2 = p_3 = p_0$ because, as before, M_0 is subcritical and stations 2 and 3 coincide. Also, since the flow is isoenergetic from t to 3, $T_3^\circ = T_2^\circ = T_t^\circ$. Finally, the net horizontal force acting on the vehicle must be zero, hence $F_2 (= F_3) = F_1$. With these conditions, Eqs. 9, 11, 13, 14, 22, 24 and 27 yield:

$y_1 = .235$	$y_3 = .95$
$M_1 = .615$	$M_3 = .84$
$\frac{T_t^\circ}{T_0} = 1.0679$	$\frac{F_1}{RA} = \frac{F_3}{RA} = 1.984$
$\frac{T_t^\circ}{T_0} = 1.25$	$\frac{p_t}{p_t^\circ} = \frac{p_2}{p_t^\circ} = .533$

It is interesting to note that, whereas the total pressure loss from station t to station 2 is higher in this case than with external propulsion, the overall entropy rise between stations 1 and 2 is actually 30% lower.

Finally,

$$\frac{P_i}{P_e} = \frac{\gamma}{\gamma-1}\,\frac{T_3^\circ - T_1^\circ}{T_0} = .638$$

Thus, the ratio between the power required with this mode of internal propulsion and the power required, for the same vehicle and at the same Mach number M_0, with external propulsion, is $P_i/P_e = .668$.

If $T_0 = 500\ ^\circ R$, hence $a_0 = 1100$ fps, the velocity of the vehicle in the condition just considered is 880 fps. The maximum velocity of the air ahead of the vehicle, relative to the tube, is 529 fps with external propulsion and 207 fps with internal propulsion. The maximum velocity of the air in the wake, relative to the tube, is 110 fps with external propulsion and 83.5 fps (in the direction opposite to the direction of motion of the vehicle) with internal propulsion.

Intermediate situations, involving both internal and external propulsion, may be investigated as follows:

For various values of y_1, Eq. 11 provides M_1, hence D_1. Then, Eqs. 13, 27, and 9 provide the corresponding values of $\frac{F_1}{p_0 A}$, $\frac{T_3^\circ}{T_1^\circ}$ and $\frac{T_1^\circ}{T_0}$, Eq. 24 gives M_3^2, and F_3/p_0A is obtained as $1 + \gamma M_3^2$. The difference between F_1 and F_3 is the thrust that must be provided by external forces to maintain the

steady motion of the vehicle. The results are plotted, for th condition under consideration, in Fig. 3. Values of y_1 intermediate between .235 and .6 are produced when propulsion is of mixed type, i.e., both internal and external, the latter compo of the thrust being $F_1 - F_3$. The power factor P decreases mo tonically as the mode of propulsion is changed from purely ex ($y_1 = .6$) to purely internal ($y_1 = .235$). The condition $y_1 <$ occurs when the internal thrust exceeds the value required to tain steady motion.

If the constant-T^* condition is replaced by the assumpt of an isoenergetic flow ahead of station 1, the following re are obtained.

With external propulsion, $M_1 = .328$ as before, but Eq. 1 yields

$$\frac{F_1}{p_0 A} = 2.945$$

Furthermore, since $T_3^\circ = T_1^\circ = T_0^\circ = 1.128\ T_0$, Eqs. 22 and 24 $M_3^2 = .64$, hence (remembering that $p_3 = p_0$, because M_0 is sub-critical)

$$\frac{F_3}{p_0 A} = 1 + \gamma M_3^2 = 1.896$$

and

$$P_e = \frac{F_1 - F_3}{p_0 A} = 1.049$$

For the case of internal propulsion, the condition $F_3 = F_1$ and Eqs. 15, 17, and 24 yield $M_1 = .621$, $T_3^o = 1.1745\ T_o\ M_3^2 = .739$, and $F_1/p_oA = F_3/p_oA = 2.03$. Then, since $T_1^o = 1.128\ T_o$,

$$P_i = \frac{\gamma}{\gamma-1}\,\frac{T_3^o - T_1^o}{T_o} = .693$$

Thus, the modified analytical model yields $P_i/P_e = .662$. This result is very close to that obtained through the use of the constant-T^{o*} assumption ($P_i/P_e = .668$). It appears, therefore, that the latter assumption can be used with confidence for all subsonic speeds up to at least $M_o = .8$. However, the calculated power required is, at this Mach number, between 8 and 10 percent higher when the flow is assumed to be isoenergetic than when the constant-T^{o*} assumption is used.

Condition 2. $M_o = 2.5$. The diameter of the vehicle is 72.7% of the inner diameter of the tube. The nose of the vehicle is designed to produce, through a train of oblique shocks, a stagnation pressure ratio (p_t^o/p_o^o) of .80 at $M_o = 2.5$ in the absence of flow disturbances ahead of station 1. The stipulated diameter ratio corresponds to $B = .525$ and $A_t/A = .475$.

With external propulsion, the flow is choked at t and subsonic at 1. If the flow in this condition is assumed to be isentropic between 1 and t, the continuity equation gives

$D_1 = .475\ (D1) = .275$, hence $M_1 = .289$ and $N_1 = .2609$. Then Eq. 15 yields $F_1/p_oA = 14.39$.

Assuming $p_2^o/p_1^o = .95$, one obtains

$$D_2 = D_1/.95 = .29, \text{ hence } M_2 = 2.194,\ N_2 = .3972$$

$$F_2/p_2A = (N_1/N_2)F_1/p_2A = 9.44$$

and finally

$$P_e = \frac{F_1 - F_2}{p_2A} = 4.95$$

The possibility that the flow may be subsonic at 2 must be excluded. In fact, with the supersonic solution ($M_2 = 2.194$) selected above,

$$\frac{p_2}{p_o} = \frac{F_2}{p_2A(1+\gamma M_2^2)} = 1.22$$

If the flow at 2 were subsonic, the pressure there would be at least five times higher and would increase further from there in the direction of the flow. This situation would be incompatible with the boundary conditions. Therefore, the flow at 2 is supersonic and underexpanded. It is possible that the flow will adjust itself to a lower pressure further downstream through a pattern of expansion waves between stations 2 and 3.

With internal propulsion, if a cryptosteady energy exchang

is used to energize the flow between 1 and t, the disturbances ahead of 1 can be "swallowed". Then the flow at 1 is undisturbed, and $F_1 = F_o$, $M_1 = M_o$, and $T_1^o = T_o^o$.

The input of energy is assumed to take place isentropically behind the oblique shocks surrounding the nose, through which the stagnation pressure ratio retains the stipulated value .8. A further 5% loss of stagnation pressure is assumed to take place between the throat and station 2. Then,

$$\frac{p_2^o}{p_1^o} = .8\left(\frac{T_2^o}{T_1}\right)^{\frac{\gamma}{\gamma-1}} \times .95$$

$$= .76\left(\frac{T_2^o}{T_1^o}\right)^{3.5}$$

and the continuity equation

$$\frac{p_2^o D_2}{\sqrt{T_2^o}} = \frac{p_1^o D_1}{\sqrt{T_1^o}} \left(= \frac{p_o^o D_o}{\sqrt{T_o^o}}\right)$$

becomes

$$.76\left(\frac{T_2^o}{T_o^o}\right)^3 = \frac{D_o}{D_2} \tag{28}$$

On the other hand, the momentum equation ($F_2 = F_o$) may be written in the form

$$\frac{T_2^o}{T_o^o} = \left(\frac{N_2}{N_o}\right)^2 \tag{29}$$

Eqs. 28 and 29 yield

$$.76\, Z_2 = Z_o = 710.5 \times 10^{-6}$$

whence

$$Z_2 = 935 \times 10^{-6}$$

$$M_2 = 2.320 \qquad N_2 = .3917$$

Therefore, $T_2^o/T_o^o = (.3917/.3846)^2 = 1.0373$, and finally

$$\frac{T_1^*}{T_o} = \frac{T^*}{T_o} = 2.25$$

$$\frac{T_2^o}{T_o^o} = 2.334$$

$$P = \frac{\gamma}{\gamma-1}\frac{T_2^o - T_1^o}{T_o} = .294$$

The ratio between the power required with this mode of internal propulsion and the power required, for the same vehicle at the same Mach number M_o, with external propulsion, is in this case $P_i/P_e = .0594$.

It can be shown that the flow is always underexpanded at with internal propulsion if the supersonic solution for M_2 is lower than M_o. Indeed, from the condition $F_2 = F_3$, one obtains

$$\frac{p_2}{p_o} = \frac{F_2}{p_o A(1+\gamma M_o^2)}$$

$$= \frac{1+\gamma M_o^2}{1+\gamma M_2^2} > 1 \quad \text{if} \quad M_o > M_2$$

This confirms that in the example just treated no shock occurs between stations t and 2. However, as before, it is likely that expansion waves will be present between stations 2 and 3.

These waves will not affect the power required.

If the mode of propulsion is of the ramjet type, the required power factor is somewhat higher, although still one order of magnitude lower than with external propulsion. It should be noted that the use of purely thermal propulsion in the type of vehicle under consideration would not be practical, not only because it would require the assistance of auxiliary devices for acceleration to the design speed, but also because it would not provide for stability of the flow ahead of the throat. This stability, as well as some of the thrust required at the lower speeds, could be provided by a fan or by an ejector pump ahead of station t. In the present analysis of cruising operation at $M_o = 2.5$ it is assumed, for simplicity, that whereas most of the energy input is in the form of heat addition to the flow between stations t and 2, the work performed by the pumping device ahead of t is just enough to make up for the loss of stagnation pressure between t and 2. The calculated power factor will, of course, account for the total power that is required for this combined operation.

Under these conditions, the loss of stagnation pressure from 1 to 2 is again 20%, and the momentum equation ($F_2 = F_o$) and continuity equation ($p^oD/\sqrt{T^o}$ = constant) become

$$.8G_2 = G_o$$

and

$$\frac{T_2^\circ}{T_0^\circ} = \left(\frac{.8 D_2}{D}\right)^2$$

whence $M_2 = 2.223$ and $T_2^\circ/T_0^\circ = 1.0601$. Then, since $T_0^\circ/T_0 =$ there follows $T_2^\circ/T_0 = 2.385$ and

$$P_i = \frac{\gamma}{\gamma-1}\,\frac{T_2^\circ - T_0^\circ}{T_0} = .472$$

This power factor is less than one tenth of the power fac for external propulsion. It should be noted, however, that th calculated value of P_i for thermal propulsion is very sensitiv changes in the losses associated with heat addition and in the tribution of mechanical and thermal input components. Even a moderate increase of stagnation pressure loss downstream of t not compensated through an increased allocation of power to th mechanical input device ahead of t, may result in a substantia increase of power required.

The input of thermal energy may be effected either through combustion of a fuel or by transfer of heat from a suitable sou (e.g., a nuclear reactor). The increase of stagnation tempera that is required for thermal propulsion is relatively small and should be obtainable with heat exchangers of acceptable size ar drag. In some cases it may be advisable to carry out the addit of heat subsonically (in order to reduce the attendant loss of

stagnation pressure) and to re-accelerate the flow to supersonic speed through a converging-diverging passage downstream of the heating region.

Internal, ramjet-type propulsion with heat addition behind the vehicle.

Under certain conditions it may be desirable to add heat to the flow between stations 2 and 3 rather than upstream of station 2. When this is done, thrust is generated in much the same manner as it is in most conventional ramjets, except for the fact that, in the case of the vehicle in the tube, the structure of the "combustion chamber" is part of the stationary tube and not of the moving vehicle. Of course, no flow process downstream of station 2 can have any effect on the vehicle unless the flow at this station - and for some distance upstream of it - is subsonic.

It has been shown that when the flow at 2 is subsonic the pressure there is too high to be supported by a stable wake under the conditions examined in the preceding examples. This difficulty is eliminated, however, when the subsonic flow condition at 2 is sustained by a Rayleigh process between 2 and 3, because the rate of heat input that is capable of maintaining this condition is always above the critical value that produces thermal choking at the downstream end of the heating region. With $M_3 = 1$, the upper limit of the pressure upstream of station 3 is no longer

controlled by the downstream boundary conditions.

The calculation of the power factor is particularly sim with this mode of propulsion because, from the conditions $F_3 = F_2 = F_o$ and $M_3 = 1$, one obtains

$$\frac{T_2^\circ}{T_o^\circ} = \left(\frac{N(1)}{N_o}\right)^2$$

whence

$$P_i = \frac{\gamma}{\gamma-1}\frac{T_o^\circ}{T_o}\left[\left(\frac{N(1)}{N_o}\right)^2 - 1\right]$$

For $M_o = 2.5$ in air, $P_i = 3.27$. This power factor is v above the value calculated above for the case of heat additi tween t and 2, mainly because of the large entropy increment is produced by the shock through which the flow becomes subs upstream of 2. Nevertheless, this mode of propulsion has se attractive features that make it worthy of consideration des its higher power requirements. Its most important advantage that it permits the input of propulsive energy, in the form heat, from sources which are activated by the passing vehicl fixed to the tube.

Discussion of results, and concluding remarks.

The simple analysis developed in this study reveals that flow disturbances that are set up by a moving vehicle in a t

are largely determined by the mode of propulsion. The same can be said, of course, of the attendant flow losses and of the power required. In other words, the thrust that is required to maintain the motion of a vehicle in a tube depends on the manner in which the thrust itself is generated. The dependence is particularly critical when the speed of the vehicle is high. This result is illustrated by the relative magnitudes of the power factors calculated in the examples above for a few, randomly selected modes of propulsion.

It is generally possible to find, for each configuration of the vehicle and for each cruising speed, an internal mode of propulsion that produces smaller velocity fluctuations in the adjacent fluid columns - and, accordingly, requires less power - than any external mode. The potential superiority of internal over external modes is small at low speeds but increases with increasing cruising speed and becomes impressive at high subsonic and at supersonic speeds.

Some merit, from the standpoint of power required, may be found under special conditions in mixed schemes, involving both internal and external propulsion.

During acceleration with internal propulsion, the air just ahead of the vehicle is induced to flow, relative to the tube, in

the direction of the acceleration of the vehicle or in the oppc direction, depending on the speed of the vehicle and on the exc of thrust over drag. An internally propelled vehicle, acceler from rest to cruising speed, generates forward-facing expansior compressior waves, in this order of succession. The net effec these waves ahead of the vehicle, in the final steady state, is most cases a forward-facing flow if the cruising speed is subs In general, it is only at supersonic speeds that an i ternal t generator can eliminate all disturbances ahead of the vehicle out producing an excess of thrust over drag.

Nevertheless, even at subsonic speeds, the flow disturban ahead of the vehicle can be reduced, by appropriate means of i nal propulsion, to a much lower amplitude than would be produce external propulsion. As a consequence, the increment of stream force (relative to the vehicle) that is imparted by wall fricti to the disturbed flow ahead of the vehicle is normally smaller internal than with external propulsion.

The flow behind the vehicle undergoes for some distance ce rapid transformations, the nature of which has been examined in tail by Hagerup in a recent study (Ref. 4). The subsequent beh of the "wake" depend on the speed of the vehicle and on the mod thrust generation. Although there is much in the behavior of t wake that is still incompletely understood, it has been ascerta

that there is a range of operating regimes within which the boundary conditions demand that the wake flow be substantially at rest relative to the tube everywhere except in close proximity to the vehicle. Outside of this range the wake is "stable", in the sense that even relatively large local perturbations within it may be compatible in steady state with the boundary conditions. Of course, if in the vehicle-fixed frame of reference the wake flow is sonic or supersonic at any station, the downstream boundary conditions can have no effect on the flow upstream of that station.

When flow disturbances are sustained in steady state over great distances ahead of the vehicle, the stagnation temperature of the air, relative to the vehicle, is lower than it would be in flight at the same Mach number through the surrounding atmosphere.

At high travel speeds, at least a portion of the power input for internal propulsion must be supplied ahead of the throat of the air transfer passage. The purpose of this arrangement is to reduce the amplitude of the flow disturbances ahead of the vehicle at high subsonic speeds and to prevent the propagation of such disturbances altogether at supersonic speeds.

At very high speeds, thermal modes of internal propulsion, in which the input of energy (except for the relatively small fraction which must be supplied ahead of the throat) is in the form of heat

addition to the flow, promise attractive advantages of economy and mechanical simplicity. These modes also lend themselves to interesting possibilities in the utilization of heat from nucl reactors.

Special attention should be given to thermal modes in whi the heat sources are fixed to the tube and successively activ in such synchromism with the passing vehicle that they produce substantially steady regime of heat addition in the vehicle-fi frame of reference.

References

1. Tollmien, W., "Luftwiderstand und Druckverlauf bei der Fahrt von Zügen in einem Tunnel," Zeitschrift des Vereines deutscher Ingenieure, 71, No. 6, 199-203, 5 February 1927.

2. Foa, J.V., Elements of Flight Propulsion, Wiley, 1960.

3. Cromack, D. and Gijsels, L., Section G of "Research on the Dynamics of a Vehicle in a Tube," Final Progress Report, Grant No. DA ORD 31-124-61-G88, Rensselaer Polytechnic Institute, June 1964.

4. Hagerup, H., "A Note on the Flow Induced by a Disturbance Traveling in a Tube," Rensselaer Polytechnic Institute Tech. Rept. TR AE 6405, June 1964.

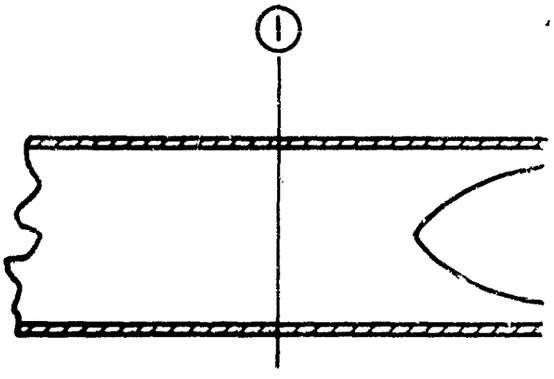

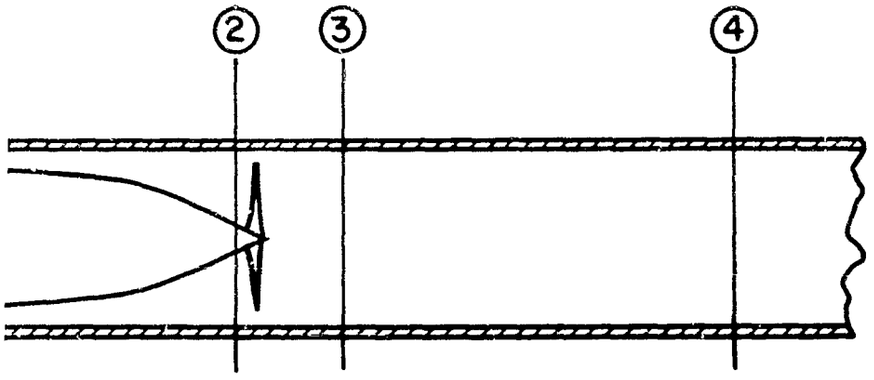

FIG. 1

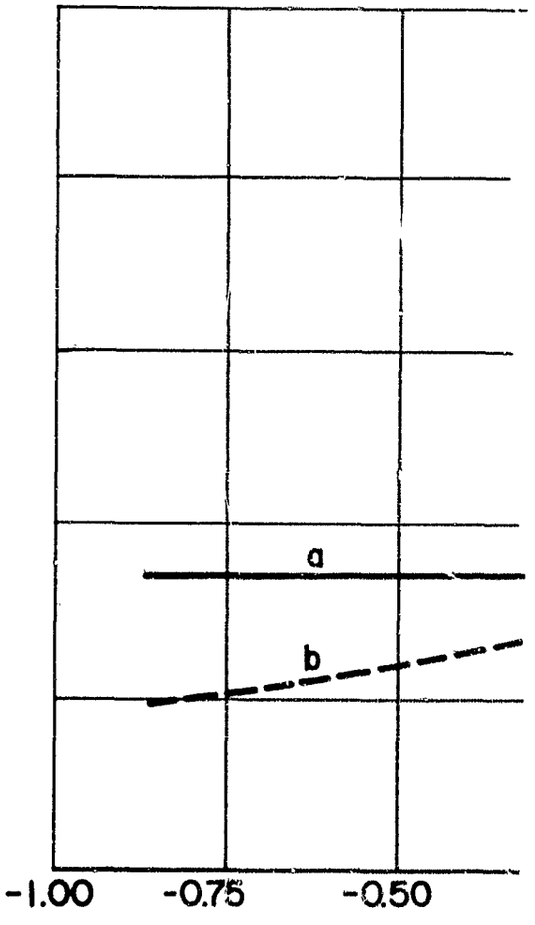
a
b
-1.00
-0.75
-0.50

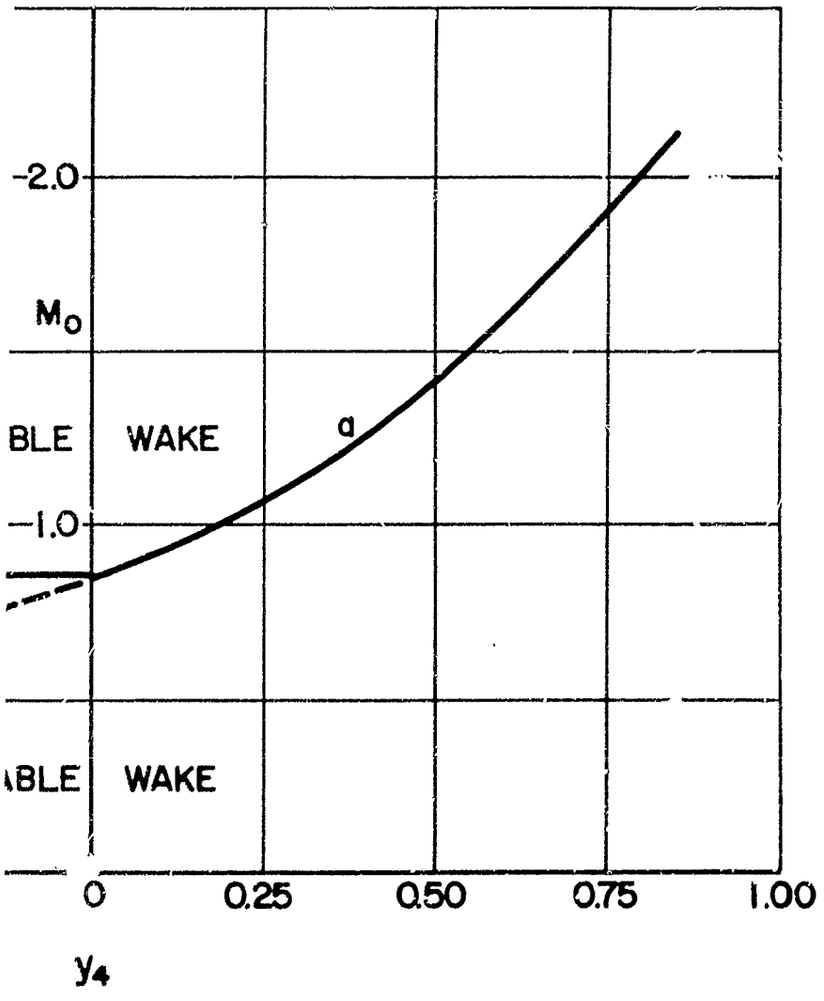

FIG. 2

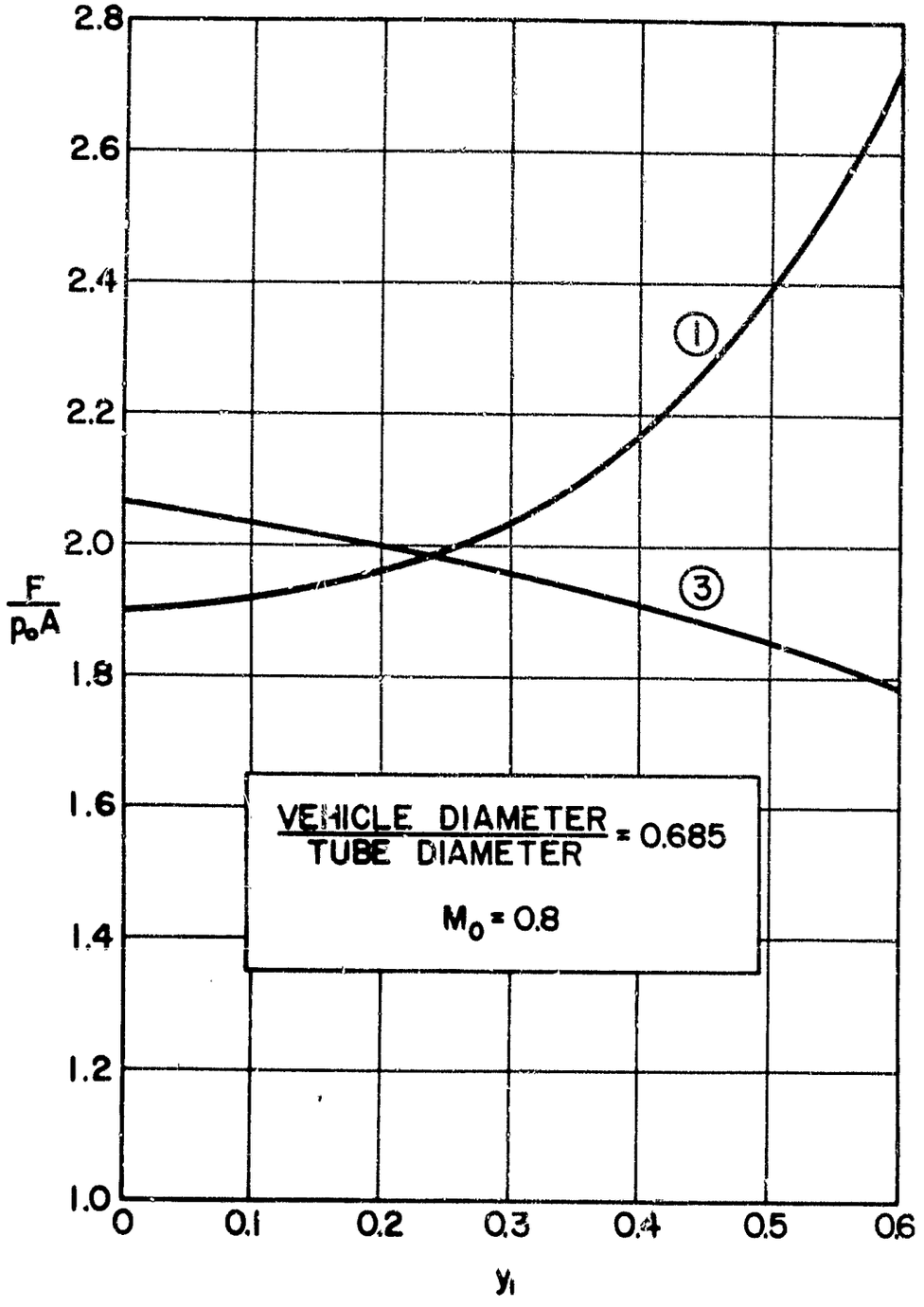
2.8
2.6
2.4
2.2
2.0
1.8
1.6
1.4
1.2
1.0
0
0.1
0.2
0.3
0.4
0.5
0.6
F / P₀A
y₁
①
③
VEHICLE DIAMETER / TUBE DIAMETER = 0.685
M₀ = 0.8

FIG. 3

APPENDIX

Function Z for $\gamma = 1.4$

M	Z	M	Z	M	Z
0.122	3.555E-07	0.202	9.833E-06	0.282	7.528E-05
0.124	3.967E-07	0.204	1.047E-05	0.284	7.842E-05
0.126	4.419E-07	0.206	1.113E-05	0.286	8.167E-05
0.128	4.913E-07	0.208	1.184E-05	0.288	8.501E-05
0.130	5.453E-07	0.210	1.257E-05	0.290	8.846E-05
0.132	6.042E-07	0.212	1.335E-05	0.292	9.201E-05
0.134	6.684E-07	0.214	1.416E-05	0.294	9.567E-05
0.136	7.382E-07	0.216	1.501E-05	0.296	9.944E-05
0.138	8.139E-07	0.218	1.590E-05	0.298	1.033E-04
0.140	8.961E-07	0.220	1.683E-05	0.300	1.073E-04
0.142	9.851E-07	0.222	1.781E-05	0.302	1.114E-04
0.144	1.081E-06	0.224	1.883E-05	0.304	1.156E-04
0.146	1.185E-06	0.226	1.990E-05	0.306	1.200E-04
0.148	1.298E-06	0.228	2.101E-05	0.308	1.244E-04
0.150	1.418E-06	0.230	2.218E-05	0.310	1.290E-04
0.152	1.549E-06	0.232	2.339E-05	0.312	1.337E-04
0.154	1.689E-06	0.234	2.466E-05	0.314	1.385E-04
0.156	1.839E-06	0.236	2.599E-05	0.316	1.435E-04
0.158	2.000E-06	0.238	2.736E-05	0.318	1.486E-04
0.160	2.173E-06	0.240	2.880E-05	0.320	1.538E-04
0.162	2.358E-06	0.242	3.029E-05	0.322	1.591E-04
0.164	2.556E-06	0.244	3.185E-05	0.324	1.646E-04
0.166	2.768E-06	0.246	3.347E-05	0.326	1.703E-04
0.168	2.994E-06	0.248	3.515E-05	0.328	1.760E-04
0.170	3.234E-06	0.250	3.690E-05	0.330	1.819E-04
0.172	3.491E-06	0.252	3.871E-05	0.332	1.879E-04
0.174	3.764E-06	0.254	4.060E-05	0.334	1.941E-04
0.176	4.055E-06	0.256	4.255E-05	0.336	2.004E-04
0.178	4.364E-06	0.258	4.458E-05	0.338	2.069E-04
0.180	4.692E-06	0.260	4.669E-05	0.340	2.135E-04
0.182	5.039E-06	0.262	4.887E-05	0.342	2.203E-04
0.184	5.408E-06	0.264	5.112E-05	0.344	2.272E-04
0.186	5.799E-06	0.266	5.346E-05	0.346	2.343E-04
0.188	6.212E-06	0.268	5.588E-05	0.348	2.415E-04
0.190	6.650E-06	0.270	5.839E-05	0.350	2.489E-04
0.192	7.112E-06	0.272	6.098E-05	0.352	2.564E-04
0.194	7.600E-06	0.274	6.365E-05	0.354	2.641E-04
0.196	8.115E-06	0.276	6.642E-05	0.356	2.720E-04
0.198	8.658E-06	0.278	6.928E-05	0.358	2.800E-04
0.200	9.231E-06	0.280	7.223E-05	0.360	2.882E-04

M	Z	M	Z	M	Z
0.362	2.965E-04	0.442	7.726E-04	0.522	1.519E-03
0.364	3.050E-04	0.444	7.881E-04	0.524	1.541E-03
0.366	3.137E-04	0.446	8.039E-04	0.526	1.562E-03
0.368	3.225E-04	0.448	8.197E-04	0.528	1.584E-03
0.370	3.315E-04	0.450	8.358E-04	0.530	1.606E-03
0.372	3.407E-04	0.452	8.521E-04	0.532	1.628E-03
0.374	3.500E-04	0.454	8.685E-04	0.534	1.650E-03
0.376	3.595E-04	0.456	8.851E-04	0.536	1.672E-03
0.378	3.692E-04	0.458	9.018E-04	0.538	1.694E-03
0.380	3.791E-04	0.460	9.187E-04	0.540	1.717E-03
0.382	3.891E-04	0.462	9.358E-04	0.542	1.739E-03
0.384	3.993E-04	0.464	9.531E-04	0.544	1.762E-03
0.386	4.097E-04	0.466	9.705E-04	0.546	1.784E-03
0.388	4.202E-04	0.468	9.881E-04	0.548	1.807E-03
0.390	4.309E-04	0.470	1.006E-03	0.550	1.830E-03
0.392	4.418E-04	0.472	1.024E-03	0.552	1.853E-03
0.394	4.529E-04	0.474	1.042E-03	0.554	1.876E-03
0.396	4.642E-04	0.476	1.060E-03	0.556	1.899E-03
0.398	4.756E-04	0.478	1.078E-03	0.558	1.922E-03
0.400	4.872E-04	0.480	1.097E-03	0.560	1.945E-03
0.402	4.990E-04	0.482	1.116E-03	0.562	1.968E-03
0.404	5.110E-04	0.484	1.135E-03	0.564	1.991E-03
0.406	5.231E-04	0.486	1.154E-03	0.566	2.015E-03
0.408	5.355E-04	0.488	1.173E-03	0.568	2.038E-03
0.410	5.480E-04	0.490	1.192E-03	0.570	2.062E-03
0.412	5.607E-04	0.492	1.211E-03	0.572	2.085E-03
0.414	5.735E-04	0.494	1.231E-03	0.574	2.109E-03
0.416	5.866E-04	0.496	1.251E-03	0.576	2.132E-03
0.418	5.998E-04	0.498	1.271E-03	0.578	2.156E-03
0.420	6.132E-04	0.500	1.291E-03	0.580	2.180E-03
0.422	6.268E-04	0.502	1.311E-03	0.582	2.203E-03
0.424	6.406E-04	0.504	1.331E-03	0.584	2.227E-03
0.426	6.546E-04	0.506	1.351E-03	0.586	2.251E-03
0.428	6.687E-04	0.508	1.372E-03	0.588	2.275E-03
0.430	6.830E-04	0.510	1.393E-03	0.590	2.299E-03
0.432	6.975E-04	0.512	1.413E-03	0.592	2.323E-03
0.434	7.121E-04	0.514	1.434E-03	0.594	2.347E-03
0.436	7.270E-04	0.516	1.455E-03	0.596	2.371E-03
0.438	7.420E-04	0.518	1.477E-03	0.598	2.395E-03
0.440	7.572E-04	0.520	1.498E-03	0.600	2.419E-03

M	Z	M	Z	M	Z
0.602	2.443E-03	0.682	3.386E-03	0.762	4.202E-03
0.604	2.467E-03	0.684	3.409E-03	0.764	4.220E-03
0.606	2.491E-03	0.686	3.431E-03	0.766	4.237E-03
0.608	2.515E-03	0.688	3.454E-03	0.768	4.255E-03
0.610	2.539E-03	0.690	3.476E-03	0.770	4.272E-03
0.612	2.563E-03	0.692	3.498E-03	0.772	4.289E-03
0.614	2.587E-03	0.694	3.520E-03	0.774	4.306E-03
0.616	2.611E-03	0.696	3.542E-03	0.776	4.323E-03
0.618	2.635E-03	0.698	3.564E-03	0.778	4.340E-03
0.620	2.659E-03	0.700	3.585E-03	0.780	4.357E-03
0.622	2.683E-03	0.702	3.607E-03	0.782	4.373E-03
0.624	2.707E-03	0.704	3.629E-03	0.784	4.389E-03
0.626	2.731E-03	0.706	3.650E-03	0.786	4.406E-03
0.628	2.755E-03	0.708	3.671E-03	0.788	4.422E-03
0.630	2.779E-03	0.710	3.693E-03	0.790	4.437E-03
0.632	2.803E-03	0.712	3.714E-03	0.792	4.453E-03
0.634	2.827E-03	0.714	3.735E-03	0.794	4.469E-03
0.636	2.851E-03	0.716	3.756E-03	0.796	4.484E-03
0.638	2.875E-03	0.718	3.776E-03	0.798	4.499E-03
0.640	2.898E-03	0.720	3.797E-03	0.800	4.514E-03
0.642	2.922E-03	0.722	3.818E-03	0.802	4.529E-03
0.644	2.946E-03	0.724	3.838E-03	0.804	4.544E-03
0.646	2.970E-03	0.726	3.858E-03	0.806	4.559E-03
0.648	2.993E-03	0.728	3.879E-03	0.808	4.573E-03
0.650	3.017E-03	0.730	3.899E-03	0.810	4.587E-03
0.652	3.040E-03	0.732	3.919E-03	0.812	4.602E-03
0.654	3.064E-03	0.734	3.938E-03	0.814	4.616E-03
0.656	3.087E-03	0.736	3.958E-03	0.816	4.629E-03
0.658	3.111E-03	0.738	3.978E-03	0.818	4.643E-03
0.660	3.134E-03	0.740	3.997E-03	0.820	4.657E-03
0.662	3.157E-03	0.742	4.016E-03	0.822	4.670E-03
0.664	3.181E-03	0.744	4.035E-03	0.824	4.683E-03
0.666	3.204E-03	0.746	4.054E-03	0.826	4.696E-03
0.668	3.227E-03	0.748	4.073E-03	0.828	4.709E-03
0.670	3.250E-03	0.750	4.092E-03	0.830	4.722E-03
0.672	3.273E-03	0.752	4.111E-03	0.832	4.734E-03
0.674	3.296E-03	0.754	4.129E-03	0.834	4.746E-03
0.676	3.318E-03	0.756	4.148E-03	0.836	4.759E-03
0.678	3.341E-03	0.758	4.166E-03	0.838	4.771E-03
0.680	3.364E-03	0.760	4.184E-03	0.840	4.783E-03

M	Z
0.842	4.794E-03
0.844	4.806E-03
0.846	4.817E-03
0.848	4.829E-03
0.850	4.840E-03
0.852	4.851E-03
0.854	4.861E-03
0.856	4.872E-03
0.858	4.882E-03
0.860	4.893E-03
0.862	4.903E-03
0.864	4.913E-03
0.866	4.922E-03
0.868	4.932E-03
0.870	4.942E-03
0.872	4.951E-03
0.874	4.960E-03
0.876	4.969E-03
0.878	4.978E-03
0.880	4.986E-03
0.882	4.995E-03
0.884	5.003E-03
0.886	5.012E-03
0.888	5.020E-03
0.890	5.027E-03
0.892	5.035E-03
0.894	5.043E-03
0.896	5.050E-03
0.898	5.057E-03
0.900	5.064E-03
0.902	5.071E-03
0.904	5.078E-03
0.906	5.085E-03
0.908	5.091E-03
0.910	5.098E-03
0.912	5.104E-03
0.914	5.110E-03
0.916	5.116E-03
0.918	5.121E-03
0.920	5.127E-03
0.922	5.132E-03
0.924	5.138E-03
0.926	5.143E-03
0.928	5.148E-03
0.930	5.152E-03
0.932	5.157E-03
0.934	5.162E-03
0.936	5.166E-03
0.938	5.170E-03
0.940	5.174E-03
0.942	5.178E-03
0.944	5.182E-03
0.946	5.186E-03
0.948	5.189E-03
0.950	5.193E-03
0.952	5.196E-03
0.954	5.199E-03
0.956	5.202E-03
0.958	5.205E-03
0.960	5.207E-03
0.962	5.210E-03
0.964	5.212E-03
0.966	5.214E-03
0.968	5.217E-03
0.970	5.219E-03
0.972	5.220E-03
0.974	5.222E-03
0.976	5.224E-03
0.978	5.225E-03
0.980	5.227E-03
0.982	5.228E-03
0.984	5.229E-03
0.986	5.230E-03
0.988	5.231E-03
0.990	5.231E-03
0.992	5.232E-03
0.994	5.232E-03
0.996	5.233E-03
0.998	5.233E-03
1.000	5.233E-03
1.002	5.233E-03
1.004	5.233E-03
1.006	5.232E-03
1.008	5.232E-03
1.010	5.231E-03
1.012	5.231E-03
1.014	5.230E-03
1.016	5.229E-03
1.018	5.228E-03
1.020	5.227E-03
1.022	5.226E-03
1.024	5.224E-03
1.026	5.223E-03
1.028	5.221E-03
1.030	5.220E-03
1.032	5.218E-03
1.034	5.216E-03
1.036	5.214E-03
1.038	5.212E-03
1.040	5.209E-03
1.042	5.207E-03
1.044	5.205E-03
1.046	5.202E-03
1.048	5.200E-03
1.050	5.197E-03
1.052	5.194E-03
1.054	5.191E-03
1.056	5.188E-03
1.058	5.185E-03
1.060	5.182E-03
1.062	5.178E-03
1.064	5.175E-03
1.066	5.171E-03
1.068	5.168E-03
1.070	5.164E-03
1.072	5.160E-03
1.074	5.156E-03
1.076	5.152E-03
1.078	5.148E-03
1.080	5.144E-03

M	Z	M	Z	M	Z
1.082	5.140E-03	1.162	4.906E-03	1.242	4.582E-03
1.084	5.135E-03	1.164	4.899E-03	1.244	4.573E-03
1.086	5.131E-03	1.166	4.892E-03	1.246	4.564E-03
1.088	5.126E-03	1.168	4.884E-03	1.248	4.555E-03
1.090	5.122E-03	1.170	4.877E-03	1.250	4.546E-03
1.092	5.117E-03	1.172	4.870E-03	1.252	4.537E-03
1.094	5.112E-03	1.174	4.862E-03	1.254	4.528E-03
1.096	5.108E-03	1.176	4.855E-03	1.256	4.519E-03
1.098	5.103E-03	1.178	4.847E-03	1.258	4.510E-03
1.100	5.098E-03	1.180	4.840E-03	1.260	4.501E-03
1.102	5.092E-03	1.182	4.832E-03	1.262	4.492E-03
1.104	5.087E-03	1.184	4.824E-03	1.264	4.483E-03
1.106	5.082E-03	1.186	4.816E-03	1.266	4.474E-03
1.108	5.077E-03	1.188	4.809E-03	1.268	4.464E-03
1.110	5.071E-03	1.190	4.801E-03	1.270	4.455E-03
1.112	5.066E-03	1.192	4.793E-03	1.272	4.446E-03
1.114	5.060E-03	1.194	4.785E-03	1.274	4.437E-03
1.116	5.055E-03	1.196	4.777E-03	1.276	4.427E-03
1.118	5.049E-03	1.198	4.769E-03	1.278	4.418E-03
1.120	5.043E-03	1.200	4.761E-03	1.280	4.409E-03
1.122	5.037E-03	1.202	4.753E-03	1.282	4.399E-03
1.124	5.031E-03	1.204	4.745E-03	1.284	4.390E-03
1.126	5.025E-03	1.206	4.736E-03	1.286	4.381E-03
1.128	5.019E-03	1.208	4.728E-03	1.288	4.371E-03
1.130	5.013E-03	1.210	4.720E-03	1.290	4.362E-03
1.132	5.007E-03	1.212	4.711E-03	1.292	4.352E-03
1.134	5.001E-03	1.214	4.703E-03	1.294	4.343E-03
1.136	4.994E-03	1.216	4.695E-03	1.296	4.333E-03
1.138	4.988E-03	1.218	4.686E-03	1.298	4.324E-03
1.140	4.981E-03	1.220	4.678E-03	1.300	4.314E-03
1.142	4.975E-03	1.222	4.669E-03	1.302	4.305E-03
1.144	4.968E-03	1.224	4.661E-03	1.304	4.295E-03
1.146	4.962E-03	1.226	4.652E-03	1.306	4.286E-03
1.148	4.955E-03	1.228	4.643E-03	1.308	4.276E-03
1.150	4.948E-03	1.230	4.635E-03	1.310	4.267E-03
1.152	4.941E-03	1.232	4.626E-03	1.312	4.257E-03
1.154	4.934E-03	1.234	4.617E-03	1.314	4.247E-03
1.156	4.927E-03	1.236	4.609E-03	1.316	4.238E-03
1.158	4.920E-03	1.238	4.600E-03	1.318	4.228E-03
1.160	4.913E-03	1.240	4.591E-03	1.320	4.218E-03

M	Z	M	Z	M	Z
1.322	4.209E-03	1.402	3.817E-03	1.482	3.430E-03
1.324	4.199E-03	1.404	3.808E-03	1.484	3.420E-03
1.326	4.189E-03	1.406	3.798E-03	1.486	3.411E-03
1.328	4.180E-03	1.408	3.788E-03	1.488	3.401E-03
1.330	4.170E-03	1.410	3.778E-03	1.490	3.392E-03
1.332	4.160E-03	1.412	3.768E-03	1.492	3.382E-03
1.334	4.151E-03	1.414	3.759E-03	1.494	3.373E-03
1.336	4.141E-03	1.416	3.749E-03	1.496	3.363E-03
1.338	4.131E-03	1.418	3.739E-03	1.498	3.354E-03
1.340	4.121E-03	1.420	3.729E-03	1.500	3.345E-03
1.342	4.112E-03	1.422	3.719E-03	1.502	3.335E-03
1.344	4.102E-03	1.424	3.710E-03	1.504	3.326E-03
1.346	4.092E-03	1.426	3.700E-03	1.506	3.316E-03
1.348	4.082E-03	1.428	3.690E-03	1.508	3.307E-03
1.350	4.073E-03	1.430	3.680E-03	1.510	3.298E-03
1.352	4.063E-03	1.432	3.671E-03	1.512	3.288E-03
1.354	4.053E-03	1.434	3.661E-03	1.514	3.279E-03
1.356	4.043E-03	1.436	3.651E-03	1.516	3.270E-03
1.358	4.033E-03	1.438	3.641E-03	1.518	3.261E-03
1.360	4.024E-03	1.440	3.632E-03	1.520	3.251E-03
1.362	4.014E-03	1.442	3.622E-03	1.522	3.242E-03
1.364	4.004E-03	1.444	3.612E-03	1.524	3.233E-03
1.366	3.994E-03	1.446	3.603E-03	1.526	3.224E-03
1.368	3.984E-03	1.448	3.593E-03	1.528	3.214E-03
1.370	3.975E-03	1.450	3.583E-03	1.530	3.205E-03
1.372	3.965E-03	1.452	3.574E-03	1.532	3.196E-03
1.374	3.955E-03	1.454	3.564E-03	1.534	3.187E-03
1.376	3.945E-03	1.456	3.554E-03	1.536	3.178E-03
1.378	3.935E-03	1.458	3.545E-03	1.538	3.168E-03
1.380	3.925E-03	1.460	3.535E-03	1.540	3.159E-03
1.382	3.916E-03	1.462	3.525E-03	1.542	3.150E-03
1.384	3.906E-03	1.464	3.516E-03	1.544	3.141E-03
1.386	3.896E-03	1.466	3.506E-03	1.546	3.132E-03
1.388	3.886E-03	1.468	3.497E-03	1.548	3.123E-03
1.390	3.876E-03	1.470	3.487E-03	1.550	3.114E-03
1.392	3.866E-03	1.472	3.477E-03	1.552	3.105E-03
1.394	3.857E-03	1.474	3.468E-03	1.554	3.096E-03
1.396	3.847E-03	1.476	3.458E-03	1.556	3.087E-03
1.398	3.837E-03	1.478	3.449E-03	1.558	3.078E-03
1.400	3.827E-03	1.480	3.439E-03	1.560	3.069E-03

M	Z	M	Z	M	Z
1.562	3.060E-03	1.642	2.716E-03	1.722	2.403E-03
1.564	3.051E-03	1.644	2.708E-03	1.724	2.395E-03
1.566	3.042E-03	1.646	2.700E-03	1.726	2.388E-03
1.568	3.033E-03	1.648	2.692E-03	1.728	2.380E-03
1.570	3.024E-03	1.650	2.684E-03	1.730	2.373E-03
1.572	3.015E-03	1.652	2.675E-03	1.732	2.366E-03
1.574	3.007E-03	1.654	2.667E-03	1.734	2.358E-03
1.576	2.998E-03	1.656	2.659E-03	1.736	2.351E-03
1.578	2.989E-03	1.658	2.651E-03	1.738	2.344E-03
1.580	2.980E-03	1.660	2.643E-03	1.740	2.336E-03
1.582	2.971E-03	1.662	2.635E-03	1.742	2.329E-03
1.584	2.963E-03	1.664	2.627E-03	1.744	2.322E-03
1.586	2.954E-03	1.666	2.619E-03	1.746	2.315E-03
1.588	2.945E-03	1.668	2.611E-03	1.748	2.307E-03
1.590	2.936E-03	1.670	2.603E-03	1.750	2.300E-03
1.592	2.928E-03	1.672	2.595E-03	1.752	2.293E-03
1.594	2.919E-03	1.674	2.587E-03	1.754	2.286E-03
1.596	2.910E-03	1.676	2.579E-03	1.756	2.279E-03
1.598	2.902E-03	1.678	2.571E-03	1.758	2.272E-03
1.600	2.893E-03	1.680	2.563E-03	1.760	2.265E-03
1.602	2.885E-03	1.682	2.556E-03	1.762	2.257E-03
1.604	2.876E-03	1.684	2.548E-03	1.764	2.250E-03
1.606	2.867E-03	1.686	2.540E-03	1.766	2.243E-03
1.608	2.859E-03	1.688	2.532E-03	1.768	2.236E-03
1.610	2.850E-03	1.690	2.524E-03	1.770	2.229E-03
1.612	2.842E-03	1.692	2.517E-03	1.772	2.222E-03
1.614	2.833E-03	1.694	2.509E-03	1.774	2.215E-03
1.616	2.825E-03	1.696	2.501E-03	1.776	2.209E-03
1.618	2.816E-03	1.698	2.493E-03	1.778	2.202E-03
1.620	2.808E-03	1.700	2.486E-03	1.780	2.195E-03
1.622	2.799E-03	1.702	2.478E-03	1.782	2.188E-03
1.624	2.791E-03	1.704	2.470E-03	1.784	2.181E-03
1.626	2.783E-03	1.706	2.463E-03	1.786	2.174E-03
1.628	2.774E-03	1.708	2.455E-03	1.788	2.167E-03
1.630	2.766E-03	1.710	2.448E-03	1.790	2.161E-03
1.632	2.758E-03	1.712	2.440E-03	1.792	2.154E-03
1.634	2.749E-03	1.714	2.433E-03	1.794	2.147E-03
1.636	2.741E-03	1.716	2.425E-03	1.796	2.140E-03
1.638	2.733E-03	1.718	2.418E-03	1.798	2.134E-03
1.640	2.725E-03	1.720	2.410E-03	1.800	2.127E-03

M	Z	M	Z	M	Z
1.802	2.120E-03	1.882	1.868E-03	1.962	1.645E-03
1.804	2.113E-03	1.884	1.862E-03	1.964	1.640E-03
1.806	2.107E-03	1.886	1.856E-03	1.966	1.635E-03
1.808	2.100E-03	1.888	1.851E-03	1.968	1.630E-03
1.810	2.094E-03	1.890	1.845E-03	1.970	1.624E-03
1.812	2.087E-03	1.892	1.839E-03	1.972	1.619E-03
1.814	2.080E-03	1.894	1.833E-03	1.974	1.614E-03
1.816	2.074E-03	1.896	1.827E-03	1.976	1.609E-03
1.818	2.067E-03	1.898	1.821E-03	1.978	1.604E-03
1.820	2.061E-03	1.900	1.816E-03	1.980	1.599E-03
1.822	2.054E-03	1.902	1.810E-03	1.982	1.594E-03
1.824	2.048E-03	1.904	1.804E-03	1.984	1.589E-03
1.826	2.041E-03	1.906	1.798E-03	1.986	1.584E-03
1.828	2.035E-03	1.908	1.793E-03	1.988	1.578E-03
1.830	2.029E-03	1.910	1.787E-03	1.990	1.573E-03
1.832	2.022E-03	1.912	1.781E-03	1.992	1.568E-03
1.834	2.016E-03	1.914	1.776E-03	1.994	1.563E-03
1.836	2.009E-03	1.916	1.770E-03	1.996	1.559E-03
1.838	2.003E-03	1.918	1.764E-03	1.998	1.554E-03
1.840	1.997E-03	1.920	1.759E-03	2.000	1.549E-03
1.842	1.990E-03	1.922	1.753E-03	2.002	1.544E-03
1.844	1.984E-03	1.924	1.748E-03	2.004	1.539E-03
1.846	1.978E-03	1.926	1.742E-03	2.006	1.534E-03
1.848	1.972E-03	1.928	1.737E-03	2.008	1.529E-03
1.850	1.965E-03	1.930	1.731E-03	2.010	1.524E-03
1.852	1.959E-03	1.932	1.726E-03	2.012	1.519E-03
1.854	1.953E-03	1.934	1.720E-03	2.014	1.515E-03
1.856	1.947E-03	1.936	1.715E-03	2.016	1.510E-03
1.858	1.941E-03	1.938	1.709E-03	2.018	1.505E-03
1.860	1.935E-03	1.940	1.704E-03	2.020	1.500E-03
1.862	1.928E-03	1.942	1.698E-03	2.022	1.495E-03
1.864	1.922E-03	1.944	1.693E-03	2.024	1.491E-03
1.866	1.916E-03	1.946	1.688E-03	2.026	1.486E-03
1.868	1.910E-03	1.948	1.682E-03	2.028	1.481E-03
1.870	1.904E-03	1.950	1.677E-03	2.030	1.476E-03
1.872	1.898E-03	1.952	1.672E-03	2.032	1.472E-03
1.874	1.892E-03	1.954	1.666E-03	2.034	1.467E-03
1.876	1.886E-03	1.956	1.661E-03	2.036	1.462E-03
1.878	1.880E-03	1.958	1.656E-03	2.038	1.458E-03
1.880	1.874E-03	1.960	1.650E-03	2.040	1.453E-03

M	Z	M	Z	M	Z
2.042	1.449E-03	2.122	1.276E-03	2.202	1.125E-03
2.044	1.444E-03	2.124	1.272E-03	2.204	1.121E-03
2.046	1.439E-03	2.126	1.268E-03	2.206	1.118E-03
2.048	1.435E-03	2.128	1.264E-03	2.208	1.114E-03
2.050	1.430E-03	2.130	1.260E-03	2.210	1.111E-03
2.052	1.426E-03	2.132	1.256E-03	2.212	1.107E-03
2.054	1.421E-03	2.13	1.252E-03	2.214	1.104E-03
2.056	1.417E-03	2.136	1.248E-03	2.216	1.100E-03
2.058	1.412E-03	2.138	1.244E-03	2.218	1.097E-03
2.060	1.408E-03	2.140	1.240E-03	2.220	1.093E-03
2.062	1.403E-03	2.142	1.236E-03	2.222	1.090E-03
2.064	1.399E-03	2.144	1.232E-03	2.224	1.087E-03
2.066	1.394E-03	2.146	1.228E-03	2.226	1.083E-03
2.068	1.390E-03	2.148	1.225E-03	2.228	1.080E-03
2.070	1.386E-03	2.150	1.221E-03	2.230	1.076E-03
2.072	1.381E-03	2.152	1.217E-03	2.232	1.073E-03
2.074	1.377E-03	2.154	1.213E-03	2.234	1.070E-03
2.076	1.372E-03	2.156	1.209E-03	2.236	1.066E-03
2.078	1.368E-03	2.158	1.205E-03	2.238	1.063E-03
2.080	1.364E-03	2.160	1.202E-03	2.240	1.060E-03
2.082	1.359E-03	2.162	1.198E-03	2.242	1.056E-03
2.084	1.355E-03	2.164	1.194E-03	2.244	1.053E-03
2.086	1.351E-03	2.166	1.190E-03	2.246	1.050E-03
2.088	1.347E-03	2.168	1.187E-03	2.248	1.047E-03
2.090	1.342E-03	2.170	1.183E-03	2.250	1.043E-03
2.092	1.338E-03	2.172	1.179E-03	2.252	1.040E-03
2.094	1.334E-03	2.174	1.175E-03	2.254	1.037E-03
2.096	1.330E-03	2.176	1.172E-03	2.256	1.034E-03
2.098	1.325E-03	2.178	1.168E-03	2.258	1.030E-03
2.100	1.321E-03	2.180	1.164E-03	2.260	1.027E-03
2.102	1.317E-03	2.182	1.161E-03	2.262	1.024E-03
2.104	1.313E-03	2.184	1.157E-03	2.264	1.021E-03
2.106	1.309E-03	2.186	1.153E-03	2.266	1.018E-03
2.108	1.305E-03	2.188	1.150E-03	2.268	1.014E-03
2.110	1.300E-03	2.190	1.146E-03	2.270	1.011E-03
2.112	1.296E-03	2.192	1.143E-03	2.272	1.008E-03
2.114	1.292E-03	2.194	1.139E-03	2.274	1.005E-03
2.116	1.288E-03	2.196	1.135E-03	2.276	1.002E-03
2.118	1.284E-03	2.198	1.132E-03	2.278	9.987E-04
2.120	1.280E-03	2.200	1.128E-03	2.280	9.956E-04

M	Z	M	Z	M	Z
2.282	9.925E-04	2.362	8.768E-04	2.442	7.757E-
2.284	9.894E-04	2.364	8.741E-04	2.444	7.734E-(
2.286	9.863E-04	2.366	8.714E-04	2.446	7.710E-(
2.288	9.832E-04	2.368	8.688E-04	2.448	7.687E-(
2.290	9.802E-04	2.370	8.661E-04	2.450	7.663E-(
2.292	9.771E-04	2.372	8.634E-04	2.452	7.640E-(
2.294	9.741E-04	2.374	8.608E-04	2.454	7.617E-(
2.296	9.711E-04	2.376	8.581E-04	2.456	7.594E-(
2.298	9.681E-04	2.378	8.555E-04	2.458	7.571E-(
2.300	9.651E-04	2.380	8.529E-04	2.460	7.548E-
2.302	9.621E-04	2.382	8.503E-04	2.462	7.525E-
2.304	9.591E-04	2.384	8.476E-04	2.464	7.502E-(
2.306	9.561E-04	2.386	8.450E-04	2.466	7.480E-(
2.308	9.532E-04	2.388	8.425E-04	2.468	7.457E-(
2.310	9.502E-04	2.390	8.399E-04	2.470	7.434E-
2.312	9.473E-04	2.392	8.373E-04	2.472	7.412E-(
2.314	9.443E-04	2.394	8.347E-04	2.474	7.389E-
2.316	9.414E-04	2.396	8.322E-04	2.476	7.367E-(
2.318	9.385E-04	2.398	8.296E-04	2.478	7.345E-(
2.320	9.356E-04	2.400	8.271E-04	2.480	7.323E-(
2.322	9.327E-04	2.402	8.246E-04	2.482	7.301E-(
2.324	9.298E-04	2.404	8.221E-04	2.484	7.279E-(
2.326	9.269E-04	2.406	8.195E-04	2.486	7.257E-(
2.328	9.241E-04	2.408	8.170E-04	2.488	7.235E-(
2.330	9.212E-04	2.410	8.145E-04	2.490	7.213E-(
2.332	9.184E-04	2.412	8.121E-04	2.492	7.191E-(
2.334	9.155E-04	2.414	8.096E-04	2.494	7.169E-(
2.336	9.127E-04	2.416	8.071E-04	2.496	7.148E-(
2.338	9.099E-04	2.418	8.046E-04	2.498	7.126E-(
2.340	9.071E-04	2.420	8.022E-04	2.500	7.105E-(
2.342	9.043E-04	2.422	7.997E-04	2.502	7.083E-(
2.344	9.015E-04	2.424	7.973E-04	2.504	7.062E-(
2.346	8.987E-04	2.426	7.949E-04	2.506	7.041E-(
2.348	8.959E-04	2.428	7.925E-04	2.508	7.020E-(
2.350	8.932E-04	2.430	7.900E-04	2.510	6.999E-(
2.352	8.904E-04	2.432	7.876E-04	2.512	6.978E-(
2.354	8.877E-04	2.434	7.852E-04	2.514	6.957E-(
2.356	8.850E-04	2.436	7.828E-04	2.516	6.936E-(
2.358	8.822E-04	2.438	7.805E-04	2.518	6.915E-(
2.360	8.795E-04	2.440	7.781E-04	2.520	6.894E-(

M	Z	M	Z	M	Z
2.522	6.873E-04	2.602	6.100E-04	2.682	5.423E-04
2.524	6.853E-04	2.604	6.082E-04	2.684	5.407E-04
2.526	6.832E-04	2.606	6.064E-04	2.686	5.391E-04
2.528	6.812E-04	2.608	6.046E-04	2.688	5.376E-04
2.530	6.791E-04	2.610	6.028E-04	2.690	5.360E-04
2.532	6.771E-04	2.612	6.011E-04	2.692	5.344E-04
2.534	6.751E-04	2.614	5.993E-04	2.694	5.329E-04
2.536	6.731E-04	2.616	5.975E-04	2.696	5.313E-04
2.538	6.710E-04	2.618	5.957E-04	2.698	5.298E-04
2.540	6.690E-04	2.620	5.940E-04	2.700	5.283E-04
2.542	6.670E-04	2.622	5.922E-04	2.702	5.267E-04
2.544	6.650E-04	2.624	5.905E-04	2.704	5.252E-04
2.546	6.631E-04	2.626	5.888E-04	2.706	5.237E-04
2.548	6.611E-04	2.628	5.870E-04	2.708	5.221E-04
2.550	6.591E-04	2.630	5.853E-04	2.710	5.206E-04
2.552	6.571E-04	2.632	5.836E-04	2.712	5.191E-04
2.554	6.552E-04	2.634	5.818E-04	2.714	5.176E-04
2.556	6.532E-04	2.636	5.801E-04	2.716	5.161E-04
2.558	6.513E-04	2.638	5.784E-04	2.718	5.146E-04
2.560	6.493E-04	2.640	5.767E-04	2.720	5.131E-04
2.562	6.474E-04	2.642	5.750E-04	2.722	5.116E-04
2.564	6.455E-04	2.644	5.733E-04	2.724	5.102E-04
2.566	6.435E-04	2.646	5.717E-04	2.726	5.087E-04
2.568	6.416E-04	2.648	5.700E-04	2.728	5.072E-04
2.570	6.397E-04	2.650	5.683E-04	2.730	5.057E-04
2.572	6.378E-04	2.652	5.666E-04	2.732	5.043E-04
2.574	6.359E-04	2.654	5.650E-04	2.734	5.028E-04
2.576	6.340E-04	2.656	5.633E-04	2.736	5.014E-04
2.578	6.321E-04	2.658	5.617E-04	2.738	4.999E-04
2.580	6.303E-04	2.660	5.600E-04	2.740	4.985E-04
2.582	6.284E-04	2.662	5.584E-04	2.742	4.971E-04
2.584	6.265E-04	2.664	5.568E-04	2.744	4.956E-04
2.586	6.247E-04	2.666	5.551E-04	2.746	4.942E-04
2.588	6.228E-04	2.668	5.535E-04	2.748	4.928E-04
2.590	6.210E-04	2.670	5.519E-04	2.750	4.913E-04
2.592	6.191E-04	2.672	5.503E-04	2.752	4.899E-04
2.594	6.173E-04	2.674	5.487E-04	2.754	4.885E-04
2.596	6.155E-04	2.676	5.471E-04	2.756	4.871E-04
2.598	6.136E-04	2.678	5.455E-04	2.758	4.857E-04
2.600	6.118E-04	2.680	5.439E-04	2.760	4.843E-04

M	Z	M	Z	M	Z
2.762	4.829E-04	2.842	4.308E-04	2.922	3.850E-0
2.764	4.815E-04	2.844	4.296E-04	2.924	3.839E-0
2.766	4.802E-04	2.846	4.284E-04	2.926	3.829E-0
2.768	4.788E-04	2.848	4.272E-04	2.928	3.818E-0
2.770	4.774E-04	2.850	4.260E-04	2.930	3.807E-0
2.772	4.760E-04	2.852	4.248E-04	2.932	3.797E-0
2.774	4.747E-04	2.854	4.236E-04	2.934	3.786E-0
2.776	4.733E-04	2.856	4.224E-04	2.936	3.776E-0
2.778	4.720E-04	2.858	4.212E-04	2.938	3.765E-0
2.780	4.706E-04	2.860	4.200E-04	2.940	3.755E-0
2.782	4.693E-04	2.862	4.188E-04	2.942	3.744E-0
2.784	4.679E-04	2.864	4.176E-04	2.944	3.734E-0
2.786	4.666E-04	2.866	4.165E-04	2.946	3.724E-0
2.788	4.652E-04	2.868	4.153E-04	2.948	3.713E-0
2.790	4.639E-04	2.870	4.141E-04	2.950	3.703E-0
2.792	4.626E-04	2.872	4.130E-04	2.952	3.693E-0
2.794	4.613E-04	2.874	4.118E-04	2.954	3.683E-0
2.796	4.600E-04	2.876	4.106E-04	2.956	3.672E-0
2.798	4.586E-04	2.878	4.095E-04	2.958	3.662E-0
2.800	4.573E-04	2.880	4.083E-04	2.960	3.652E-0
2.802	4.560E-04	2.882	4.072E-04	2.962	3.642E-0
2.804	4.547E-04	2.884	4.060E-04	2.964	3.632E-0
2.806	4.534E-04	2.886	4.049E-04	2.966	3.622E-0
2.808	4.521E-04	2.888	4.038E-04	2.968	3.612E-0
2.810	4.509E-04	2.890	4.026E-04	2.970	3.602E-0
2.812	4.496E-04	2.892	4.015E-04	2.972	3.592E-0
2.814	4.483E-04	2.894	4.004E-04	2.974	3.582E-0
2.816	4.470E-04	2.896	3.993E-04	2.976	3.572E-0
2.818	4.458E-04	2.898	3.981E-04	2.978	3.563E-0
2.820	4.445E-04	2.900	3.970E-04	2.980	3.553E-0
2.822	4.432E-04	2.902	3.959E-04	2.982	3.543E-0
2.824	4.420E-04	2.904	3.948E-04	2.984	3.533E-0
2.826	4.407E-04	2.906	3.937E-04	2.986	3.523E-0
2.828	4.395E-04	2.908	3.926E-04	2.988	3.514E-0
2.830	4.382E-04	2.910	3.915E-04	2.990	3.504E-0
2.832	4.370E-04	2.912	3.904E-04	2.992	3.495E-0
2.834	4.357E-04	2.914	3.893E-04	2.994	3.485E-0
2.836	4.345E-04	2.916	3.882E-04	2.996	3.475E-0
2.838	4.333E-04	2.918	3.872E-04	2.998	3.466E-0
2.840	4.320E-04	2.920	3.861E-04	3.000	3.456E-0

SECTION G

ANALYSIS OF THE WAKE OF A SELF-PROPELLED VEHICLE IN A DUCT WITH CONSIDERATION OF HEAT TRANSFER AND FRICTION

by

Duane E. Cromack

and

Leo F. Gijsels

SUMMARY

This report concerns the flow in the wake of a self-propelled vehicle traveling in an infinite tube. The analysis includes the effects of compressibility, friction and heat transfer and makes use of the Reynolds analogy to relate the latter two effects.

SYMBOLS

a speed of sound (fps)

c_p specific heat at constant pressure (ft-lb/slug)

C_τ non-dimensional friction factor

$D = M\left(1 + \frac{\gamma-1}{2}M^2\right)^{\frac{\gamma+1}{2(\gamma-1)}}$

F stream force relative to the vehicle (lb)

g gravitational constant (ft/sec^2)

h convective heat transfer coefficient (Btu/ft^2 sec $^\circ$R)

K heat transfer factor in eq. 3 (ft-lb/slug $^\circ$R)

$\dot{m}$ mass flow rate relative to the vehicle (slugs/sec)

M Mach number of the flow relative to the vehicle

$M_\circ = \left(\frac{u_w^2}{\gamma g R T_\circ}\right)^{\frac{1}{2}}$ = const.

p static pressure (psf)

p° stagnation pressure ( )

q_a heat input in combustion process per unit mass (ft-lb/slug)

r duct radius (ft)

R gas constant (ft-lb/slug $^\circ$R)

T static temperature ($^\circ$R)

T° stagnation temperature relative to the vehicle ($^\circ$R)

$T^{\circ *}$ stagnation temperature relative to the wall ($^\circ$R)

u velocity of the flow relative to the vehicle (fps)

u_w velocity of the wall relative to the vehicle (fps)

v velocity of the vehicle relative to the wall (fps)

x duct axial coordinate (ft)

α duct cross-sectional area (ft^2)

β non-dimensional velocity ratio, u/u_w

γ specific heat ratio

η non-dimensional axial coordinate, x/r

Subscripts (see Fig. G-1)

0 conditions outside the tube, assumed uniform

1 nearest station ahead of the vehicle where the flow can be considered one-dimensional

2 station at tail end of vehicle

3 terminal station of energy addition in internal propulsion; upstream end of wake

INTRODUCTION

The general concept of high speed vehicles propelling themselves through ducts was presented by Foa in reference 1. In the calculation of the power required for such systems, the flow induced by the vehicle must be determined.

This problem has been treated in different ways by various authors (Refs. 2 through 6). Tollmien (Ref. 2) was the first to study the flow produced by a train in a tunnel and the effect of this flow on the power required. Reference 3 considers the flow induced by a self-propelled subsonic vehicle through a quasi static analysis in which viscous stresses are neglected and the thrust generator is represented as an actuator disc. Reference 4 also considers an incompressible and inviscid fluid in a simplified treatment of the same problem. Reference 5 includes viscous effects and follows a boundary-layer approach. Reference 6 develops the general equations for the one-dimensional analysis of the flow in the frame of reference of a vehicle moving in a tube of infinite length, with consideration of friction and heat transfer. Closed-form solutions are obtained for regions ahead of and at some distance behind the vehicle, where heat exchanges are assumed to take place according to such a schedule that the stagnation enthalpy relative to the walls remains constant.

In the present analysis, the equations of Ref. 6 are applied

to the region behind the vehicle without the simplifying assumptions that are required to yield closed-form solutions.

ANALYSIS

The present analysis considers a tube of infinite length in which a vehicle is moving at constant speed. In a vehicle-fixed frame of reference (see Fig. G-1) the flow is steady. The walls are moving at a velocity equal and opposite to the velocity of the vehicle. The energy and momentum equations for this situation are (Ref. 6):

$$\dot{m} g C_p dT^\circ = u_w dF + dq \tag{1}$$

where $$dT^\circ = dT + \frac{u\,du}{g C_p}$$

$$dF = -\rho \alpha \frac{C_f}{r}(u - u_w)|u - u_w|\,dx \tag{2}$$

The wall temperature is assumed here to remain constant and equal to the external ambient temperature T_o. Thus, the instantaneous rate of heat transfer can be expressed as

$$dq = -K(u)\left(T^{\circ *} - T_o\right)dx \tag{3}$$

where T^{o*} is the stagnation temperature of the flow in the vicinity of and relative to the wall. Thus

$$T^{\circ *} = T + \frac{(u - u_w)}{2 g C_p} \tag{4}$$

K(u) is a function of the convective film coefficient and through the Reynolds analogy becomes a function of the friction coefficient and of the absolute velocity of the flow relative to the wall, $|u - u_w|$. From the Reynolds analogy, the Stanton Number for the case of moving walls can be written as

$$S_t \equiv \frac{h}{g\rho C_p |u-u_w|} = \frac{C_f}{2} .$$

Thus the film coefficient becomes

$$h = \frac{C_f}{2} g\rho C_p |u-u_w|$$

and K(u) becomes

$$K(u) = 2\pi r h = \pi r C_f C_p g\rho |u-u_w| .$$

Substitution of equations 2, 3, and 4 into 1 gives

$$\dot{m} g C_p dT + \dot{m} u du = -\rho \alpha u_w \frac{C_f}{r}(u-u_w)|u-u_w| dx$$

$$-\pi r C_f C_p g\rho |u-u_w| \left(T + \frac{(u-u_w)^2}{2g C_p} - T_o\right) dx . \qquad (5)$$

The mass flow rate $\dot{m}$, may be written as

$$\dot{m} = \rho \alpha u = \frac{p \alpha u}{gRT} = \frac{(F - \dot{m}u)u}{gRT}$$

Therefore

$$\dot{m} g R T = (F - \dot{m}u)u$$

and differentiating gives

$$\dot{m} g R dT = u dF + F du - 2\dot{m} u du . \qquad (6)$$

Eqs. 5 and 6 give

$$\left(\frac{\gamma}{\gamma-1}\right)\frac{1}{\dot{m}}\left(u dF + F du - 2\dot{m} u du\right) + u du =$$

$$-\frac{C_f}{r}\frac{u_w}{u}(u-u_w)|u-u_w|dx - g\frac{C_f}{r}C_p\frac{|u-u_w|}{u}\left(\frac{Fu}{\dot{m}gR} - \frac{u^2}{gR} + \frac{(u-u_w)^2}{2g C_p} - T_o\right)dx.$$

Substituting for dF from eq. 2 and rearranging, one obtains

$$\left(\frac{\gamma}{\gamma-1}\frac{F}{\dot{m}} - \left(\frac{\gamma+1}{\gamma-1}\right)u\right)\frac{du}{dx} = \left(\frac{\gamma}{\gamma-1} - \frac{u_w}{u}\right)\frac{C_f}{r}(u-u_w)|u-u_w| \qquad (7)$$

$$-\left(\frac{\gamma}{\gamma-1}\right)\frac{C_f}{r}\frac{|u-u_w|}{u}\left(\frac{Fu}{\dot{m}} - u^2 + \left(\frac{\gamma-1}{2\gamma}\right)(u-u_w)^2 - gRT_o\right)$$

Differentiation with respect to x and the elimination of F/$\dot{m}$ between the resulting equation and eq. 7 leads to the following second order non-linear differential equation in non-dimensional form with $\beta = \frac{u}{u_w}$ and $\eta = \frac{x}{r}$:

$$\frac{d^2\beta}{d\eta^2} = \left\{\frac{1}{\beta - \left(\gamma - \frac{\gamma-1}{\beta}\right)(\beta-1) + \left(\frac{\gamma-1}{2}\right)\frac{(\beta-1)^2}{\beta} - \frac{1}{M_o^2\beta}}\right\}\left\{-\frac{(\gamma+1)}{C_T}\frac{1}{|\beta-1|}\left(\frac{d\beta}{d\eta}\right)^3\right.$$

$$-\left[\left(1+\frac{\gamma-1}{\beta}\right)\left(\frac{\beta-1}{\beta}\right)+\left(4\gamma+1-\frac{2(\gamma-1)}{\beta}\right)+\left(\frac{\gamma-1}{2}\right)\left(\frac{\beta-1}{\beta}\right)^2-\frac{\beta}{(\beta-1)}+\frac{1}{M_o^2\beta^2(\beta-1)}\right]\left(\frac{d\beta}{d\eta}\right)^2$$

$$-\left[\left(\gamma+1+\frac{\gamma-1}{\beta}\right)\left(\frac{\beta-1}{\beta}\right)+\left(2\gamma-\frac{(\gamma-1)}{\beta}\right)+\left(\frac{\gamma-1}{2}\right)\left(\frac{\beta-1}{\beta}\right)^2-\frac{1}{M_o^2\beta^2}\right]C_T|\beta-1|\left(\frac{d\beta}{d\eta}\right)$$

$$\left.-\left[\gamma C_T^2\,\frac{(\beta-1)^3}{\beta}\right]\right\} \qquad (8)$$

The values for β and $\frac{d\beta}{d\eta}$ at $\eta = 0$ i.e., immediately behind the vehicle, are obtained in the following manner: Rearranging eq. 7 in terms of $\frac{d\beta}{d\eta}$ gives

$$\frac{d\beta}{d\eta} = \left[\frac{C_T|\beta-1|}{\frac{\gamma F}{\dot{m}u_\omega} - (\gamma+1)\beta}\right]\left\{\left(\gamma - \frac{(\gamma-1)}{\beta}\right)(\beta-1) - \left(\frac{\gamma F}{\dot{m}u_\omega} - \gamma\beta + \left(\frac{\gamma-1}{2}\right)\frac{(\beta-1)^2}{\beta} - \frac{1}{M_o^2\beta}\right)\right\} \qquad (9)$$

where all terms can be evaluated at $\eta = 0$ for a given $\beta(0)$. The initial value of β must be expressed as a relation between appropriate parameters of the propulsive device.

Equation 8, with the appropriate initial values of β and $\frac{d\beta}{d\eta}$, may be used to describe the flow in the wake of a subsonic or a supersonic vehicle traveling in a tube.

REFERENCES

1. Foa, J.V., "A Fast Carrier", Rensselaer Polytechnic Institute Tech. Rept. TR AE 6206, May 1962.

2. Tollmien, W., "Luftwiderstand und Druckverlauf bei der Fahrt von Zugen in einem Tunnel," Zeitschrift des Vereines deutscher Ingenieure, 71, No. 6, 199-203, 5 February 1927.

3. McGrath, P., J.W.Burr, W.R.Adair, "The Flow Induced by a New Type of Self-Propelled Vehicle in a Duct," Rensselaer Polytechnic Institute Tech. Rept. TR AE 6204, October 1962.

4. von Keszycki, H.J., "The Motion of a Self-Propelled Body in a Tube," Rensselaer Polytechnic Institute Tech. Rept. TR AE 5905, December 1959.

5. Hagerup, H., "A Note on Compressible Viscous Flow in Tubes," Rensselaer Polytechnic Institute Tech. Rept. TR AE 6405, June 1964.

6. Foa, J.V., "Propulsion of a Vehicle in a Tube," Rensselaer Polytechnic Institute Tech. Rept. TR AE 6404, June 1964.

7. Gijsels, L., "Preliminary Design Considerations for a 3 ft. Diameter Tube Transport Pilot Model," Section J of "Research on the Dynamics of a Vehicle in a Tube," Final Progress Report Grant DA-ORD-31-124-61-G88, Rensselaer Polytechnic Institute, June 1964.

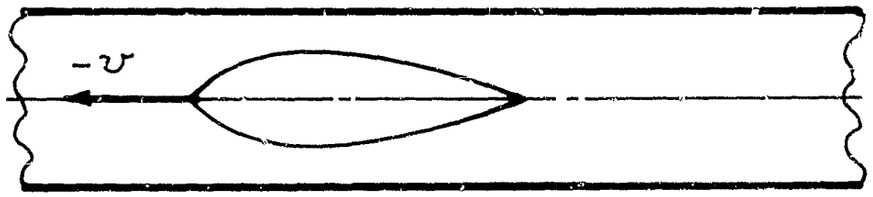

WALL-FIXED FRAME OF REFERENCE

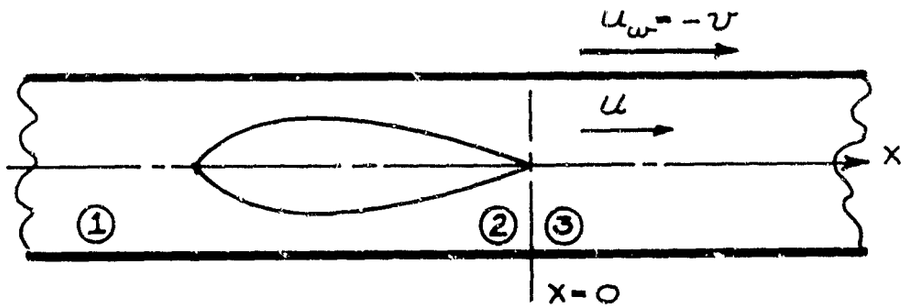

VEHICLE-FIXED FRAME OF REFERENCE

FIGURE G-1
SCHEMATIC OF VEHICLE IN A TUBE

SECTION H

A NOTE ON THE FLOW INDUCED BY A DISTURBANCE TRAVELING IN A TUBE

by

Henrik J. Hagerup

LIST OF SYMBOLS

α Mach number function, $\alpha \equiv \frac{1+(\gamma-1)M^2}{1-M^2}$

c_i coefficients of velocity transform

γ specific heat ratio

Δ initial mass flow disturbance

Δp pressure increment relative to initial value, $\Delta p \equiv p - p_1$

δ initial velocity disturbance

ε initial enthalpy disturbance

$f(\alpha)$ arbitrary function

h enthalpy perturbation

$I_i(z)$ Modified Bessel functions of the first kind

i, j indices

$K_i(z)$ Modified Bessel functions of the second kind

k constant

m_i coefficients of enthalpy transform

M Mach number upstream

μ viscosity perturbation

p pressure perturbation

$q(x)$ heat transfer function, $q(x) \equiv -\left.\frac{\partial h}{\partial r}\right|_{wall}$

R tube radius

r radial coordinate

Re Reynolds number, $Re \equiv \frac{\rho_0 u_0 R}{\mu_0}$

ρ density perturbation

σ Prandtl number

u axial velocity perturbation

v radial velocity perturbation

x axial coordinate, positive downstream

s Laplace transform variable

$\tau(x)$ shear function, $\tau(x) \equiv -\left.\frac{\partial u}{\partial r}\right|_{wall}$

$\overline{(\,)}$ Laplace transform of $(\,)$

$(\,)^*$ dimensional physical quantity complete

$(\,)_0$ dimensional upstream reference value

$(\,)_1$ value immediately behind disturbance

Summary

Linearized two-dimensional analysis indicating some general features of flow induced by disturbance propagating at constant velocity along slender tube. Formulation applies to small disturbances, includes effects of viscosity and heat conduction for gases of arbitrary Prantl number, neglects viscous dissipation. Typical subsonic and supersonic solutions have been calculated for case of Prandtl number one.

A new transportation system in which a vehicle propels itself at high velocity through a long tube has been proposed (Ref. 1). The investigation of the turbulent flow field in the tube downstream of the vehicle forms an important part of the complete system analysis. The purpose of the present discussion is to explore in simpler terms some aspects of the induced flow field associated with a local disturbance on a more modest scale, traveling at constant velocity along an essentially infinite tube.

To an observer stationary in the tube, the passage of the disturbance is felt as a sudden change in velocity, pressure and temperature, followed by a gradual return to the undisturbed state. To an observer traveling with the origin of the disturbance, it might reasonably be expected that the flow would appear steady, and the conservation equations would be simpler in this case; however, the assumption of steady flow is of course admissible only if the induced flow field predicted on this basis decays asymptotically with distance downstream, so that the end conditions are automatically satisfied.

The two-dimensional analysis reported in this preliminary note is confined to the laminar version of the steady flow problem. The problem situation referred to the moving coordinate system is formalized in the following terms: a frontal discontinuity at some

station $X=0$ in a tube of circular cross section imparts to the flow immediately behind it a velocity $u^* = u_\infty + u_\infty \delta$ parallel to the axis and an enthalpy $h^* = h_\infty + h_\infty \varepsilon$, both perturbations here chosen as initially constant across the tube. Other distributions would however be equally admissible within the two-dimensional formulation. The walls as well as the fluid upstream are taken to be at conditions $u^* = u_\infty$ and $h^* = h_\infty$, though the upstream state enters the mathematical problem only as a reference state. The objective of the analysis is to describe the development of the initial block perturbation profiles $u_\infty \delta$ and $h_\infty \varepsilon$ in the flow field downstream.

The problem may for present purposes be regarded as in the nature of a boundary layer situation, with x-derivatives and r-components of velocity generally negligible compared to r-derivatives and x-components, and x-derivatives of enthalpy generally negligible compared to r-derivatives. Assuming the flow also to be axisymmetric and without swirl, we have the simplified governing system of equations for the steady flow of a perfect gas with constant Prandtl number in the form

$$\rho^* u^* \frac{\partial u^*}{\partial x^*} + \rho^* v^* \frac{\partial u^*}{\partial r^*} = - \frac{\partial p^*}{\partial x^*} + \frac{1}{r^*} \frac{\partial}{\partial r^*} \left(\mu^* r^* \frac{\partial u^*}{\partial r^*} \right)$$

$$\frac{\partial p^*}{\partial r^*} = 0 \qquad \frac{\partial}{\partial x^*} (\rho^* u^*) + \frac{1}{r^*} \frac{\partial}{\partial r^*} (r^* \rho^* v^*) = 0$$

$$\rho^* u^* \frac{\partial h^*}{\partial x^*} + \rho^* v^* \frac{\partial h^*}{\partial r^*} = u^* \frac{\partial p^*}{\partial x^*} + \frac{1}{r^*} \frac{\partial}{\partial r^*} \left(r^* \frac{\mu^*}{\sigma} \frac{\partial h^*}{\partial r^*} \right) + \mu^* \left(\frac{\partial u^*}{\partial r^*} \right)^2$$

$$p^* = \frac{\gamma - 1}{\gamma} \rho^* h^*$$

The boundary and initial conditions are

$$r^* = R \qquad u^* = u_0 \qquad v^* = 0 \qquad h^* = h_0$$

$$x^* = 0 \qquad u^* = u_0 + u_0\delta \qquad v^* = 0 \qquad h^* = h_0 + h_0\varepsilon$$

Because of the finite velocity at the wall, the local velocity in the flow field need nowhere depart significantly from some reasonably defined mean, and the Oseen approximation suggests itself as a promising approach to the problem. The equations are accordingly linearized by replacing the transport derivative operator as follows

$$u^* \frac{\partial}{\partial x^*} + v^* \frac{\partial}{\partial r^*} \Rightarrow h u_0 \frac{\partial}{\partial x^*}$$

where h is an unspecified constant, which in the small perturbation analysis to follow may be taken as $h = 1$. Introducing non-dimensional variables through the expressions

$$r^* = Rr \qquad x^* = Re\,Rx \qquad u^* = u_0 + u_0 u \qquad h^* = h_0 + h_0 h$$

$$p^* = p_0 + p_0 p \qquad \rho^* = \rho_0 + \rho_0 \rho \qquad \mu^* = \mu_0 + \mu_0 \mu \qquad Re \equiv \frac{\rho_0 u_0 R}{\mu_0}$$

one obtains under the restriction to small perturbations the linearized formulation for the compressible flow development in terms of the normalized system

$$\frac{1}{r}\frac{\partial}{\partial r}\left(r \frac{\partial u}{\partial r}\right) - \frac{\partial u}{\partial x} = \frac{1}{\gamma M^2}\frac{dp}{dx}$$

$$\frac{1}{r}\frac{\partial}{\partial r}\left(r \frac{\partial h}{\partial r}\right) - 6\frac{\partial h}{\partial x} = -6\,\frac{\gamma - 1}{\gamma}\frac{dp}{dx}$$

$$p = \rho + h$$

where it should be noticed in particular that the viscous dissipation term in the energy equation has been neglected, as a higher order effect. The system is subject to the conditions

$$r = 1 \qquad u = h = 0$$

$$x = 0 \qquad u = \delta \quad h = \varepsilon$$

The nature of the problem suggests now the use of the Laplace transformation

$$\bar{u}(s,r) \equiv \int_0^\infty u(x,r)\, e^{-sx}\, dx$$

Transforming first the momentum equation, one obtains an ordinary differential equation

$$\frac{1}{r}\frac{d}{dr}\left(r\frac{d\bar{u}}{dr}\right) - s\bar{u} = \frac{s}{\gamma M^2}\bar{p} - \frac{p_1}{\gamma M^2} - \delta$$

which has the solution (Ref. 2)

$$\bar{u}(s,r) = c_1 I_0(\sqrt{s}\,r) + c_2 K_0(\sqrt{s}\,r) + c_3$$

The axis $r = 0$ is within the flow field, so $\bar{u}(s,0)$ must be bounded; hence $c_2 = 0$. The velocity boundary condition at the wall $r = 1$ gives

$$c_3 = -I_0(\sqrt{s})\, c_1$$

But the particular solution is by inspection

$$c_3 = -\frac{\bar{p}}{\gamma M^2} + \frac{1}{\gamma M^2}\frac{p_1}{s} + \frac{\delta}{s}$$

with the initial pressure given by the equation of state as $p_1 = \Delta - \delta + \varepsilon$ where Δ is a term allowing for the possibility of mass addition as part of the initial disturbance mechanism. Solving for the transformed pressure one obtains

$$\bar{p}(s) = \gamma M^2 \left[\frac{\delta}{s} + I_0(\sqrt{s})\, c_1 \right] + \frac{\Delta - \delta + \varepsilon}{s}$$

A third constraint is provided by the constant mass flow requirement for steady flow:

$$\int_0^R \rho^* u^* 2\pi r^* dr^* = \rho_0 u_0 \pi R^2 + \Delta \rho_0 u_0 \pi R^2$$

Normalizing this and taking the Laplace transform, one obtains with the equation of state the mass flow constraint in the linearized form

$$\int_0^1 \left[\bar{u} + \bar{\rho} - \bar{h} \right] 2r\, dr = \frac{\Delta}{s}$$

From the energy equation, next, it follows by transformation

$$\frac{1}{r} \frac{d}{dr} \left(r \frac{d\bar{h}}{dr} \right) - \sigma s \bar{h} = -\sigma \frac{\gamma - 1}{\gamma} s \bar{p} + \sigma \frac{\gamma - 1}{\gamma} p_1 - \sigma \varepsilon$$

and the admissible part of the solution is again of the form

$$\bar{h}(s, r) = h_1 I_0(\sqrt{s\sigma}\, r) + h_3$$

with

$$h_1 = - \frac{h_3}{I_0(\sqrt{s\sigma})}$$

from the wall temperature boundary condition. The particular solution, using the pressure as already obtained, is

$$h_3 = (\gamma-1) M^2 \left[\frac{\delta}{\lambda} + I_0(\sqrt{\lambda})\, c_1 \right] + \frac{\varepsilon}{\lambda}$$

Substitution of the expressions for $\bar{u}$, $\bar{h}$, and $\bar{\rho}$ into the mass flow constraint provides an implicit relation for c_1 and upon integration leads to the result eventually, neglecting perturbation products:

$$c_1 = -\frac{1}{\lambda I_0(\sqrt{\lambda})} \frac{(1-M^2)\delta - \left[\varepsilon + (\gamma-1)M^2\delta\right] \dfrac{2 I_1(\sqrt{\lambda\sigma})}{\sqrt{\lambda\sigma}\, I_0(\sqrt{\lambda\sigma})}}{(1-M^2) - \dfrac{2}{\sqrt{\lambda}} \dfrac{I_1(\sqrt{\lambda})}{I_0(\sqrt{\lambda})} - (\gamma-1)M^2 \dfrac{2 I_1(\sqrt{\lambda\sigma})}{\sqrt{\lambda\sigma}\, I_0(\sqrt{\lambda\sigma})}}$$

The analysis is capable of greater accuracy, but for the pres exploratory purpose the first approximation is adequate.

Rather than to attempt at this point the description of t entire velocity and temperature fields, we confine the followi discussion to the more essential parameters of wall shear, hea transfer, and pressure as functions of x. The normalized shea transform is given by the expression

$$\bar{\tau} \equiv -\left.\frac{\partial u}{\partial \lambda}\right|_{\lambda=1} = -c_1 \sqrt{\lambda}\, I_1(\sqrt{\lambda})$$

The theory as formulated applies to a gas of arbitrary Prandtl number, but in the following we consider the special case of $\sigma = 1$ for algebraic convenience. The shear transform follow

then from the general expression for c_1 in the relatively simple form:

$$\bar{\tau}(s) = \frac{I_1(\sqrt{s})}{I_0(\sqrt{s})}\frac{\delta}{s} + \left[\frac{I_1(\sqrt{s})}{I_0(\sqrt{s})}\right]^2 \frac{\frac{2}{\sqrt{s}}\frac{\delta-\varepsilon}{1-M^2}}{\sqrt{s}\left[1-\frac{2}{\sqrt{s}}\frac{1+(\gamma-1)M^2}{1-M^2}\frac{I_1(\sqrt{s})}{I_0(\sqrt{s})}\right]}$$

The transform of normalized heat transfer to the wall is given by

$$\bar{q} \equiv -\left.\frac{\partial h}{\partial \lambda}\right|_{\lambda=1} = -k_1\sqrt{s\sigma}\, I_1(\sqrt{s\sigma})$$

and it follows similarly that

$$\bar{q}(s) = \frac{I_1(\sqrt{s})}{I_0(\sqrt{s})}\frac{\varepsilon}{\sqrt{s}} - (\gamma-1)M^2\left[\frac{I_1(\sqrt{s})}{I_0(\sqrt{s})}\right]^2 \frac{\frac{2}{\sqrt{s}}\frac{\delta-\varepsilon}{1-M^2}}{\sqrt{s}\left[1-\frac{2}{\sqrt{s}}\frac{1+(\gamma-1)M^2}{1-M^2}\frac{I_1(\sqrt{s})}{I_0(\sqrt{s})}\right]}$$

The transform of the pressure change referred to the initial condition p_1 is given as

$$\overline{\Delta p} \equiv \bar{p} - \frac{\Delta-\delta-\varepsilon}{s} = \gamma M^2\left[\frac{\delta}{s} + I_0(\sqrt{s})\,c_1\right]$$

and takes the form

$$\overline{\Delta p}(s) = -\gamma M^2\frac{I_1(\sqrt{s})}{I_0(\sqrt{s})} \frac{\frac{2}{\sqrt{s}}\frac{\delta-\varepsilon}{1-M^2}}{s\left[1-\frac{2}{\sqrt{s}}\frac{1+(\gamma-1)M^2}{1-M^2}\frac{I_1(\sqrt{s})}{I_0(\sqrt{s})}\right]}$$

The remaining problem is to establish the inverse transforms of the functions $\bar{\tau}(s)$, $\bar{q}(s)$, and $\overline{\Delta p}(s)$.

The inversion is most readily accomplished by power series expansion and by residue calculus for the two ranges corresponding to small x and large x respectively. For the initial part of the flow, the asymptotic representations for Bessel functions of large

argument lead to the expansion

$$\bar{\tau}(s) = \delta\left\{\frac{1}{\sqrt{s}} - \frac{1}{2s} - \frac{1}{8s\sqrt{s}} - \frac{1}{8s^2}\right\} + (\delta-\varepsilon)\frac{2}{1-M^2}\left\{\frac{1}{s} + \frac{2\alpha-1}{s\sqrt{s}} + \frac{\alpha(4\alpha-3)}{s^2}\right\} + O\left(\frac{1}{s^2\sqrt{s}}\right); \qquad \alpha \equiv \frac{1+(\gamma-1)M^2}{1-M^2}$$

The inverse transform representing the normalized local shear for small x follows from this in the form

$$\tau(x) = \delta\left\{\frac{1}{\sqrt{\pi}}\frac{1}{\sqrt{x}} - \frac{1}{2} - \frac{1}{4\sqrt{\pi}}\sqrt{x} - \frac{1}{8}x\right\} + (\delta-\varepsilon)\frac{2}{1-M^2}\left\{1 + \frac{2(2\alpha-1)}{\sqrt{\pi}}\sqrt{x} + \alpha(4\alpha-3)x\right\} + O(x\sqrt{x})$$

For the heat transfer one obtains in the same manner the result

$$q(x) = \varepsilon\left\{\frac{1}{\sqrt{\pi}}\frac{1}{\sqrt{x}} - \frac{1}{2} - \frac{1}{4\sqrt{\pi}}\sqrt{x} - \frac{1}{8}x\right\} - (\delta-\varepsilon)\frac{2(\gamma-1)M^2}{1-M^2}\left\{1 + \frac{2(2\alpha-1)}{\sqrt{\pi}}\sqrt{x} + \alpha(4\alpha-3)x\right\} + O(x\sqrt{x})$$

and for the pressure change similarly:

$$\Delta p(x) = -(\delta-\varepsilon)\frac{2\gamma M^2}{1-M^2}\left\{\frac{2}{\sqrt{\pi}}\sqrt{x} + \frac{4\alpha-1}{2}x + \frac{16\alpha(2\alpha-1)-1}{6\sqrt{\pi}}x\sqrt{x}\right\} + O($$

The asymptotic expansions of the same flow properties for large values of x are obtainable, with a little caution, from the simple expansion formula (Ref. 3)

$$\mathcal{L}^{-1}\{f(s)\} \equiv \mathcal{L}^{-1}\left\{\frac{a(s)}{b(s)}\right\} = \sum_{i=1}^{\infty}\left\{\frac{a(s_i)}{b'(s_i)}e^{s_i x}\right\}$$

when the singularities of $f(s)$ are simple poles at $s = s_i$.

For the shear one obtains for large x the result

$$\tau(x) \cong \sum_{i=1} \left\{ 2\delta - (\delta-\varepsilon)\frac{2}{1+(\gamma-1)M^2} \right\} e^{\lambda_i x}$$

$$+ \sum_{j=1} \left\{ (\delta-\varepsilon)\left[\frac{I_1(\sqrt{\lambda_j})}{I_0(\sqrt{\lambda_j})}\right]^2 \frac{2}{(1-M^2)\left[1-\kappa\left(1-\left[\frac{I_1(\sqrt{\lambda_j})}{I_0(\sqrt{\lambda_j})}\right]^2\right)\right]} \right\} e^{\lambda_j x}$$

where the location of the singularities follow from the transcendental equations

$$\left.\begin{aligned} I_0(\sqrt{\lambda_i}) &= 0 \\ \frac{2\kappa}{\sqrt{\lambda_j}}\frac{I_1(\sqrt{\lambda_j})}{I_0(\sqrt{\lambda_j})} &= 1 \end{aligned}\right\} \quad i,j = 1,2,3,\ldots$$

The heat transfer is given for large x similarly by

$$q(x) \cong \sum_{i=1} \left\{ \frac{2\left[\varepsilon+(\gamma-1)M^2\delta\right]}{1+(\gamma-1)M^2} \right\} e^{\lambda_i x}$$

$$- \sum_{j=1} \left\{ (\delta-\varepsilon)\left[\frac{I_1(\sqrt{\lambda_j})}{I_0(\sqrt{\lambda_j})}\right]^2 \frac{2(\gamma-1)M^2}{(1-M^2)\left[1-\kappa\left(1-\left[\frac{I_1(\sqrt{\lambda_j})}{I_0(\sqrt{\lambda_j})}\right]^2\right)\right]} \right\} e^{\lambda_j x}$$

while the pressure change for large x is

$$\Delta p(x) \cong -\sum_{j=1} \left\{ (\delta-\varepsilon)\frac{\gamma M^2}{1+(\gamma-1)M^2} \frac{1}{\left[1-\kappa\left(1-\left[\frac{I_1(\sqrt{\lambda_j})}{I_0(\sqrt{\lambda_j})}\right]^2\right)\right]} \right\} e^{\lambda_j x}$$

in terms of the roots of the second transcendental equation above.

Results of sample calculations of shear, heat transfer, and pressure variation along the tube for $\sigma = 1$ and for characteristic velocities upstream corresponding to M = 0, .5, 1.5, and 2.5 are presented at the end of this note. The first figure shows the steady flow response of the wall shear to unit initial block profile perturbations in velocity (δ) and in enthalpy (ε), the second

figure shows the corresponding heat transfer response, and the third figure shows the pressure response to a velocity/enthalpy input sufficient to give a unit initial perturbation in pressure. The results are interesting in their own right, being directly pertinent to the compressible version of the classical inlet problem with or without moving walls. This and related applications will be discussed in detail elsewhere.

In terms of the problem of present concern, in the supersonic case the linearized solution as based on the steady flow assumption displays the proper asymptotic decay and is thus acceptable for the vehicle-in-the-tube problem situation: the failure of the end condition to communicate upstream in this case could indeed have been anticipated by considering the signal propagation within the flow field under supersonic conditions. The results shown in the final figure, representing for illustrative purposes the response of the flow at $M = 1.5$ to initial perturbations of 10% velocity decrement and 25% enthalpy rise, reveal some interesting circumstances of the laminar problem. As reflected in the wall shear variation, the downstream flow field turns out for these conditions to be characterized by a temporary reversal in flow direction rather than by the initially expected gradual decay. A significant feature is the finite heat transfer at the station where the wall shear passes through zero: obviously the use of Reynolds analogy on the problem must be handled with particular care.

In the subsonic case, on the other hand, the steady flow assumption leads to a response which according to the dissipationless linearized theory in general diverges exponentially for large x. The solution and one or more of its underlying assumptions are therefore fundamentally inapplicable to the subsonic vehicle-in-the-tube problem situation, except when $(\delta - \varepsilon) = 0$. According to the linearized theory, however, in this particular case the pressure perturbation is everywhere zero, the divergent terms in shear and heat transfer cancel out, and the subsonic solution then satisfies the end conditions after all. This special situation recalls superficially the problem of the propagation of a laminar flame at essentially constant pressure, but it remains to be seen if this precarious balance of oppositely divergent terms is the only steady subsonic solution of interest.

A useful next application of the linearized theory would be to the initial, unsteady phase of the problem when the disturbance is nearer to the end of the tube, in order to check the extent to which the subsonic asymptotic behavior for large time would reflect the constant pressure solution indicated above. The role of viscous dissipation in the problem should also be reconsidered, but that is outside the scope of the linearized formulation. Another problem outstanding is the much more difficult question of turbulent effects. The quantitative results derived above apply

of course specifically to the laminar problem; however, the general conjectures suggested are basic to the problem situation and would appear to apply to the turbulent case as well.

References

1. Foa, J.V., "Land transport at air transport speeds" National Transportation Journal, July-August 1962.

2. Jahnke, E. and Emde, F., Tables of Functions, 4th ed. Dover Publications, New York 1945.

3. Jaeger, J.C., The Laplace Transformation, 2nd ed. Wiley and Sons, 1961.

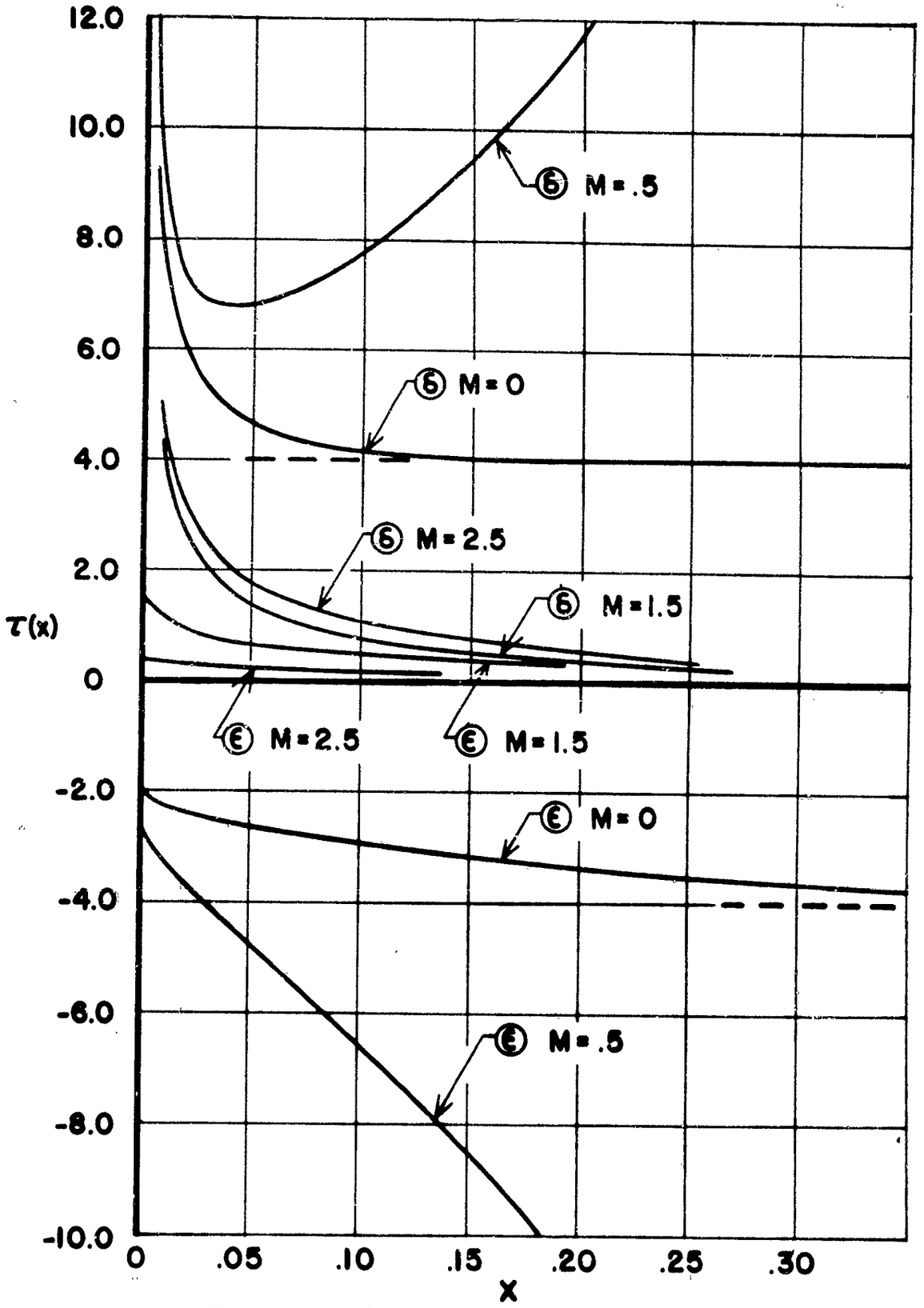

Fig. 1. Wall shear vs. Distance downstream

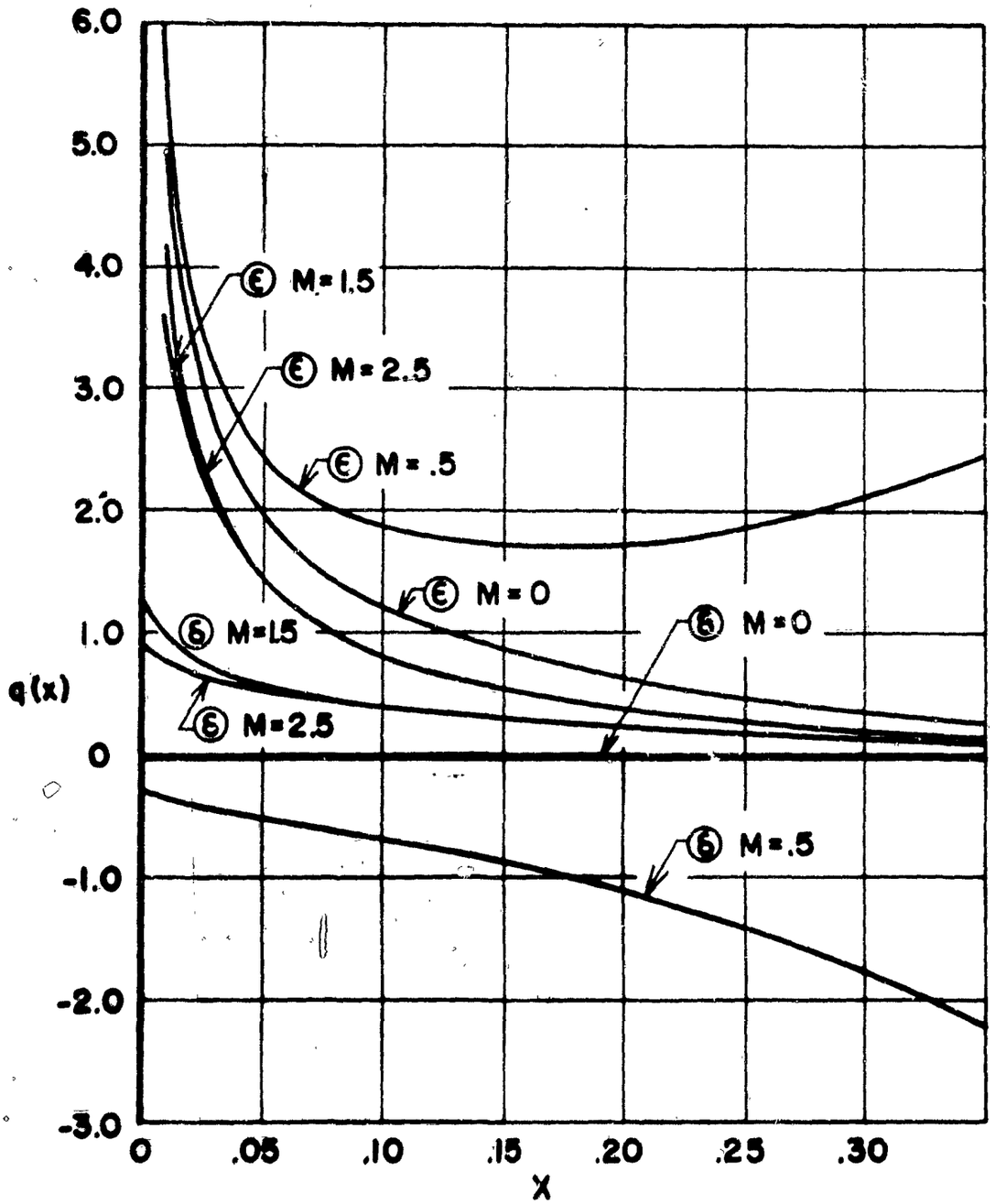

Fig. 2. Heat transfer to wall vs. Distance downstream

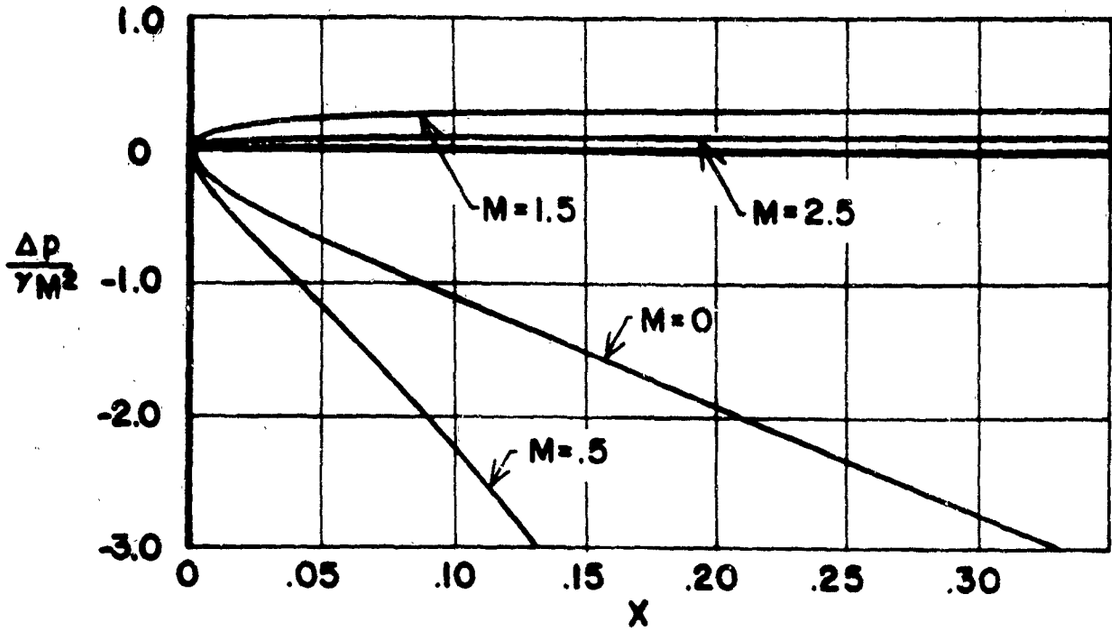

Fig. 3. Local pressure vs. Distance downstream

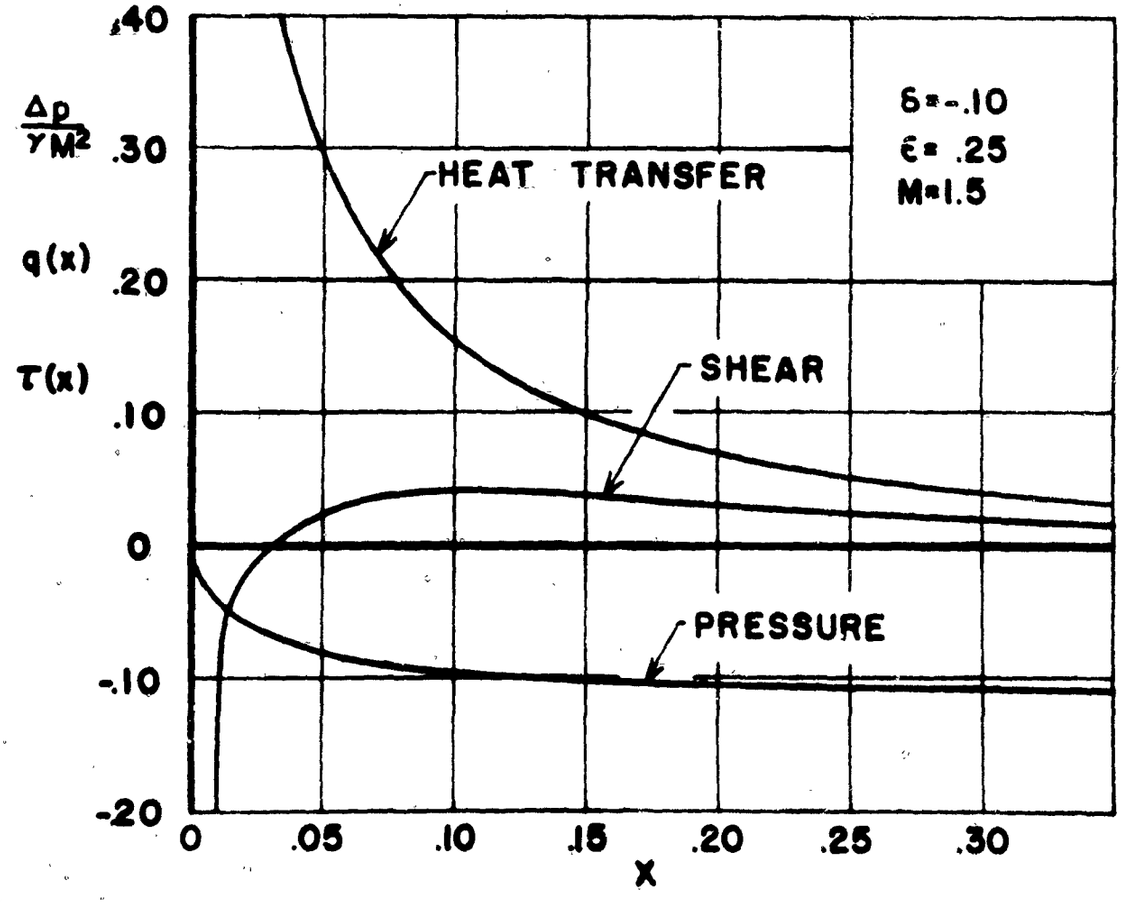

Fig. 4. Typical supersonic response to combined perturbation

SECTION I

ON TWO PROBLEMS OF TRANSONIC NONSTEADY MOTION OF A VEHICLE IN A TUBE

by

John W. Burr

SYMBOLS

a - speed of sound (ft/sec)

A - speed of sound nondimenionalized ($\frac{a}{a_o}$)

b - acceleration of vehicle (ft/sec^2)

b' - acceleration of the air (ft/sec^2)

B - percent mass flow blead off

D - Mach number function (see page I-8)

F - stream force

G - Mach number function (see page I-8)

g - acceleration of gravity

M - Mach number

$\dot{m}$ - mass flow rate

N - Mach number function (see page I-8)

P - Riemann parameter on right running characteristic

p - pressure (lb/ft^2)

Q - Riemann parameter on left running characteristic

R - gas constant

T - temperature (^oR)

τ - time

u - velocity (ft/sec)

U - velocity nondimensionalized ($\frac{u}{a_o}$)

x - distance along tube

α - cross sectional area

γ - specific heat ratio

Subscripts

i - initial values

0 - reference state

R - pertaining to the flow on the right hand side of the vehicle relative to the tube

S - shock

V - vehicle

VR - pertaining to the flow on the right hand side of the vehicle relative to the vehicle

3 - region in time-distance plane (See fig. I-1)

4 - region in time-distance plane (See fig. I-1)

Superscripts

0 - stagnation conditions

INTRODUCTION

The problem of accelerating through the transonic region to reach supersonic speeds has always been a difficult problem and is even more difficult for the case of a vehicle in a tube. When a vehicle travels at supersonic speeds, either through a tube or in open air, there usually exists a shock wave at the nose of the vehicle. It may be attached to the vehicle or be only a small fraction of a body length ahead of the vehicle, but there is always a shock wave present. When a self-propelled vehicle, which uses the air in the tube as the propulsive medium, accelerates from rest in a tube it usually sends out an expansion wave initially. Since a shock wave will exist ahead of the vehicle in supersonic flow, there must be some point during the acceleration at which the wave being sent upstream changes from an expansion to a compression type wave.

This acceleration of a vehicle in a duct through transonic speeds was first investigated in 1957 and reported in RPI report TR AE 6101 (Ref. 1). This investigation showed that, although it may be possible to reach supersonic speeds, many unusual and interesting flow situations occur during the transonic acceleration period.

The problem of obtaining supersonic speeds within a tube is very similar to the problem of starting a supersonic inlet. The

presence of the vehicle in the tube forms a "throat" and before a supersonic type flow is obtained the normal shock which forms in the tube ahead of the vehicle must be "swallowed". At some subsonic Mach number the flow around the vehicle will reach sonic velocity relative to the vehicle and will become "choked". As the vehicle accelerates beyond this point, the vehicle will be forced to "push along" some of the air ahead of it and the disturbances which are sent upstream will no longer be expansion waves as in the initial acceleration but rather compression waves. These compression waves will coalesce and form a normal shock some distance ahead of the vehicle and the flow around the vehicle will remain choked until the vehicle overtakes the shock. This can only occur after the vehicle has reached or exceeded the Mach number, relative to the duct, at which the vehicle was designed to pass the normal shock.

If there is an appreciable region of disturbed flow between the shock and the vehicle, a great deal of power will be required to push this slug of high speed air through the tube. The first part of this report deals with the determination of the distance at which the shock forms ahead of the vehicle and of its standoff distance during the transition time before it is overtaken by the vehicle.

The second part of this report deals with the problem of slowing down the shock and of shortening the distance and time required to

overtake it. There are several ways of doing this, but the only technique considered here is that of the "shock trap" which consists of a section of tube with perforations through which the overpressure produced by the shock can be relieved.

SHOCK FORMATION AND GROWTH

Formation of a Shock by a Permeable Piston

The technique used to determine the time and position of the initial formation of the shock is similar to those used by Foa (Ref. 2) and Rudinger (Ref. 3). Consider a vehicle moving in an infinite tube at a velocity such that the flow around the body is choked. If the ratio of the area of the tube to the area of the annular space between the vehicle and the tube, is fixed, then the Mach number of the flow just ahead of the vehicle, relative to the vehicle,

$$M_{VR} = \frac{u_v - u_.}{a_a} = \frac{U_v - U_R}{A_R}$$

will remain constant as the vehicle accelerates.

The vehicle is moving at u_{vi} and the flow velocity just ahead of the vehicle is u_{Ri} (both relative to the tube) and the Riemann Parameter, Q on the left running characteristic is constant ahead of the vehicle. At time t=o consider that the vehicle is accelerated steadily at a rate $b = \frac{du_R}{dt}$. Since the flow around the vehicle is choked, the flow will also be pushed along or accelerated as the

vehicle accelerates. However, the flow will not be accelerated at the same rate as the vehicle but at some slower rate, $b' = \frac{du_R}{dt}$ Now the velocity of the flow just ahead of the vehicle, relative to the vehicle, is

$$u_{VR} = u_V - u_R \tag{1}$$

Hence $$u_R = u_V - u_{VR}$$

$$= u_V - M_{VR} a_R \tag{2}$$

Since M_{VR} is constant $\frac{du_R}{dt} = 0 = \frac{2}{\gamma-1} \frac{du_V}{dt} - M_{VR} \frac{da_R}{dt}$

or $$b' = b - M_{VR} \frac{da_R}{dt} \tag{3}$$

Also, since $$Q = \frac{2}{\gamma-1} A_R + U_R = Const.$$

then $$\frac{dQ}{dt} = 0 = \frac{2}{\gamma-1} \frac{dA_R}{dt} - \frac{dU_R}{dt}$$

and therefore

$$\frac{du_R}{dt} = \frac{2}{\gamma-1} \frac{da_R}{dt} \tag{4}$$

and the acceleration of the flow just ahead of the vehicle is

$$b' = \frac{b}{1 + \frac{\gamma-1}{2} M_{VR}} \tag{5}$$

If we now consider this acceleration as the acceleration of an equivalent piston, and employ the technique used by Foa (Ref. 2) fo

the formation of a shock by a uniformly accelerated piston, we find that the time required for the first formation of the shock is

$$t = \left(u_{Ri} + a_{Ri} - u_{vi}\right) \frac{2}{\gamma+1} \frac{1}{b'} \tag{6}$$

During this time both the wave and the vehicle have been moving down the tube. The distance traveled by the first wave is

$$x_s = \left(u_{Ri} + a_{Ri}\right)\left(u_{Ri} + a_{Ri} - u_{vi}\right)\frac{2}{\gamma+1} \frac{1}{b'} \tag{7}$$

and the distance traveled by the vehicle is

$$x_v = u_{vi} t + b \frac{t^2}{2} \tag{8}$$

Combining these with eq. (6) the distance at which the shock first appears ahead of the vehicle can be found from eqs. 7 and 8.

$$x_s - x_v = \left(1 - \frac{b}{b'} \frac{1}{\gamma+1}\right)\left(a_{Ri} + u_{Ri} - u_{vi}\right)^2 \frac{2}{\gamma+1} \frac{1}{b'} \tag{9}$$

Numerical Example

Consider a vehicle designed to pass a normal shock at Mach number 2.0. With this condition the flow velocity behind the normal shock is 577 ft/sec. If the vehicle is designed so that it can accelerate up to 577 ft/sec. before the annular passage around it becomes choked then it will be able to travel at the same speed, relative to the flow behind the shock, as the shock itself. In this

way it can swallow a normal shock at Mach number 2.0.

Also at this point let $u_{Ri} = 0$, $a_{Ri} = 1000$ ft/sec. and let the vehicle be accelerated at 30 ft/sec. Under these conditions $M_{VR} = .577$ and eq. (14) gives a value of $x_s = 12900$ ft. or 2.45 miles. However the distance of the shock ahead of the vehicle $x_s - x_v$ is only 2970 ft. or .56 miles.

From this point on the growth of the shock can be calculated by means of one-dimensional non-steady characteristic theory (See Ref. 1). Since the Mach number of the flow just ahead of the vehicle, relative to the vehicle, remains constant then

$$U_v = M_{VR} A_R + U_R \tag{10}$$

The left running characteristic reaches the vehicle from upstream after passing through the shock. The Riemann parameter on this characteristic is

$$Q_R = \frac{2}{\gamma-1} A_R - U_R \tag{11}$$

Adding these two equations we have

$$U_R + Q_R = \left(\frac{2}{\gamma-1} + M_{VR}\right) A_R \tag{12}$$

or

$$A_R = \frac{U_v + Q_R}{\frac{2}{\gamma-1} + M_{VR}} \tag{13}$$

Now, substituting this into eq. (17) we have

$$u_v = M_{VR} \frac{U_v + Q_R}{\frac{2}{\gamma-1} + M_{VR}} + U_R$$

or

$$U_R = \left(1 - \frac{M_{VR}}{\frac{2}{\gamma-1} + M_{VR}}\right) U_v - Q_R \qquad (14)$$

Now, by the use of equations (13) and (14) the Riemann parameter on the right running characteristic,

$$P_R = \frac{2}{\gamma-1} A_R + U_R$$

which originates at the vehicle can be determined, and the characteristics net can be constructed between the vehicle and the shock.

The results of a calculation of this type are shown on Fig. I-1. Although the vehicle in the case considered is designed to swallow a normal shock at $M_s = 2.0$, the shock is still a distance ahead of the vehicle at the time the shock first reaches $M_s = 2.0$. As a consequence, the vehicle continues to accelerate and strengthen the shock and does not overtake it until $M_v = 2.53$ and $M_s = 2.42$.

SHOCK TRAP

The shock trap consists of a section of the tube with wall perforation which connect the tube to either the atmosphere outside or to some large sealed chambers. Before the shock passes through the perforated section, the tube is under the same pressure as either the

outside atmosphere or the sealed chambers. When the shock passes the perforated section, the high pressure behind the shock causes some of the air in the tube to pass out through the perforations. Hence the mass flow rate in the tube behind the shock is less downstream of the perforations than it is upstream and the shock is weakened.

One possible advantage of having the perforations connected to large sealed chambers instead of open to the atmosphere is that the air which passes out of the tube will be stored in the chambers at the high pressure produced by the shock. After the vehicle passes through the perforated section the air will be forced back into the tube and thereby provide additional thrust to the vehicle.

For simplicity in analyzing the operation of the shock trap, perforations will be assumed to exist at only one station and to be arranged and sized to remove a fixed percentage B of the flow behind any normal shock. Prior to the arrival of the shock the conditions in the tube are uniform and the air is at rest throughout the tube. Now consider that a shock is propagating through the tube at a constant Mach number M_s (see Fig. I-2).

After the shock has passed the perforations the continuity and momentum equations across the perforated section are

$$\dot{m}_3 = \dot{m}_4 (1 - B) \qquad (1$$

and $$F_3 - F_4 = (\dot{m}_4 - \dot{m}_3)\, u_4 \qquad (16)$$

Using the continuity equation, the momentum equation reduces to

$$F_3 - F_4 = B\, \dot{m}_4\, u_4 \qquad (17)$$

where the mass flow rate is

$$\dot{m} = \sqrt{\frac{\gamma}{gR}}\, \frac{P^\circ \alpha\, D}{\sqrt{T^\circ}}$$

the stream force is $F = \dot{m}\, u + P\alpha$

$$= P^\circ \alpha\, G$$

and $$G = \frac{1 + \gamma M^2}{\left(1 + \frac{\gamma-1}{2} M^2\right)^{\frac{\gamma}{\gamma-1}}}$$

$$D = \frac{M}{\left(1 + \frac{\gamma-1}{2} M^2\right)^{\frac{\gamma+1}{2(\gamma-1)}}}$$

The momentum equation can be reduced to

$$\frac{P_3^\circ}{P_4^\circ} = \left\{ 1 + \frac{\gamma B M_4^2}{1 + \gamma M_4^2} \right\} \frac{G_4}{G_3} \qquad (18)$$

and the continuity equation becomes

$$\frac{P_3^\circ}{P_4^\circ} = \frac{D_4}{D_3} (1 - B) \qquad (19)$$

Combining these two equations gives

$$\frac{N_4}{N_3} = \frac{1}{1-B}\left\{1 + B\,\frac{\gamma M_4^2}{1+\gamma M_4^2}\right\} \qquad (2$$

where

$$N = \frac{D}{G} = \frac{M\left(1 + \frac{\gamma-1}{2}M^2\right)^{\frac{1}{2}}}{1+\gamma M^2}$$

Now

$$P_4 = \frac{2}{\gamma-1} A_4 \left(1 + \frac{\gamma-1}{2} M_4\right)$$

$$= \frac{2}{\gamma-1}\,\frac{1}{a_0}\left(\frac{\gamma g R T_4^\circ}{1+\frac{\gamma-1}{2}M_4^2}\right)^{\frac{1}{2}}\left(1 + \frac{\gamma-1}{2} M_4\right) \qquad (2$$

Likewise

$$Q_3 = \frac{2}{\gamma-1}\,\frac{1}{a_0}\left(\frac{\gamma g R T_3^\circ}{1+\frac{\gamma-1}{2}M_3^2}\right)^{\frac{1}{2}}\left(1 - \frac{\gamma-1}{2} M_3\right) \qquad (2$$

Now since there is no energy added or removed from the flow, $T_3^\circ = T_4^\circ$ and

$$\frac{P_4}{Q_3} = \frac{1+\frac{\gamma-1}{2}M_4}{1-\frac{\gamma-1}{2}M_3}\left\{\frac{1+\frac{\gamma-1}{2}M_3}{1+\frac{\gamma-1}{2}M_4}\right\}^{\frac{1}{2}} \qquad (2$$

Since the values of P_4 and Q_3 are known equation (20) and (23) can be solved graphically to yield the Mach number on either side of the perforated section. This solution is shown on Fig. I-3. By

using an iterative procedure to determine the value of Q across the shock, the shock attenuation resulting from any given flow diversion can be determined.

For example, if a shock trap is so located that the shock reaches the perforated station when $M_s = 1.43$ then $\frac{P_4}{Q_3}$ is approximately 1.24 and if 10% of the flow is removed then $\frac{P_3}{Q_3}$ is approximately 1.22 and M_s immediately downstream of the perforated section is approximately 1.38. This shows that a shock trap may be useful in reducing the strength of the shock.

For shock Mach numbers greater than about 2.0 the value of $\frac{P_4}{Q_3}$ will exceed 1.5 and this analysis will not apply. A more complicated analysis which includes sonic conditions at the perforated section must be developed.

REFERENCES

1. Burr, John W.: "A Contribution to the Dynamics of a Self-Propelled Vehicle in an Infinite Duct", Rensselaer Polytechnic Institut Troy, New York, Jan. 1961.

2. Foa, J.V.: Elements of Flight Propulsion, John Wi & Sons, Inc., New York, New York 1960

3. Rudinger, George: Wave Diagrams for Nonsteady Flow in D D. Van Nostrand Company, New York, New York, 1955.

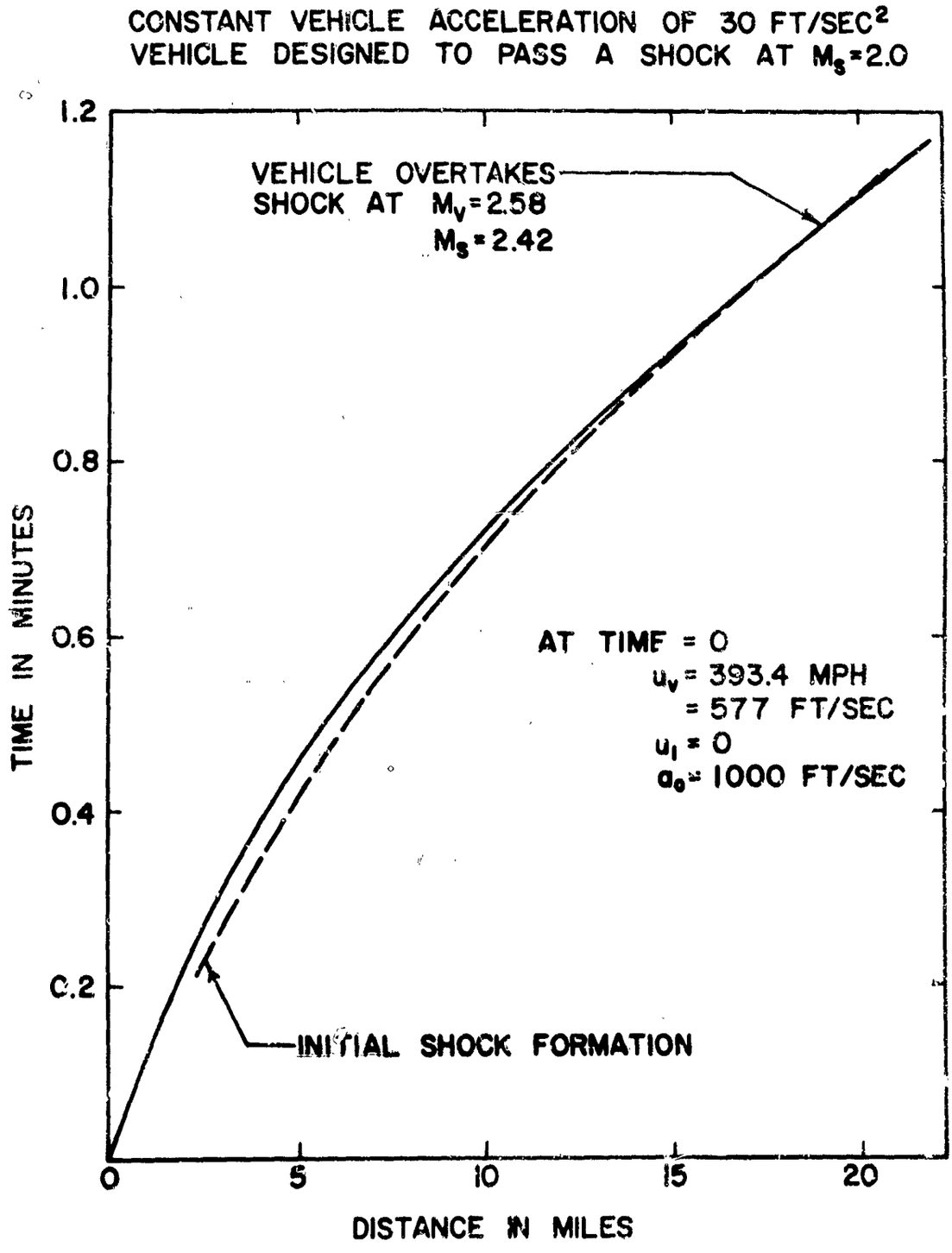

Fig. I-1: Formation and Growth of the Shock caused by a Uniformly Accelerating Vehicle

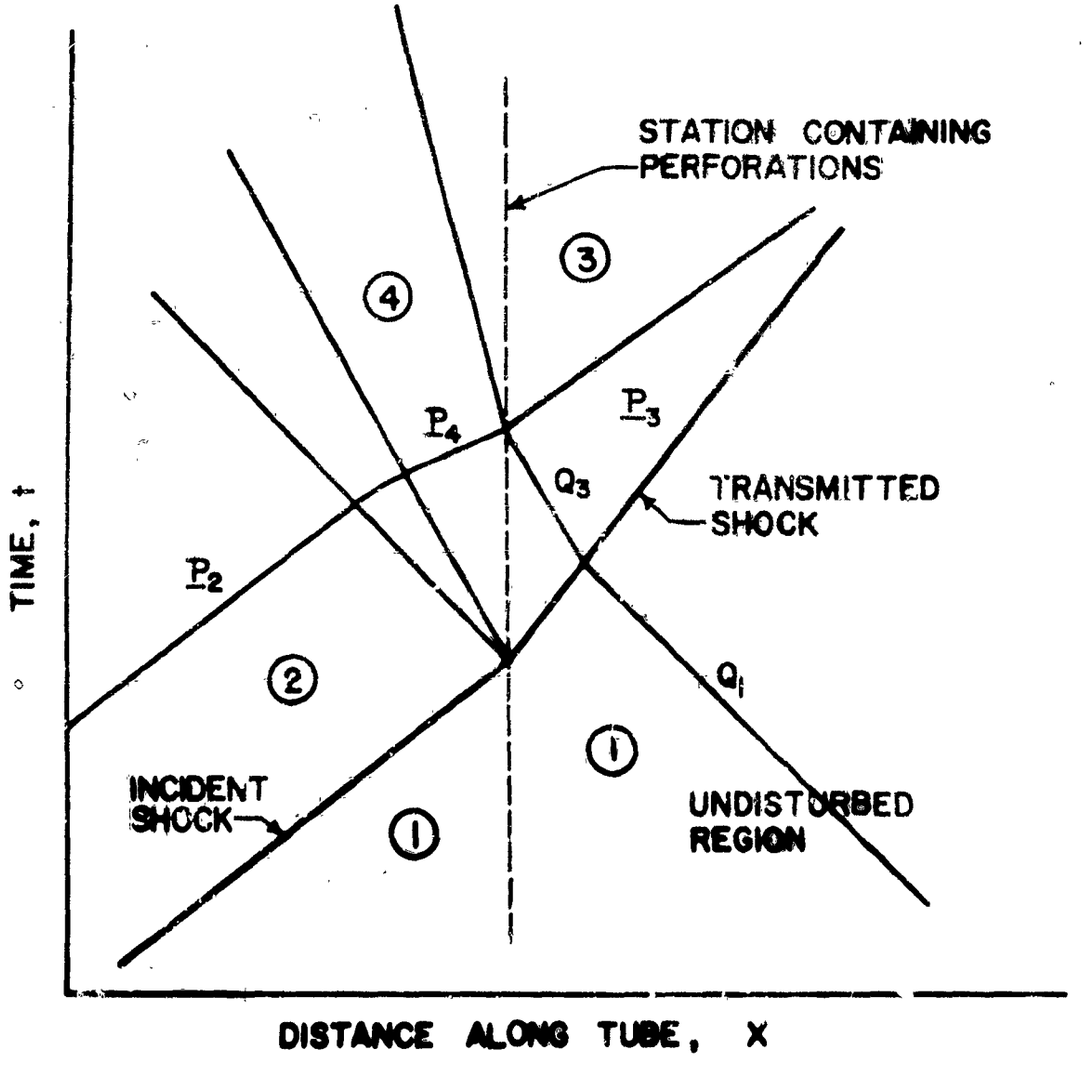

Fig. I-2: Schematic Representation of the Operation of a Shock Trap.

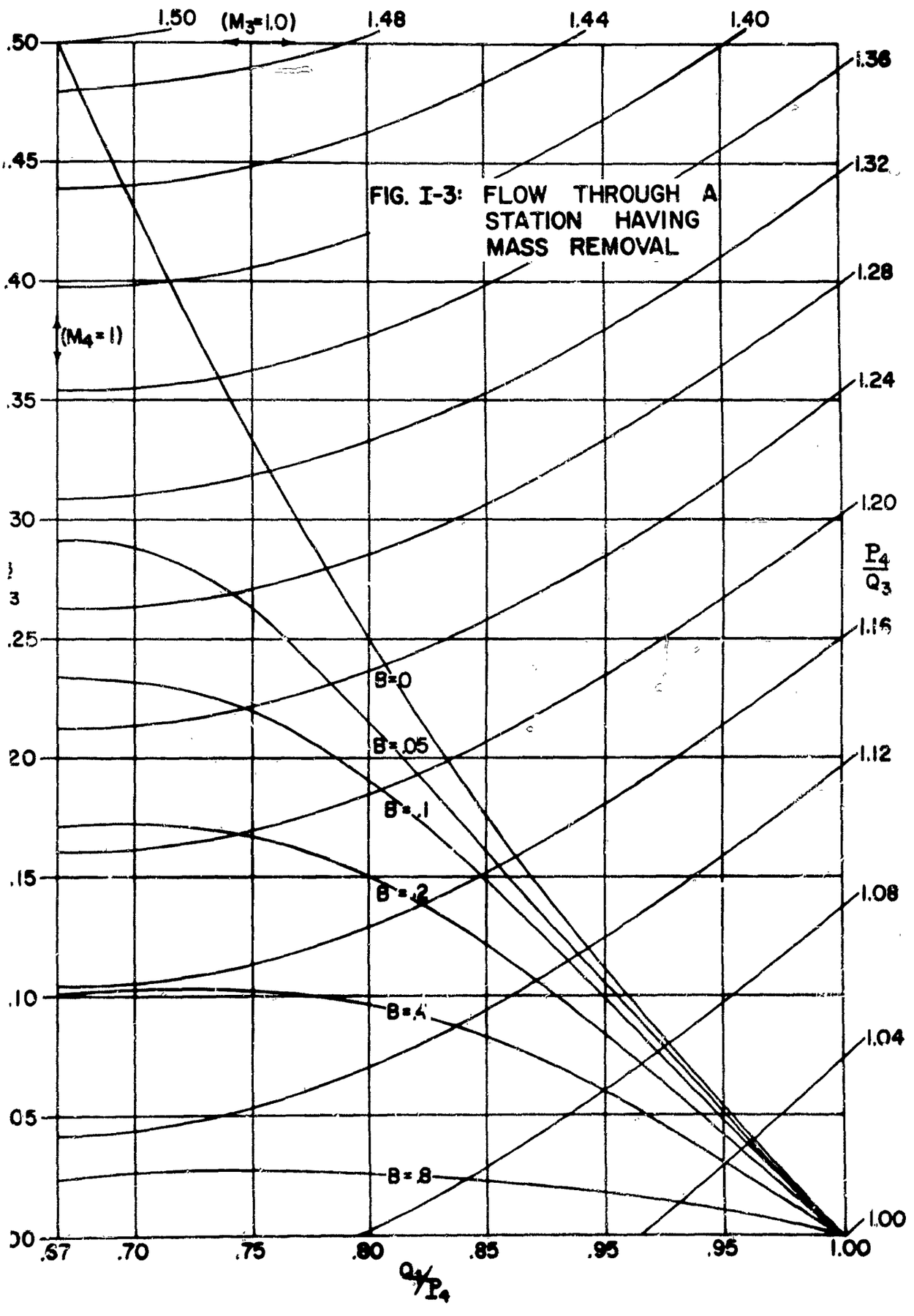

FIG. I-3: FLOW THROUGH A STATION HAVING MASS REMOVAL

SECTION J

PRELIMINARY DESIGN CONSIDERATIONS FOR A 3-FT DIAMETER TUBE TRANSPORT PILOT MODEL

by

Leo F. Gijsels

ABSTRACT

This report deals with the design of a pilot model of the tube transport system. The means of propulsion considered here is a jet engine, placed behind the vehicle and acting as the driver of an ejector pump which sucks the air from ahead of the vehicle and transfers it to the rear. The paper only covers the selection of some of the basic parameters involved.

SYMBOLS

α cross sectional area (sq ft)

$\dot{m}$ mass flow rate (slugs/sec)

p pressure (lb/sq ft)

T temperature (^{o}R)

ϱ density (slugs/cu ft)

u flow velocity (ft/sec)

a speed of sound (ft/sec)

M Mach number

F stream force (lb)

$\mathcal{D}$ drag (lb)

θ thrust (lb)

d diameter of tube (ft)

S entropy (Btu/^{o}R lb)

P power (HP)

$$D = M\left[1 + \frac{\gamma-1}{2} M^2\right]^{-\frac{\gamma+1}{2(\gamma-1)}}$$

$$G = \left[1+\gamma M^2\right]\left[1 + \frac{\gamma-1}{2} M^2\right]^{-\frac{\gamma}{\gamma-1}}$$

$$N = \frac{D}{G} = M\left[1 + \frac{\gamma-1}{2} M^2\right]^{\frac{1}{2}}\left[1+\gamma M^2\right]^{-1}$$

SUBSCRIPTS

1 undisturbed ambient conditions

2 conditions between vehicle and engine

3 conditions after vehicle and engine

4 conditions after mixing

5 final conditions after heat extraction

p primary

s secondary

SUPERSCRIPTS

o stagnation values

INTRODUCTION

The problem considered here is that of selecting a power plant for a pilot model of the tube transport system. It is specified that the vehicle is to travel at 300 mph. (M = 0.4) in a tube of 3 ft. diameter.

The analytical model used is that of an entropy and drag producer (the vehicle), followed by a thrust generator, an adiabatic mixing region and a heat extraction region (Fig. J-1).

The equations are simplified by changing the frame of reference from that fixed to the walls to one moving with the vehicle. In the latter frame of reference the flow is substantially steady or quasi steady. The air undergoes a complete cycle from a station some distance upstream of the vehicle to a station 5 some distance downstream of it.

DRAG PRODUCTION

The first step is to analyze what is happening between sections 1 and 2, around the vehicle. The flow conditions at station 1 are taken to be $T_1^o = 500^oR$ and $p_1 = 2{,}120$ psf, hence $\rho_1 = 0.0024$ slugs/cu ft; $u_1 = 300$ mph $= 440$ fps ($M_1 = 0.4$). With $\alpha_1 = \frac{\pi d^2}{4} = 7.07$ sq ft, the mass flow rate is: $\dot{m}_1 = \rho_1 \alpha u_1 = 7.68$ slugs/sec.

The flow transformation from section 1 to 2 is isoenergeti hence: $T_2^\circ = T_1^\circ = 516^\circ R$.

The best criterion presently available for the design of the air passage around the vehicle is to follow the current practice for jet-engine air intakes. If this is done, it is permissible to assume $\frac{p_2^\circ}{p_1^\circ} = 0.95$, hence $p_2^\circ = 2{,}240$ psf.

The other flow parameters at station 2 are obtained from the conservation equations (Ref. 1).

Continuity eqn.: $$\frac{p_A^\circ \alpha_A D_A}{\sqrt{T_A^\circ}} = \frac{p_B^\circ \alpha_B D_B}{\sqrt{T_B^\circ}} \qquad (1)$$

or $$\frac{F_A N_A}{\sqrt{T_A^\circ}} = \frac{F_B N_B}{\sqrt{T_B^\circ}} \qquad (2)$$

Momentum eqn.: $$F_B - F_A = p_B^\circ \alpha_B G_B - p_A^\circ \alpha_A G_A \qquad (3)$$

Energy eqn.: $$T_B^\circ - T_A^\circ = \frac{q_{AB} + w_{AB}}{c_p} \qquad (4)$$

One easily finds from the continuity eqn: $M_2 = 0.426$, whil the momentum eqn. gives the drag $\mathcal{D} = F_2 - F_1 = -745$ lb.

The entropy production is given by:

$$\Delta S = c_p \ln \frac{T_2^\circ}{T_1^\circ} - R \ln \frac{p_2^\circ}{p_1^\circ} = -53.3 \ln 0.95 = 2.73 \ \frac{Btu}{^\circ R\, lb}$$

THRUST GENERATOR

Since the three conservation eqns. have five unknowns:

P_3^o, T_3^o, M_3, θ , q_a , two additional relationships are required. One of those requirements is that the thrust θ must exactly balance the drag $\mathcal{D}$, or $\theta = -\mathcal{D} = 745$ lb.

Now the eqns. can be solved for T_3^o, P_3^o, M_3 with q_a as parameter. However, the values for q_a are limited in both directions. Due to the second law of thermodynamics, the total entropy change (i.e. ΔS of the flow plus the surroundings) must be positive for a spontaneous process. Hence a minimum value for q_a is established. On the other hand, from the continuity eqn. $\frac{F_2 N_2}{\sqrt{T_2^o}} = \frac{F_3 N}{\sqrt{T_3^o}}$ (2), follows that, for the subsonic case and in absence of shocks, T_3^o is limited. Hence from the energy eqn. (4) $q_{a\,max}$ can be found.

An approximate expression for the power required is found in Ref. 2, nl.:

$$P \cong \rho_1 \propto u_1 (1 - p_r^o) \qquad (5)$$

where p_r^o = stagnation pressure ratio.

Hence $P = 2{,}120 \times 7.07 \times 440 \times (1 - 0.95) \times 1.818 \times 10^{-13} =$ 600 HP.

With these two parameters, nl. the thrust $\theta = 745$ lb and the power $P = 600$ HP, the two determining characteristics for the power plant are fixed. Furthermore the mass flow rate through

the engine should be less than $\dot{m}_1 = 7.68$ slugs/sec while its cross sectional area is also limited (such that always $M < 1$).

The thrust of the power plant and also its cycle efficiency can be increased by using an inlet diffuser ahead of the jet engine.

The available catalogues give several possible power plants, which satisfy the above stated requirements of thrust, power, diameter and mass flow rate (see e.g., Ref. 3).

The following numerical example gives an idea of the order of magnitude of the different parameters involved. The jet engine has a constant cross sectional area: $\alpha_p = 1.67$ sq ft.

The parameters at stations 1 and 2 are already known.

At station 2, the flow is divided into two parts:

1. the primary flow (p) through the engine undergoes a Rayleigh process with heat addition.
2. the secondary flow (s) around the engine undergoes an isoenergetic process with a drop in stagnation pressure.

A uniform flow is assumed at the inlet over the whole cross sectional area, hence $\frac{\dot{m}_p}{\dot{m}_s} = \frac{\alpha_p}{\alpha_s}$ or $\dot{m}_p = 1.815$ slugs/sec and $\dot{m}_s = 5.865$ slugs/sec.

For the secondary flow process, with $T^o_{3s} = T^o_2 = 516^oR$ and $p^o_{3s} = 0.96\ p^o_2 = 2.150$ psf, the conservation eqns. yield $M_{3s} = 0.450$ and $R_s = 432$ lb. This additional drag must also be balanced by the thrust of the primary flow. Hence the total thrust is: $\Theta_p = 745 + 432 = 1{,}177$ lb.

For the primary flow process, the amount of heat to be added is:

$$q_a = \frac{P}{\dot m_p} HP_{sec} = \frac{550\ P}{777.5\ \dot m_p\ g}\ \text{Btu/lb} = 7.27\ \text{Btu/lb}$$

The conservation eqns. give further: $T^o_{3p} = 546.3^oR$; $F_{3p} = 5{,}320$ lb; $M_{3p} = 0.312$ and $p^o_{3p} = 3{,}000$ lb.

The flow conditions at station 4 are determined by applying the equations for isoenergetic mixing in a constant area duct.

From Ref. 1 one gets:

$$z = \left[1 - 2(\gamma+1) \frac{\left(\sum_{j=1}^{n} \dot m_j\right)\left(\sum_{j=1}^{n} \dot m_j\, T^o_{ji}\right)}{\left(\sum_{j=1}^{n} \dot m_j\, \frac{\sqrt{T^o_{ji}}}{N_{ji}}\right)^2} \right]^{\frac{1}{2}}$$

hence $z = 0.6825$.

Furthermore: $M_f^2 = \frac{1-z}{1+\gamma z}$ yields $M_f = 0.403$

$p_f = \frac{F}{(\gamma+1)\alpha}(1+\gamma z)$ with $F = F_{3p} + F_{3s} = 18{,}300$ lb gives $p_f = 2{,}110$ lb

$u_f = \frac{\gamma}{\gamma+1} \frac{F}{\dot m} (1-z) = 441$ ft/sec

$$T_f = \frac{\varepsilon}{c_p}\left(1 - \frac{\gamma-1}{\gamma+1}\,\frac{1-\alpha}{1+\alpha}\right) \text{ with } \frac{\varepsilon}{c_p} = \frac{\sum_{j=1}^{n} \dot{m}_j T_{ji}^{o}}{\sum_{j=1}^{n} \dot{m}_j} = 523$$

and $T_f = 506.6\ ^{o}R$

Reference 4 gives now: $p_4^o = 2{,}360$ psf and $T_4^o = 523.3\ ^{o}R$.

In the next part of the duct, between stations 4 and 5, heat is extracted in such an amount that the net result between 2 and 5 is zero energy addition. Hence: $q_2 \dot{m}_p = - q_4 \dot{m}_5$ or $q_4 = - 1.72$ Btu/lb.

Furthermore from the conservations eqns. $T_5^o = 515.1\ ^{o}R$ $M_5 = 0.399$ and $P_5^o = 2{,}360$ psf. Except for some minor calculation errors, the final state is the same as the initial one. Hence it is possible for the flow to undergo the above transformations and to come back to the same original state. However nothing is said about the relative distances involved. Probably a compression wave travels ahead of the vehicle, so that the undisturbed section 1 is far upstream. Maybe the compression wave is weakened by an expansion caused by the sucking of air around the vehicle through the engine. This problem is still under further study. On the other hand, the length of the mixing regi and energy extraction region can be very large too. A more detailed study of the mechanism of energy decay is found in Ref. 5.

CONCLUSION

From the vehicle under consideration, moving at a speed of 300 mph (M = 0.4) in a duct of 3 ft. diameter, a jet engine is needed which can produce, in steady motion, a thrust of 750 lb corresponding to a power of 600 HP. However during acceleration, the required values of Θ and P are higher so that the capacity of the power plant must be higher too, depending upon the desired acceleration. The diameter of the engine must be less than a certain critical value (to keep M 1).

About the support for the vehicle, some basic calculations can be found in Ref. 2.

For the calculation of the power required, the following expression from Ref. 2 was used: $P \equiv p_1 \propto u_1 (1 - p_r^o)$ (5)

P is a linear function of u_1, hence of M_1, but is independent of the weight of the vehicle. However the power calculated with eqn. (5) is the power required for steady operation only, and is determined rather by the shape of the vehicle (determines drag and p_r^o) than by its weight. The power required for the acceleration, however, is proportional to the weight of the vehicle. Furthermore, for an aerodynamic suspension system, the additional power for the air support would increase with the weight. Though this power is very low because of "ground effect" it has been

shown in Ref. 6 that most of this energy can be recovered for thrust generation. A separate power source in the nose of the vehicle could deliver this airstream for the "aerodynamic cushions" (see Ref. 2).

REFERENCES

1. Foa, J.V., Elements of Flight Propulsion, Wiley, 1960.

2. Foa, J.V., "A Fast Carrier," Rensselaer Polytechnic Inst., Tech. Rept. TR AE 6206, May 1962.

3. Jane's All the World's Aircraft 1962-1963, McGraw-Hill.

4. Foa, J.V., "Mach Number Functions for Ideal Diatomic Gases", Cornell Aeronautical Lab., October 1949.

5. Cromack, D. and Gijsels, L., Section G of "Research on the Dynamics of a Vehicle in a Tube", Final Progress Report, Grant No. DA ORD 31-124-61G-88, Rensselaer Polytechnic Inst., June 1964.

6. West, A.A., "The Effect of Simulated High Forward Speed on a Two-Dimensional Ground Effect Support," Rensselaer Polytechnic Inst., Tech. Rept. TR AE 6304, October 1963.

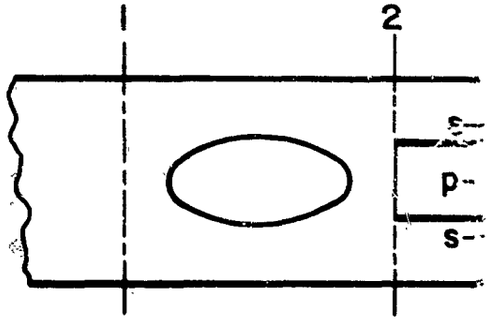

FIG. J-1: Schematic

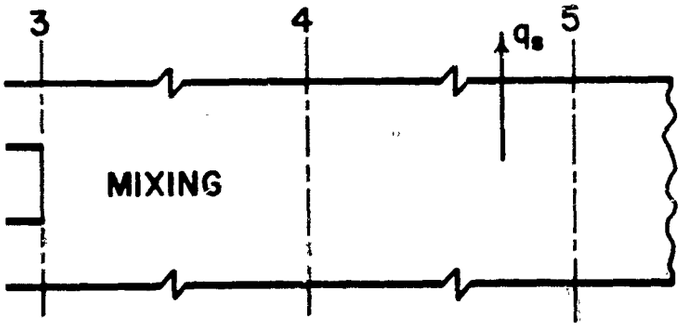

ntation of the Vehicle in a Tube

SECTION K

RECOMMENDATIONS FOR FUTURE WORK

by

Joseph V. Foa and Russell M. Lewis

RECOMMENDATIONS

A radically new mode of transportation cannot be properly evaluated in the light of today's problems and needs; rather it must be judged on the basis of its adequacy to serve the demands of tomorrow, and of its probable influence on the development and use of the land and on the patterns of living for generations to come.

A tube-transport system of the type discussed in the preceding sections would provide a mode of movement characterized by very high speed, a high level of inherent safety, and complete independence from atmospheric and surface conditions. This mode could directly penetrate the large urban centers and also provide direct access to large regional airports.

The immediate benefit would be the provision of very high speed, all-weather, direct mass transit between distant cities and within large metropolitan areas. Its greatest eventual value, however, will in all likelihood be the impetus provided to urban growth and the freedom permitted to the patterns of growth as the restrictions of our present forms of transportation are removed.

It is believed that this system would be best suited for operation at speeds from 250 to 2000 mph over distances where the

use of such speeds would be economically justifiable.

The first step in its implementation should probably be a pilot, mail-carrying line; a second step could be a shuttle service for passengers between two cities not too far apart (e.g., New York and Philadelphis or Washington) or between one of these metropolitan centers and its relocated "super airport". The operating frequency of these shuttle services could be very high, because of the intrinsic safety of this transportation system.

It should be noted that the engineering know-how for the implementation of these first steps (covering speeds up to 300 or 350 mph) is already available. Thus, from the standpoint of technical feasibility, it is believed that these steps could be undertaken immediately. The utilization of the system over longer distances and at higher speeds would have to be a gradual development, following the successful solution of the engineering problem associated with the transition to supersonic speeds and with the propulsion, support and stability of the vehicle at supersonic speeds. An effort in this direction is believed to be highly desirable from the very start, no matter how successful the "low-speed" versions may turn out to be, because all indications of the analysis are that the superiority of the proposed carrier over existing

transport systems would be far greater at supersonic than at subsonic speeds.

The successful development of a transportation system based on the ideas discussed in this report will undoubtedly take several years. Unfortunately, the novelty of the concept makes it impossible to predict all the problems that will arise in this work and to plan the developmental program very far in advance. Recommendations for further work will, therefore, be confined to a program for the first two years.

This program should consist of:

(a) engineering analyses and research aimed at the determination of quantitative information required for a study of the economic feasibility of the proposed system;

(b) design of a three-mile pilot model, and

(c) a preliminary feasibility study of the proposed system.

The engineering analysis should deal with the following areas:

(1) Propulsion. Various energy sources and thrust-generating cycles should be considered and analyzed, including - for very high speeds - thermal propulsion systems of the type diagrammatically illustrated in Fig. 6.

(2) Transonic acceleration. Attention should be given to non-steady flow means for overcoming the choking difficulties,

and to the use of suitable wall slots and perforations over those portions of the tube where the transonic acceleration is expected to take place;

(3) Vehicular support and stability. The study of stability and ground-effect support should be extended to higher speeds and larger models, with special attention to new means for increasing the stability derivatives of the proposed system, thereby permitting larger vehicular loads and higher speeds in turn. Improvements in curtain momentum recovery for thrust should also be sought, through a detailed study of the flow around the ground support pads. Finally, alternative systems of vehicular support should be explored.

The design of the pilot model will also involve a considerable amount of research. The problems of elastic stability and structural dynamics of high-speed tubed vehicles are believed to be similar in many respects, to those of high-speed aircraft. Therefore, the tools for the design and analysis of vehicular structures are already available to a great extent in aeroelasticity and in aircraft structural dynamics. In addition, there are special structural problems that are associated with the peculiar pressure distribution in the annular transfer space around the vehicle. Other design problems that should receive special attention are those of cabin air

conditioning and structural cooling at the higher speeds, of air purging in the tube, and of automatic control. The design of the tube itself, its methods of support, and limitations in alignment should also be studied during this phase of the project.

The economic analysis should be conducted concurrently with the other phases of the proposed research. The economic feasibility study must of necessity be of a preliminary nature until all design factors and operational characteristics are resolved. Consideration should be given, however, to the probable public acceptance and use, to the effects on complementing and competing modes of transportation, and to estimates of capital and operating costs.